OPERATIVE DENTISTRY

July/August 2017
Volume 42
Number 4
345–456

Academy of Operative Dentistry • American Academy of Gold Foil Operators • Academy of R.V. Tucker Study Clubs

OPERATIVE DENTISTRY

Volume 42 / Number 4
July/August 2017

www.jopdent.org

Aim and Scope

Operative Dentistry publishes articles that advance the practice of operative dentistry. The scope of the journal includes conservation and restoration of teeth; the scientific foundation of operative dental therapy; dental materials; dental education; and the social, political, and economic aspects of dental practice. Review papers, book reviews, letters and classified ads for faculty positions are also published.

Subscriptions: Fax 317-852-3162

Current pricing for individual, institutional, and dental student subscriptions (both USA and all other countries) can be found at our website: www.jopdent.org, or by contacting our subscription manager via email at editor@jopdent.org. Payment must be in USD and accompany orders. Online payment by credit card (American Express, Discover, Mastercard, and Visa) is available on our website.

Operative Dentistry (ISSN 0361-7734) is published bimonthly by Operative Dentistry, Indiana University School of Dentistry, Room S411, 1121 West Michigan Street, Indianapolis, IN 46202-5186. Periodicals postage paid at Indianapolis, IN and additional mailing offices. Postmaster: Send address changes to: Operative Dentistry, Indiana University School of Dentistry, Room S411, 1121 West Michigan Street, Indianapolis, IN 46202-5186.

Author Instructions

Please refer to author instructions at www.jopdent.org in the preparation of manuscript submissions and for journal policies.

Journal Policies

The Operative Dentistry Policy Manual which details journal policies, including late fees and claims, is available online at:

https://www.jopdent.com/journal/policies.pdf

Permissions

For permission to reproduce material from Operative Dentistry please apply to Operative Dentistry at the Editorial Office address or via email at editor@jopdent.org.

Online Access

Register for online access, manage subscriptions, save favorite articles and searches, get email alerts, and more at:

http://www.jopdentonline.org/action/registration

Editorial Board

Reviewer names available at: www.jopdent.com/journal/editorial_board.html

We thank all our reviewers for their time and dedication to Operative Dentistry.

On The Cover

"Thanksgiving Point" Lehi, UT USA. Photo provided by Larry Thompson of South Jordan, UT USA. Photo taken with an iPhone 6, 4 mm, f/2.2 1/719 sec. ISO-32

We welcome the submission of pictures for consideration for use on the cover of Operative Dentistry! All photographs should be submitted via the forms at:

https://www.jopdent.com/journal/journal.html

Editorial Office

The views expressed in Operative Dentistry do not necessarily represent those of the academies or the editors.

Operative Dentistry
Indiana University School of Dentistry, Room S411
1121 West Michigan Street, Indianapolis, IN 46202-5186
Phone 317-278-4800, Fax: 317-278-4900
http://www.jopdent.org

Editorial Staff

OPERATIVE DENTISTRY

CORPORATE SPONSORS

These Dental Manufacturers have joined Operative Dentistry in our commitment to publish quality dental literature in a timely manner. We thank them for their support.

DENTSPLY CAULK

ivoclar vivadent

Kerr™

AMERICAN BOARD OF OPERATIVE DENTISTRY
IN PURSUIT OF EXCELLENCE
ABOD
FOUNDED 1980

ULTRADENT

OPERATIVE DENTISTRY

Volume 42 / Number 4
July/August 2017

www.jopdent.org
345–456

In Memoriam

Clinical Tech/Case Report

Laboratory Research

Departments

Online Only Articles

Vol 42/No 4 July/August 2017 Pages 345–456 OPERATIVE DENTISTRY ISSN 0361-7734

©Operative Dentistry, 2017, **42-4,** 345-346

In Memoriam

Ivar Andreas Mjør 1933-2017

Ivar Mjør was one of the giants of 20th century dentistry -a man of many important academic achievements and special accolades. In addition to his numerous, diverse personal contributions of international significance to the art and science of contemporary dentistry, Ivar nurtured and mentored a large number of now eminent basic and clinical scientists, widely distributed across the world, with the common bond of pursuing research, tempered by Ivar's exemplary ethos and commitment to excellence. Furthermore, Ivar was as a distinguished and inspirational leader, heading up various organisations, including the Nordic Institute of Dental Materials Testing (NIOM) -inaugural Director 1973-1993, and the International Association for Dental Research (IADR), which he served as President in 1986-87.

Born and brought up in Norderhov Ringerike, Norway, Ivar studied dentistry at the University of Dundee, Scotland, graduating Bachelor of Dental Surgery (BDS) with commendation in 1957. Following compulsory service in the Norwegian Army, Ivar, accompanied by his devoted, surviving wife Birgit, crossed the Atlantic to study at the University of Alabama where he graduated Master of Science in Dentistry (MSD) in Pedodontics in 1960 and Master of Science (MS) in Anatomy in 1961. He then returned to Norway to the University of Oslo where he graduated Doctor of Odontology (Dr Odont) in 1966, following the successful completion and defence of a thesis entitled "Studies of normal and experimentally altered human coronal dentine". In 1970, a mere thirteen years after the successful completion of his primary qualification in dentistry, Ivar was appointed Professor of Dentistry and Chairman, Department of Anatomy, Dental Faculty, University of Oslo.

With leave of absence from the University in 1973, Ivar assumed the position of founding Director and Head, Biological/Clinical Division, Scandinavian Institute of Dental Materials (NIOM) -a position he held with distinction for 20 years. During his time at the University of Oslo and NIOM, Ivar's research

output was consistently remarkable and of international significance -many of his highly cited papers remained state of the knowledge to this day. Before moving on from NIOM in 1993, Ivar had amassed a large list of honours, including five honorary doctorate degrees, the IADR Wilmer Souder Award, two Medals of Honour of the Norwegian Dental Association -a silver in 1971, followed by gold in 1986, the Eero Tammisalo Medal and Honorary membership of the Finnish Dental Association and the Centennial Medal of the Finish Dental Society, to mention but a few!

On his retirement from NIOM in 1993, Ivar moved back across the Atlantic, together with Birgit of course, to be appointed Academy 100 Eminent Scholar Chair at the College of Dentistry, University of Florida -a position he held until 2008. In this position Ivar continued to publish widely and extensively, producing his fifth book – "Pulp-Dentin Biology in Restorative Dentistry"[1], editing two others, and authoring/co-authoring the last hundred or so of his c.400 papers, together with numerous other miscellaneous articles, editorials and opinion pieces. A focus in many of Ivar's more recent papers and opinion pieces is the growing importance of evidence-based knowledge, with an emphasis on the need for practice-based research, which he championed with vigour and great passion.

During his time in Florida, Ivar continued to lecture extensively around the world -one of his career-long activities, to give generously of his time to many, different organisations, including the Academy of Operative Dentistry, which he served for many years as Chair of the Academy's Research Committee. As in all things Ivar did, if he thought it was worth doing, the only way to do it was to do it to the best of his ability, and this meant doing it exceptionally well. In addition, Ivar finished his remarkable career the way he started it by being a highly committed, greatly acclaimed teacher and much-loved supervisor and mentor. That said, Ivar did not 'suffer fools gladly' and would be quick to challenge anyone who, to his analytic, encyclopaedic thinking, spoke or wrote "nonsense."

The authors of this obituary are but two of the countless people who advanced their careers and learnt a great deal in the process under Ivar's exceptional tutelage. Many might say a tough, demanding man to work for and with, but given his academic qualities, ability to make people realise their potential and infectious enthusiasm, let alone his great sense of humour, it remains for all those he 'helped along the way' a great honour, privilege and matter of pride to be able to say: "I worked with Ivar Mjør."

As to his legacy, over and above his three children -Per Ivar, Siri and Thor, and eight grandchildren, Ivar, while acknowledging the many advances in oral and dental science credited to him, might well have said on retiring back to Norway, where he spent his remaining years, more common sense and sense of purpose in dentistry than when he entered it in the early 1950s, notably the shift to prevention rather than cure. Also, the growing appreciation of the value and need for "real world" research in the interest of patients and dentistry appreciating its shortcomings – "At best we repair diseased and damaged teeth, and the only permanent fillings are the ones people die with". Always a pragmatist, Ivar appreciated that not everyone clung to his every word, but in not doing so, you had to have good reason, or new evidence to justify your position.

For once with Ivar, we may have the last word: thank you on behalf of dentistry and all the patients who benefited from your unswerving commitment and dedication to teaching, excellence in clinical practice and research. Rest in peace, colleague, friend and, above all, great man of oral and dental science.

Nairn Wilson and Valeria Gordan

REFERENCES

1. Mjor IA (2002) Pulp-Dentin Biology in Restorative Dentistry, Chicago, Quintessence

©Operative Dentistry, 2017, **42-4,** 347-356

Clinical Technique/Case Report

Masking of Enamel Fluorosis Discolorations and Tooth Misalignment With a Combination of At-Home Whitening, Resin Infiltration, and Direct Composite Restorations

J Perdigão • VQ Lam • BG Burseth • C Real

Clinical Relevance

Successful masking of enamel fluorosis discolorations can be achieved conservatively using a combination of at-home whitening with 10% carbamide peroxide and resin infiltration after enamel etching, resulting in a very satisfactory result.

SUMMARY

This clinical report illustrates a conservative technique to mask enamel discolorations in maxillary anterior teeth caused by hypomineralization associated with enamel fluorosis and subsequent direct resin composite to improve the anterior esthetics. The treatment consisted of at-home whitening with 10% carbamide peroxide gel with potassium nitrate and sodium fluoride in a custom-fitted tray to mask the brown-stained areas, followed by resin infiltration to mask the white spot areas. An existing resin composite restoration in the maxillary right central incisor was subsequently replaced after completion of the whitening and resin infiltration procedures, whereas the two misaligned and rotated maxillary lateral incisors were built up with direct resin composite restorations to provide the illusion of adequate arch alignment, as the patient was unable to use orthodontic therapy.

*Jorge Perdigão, DMD, MS, PhD, Department of Restorative Sciences, University of Minnesota School of Dentistry, Minneapolis, MN, USA

Viet Q. Lam, BS, University of Minnesota School of Dentistry, Minneapolis, MN, USA

Brian G. Burseth, DDS, Private Practice, Crystal Lake, IL, USA

Carmen Real, DDS, Department of Primary Dental Care, University of Minnesota School of Dentistry, Minneapolis, MN, USA

*Corresponding author: 515 SE Delaware Street, 8-450 Moos Tower, Minneapolis, MN 55455, USA; e-mail: perdi001@umn.edu

DOI: 10.2341/16-181-T

INTRODUCTION

Excessive fluoride intake may result in dental fluorosis, which is a hypomineralization of enamel

characterized by opaque white areas or discolorations ranging from light yellow to dark brown.[1] The dosage and duration of fluoride ingestion during tooth development determines the severity of fluorosis.[2] The degree of enamel hypomineralization may vary in different parts of the tooth surface due to the variation in enamel thickness.[3] Not all white or brown demineralized enamel areas are caused by fluorosis; therefore, they may be considered idiopathic.[4,5] The term enamel "dysmineralization" has been used when referring to fluorosis-like enamel discolorations.[6]

Although the corresponding enamel abnormality had been described in the beginning of the 20th century,[7,8] the etiology of dental fluorosis was not independently established until 1930.[9] In 1901 J. M. Eager, of the US Marine Hospital service, reported in Public Health Reports[7] and the following year in The Dental Cosmos[8] a frequent dental abnormality among the inhabitants of Naples, Italy, known as "denti di Chiaie" (named after Prof Chiaie who first described the condition) and attributed the enamel discoloration to the water supply. Dr Eager also noticed that the incidence of the condition among infants had greatly diminished since water brought from a distant mountain had been in use in lieu of the water from local wells. In 1916, McKay and Black[10] described the same condition, calling it "mottled enamel," localized to the area of Colorado Springs, CO. The authors also hypothesized that the water supply might be the cause of this condition.

The esthetic imbalance caused by enamel fluorosis has been treated with enamel macroabrasion or microabrasion, alone or combined with in-office or at-home whitening.[11-16] The enamel microabrasion technique was described by Croll and Cavanaugh[17] in 1986. The microabrasion paste, which contains hydrochloric acid (HCl) and silicon carbide, is applied by rubbing it onto the enamel surface and removing a microscopic layer of enamel,[18,19] therefore combining chemical erosion with mechanical abrasion. Depending on the concentration of HCl, the abrasive material, and the duration of each application, enamel microabrasion removes up to 200 μm of the outer enamel surface.[20,21] In some cases, a residual yellow color has been reported after the enamel microabrasion treatment, which may be a result of the thinner enamel exposing more of the underlying dentin.[20] Although a few applications of a microbrasion suspension have been recommended to mask white spots,[17,22] the technique is more successful in removing brown stains than white opaque areas.[23,24] However, it is difficult to predict when enamel microabrasion will remove a stain completely from a tooth,[25] as the defect may be deeper than microabrasion can reach.

The combination of HCl enamel etching with the infiltration of a low-viscosity resorcinol-formaldehyde resin into etched enamel was introduced in 1976 as a potential cariostatic treatment.[26] Croll[27] used a clear resin sealant on phosphoric acid-etched enamel to saturate the surfaces with resin for smooth surface enamel defects. In 2009, the masking of white spots with resin infiltration using 15% HCl etching followed by a drying step with ethanol, and the application of a low-viscosity light-cured resin (tetraethylene glycol dimethacrylate [TEGDMA]) was described in the literature, which is the current technique recommended for resin infiltration.[28] Compared with enamel microabrasion, the enamel resin infiltration technique is more conservative.[29] The sequential combination of at-home whitening in a custom-fitted tray with enamel resin infiltration described in this article has not been often reported in the dental literature. Therefore, the purpose of this clinical report is to describe the technique used to mask the discoloration of the maxillary anterior teeth in a patient with dental fluorosis, through the combination of at-home whitening with 10% carbamide peroxide in a custom-fitted tray and enamel resin infiltration, followed by recontouring the teeth with direct resin composite restorations.

CASE REPORT

The chief complaint of this 20-year-old male patient was "I want to get permanent crowns on my front teeth." The patient was not satisfied with the yellowish color of his teeth.

The patient's medical history was noncontributory. The periodontal status of the patient was normal and being monitored every six months. The patient had class I molar classification bilaterally, with anterior overbite of 5 mm and 3-mm overjet. Clinically, teeth 7 and 10 were retroclined relative to teeth 8 and 9. Tooth 7 was mesially rotated in relation to tooth 10. There was a history of trauma to the right maxillary central incisor (tooth 8) within the last six years, with fracture of the incisal border, but the pulp responded to vitality tests within normal limits. This tooth had been restored with resin composite. Radiographically, teeth 8 and 9 displayed a uniform periodontal ligament space and intact lamina dura consistent with the other anterior teeth. A normal generalized pattern of bone trabeculation was observed. Tooth 8 had a coronal

Figure 1. *(a) Baseline frontal view of compromised esthetics as a result of fluorosis brown and white stains and misaligned maxillary incisors. (b) Closer view of maxillary central incisors. Tooth 8 has an incisal resin composite restoration that includes the distal angle.*

radiopacity consistent with the clinical presence of a resin-based restorative material.

In addition to the clinical and radiographic findings, from the medical history we noticed that the patient was born in an area that has been described as a naturally fluoridated region (for privacy issues, we decided to keep this geographic reference confidential), which led us to the diagnosis of enamel fluorosis (Figure 1). The enamel fluorosis in this case corresponds to a tooth surface index of fluorosis (TSIF) of 4.[1]

The initial treatment plan presented to patient included at-home whitening with 10% carbamide peroxide gel with potassium nitrate and sodium fluoride (Opalescence PF 10%, Ultradent Co., South Jordan, UT, USA) in a custom-fitted tray overnight for a minimum of 5-10 weeks to mask the brown stains, followed by resin infiltration of the white spot areas with Icon (DMG America, Englewood, NJ, USA). The patient was informed that the existing resin composite restoration of tooth 8 would have to be replaced after successful completion of the

Figure 2. *Clinical aspect after 5 weeks of at-home whitening overnight with 10% carbamide peroxide with potassium nitrate and sodium fluoride (Opalescence PF 10%, Ultradent Co) in a custom-fitted tray. Compare with Figure 1a to evaluate the significant improvement of the brown stains.*

whitening and resin infiltration procedures. A consultation with Orthodontics concerning the misaligned maxillary anterior teeth was also recommended at this time.

The list of materials used is provided in Table 1. After intraoral photographs and preliminary alginate impressions to fabricate bleaching trays, a 0.035-in-thick ethylene vinyl acetate sheet was heated prior to forming the tray around the stone model in a vacuum device. The tray was then trimmed in a horseshoe shape and trimmed following the scalloped contour of the free gingival margin.[30] The tray was kept slightly short of the free gingival margin (0.5-1.0 mm) to prevent possible irritation caused by the contact of the gel with the soft tissues.[31,32] Spacers were not used to create reservoirs for the bleaching gel, as they do not increase the success of at-home bleaching.[33,34] It has been shown that the bleaching gel remains active for longer periods when reservoirs are used,[34] which may be the reason why tray reservoirs result in higher rates and higher intensity of gingival inflammation during at-home bleaching.[35] After demonstrating how to insert the gel into the tray, eight syringes of 10% carbamide peroxide gel were prescribed to patient, with the respective take-home written instructions.

Figure 2 depicts the clinical aspect after five weeks of at-home whitening overnight. The patient reported no sensitivity, and no alterations were observed in the soft tissues. The patient had been informed that an interval of two weeks would be necessary between the final application of the bleaching gel and the

Table 1: *Materials used in the clinical case*

Material (manufacturer)	Composition
Opalescence 10% PF (Ultradent Co)	10% carbamide peroxide, potassium nitrate, 0.25% sodium fluoride, xylitol, polyacrylic acid thickener, sodium hydroxide
Icon (DMG America)	Icon Etch: 15% hydrochloric acid
	Icon Dry: 100% ethyl alcohol
	Icon Infiltrant: TEGDMA, additives, and initiators
Scotchbond Universal Adhesive (3M ESPE)	10-MDP, dimethacrylate resins, HEMA, methacrylate-modified polyalkenoic acid copolymer, nanofiller, ethanol, water, initiators, silane
Filtek Supreme Ultra (3M ESPE)	Bis-GMA, UDMA, TEGDMA, Bis-EMA, silanated silica, silanated zirconia; photoinitiators

Abbreviations: 10-MDP, methacryloyloxydecyl dihydrogen phosphate; Bis-EMA, bisphenol A ethoxylated dimethacrylate; Bis-GMA, bisphenol glycidyl methacrylate; HEMA, 2-hydroxy ethylmethacrylate; TEGDMA, tetraethylene glycol dimethacrylate; UDMA, urethanedimethacrylate.

resin infiltration session. Figure 3a-c illustrates the resin infiltration clinical procedure. Figure 4a is the clinical aspect of the dehydrated teeth immediately after the resin infiltration treatment and rubber dam removal. After 48 hours, the teeth had rehydrated (Figure 4b). At this point, we informed patient that additional at-home whitening might mask slightly better the residual yellow color from the anterior teeth but that he would have to apply the whitening gel from the lingual aspect of the teeth, as a thin transparent resin layer was now coating the labial surfaces. The patient agreed with the plan and started another whitening treatment sequence.

Two weeks after the resin infiltration session, we noticed that the four maxillary incisors had become lighter (Figure 5). The patient returned to the clinic three weeks later, at which point further lightening of teeth 7 and 8 (Figure 6) was even more evident. At this stage, we informed the patient that the resin composite restoration on tooth 8 would have to be replaced after a few weeks. The patient did not pursue orthodontic treatment for the misaligned anterior teeth due to financial constraints. An alternative plan, which included a more affordable solution, was presented to the patient including advantages and disadvantages. This alternative consisted of minimal enamel reduction and building the maxillary lateral incisors with direct resin composite to change the labial alignment of the anterior teeth.

A waxed-up model was shown to patient for the patient's approval, which included the following: (1) labial realignment of the lateral incisors with direct resin composite; (2) increase of the length of the clinical crown of tooth 8 by adding resin composite to the incisal aspect while performing the replacement of the existing resin composite restoration; (3) a slight reduction of enamel (0.5 mm) on the distal and incisal aspects of the labial surface of tooth 7; and (4) adjustment of the central portion of the incisal edge of tooth 9 with a Sof-Lex XT (3M ESPE, St Paul, MN, USA) disk to establish symmetry between the two central incisors from a frontal aspect.

The resin composite shade was selected using a Vita EasyShade Advance 4.0 spectrophotometer (VITA Zahnfabrik H. Rauter GmbH, & Co KG, Bad Säckingen, Germany). A direct mockup was performed with the selected resin composite shades (A1D and A1E, Filtek Supreme Plus, 3M ESPE). The existing restoration of tooth 8 was removed, and the peripheral enamel was roughened with a diamond bur. The enamel was etched with 35% phosphoric acid gel (Ultra-Etch, Ultradent Co) (Figure 7) for 15 seconds, rinsed with water for 10 seconds, and gently air-dried. Scotchbond Universal Adhesive (3M ESPE) was applied in a rubbing motion for 15 seconds (Figure 8) and gently air dried for 10-15 seconds[36] to evaporate water and ethanol, followed by light-curing from the labial and lingual surfaces for 20 seconds each using a QHL75 halogen curing light (Dentsply Caulk, Milford, DE, USA). A putty-consistency polyvinyl siloxane guide was prepared from the waxed-up model and used to build tooth 8 in layers starting with A1E (A1 enamel shade) from the lingual aspect, followed by A1D (A1 dentin shade) to replace missing dentin and A1E on the labial aspect. Each layer was irradiated with the same curing light for 40 seconds from the both facial and lingual aspects. Finishing and polishing were carried out with fine diamond points and Sof-Lex XT disks (3M ESPE). The enamel in the lateral incisors was roughened with a medium-grit Sof-Lex XT disc (3M ESPE), followed by etching with 35% phosphoric acid gel (Ultra-Etch, Ultradent Co) for 15 seconds and the application of Scotchbond Universal Adhesive (3M ESPE) exactly as described above. Filtek Supreme Ultra (3M ESPE) resin composite, A1 body shade (A1B), was applied and light-cured on tooth 7,

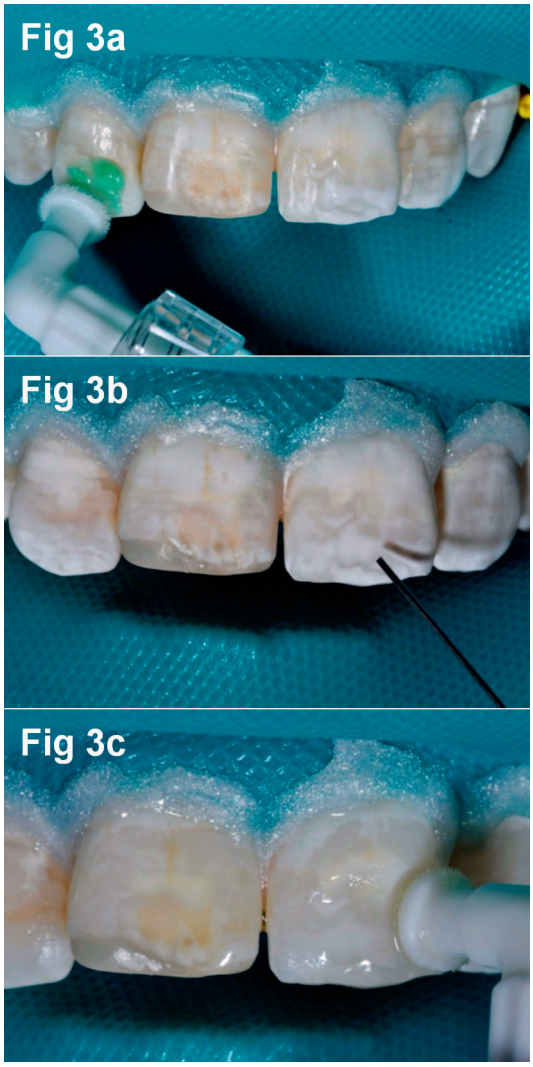

Figure 3. *(a) Teeth were cleaned with a suspension of pumice and water and thoroughly washed with water. The rubber dam was sealed cervically with a light-cured resin barrier (OpalDam, Ultradent Co). A 15% HCl gel (Icon-Etch, DMG America) was applied to the white spot areas and left undisturbed for two minutes. The manufacturer provides an application tip in the respective kit. The gel was thoroughly rinsed with water for 30 seconds with the high-speed suction tip positioned as close as possible to the area being washed. The teeth were air-dried with water- and oil-free air for 15 seconds. (b) The tip of the Icon-Dry (DMG America) syringe was positioned over the etched areas. A generous amount of Icon-Dry, which is composed of ethanol, was applied to the white spot areas and left undisturbed for 30 seconds. The teeth were air-dried with water- and oil-free air for 15 seconds. (c) An abundant amount of Icon-Infiltrant (DMG America), which contains tetraethylene glycol dimethacrylate (TEGDMA) (Table 1) initiators and stabilizers, was applied and left undisturbed for three minutes. Excess material was gently air-blown for five seconds to prevent pooling around the incisal edge. Excess resin was removed with cotton pellets and dental floss. The resin was light-cured for 40 seconds in each tooth.*

Figure 4. *(a) Clinical aspect of the dehydrated teeth immediately after the resin infiltration procedure and rubber dam removal. (b) After 48 hours, the teeth had rehydrated. The patient was informed that additional at-home whitening might improve the residual yellow color from the front teeth.*

whereas tooth 10 was restored with Filtek Supreme Ultra (3M ESPE), shade A1E. Finishing and polishing procedures were carried out as described above. The final clinical aspect is shown in Figure 9a,b. Figure 10 shows the nine-month postoperative view.

DISCUSSION

Haywood and Heymann introduced the nightguard vital bleaching technique in 1989[37] using a vacuum-formed custom-fitted soft plastic night guard filled with a 10% carbamide peroxide gel that was available over the counter. Several clinical studies have validated the effectiveness and safety of this bleaching modality.[38,39] Other authors have advocated the use of higher concentrations of carbamide peroxide.[40] Although higher concentrations of peroxides may result in a faster rate of whitening than that of 10% carbamide peroxide, they all reach a similar final result.[41,42] Higher concentrations, however, increase the incidence of tooth sensitivity.[41,42] Overnight tray whitening with 10% carbamide peroxide results in whiter teeth and more durable results than whitening for a few hours during the daytime.[43,44] The efficacy of at-home whitening to treat enamel discolorations caused by fluorosis or of

Figure 5. *Clinical aspect two weeks after the resin infiltration procedure. Due to the presence of a coating of resin infiltrant on the labial surfaces, the patient applied the carbamide peroxide gel from the lingual aspect of the teeth for 2 weeks. No sensitivity was reported. Soft tissues did not present any alteration.*

Figure 6. *Patient returned to clinic after three weeks of further at-home whitening. The patient was very satisfied with the color of his teeth. We reminded the patient that a minimum interval of two weeks was necessary between the final whitening treatment and the restorative procedure.*

idiopathic origin depends on the type of stain.[31] At-home whitening usually lightens enamel brown stains, but it may not work so well for some white areas.[45-47] At-home whitening may emphasize the whitish areas in cases of deeper white spots.

Recent clinical reports have recommended masking the enamel fluorosis stains by removing enamel with microabrasion or macroabrasion, followed by whitening.[11-16] Pontes and others[11] used an ultrafine diamond bur (macroabrasion) to remove the outer layer of the fluorotic enamel, followed by eight applications of 10 seconds each of an enamel microabrasion compound, with water rinsing between applications. One week later, the enamel microabrasion technique was repeated, followed by three sessions of in-office whitening with 35% hydrogen peroxide. Although the final result was pleasant, it is questionable whether this was a conservative treatment as enamel was removed with a diamond bur and two separate sessions of enamel microabrasion. In another clinical report,[12] enamel fluorosis stains were treated using micro-

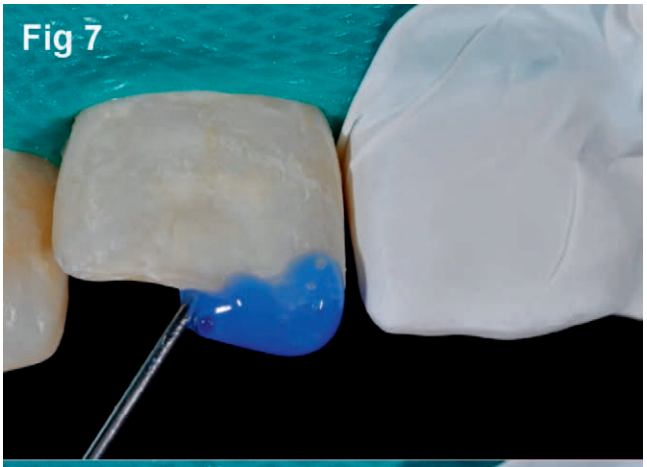

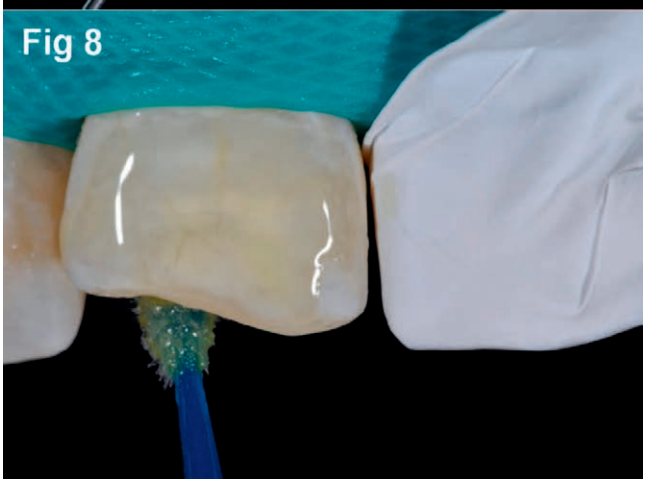

Figure 7. *The resin composite shade was selected with a Vita EasyShade Advance 4.0 spectrophotometer (VITA Zahnfabrik H. Rauter GmbH, & Co) prior to inserting the rubber dam. After removal of the existing restoration of tooth 8, a long bevel was prepared on the enamel labial surface with a diamond bur. All prepared enamel was etched with 35% phosphoric acid gel for 15 seconds (Ultra-Etch, Ultradent Co), rinsed with water for 10 seconds, and gently air-dried.*

Figure 8. *Scotchbond Universal Adhesive (3M ESPE) was applied in a rubbing motion for 15 seconds and gently air-dried for 10-15 seconds to evaporate water and ethanol, followed by light curing from the labial and lingual surfaces for 20 seconds. Filtek Supreme Ultra (3M ESPE) was then inserted and light-cured, and the restorations were finished, as described in the text.*

abrasion to eliminate the superficial enamel layer, followed by at-home bleaching and direct resin-based composite restorations. According to these authors, they started with enamel microabrasion and then prescribed a home bleaching technique "to better harmonize tooth color and produce whiter teeth."

One clinical case[16] started with two sessions of in-office whitening with three applications of 35% hydrogen peroxide in each session. The second phase of the treatment was enamel microabrasion with a paste of 12% HCl with silicon carbide that

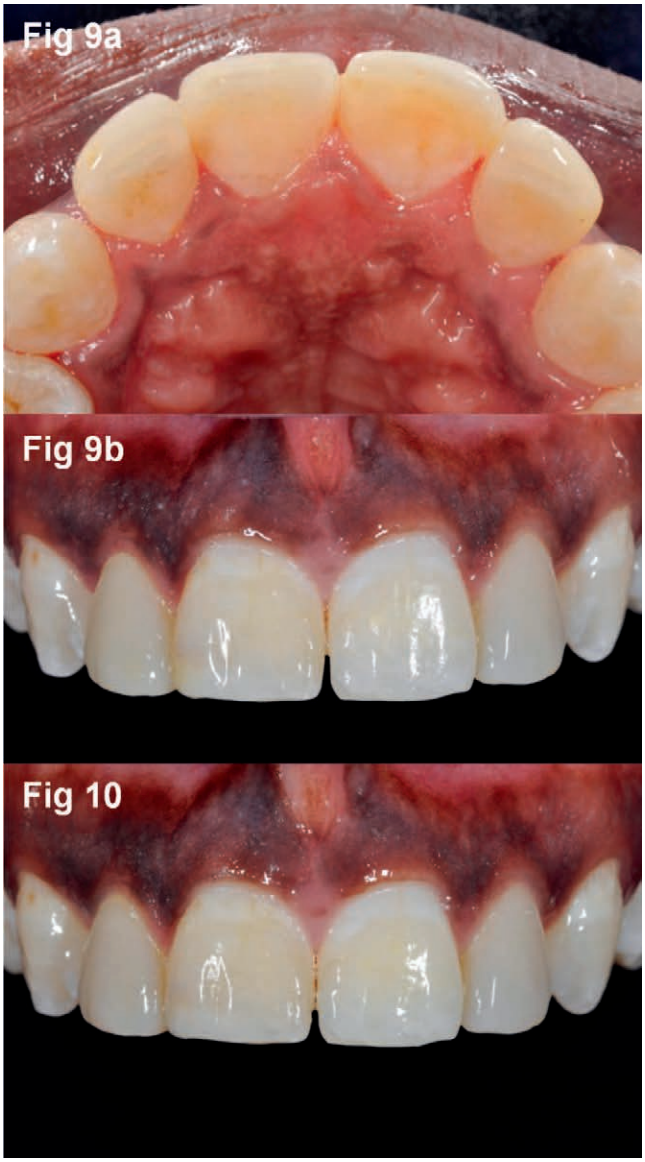

Figure 9. *(a) Final clinical aspect, mirror lingual view. (b) Final clinical aspect, frontal view.*

Figure 10. *Clinical aspect after nine months.*

was rubbed 12 consecutive times for 10 seconds each, with a 20-second water rinse between each application. However, the effect of the in-office whitening component of the treatment was not clear in this article, as no preoperative image was published. Additionally, two sessions of in-office whitening with 35% hydrogen peroxide (with three applications in each session) are more damaging to the pulp tissue than at-home whitening with 10% carbamide peroxide use in the clinical case described in the present article. For carbamide peroxide, the application of a 10% concentration from 1.5 to 8.0 hours onto enamel does not result in significant toxic effects on both odontoblast-like cells and human dental pulp cells.[48-50] When teeth were treated in-office with 35% hydrogen peroxide for three consecutive periods of 15 minutes each, 76.6% of lateral incisors, 53.3% of central incisors, and 30% of canines experience posttreatment sensitivity, with no discomfort reports for premolars.[51,52] The thinner enamel and dentin of anterior teeth may be a strong contraindication for in-office whitening, especially in young patients, as pulp necrosis may occur.[53]

For the resin infiltration technique, 15% HCl applied for 120 seconds removes ≈40 μm of enamel from the surface.[29] Using scanning electron microscopy, Sundfeld and others reported that Opalustre (Ultradent Co), which contains 6.6% HCl and silicon carbide, resulted in enamel loss ranging from 25 to 200 μm corresponding to one and 10 applications of the product for 60 seconds on each tooth, respectively.[20] Thus, the enamel surface loss is more pronounced with the enamel microabrasion technique compared with the resin infiltration technique, most likely because no pressure is applied with resin infiltration, which results in a more uniform enamel removal.

Taking into account that resin infiltration after enamel etching with HCl is a more conservative technique, it is the current treatment modality recommended for masking white spots.[28,54] The clinical sequence that we currently prescribe for yellow or brown enamel fluorosis stains starts with at-home whitening with 10% carbamide peroxide in a custom-fitted tray. In the past, we used enamel microabrasion as the second step of the treatment sequence. Currently, we prescribe enamel resin infiltration in case residual white areas persist after the whitening treatment. In this clinical report, we recontoured teeth 7 and 10 with direct resin composite restorations. This option offers an excellent solution for misaligned teeth in the anterior region,[55,56] especially in patients unwilling or unable to use orthodontic treatment. This treatment provides a very conservative approach compared with porcelain restorations, despite resin composite restorations being more susceptible to chipping and staining than ceramic restorations.[55,56] Through the selective addition of resin composite, an illusion of alignment can be created, which, in many cases, provides a very satisfactory result to our patients. Limitations include the potential interference with a balanced occlusal relationship or when the periodontal condition is affected by changes of

the emergency profiles. A short-term nine-month postoperative evaluation (Figure 10) highlighted the patient's satisfaction with the treatment outcome, without any clinical signs of soft tissue inflammation caused by change in the profile of the maxillary lateral incisors.

CONCLUSION

Successful esthetic treatment of brown and white stains caused by enamel fluorosis is possible using at-home whitening with 10% carbamide peroxide in a custom-fitted tray to whiten the brown enamel areas, followed by resin infiltration to camouflage the white spots. Direct resin composite restorations may be used to augment the esthetic outcome in cases of replacement of existing restorations and create an illusion of alignment of slight tooth misalignments.

Regulatory Statement

This study was conducted in accordance with all the provisions of the local human subjects oversight committee guidelines and policies of the University of Minnesota.

Conflict of Interest

Dr. Perdigao has received compensation for speaking at events sponsored by 3M ESPE. This relationship has been reviewed and managed by the University of Minnesota in accordance with its conflict of interest polices. All other authors certify that they have no proprietary, financial, or other personal interest of any nature or kind in any product, service and/or company presented in this article.

(Accepted 10 December 2016)

REFERENCES

1. Horowitz HS, Driscoll WS, Meyers RJ, Heifetz SB, & Kingman A (1984) A new method for assessing the prevalence of dental fluorosis—The Tooth Surface Index of Fluorosis *Journal of the American Dental Association* **109(1)** 37-41.
2. Robinson C, & Kirkham J (1990) The effect of fluoride on the developing mineralized tissues *Journal of Dental Research* **69(Special No)** 685-691, discussion 721.
3. Fejerskov O, Manji F, & Baelum V (1990) The nature and mechanisms of dental fluorosis in man *Journal of Dental Research* **69(Special No)** 692-700, discussion 721.
4. Cutress TW, & Suckling GW (1990) Differential diagnosis of dental fluorosis *Journal of Dental Research* **69(Spec No)** 714-720. discussion 721.
5. Croll TP (2009) Fluorosis *Journal of the American Dental Association* **140(3)** 278-279.
6. Croll TP (1990) Enamel microabrasion for removal of superficial dysmineralization and decalcification defects *Journal of the American Dental Association* **120(4)** 411-415.
7. Eager JM (1901) Denti di Chiaie (Chiaie teeth) *Public Health Reports* **16(44)** 2576-2577.
8. Eager JM (1902) Periscope—Chiaie teeth *The Dental Cosmos* **XLIV** 301-302.
9. Fichardt T, Van Rhyn JL, & Van Selm GW (1955) A case of fluorosis *Journal of the Faculty of Radiologists* **7(2)** 130-135.
10. McKay FS, & Black GV (1916) An investigation of mottled teeth: an endemic developmental imperfection of the enamel of the teeth, heretofore unknown in the literature of dentistry *The Dental Cosmos* **58(6)** 627-644.
11. Pontes DG, Correa KM, & Cohen-Carneiro F (2012) Re-establishing esthetics of fluorosis-stained teeth using enamel microabrasion and dental bleaching techniques *European Journal of Esthetic Dentistry* **7(2)** 130-137.
12. Ardu S, Stavridakis M, & Krejci I (2007) A minimally invasive treatment of severe dental fluorosis *Quintessence International* **38(6)** 455-458.
13. Higashi C, Dall'Agnol AL, Hirata R, Loguercio AD, & Reis A (2008) Association of enamel microabrasion and bleaching: A case report *General Dentistry* **56(3)** 244-249.
14. Sundfeld RH, Rahal V, de Alexandre RS, Briso AL, & Sundfeld Neto D (2011) Smile restoration through use of enamel microabrasion associated with tooth bleaching *Compendium of Continuing Education in Dentistry* **32(3)** e53-e57.
15. Sundfeld RH, Franco LM, Goncalves RS, de Alexandre RS, Machado LS, & Neto DS (2014) Accomplishing esthetics using enamel microabrasion and bleaching—A case report *Operative Dentistry* **39(3)** 223-227.
16. Bertassoni LE, Martin JMH, Torno V, Vieira S, Rached RN, & Mazur RF (2008) In-office dental bleaching and enamel microabrasion for fluorosis treatment *Journal of Clinical Pediatric Dentistry* **32(3)** 185-188.
17. Croll TP, & Cavanaugh RR (1986) Enamel color modification by controlled hydrochloric acid-pumice abrasion. I. Technique and examples *Quintessence International* **17(2)** 81-87.
18. Donly KJ, O'Neill M, & Croll TP (1992) Enamel microabrasion: A microscopic evaluation of the "abrosion effect" *Quintessence International* **23(3)** 175-179.
19. Paic M, Sener B, Schug J, & Schmidlin PR (2008) Effects of microabrasion on substance loss, surface roughness, and colorimetric changes on enamel in vitro *Quintessence International* **39(6)** 517-522.
20. Sundfeld RH, Croll TP, Briso AL, de Alexandre RS, & Sundfeld Neto D (2007) Considerations about enamel microabrasion after 18 years *American Journal of Dentistry* **20(2)** 67-72.
21. Kendell RL (1989) Hydrochloric acid removal of brown fluorosis stains: Clinical and scanning electron micrographic observations *Quintessence International* **20(11)** 837-839.
22. Croll TP, & Cavanaugh RR (1986) Hydrochloric acid-pumice enamel surface abrasion for color modification: results after six months *Quintessence International* **17(6)** 335-341.

23. Welbury RR, & Shaw L (1990) A simple technique for removal of mottling, opacities and pigmentation from enamel *Dental Update* **17(4)** 161-163.
24. Willis GP, & Arbuckle GR (1992) Orthodontic decalcification management with microabrasion *Journal of the Indiana Dental Association* **71(4)** 16-19.
25. Celik EU, Yildiz G, & Yazkan B (2013) Clinical evaluation of enamel microabrasion for the aesthetic management of mild-to-severe dental fluorosis *Journal of Esthetic and Restorative Dentistry* **25(6)** 422-430.
26. Robinson C, Hallsworth AS, Weatherell JA, & Künzel W (1976) Arrest and control of carious lesions: A study based on preliminary experiments with resorcinol-formaldehyde resin *Journal of Dental Research* **55(5)** 812-818.
27. Croll TP (1987) Bonded resin sealant for smooth surface enamel defects: New concepts in "microrestorative" dentistry *Quintessence International* **18(1)** 5-10.
28. Paris S, & Meyer-Lueckel H (2009) Masking of labial enamel white spot lesions by resin infiltration—A clinical report *Quintessence International* **40(9)** 713-718.
29. Meyer-Lueckel H, Paris S, & Kielbassa AM (2007) Surface layer erosion of natural caries lesions with phosphoric and hydrochloric acid gels in preparation for resin infiltration *Caries Research* **41(3)** 223-230.
30. Haywood VB (1997) Nightguard vital bleaching *Dentistry Today* **16(6)** 86, 88, 90-91.
31. Haywood VB (2003) Frequently asked questions about bleaching *Compendium of Continuing Education in Dentistry* **24(4A)** 324-338.
32. Haywood VB (1997) Nightguard vital bleaching: Current concepts and research *Journal of the American Dental Association* **128(Suppl)** 19S-25S.
33. Javaheri DS, & Janis JN (2000) The efficacy of reservoirs in bleaching trays. *Operative Dentistry* **25(3)** 149-151.
34. Matis BA, Yousef M, Cochran MA, & Eckert GJ (2002) Degradation of bleaching gels in vivo as a function of tray design and carbamide peroxide concentration. *Operative Dentistry* **27(1)** 12-18.
35. Kirsten GA, Freire A, de Lima AA, Ignácio SA, & Souza EM (2009) Effect of reservoirs on gingival inflammation after home dental bleaching *Quintessence International* **40(3)** 195-202.
36. Luque-Martinez IV, Perdigão J, Munoz MA, Sezinando A, Reis A, & Loguercio A (2014) Effects of solvent evaporation time on immediate adhesive properties of universal adhesives to dentin *Dental Materials* **30(10)** 1126-1135.
37. Haywood VB, & Heymann HO (1989) Nightguard vital bleaching *Quintessence International* **20(3)** 173-176.
38. Matis BA, Cochran MA, Eckert G, & Carlson TJ (1998) The efficacy and safety of a 10% carbamide peroxide bleaching gel *Quintessence International* **29(9)** 555-563.
39. Leonard RH Jr, Van Haywood B, Caplan DJ, &Tart ND (2003) Nightguard vital bleaching of tetracycline- stained teeth: 90 months post treatment *Journal of Esthetic and Restorative Dentistry* **15(3)** 142–152, discussion 153.
40. Meireles SS, Heckmann SS, Leida FL, dos Santos Ida S, Della Bona A, & Demarco FF (2008) Efficacy and safety of 10% and 16% carbamide peroxide tooth-whitening gels: A randomized clinical trial *Operative Dentistry* **33(6)** 606-612.
41. Matis BA, Mousa HN, Cochran MA, & Eckert GJ (2000) Clinical evaluation of bleaching agents of different concentrations *Quintessence International* **31(5)** 303-310.
42. Basting RT, Amaral FL, França FM, & Flório FM (2012) Clinical comparative study of the effectiveness of and tooth sensitivity to 10% and 20% carbamide peroxide home-use and 35% and 38% hydrogen peroxide in-office bleaching materials containing desensitizing agents *Operative Dentistry* **37(5)** 464-473.
43. Matis BA, Cochran MA, & Eckert G (2009) Review of the effectiveness of various tooth whitening systems *Operative Dentistry* **34(2)** 230-235.
44. Cardoso PC, Reis A, Loguercio A, Vieira LC, & Baratieri LN (2010) Clinical effectiveness and tooth sensitivity associated with different bleaching times for a 10 percent carbamide peroxide gel *Journal of the American Dental Association* **141(10)** 1213-1320.
45. Haywood VB, & Leonard RH (1998) Nightguard vital bleaching removes brown discoloration for 7 years: A case report *Quintessence International* **29(7)** 450-451.
46. Bodden MK, & Haywood VB (2003) Treatment of endemic fluorosis and tetracycline staining with macroabrasion and nightguard vital bleaching: A case report *Quintessence International* **34(2)** 87-91.
47. Perdigão J (2010) Dental whitening—Revisiting the myths *Northwest Dentistry* **89(6)** 19-21, 23-26.
48. Soares DG, Ribeiro AP, Sacono NT, Coldebella CR, Hebling J, & Costa CA (2011) Transenamel and transdentinal cytotoxicity of carbamide peroxide bleaching gels on odontoblast-like MDPC-23 cells *International Endodontic Journal* **44(2)** 116-125.
49. Duque CC, Soares DG, Basso FG, Hebling J, de Souza Costa CA (2014) Bleaching effectiveness, hydrogen peroxide diffusion, and cytotoxicity of a chemically activated bleaching gel *Clinical Oral Investigations* **18(6)** 1631-1637.
50. de Almeida LC, Soares DG, Azevedo FA, Gallinari Mde O, Costa CA, dos Santos PH, & Briso AL (2015) At-home bleaching: Color alteration, hydrogen peroxide diffusion and cytotoxicity *Brazilian Dental Journal* **26(4)** 378-383.
51. de Almeida LC, Costa CA, Riehl H, dos Santos PH, Sundfeld RH, & Briso AL (2012) Occurrence of sensitivity during at-home and in-office tooth bleaching therapies with or without use of light sources *Acta Odontológica Latinoamericana* **25(1)** 3-8.
52. Bonafé E, Bacovis CL, Iensen S, Loguercio AD, Reis A, & Kossatz S (2013) Tooth sensitivity and efficacy of in-office bleaching in restored teeth *Journal of Dentistry* **41(4)** 363-369.
53. Costa CA, Riehl H, Kina JF, Sacono NT, & Hebling J (2010) Human pulp responses to in-office tooth bleaching *Oral Surgery, Oral Medicine, Oral Pathology, Oral Radiology, and Endodontology* **109(4)** e59-e64.
54. Senestraro SV, Crowe JJ, Wang M, Vo A, Huang G, Ferracane J, & Covell DA Jr (2013) Minimally invasive

resin infiltration of arrested white-spot lesions: A randomized clinical trial *Journal of the American Dental Association* **144(9)** 997-1005.

55. Peumans M, Van Meerbeek B, Lambrechts P, & Vanherle G (1997) The 5-year clinical performance of direct composite additions to correct tooth form and position. I. Esthetic qualities *Clinical Oral Investigations* **1(1)** 12-18.

56. Peumans M, Van Meerbeek B, Lambrechts P, & Vanherle G (1997) The 5-year clinical performance of direct composite additions to correct tooth form and position. II. Marginal qualities *Clinical Oral Investigations* **1(1)** 19-26.

©Operative Dentistry, 2017, **42-4,** 357-366

Laboratory Research

Chemical Interaction Analysis of an Adhesive Containing 10-Methacryloyloxydecyl Dihydrogen Phosphate (10-MDP) With the Dentin in Noncarious Cervical Lesions

BMB Oliveira • ALM Ulbaldini • F Sato • ML Baesso
AC Bento • LHC Andrade • SM Lima • RC Pascotto

Clinical Relevance

The results suggest that it is unnecessary to remove the hypermineralized layer with burs, as this may decrease the chemical bonding potential of 10-MDP.

SUMMARY

The purpose of this study was to evaluate the chemical bonds of a self-etch 10-methacryloyloxydecyl dihydrogen phosphate (10-MDP) adhesive to natural noncarious cervical lesions (NCCLs) and compare them with those occurring in sclerotic dentin in artificially prepared defects (APDs). Four human teeth with natural NCCLs on the buccal surface were selected. Artificial defects matching the natural lesions were prepared on the lingual surface of the same teeth serving as control. Micro-Raman (MR) spectroscopy was used to quantify mineral content in natural NCCLs and in APDs. Fourier transform infrared-photoacoustic spectroscopy (FTIR-PAS) readouts were taken before and after adhesive application to analyze the protein matrix/mineral (M:M) ratio and chemical interactions between 10-MDP adhesive and dentin. The MR and FTIR-PAS spectra collected from natural NCCLs demonstrated a larger area of the band (961 cm^{-1},

*Bruna M. B. Oliveira, DDS, MSc, Dentistry, State University of Maringá, Maringá, Paraná, Brazil

Adriana L.M. Ulbaldini, Maringá, DDS, MSc, Dentistry, State University of Maringá, Maringá, Paraná, Brazil

Francielle Sato, PhD, Physics, State University of Maringá, Maringá, Paraná, Brazil

Mauro L. Baesso, PhD, Physics, State University of Maringá, Maringá, Paraná, Brazil

Antonio Carlos Bento, PhD, Physics, State University of Maringá, Paraná, Brazil

Luis H. C. Andrade, PhD, Physics, State University of Mato Grosso do Sul, Cidade Universitária de Dourados, Dourados, Mato Grosso do Sul, Brazil

Sandro M. Lima, PhD, Physics, State University of Mato Grosso do Sul, Cidade Universitária de Dourados, Dourados, Mato Grosso do Sul, Brazil

Renata C. Pascotto, DDS, MSc, PhD, Dentistry, State University of Maringá, Maringá, Paraná, Brazil

*Corresponding author: Av Mandacaru, 1550 Maringá, Paraná 87010-060, Brazil; e-mail: bru.bertol@gmail.com

DOI: 10.2341/16-062-L

PO_4) and lower M:M ratio, respectively, characterizing a hypermineralized dentin, compared with APDs. FTIR-PAS demonstrated emergence of a peak (1179 cm^{-1}, P=O) in spectra after adhesive treatment, demonstrating a more intense chemical interaction in natural NCCLs. The results demonstrated that chemical bonding of 10-MDP adhesive to natural NCCLs is more intense, due to the hypermineralized surface, and suggest that it is unnecessary to remove the hypermineralized layer with burs, as this may decrease the chemical bonding potential of 10-MDP.

INTRODUCTION

Noncarious cervical lesions (NCCLs) are a challenge in dental practice, and multifactorial etiologies are involved in their development.[1,2] Noncarious cervical lesions usually form as a result of slow and progressive loss of mineralized dental structure caused by the association of different phenomena such as erosion, abrasion, and abfraction.[3]

Laboratory studies have demonstrated that adhesion to sclerotic dentin in NCCLs is compromised, resulting in reduced bond strength compared with artificial lesions created in sound cervical dentin.[4,5] This reduction in bond strength in NCCLs occurs due to molecular/chemical structural alterations that may result in dentin less favorable to bonding.[6] The presence of a sclerotic layer in NCCLs could make it difficult for the hybrid layer to form, because of the lower degree of primer diffusion and adhesive infiltration.[7]

Recent studies have, however, turned their attention to the additional chemical bonding potential between the functional monomers present in some adhesive systems and the components of dentin,[8-12] which seems to be particularly important for restorations placed in NCCLs.[10,13-15] The functional monomer 10-methacryloyloxydecyl dihydrogen phosphate (10-MDP) is present in some commercially available adhesive systems and has demonstrated good chemical bonding potential to hydroxyapatite through the formation of a "nanolayer" capable of enhancing the effectiveness and longevity of bonds.[11,16] Studies have shown this bond to be more stable to hydrolytic degradation than other functional monomers and to have a low solubility of calcium salts and long and hydrophobic spacer carbon chain, such as 4-methacryloyloxyethyl trimellitic acid (4-MET), and 2-methacryloxyethyl phenyl hydrogen phosphate (phenyl-P).[11,17] Based on the survival rates of restorations placed in NCCLs with a mild self-etch adhesive containing 10-MDP, a recent review of the literature has suggested that chemical bonding to NCCL not only occurs, but it would also be more intense due to its hypermineralized surface.[13] However, this improved chemical interaction between the hypermineralized dentin in the natural NCCLs and adhesive systems containing 10-MDP has yet to be demonstrated.

Some studies have suggested the need for roughening the surface of NCCLs to remove the hypermineralized layer to achieve dentin with characteristics closer to those of prepared cavities and better results in the clinical retention of composite restorations.[18,19] Thus, to assess the necessity of cavity preparation in NCCL surfaces before bonding procedures, it is appropriate to evaluate whether the chemical interaction between an adhesive system containing the 10-MDP and dentin in natural NCCLs is reduced compared with the dentin in prepared artificial defects of the same tooth.

Therefore, the objective of this study was to evaluate the chemical interactions that characterize the bond of a self-etch adhesive containing 10-MDP as the functional monomer to hypermineralized dentin in natural NCCLs and compare these chemical interactions with those in sclerotic dentin in artificially prepared defects (APDs).

METHODS AND MATERIALS

This *in vitro* study was conducted after obtaining approval from the local Institutional Review Board (CAAE:25006614.3.0000.0104). The four incisor teeth used in this study were extracted for periodontal or orthodontic reasons and were donated by patients through signature of a term of informed consent. After extraction, the teeth were cleaned and stored in physiologic solution at 4°C. All the teeth presented grade 4 dental sclerosis, according to the modified sclerosis scale defined by Ritter and others.[20] Grade 4 is attributed to NCCLs with the presence of significant sclerosis. The dentin is dark yellow or brownish with a petrified appearance and significant translucence or evident transparency.[20] Noncarious cervical lesions were located in the cervical region of the buccal surface.

Dental Fragment Preparation

Artificial defects (class V cavities) were prepared in the cervical region of the sound lingual surface of the same teeth, with the use of CVDentus cylindri-

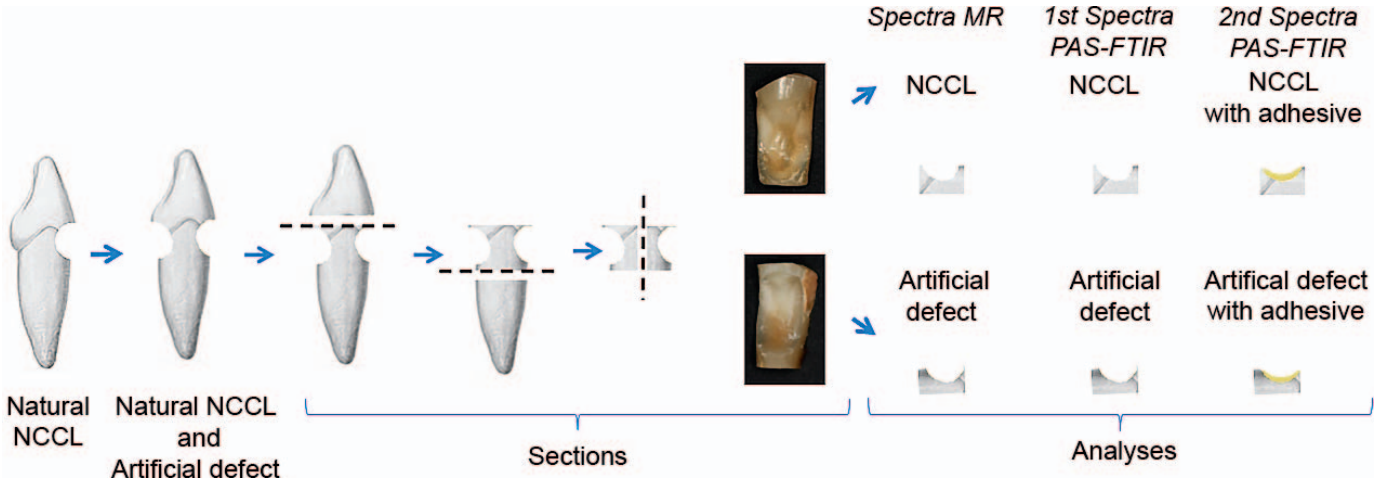

Figure 1. *Illustration showing the natural NCCL, artificial defect preparation, and tooth sectioning for MR and FTIR-PAS spectra acquisition.*

cal diamond burs (C1 1.0 × 4.0 mm) mounted in an ultrasound device (CVDent1000, CVDVale, São Carlos, Brazil), under constant water cooling. The APDs were created in dentin, with approximately the same size, shape, and location as those of their corresponding natural NCCL and served as controls.

After this, dental fragments were obtained from the buccal and palatal surfaces of each tooth, containing the natural NCCLs and the APDs, respectively. The teeth were sectioned with a low-speed diamond saw under water cooling. First, the occlusal crown and apical root were removed from the teeth, immediately above and below the lesions, respectively. Then, the teeth were sectioned in the occlusal-apical direction to separate the buccal and lingual surfaces of the specimens containing the natural NCCLs and the APDs (Figure 1).

Adhesive System Application

The composition of the self-etch adhesive containing the functional monomer 10-MDP used in this study is presented in Table 1. The adhesive was actively applied on the cavities for 20 seconds, by using a microbrush slightly impregnated with the product, without excesses, in accordance with the manufacturer's recommendations. A light stream of air was then applied over the liquid for approximately five seconds, until no movement was seen and the solvent had evaporated completely. Finally, the adhesive system was light polymerized (LED Radii, SDI, Bayswater, Australia; 1200 mW/cm^2) for 10 seconds. After polymerization, the specimens were immediately analyzed by Fourier transform infrared-photoacoustic spectroscopy (FTIR-PAS). No composite resin was applied on the surface.

Mineral Composition Analysis of Dentin

The sclerotic dentin mineral composition in the natural NCCLs and in the APDs was analyzed by means of micro-Raman (MR) spectroscopy. The experiments were carried out in a Raman Bruker spectrometer, equipped with a Senterra confocal microscope (Bruker Optik GmbH, Ettlingen, Germany).

The spectra of specimens containing the natural NCCLs and the APDs were collected in three different points along the surface. All the data were collected with a resolution of 4 cm^{-1} in the spectral range of 3500-450 cm^{-1}. To improve the signal-to-noise ratio, each spectrum was obtained from the

Table 1: *Composition and Lot Number of Self-Etching Adhesive Systems Used in This Study*

Product	Composition	Lot no.
Scotchbond Universal Adhesive (3M/ESPE Dental Products, St. Paul, MN, USA)	MDP ($C_{14}H_{27}O_6P$) TEDGMA ($C_{14}H_{22}O_6$) Bis-GMA ($C_{29}H_{36}O_8$) Polyalkenoic acid copolymer ($C_{21}H_{33}O_8$) HEMA ($C_6H_{10}O_3$) Modified methacrylate ($C_5H_8O_2$) Filler load (SiO_2) Water (H_2O) Silane (SiH_4) Alcohol (C_2H_6O) Primers	507329

Abbreviations: MDP, 10-methacryloxydecyl dihydrogen phosphate; TEDGMA, triethyleneglycol dimethacrylate; Bis-GMA, bisphenol-A glycidyl methacrylate; HEMA, 2-hydroxyethylmethacrylate.

average of 1000 scans at a laser wavelength of 1064 nm, power of 150 mW, and 40× magnification. Apart from the high number of scans, the detector temperature was also reduced to −84°C to improve the signal obtained. All readouts were standardized with the use of a support mirror, selection of the area to be measured, and manual and automatic focusing.

All the spectra collected were placed in the same baseline and normalized with the assistance of the OPUS spectroscopy software (Bruker Optics, Ettlingen, Germany). Origin software (OriginPro 8 Corporation, Northampton, MA, USA) was used to obtain the numerical quantifications of the MR spectra by integration of each curve of the absorption band at 961 cm^{-1} (phosphate) to calculate the respective area. Final area values were obtained from the mean result of the three different preset points (determined before measuring) used for MR spectra acquisition.

NCCL sample homogeneity after adhesive treatment was proved by the calculation of dentin surface matrix:mineral ratio (M:M = the ratio of the intensities of the photoacoustic absorption bands of the amide I [1650 cm^{-1}] divided by the intensities of the phosphate band at 1040 cm^{-1}). These ratios were submitted to a Shapiro-Wilk normality test (R statistic software, R Foundation for Statistical Computing, Vienna, Austria), and were represented by means and SD.

To assess the differences in the M:M ratio between the sclerotic dentin in the natural NCCLs and the control dentin in the APDs, the relative intensities of the absorption bands attributed to amide I and phosphate obtained with FTIR-PAS were compared. To calculate the M:M ratio of the samples, the intensities of the photoacoustic absorption bands of the amide I (1650 cm^{-1}) were divided by the intensities of the phosphate bands (560, 600, and 1040 cm^{-1}). Calculations were conducted using the spectrum obtained using the mean spectrum obtained from the dentin in the natural NCCLs and APDs after the application of the adhesive. These ratios were submitted to Shapiro-Wilk normality and Student *t*-tests at the 5% significance level (R statistic software).

Analysis of the Chemical Interaction Between the Adhesive and Dentin

The optical absorption bands obtained with FTIR-PAS work as fingerprints of specific molecules contained in the specimens, and as a result, provide information on the chemical interactions, expressed through alterations and/or appearance of new peaks.[21]

To determine the depth of the analysis, it is important to consider that the reading depth with FTIR-PAS technique is defined by the thermal diffusion length (cm) as $\mu = [D\lambda/(2\pi v)]^{1/2}$, in which D is the thermal diffusivity of the sample (cm^2/s), v is the speed of the mirror (cm/s), and λ is the wavelength of the incident radiation (cm). This parameter reflects the attenuation of the thermal wave amplitude and was used to analyze the approximate depth at which the photoacoustic signal is generated in the sample.

In this experimental condition, the sample treated with the adhesive was composed of two surfaces with a hybrid interface, both with effective values for thermal diffusivity. The value of μ depends on the value of these parameters, according to the wavelength of the incident radiation. Thermal diffusivity for dentin in the tubular direction has been defined as $D = 2.5 \times 10^{-3}$ cm^2/s.[22] For the adhesive, thermal diffusivity readouts were taken by using the thermal lens technique,[23,24] which provided $D = (1.58 \pm 0.07) \times 10^{-3}$ cm^2/s. As there was exciting radiation incident on the adhesive placed in the cavities, μ was estimated using the value of the thermal diffusivity obtained for the adhesive. Thus, using v = 0.63 cm/s, the measurement depth calculated for the energy of 1176 cm^{-1} ($\lambda = 8.5 \times 10^{-4}$ cm) was μ = 5.8 μm. In other words, the inspection depth of the technique for the readouts taken in this study was about 6 μm. Considering that the adhesive film varies between 2 and 3 μm,[24,25] it may be affirmed that technique was capable of taking the readouts on the dentin in the hybrid region beneath the adhesive system.

The FTIR-PAS spectra were recorded by a Nicolet spectrometer, equipped with a MTEC Photoacoustic Model 200 photoacoustic cell (MTEC Photoacoustics, Inc. Ames, IA). This equipment allows the absorption bands of the matter of interest to be monitored at a specific depth of the sample, providing the distribution profile of the matter throughout the sample. All spectra were collected at a resolution of 8 cm^{-1}, with a scan speed of 0.63 cm/s, in the spectral range of 4000-400 cm^{-1}.

After placing the specimen into the device, the photoacoustic cell was filled with helium gas to minimize interference in the optical absorption spectra caused by molecules of oxygen and water present in the air and on the specimen surface. The

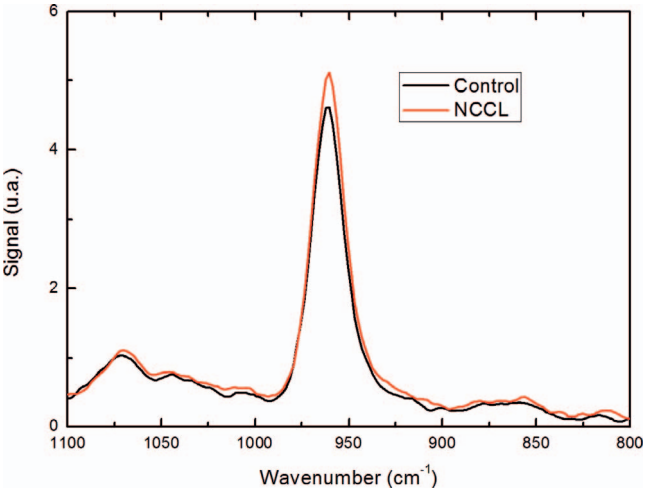

Figure 2. *Mean of the absorption spectra at 961 cm^{-1} (phosphate), demonstrating different intensities between the dentin in the natural NCCLs and the dentin the APDs (control).*

spectra of specimens were collected before and after they were submitted to treatment with the adhesive system. A disk of pure adhesive was prepared by placing 1 mL of the material on a glass slide that was light activated for 20 seconds (LED Radii, SDI; 1200 mW/cm^2). The slide was submitted to MR, and the spectrum of the pure adhesive was collected. This was an important methodologic step to differentiate the composition of the adhesive alone from that of the dental structure, so that the differences in the photoacoustic absorption peaks obtained from the adhesive and from the dentin could be verified.

The FTIR-PAS spectral data obtained were transferred to Origin software (OriginPro 8 Corporation). The spectral interval measured was divided into two spectral ranges (2180-400 and 1800-550 cm^{-1}). For each spectral range, a specific wavelength was established for the normalization of the data at 1460 cm^{-1} (CH stretch). This particular band was selected because it was present simultaneously with constant intensity in the spectra collected from the dentin in the natural NCCLs and in the APDs. Graphs were generated for each individual tooth, from which the average spectrum of the dentin in the natural NCCLs and in the APDs was calculated.

With the objective of observing the chemical interactions between the dental substrate and the adhesive system, the spectrum collected from the pure adhesive was subtracted from the spectrum acquired from the natural NCCL dentin with adhesive and the APD with adhesive. Possible overlaps of the bands associated with the adhesive with the spectral bands of the dental substrate could then be eliminated. As a result, small alterations or appearance of peaks in the spectra associated with the dentin due to the application of adhesive could be visualized. In addition, numerical quantifications of the spectra were obtained by integrating the curve of the band at 1179 cm^{-1} (v1 P=O) in the specimens with those of the natural NCCL and APD.

Table 2: *Means Values and SDs of the Organic M:M Ratio From the Dentin in the Natural NCCLs and in the Artificial Defects (Control) Before and After the Application of the Adhesive Containing 10-MDP*

Treatment with adhesive	Substrate	M:M	SD
Before	Control	1.11	0.06
	NCCL	1.09	0.11
After	Control	0.74	0.07
	NCCL	0.68	0.06

RESULTS

Dentin Mineral Composition Analysis

Spectra of the four NCCL dentin surfaces after adhesive treatment showed homogeneity in organic and inorganic composition (0.68 ± 0.06).

Mean values and SDs obtained from the integrated areas of the MR scans of the band at 961 cm^{-1} (phosphate) performed at three different points (total of 12 scans for each group) on the surface of the dentin in the natural NCCL and APD (control) were 140 ± 7 and 130 ± 10, respectively. Figure 2 illustrates the difference in the intensities of the phosphate absorption band at 961 cm^{-1} between the two studied groups.

The M:M ratios obtained with FTIR-PAS after the application of the adhesive are presented in Table 2. Dentin in natural NCCL cavities treated with adhesive presented a lower M:M ratio than dentin in APD ($p<0.05$).

Analysis of the Chemical Interaction Between the Adhesive and Dentin

The photoacoustic absorption spectra of the pure adhesive dentin in the natural NCCLs and dentin in the APDs were mapped, and they identified the functional groups in their composition (Figure 3A,B). The 1800-500 cm^{-1} spectral range represents the region of interest in this study. Figure 3B illustrates the spectra of the dentin in the natural NCCLs and in the APDs. The observed spectra revealed vibrations of both organic and inorganic components. The absorption bands indicated the major organic contributions at 1650 cm^{-1} (amide I, C=O), 1550 cm^{-1} (amide II, N-H and C-N), and 1240 cm^{-1} (amide III,

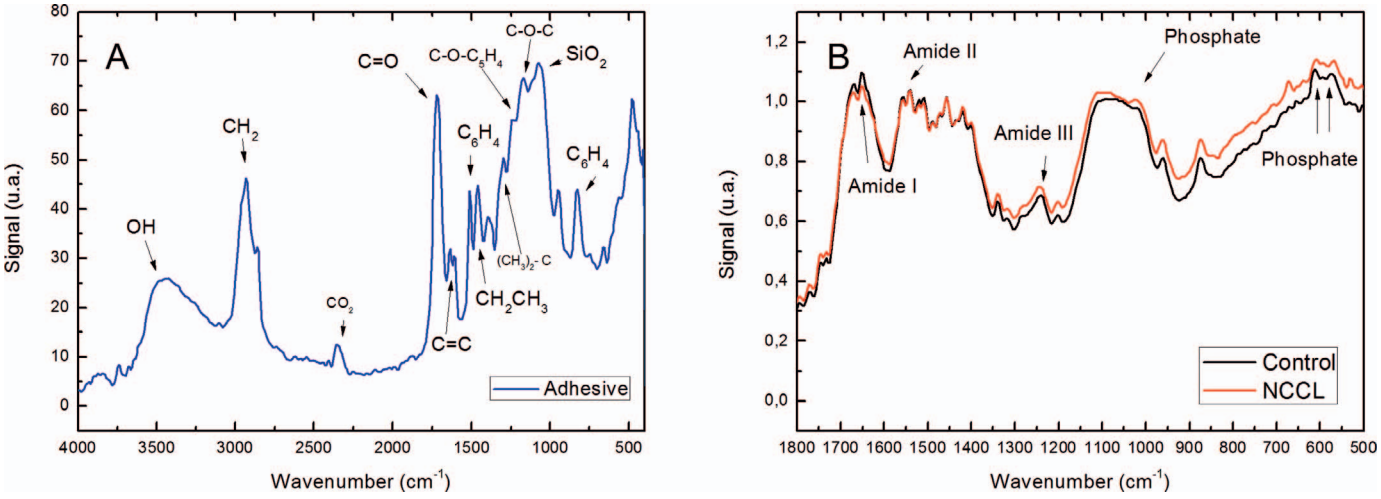

Figure 3. *(A) Photoacoustic absorption spectrum acquired from pure adhesive with the functional groups identified. (B) Photoacoustic absorption spectra acquired from the dentin in the natural NCCLs and in APDs (control).*

C-N and N-H). Contributions from the mineral phase were the orthophosphate bands (PO_4) at 600-560 and 1200-900 cm^{-1}.

After the adhesive was applied on the specimen surfaces (Figure 4), the main contributions from the functional groups with reference to the adhesive system were the methacrylate monomer bands at 1720 cm^{-1} (carbonyl, C=O) and 1457 cm^{-1} (CH_2CH_3); the bisphenol-A glycidyl methacrylate (Bis-GMA) bands at 1638 cm^{-1} (C=C), 1140 cm^{-1} (C-O-C), 1300 cm^{-1} [$(CH_3)_2$], 1260 cm^{-1} (C, C-O-C_5H_4), and 840 cm^{-1} (C_6H_4); and filler load band at 1105 cm^{-1} (SiO_2). The contributions from the

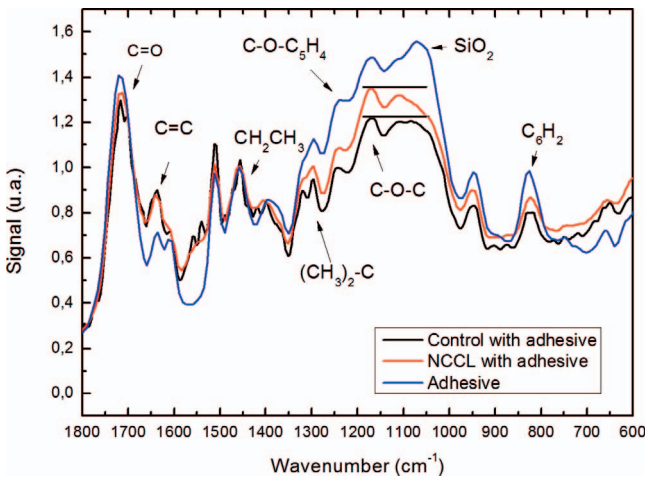

Figure 4. *Mean photoacoustic absorption spectra acquired from the adhesive, dentin in the natural NCCLs with adhesive, and in the APDs (control with adhesive) after treatment. The horizontal bars demonstrate higher relative intensity of the peak at 1179 cm^{-1}, in comparison with the band at 1100 cm^{-1}, for the dentin in natural NCCLs compared with dentin in APDs (control).*

mineral and organic composition in the spectra of dentin in the natural NCCLs and APDs were at 1179 cm^{-1} (P=O), 1650 cm^{-1} (amide I), 1550 cm^{-1} (amide II), and 1240 cm^{-1} (amide III). The horizontal bars in Figure 4 show the appearance of a new band at 1179 cm^{-1} that was more intense compared with the band at around 1100 cm^{-1}, indicating a (more intense) chemical interaction of the adhesive with the natural NCCLs in comparison with that of the APDs. This interaction was more intense for the dentin in the natural NCCLs.

Figure 5A displays the spectra of dentin in the natural NCCLs with adhesive and the control dentin in the APDs with adhesive after subtracting the spectrum acquired from the pure adhesive, to eliminate all the bands of the pure adhesive and show alterations on the spectra. This figure illustrates the new emerging behavior of the band at 1179 cm^{-1} (P=O). The peak in this band was more intense and narrow for the hypermineralized dentin in the natural NCCLs with the adhesive than in the APDs with adhesive. In Figure 5B, the dentin spectra were corrected, so that subtraction would coincide with line zero and allow us to calculate the areas of the band at 1179 cm^{-1}. Mean values and SDs for the integrated areas of the band at 1179 cm^{-1} (v_1 P=O) were 18 ± 4 in the dentin in the NCCLs with adhesive and 12 ± 5 in the APDs with the adhesive, numerically confirming the relatively higher intensity of this band in the natural NCCLs.

DISCUSSION

This study demonstrated differences in the intensity of chemical interactions of a self-etch adhesive

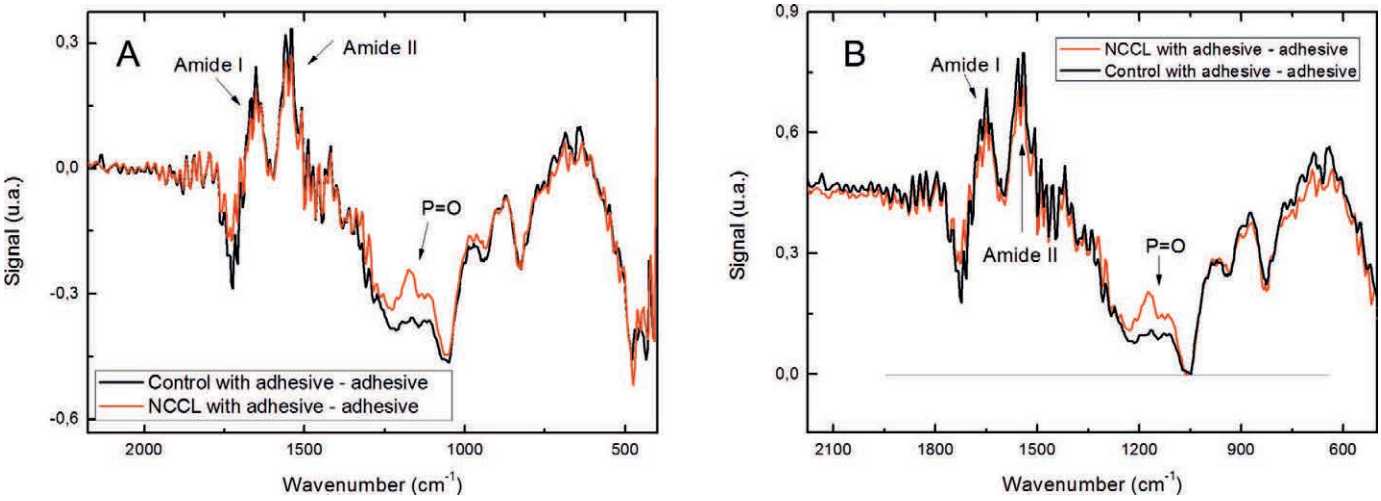

Figure 5. *Photoacoustic absorption spectra obtained after subtracting the adhesive system spectrum from the spectra acquired from the dentin in the natural NCCLs with adhesive and from the dentin in APDs (control) with adhesive. (A) Spectra after subtraction normalized at 1460 cm^{-1}. (B) Spectra after subtraction corrected to coincide with line zero.*

system containing the functional monomer 10-MDP between the sclerotic dentin in natural NCCLs and the control dentin in APDs.

When spectroscopy is used to assess whether there is a chemical bond between an adhesive system and the organic or inorganic portions of the dentin, changes in the absorption bands attributed to the dental substrate must be disclosed.[26] After treatment with the adhesive system (Figure 4), it may be observed that the silica band (SiO_2) at 1179 cm^{-1} in the mean spectra of the hypermineralized dentin in the natural NCCLs presented higher intensity compared with the normal dentin in the APDs, as illustrated by the parallel bars.

However, an overlap of the bands of the adhesive system over the dental substrate could also be observed. Wang and others,[27] using the FTIR-PAS technique, also observed that the bands attributed to the phosphate in the dentin (1200-900 cm^{-1}) overlapped with the band attributed to the SiO_2 in the adhesive, whereas the region of the amide I (1650 cm^{-1}) overlapped with the band at 1680-1620 cm^{-1} in the adhesive. As a result, in the univariate analyses, the limitation caused by the overlapping hindered the disclosure of minimal changes in the spectra.[27] Taking the overlapping issue into consideration, the analysis in the present study was enhanced by subtracting the spectrum of the pure adhesive from the spectra collected from the dentin after applying the adhesive system (Figure 5), thereby allowing the alterations/ appearance of peaks to become more evident. This procedure allowed us to improve visualization of what happened to the band at 1179 cm^{-1}, characteristic of optical absorption of the phosphoric group that was more intense and narrower in the dentin (v1 P=O) of the natural NCCL samples than in that of the APDs samples.

The increase in intensity of the band at 1179 cm^{-1} was related to the chemical interaction of the adhesive with the inorganic matrix of the dentin, more specifically between the ester group in the adhesive and the molecules of calcium and phosphate in the dentin, leading to the formation of a calcium/phosphate ester complex.[11,24] Thus, with the objective of quantitatively assessing possible differences between the sclerotic dentin in natural NCCLs and in the control dentin of APDs impregnated with the adhesive, in the present study, the integrated areas of the band at 1179 cm^{-1} were calculated in the 1218-1052 cm^{-1} band interval. The higher mean value found for the sclerotic dentin in the natural NCCLs (18±4) in comparison with the control dentin in the APDs (12±5) demonstrated that the chemical interaction with the hypermineralized dentin was more intense.

The literature has suggested that the functional monomer 10-MDP that is present in the self-etch adhesive system used in this study is capable of forming chemical bonds with hydroxyapatite (calcium-MDP salts) and therefore improves the performance and longevity of the bond in adhesive restorations.[8,11,16] Studies have justified this process by the formation of a "nanolayer," composed of two molecules of 10-MDP with their methacrylate groups directed toward each other and their functional hydrogen phosphate groups directed away from each

other, in which the methacrylate binds to the calcium ions, and the hydrogen phosphate group binds to the dentin.[17] The chemical bonds between the ester group in the adhesive (methacrylate) and the molecules of calcium and phosphate in the dentin shown in this study (Figure 5) may be attributed to the formation of calcium-MDP salts in the nanolayer as a response to the chemical interaction between the adhesive system and the dental structures.

To promote an effective chemical bond with the dentin, the functional monomer 10-MDP needs to be present in high concentrations. Studies have speculated that the addition of other compounds to the formulation of adhesive systems may decrease the formation of a nanolayer, and as a result, affect the potential chemical interaction of self-etch adhesive systems with the dentin.[28] The presence of 10-MDP in the adhesive and chemical bonding to dentin is modulated by 2-hydroxyethylmethacrylate (HEMA) that is part of the adhesive composition. Yoshida and others[29] demonstrated that HEMA significantly reduced nanolayering, because it reduced the hydroxyapatite (HAp) demineralization rate, a prerequisite to the formation of MDP-Ca salts. HEMA does interfere with, but does not completely inhibit, MDP from interacting chemically with HAp. When Yoshida and others[16] investigated the effect of commercially available adhesive systems containing 10-MDP on the formation of a nanolayer by means of X-ray diffraction, X-ray energy dispersive spectroscopy, and transmission electron microscopy, they observed that the same adhesive system used in the present study presented a less prominent nanolayer in normal human dentin compared with Clearfil SE Bond (Kuraray, Tokyo, Japan). This was attributed to the lower concentration of 10-MDP and the presence of polyalkenoic acid (copolymer) in the Scotchbond Universal Adhesive (3M/ESPE Dental Products, St. Paul, MN, USA), which may have competed with the 10-MDP for the same Ca-bond site in hydroxyapatite. In the present study, however, the relatively low concentration of 10-MDP of the Scotchbond Universal Adhesive (3M/ESPE) was sufficient to produce more intense changes in the spectra of the hypermineralized sclerotic dentin in the natural NCCLs compared with control dentin. Furthermore, when the adhesive system is applied actively (as recommended by the manufacturer), contact of the 10-MDP molecules with dentin is improved, increasing the concentration of 10-MDP in contact with the hydroxyapatite.[28] Considering these factors, when using adhesive systems with higher concentrations of 10-MDP, it would be expected that an enhanced chemical interaction would occur in the hypermineralized dentin in natural NCCLs.

Analysis of the mineral content on the surface of the dentin tested indicated that the sclerotic dentin in natural NCCLs is hypermineralized in comparison with the APDs. The MR analysis demonstrated the areas corresponding to the band at 961 cm^{-1} (v1 phosphate) were more intense in the dentin in the natural NCCLs than in the APDs, characterizing a zone of hypermineralized dentin (Figure 2). This was confirmed by calculating the integrated areas of the bands, which demonstrated that the numerical value of the mineral content found in the dentin in natural NCCLS (140 ± 7) was higher than that found in the control dentin of APDs (130 ± 10). Furthermore, FTIR-PAS analysis also demonstrated that the dentin in natural NCCLs presented a lower M:M ratio than the APDs after adhesive treatment ($p=0.04$). It is very difficult to obtain extracted anterior teeth with NCCL to analysis. Although a sample size of four incisors were used for chemical interaction analysis, the results showed homogeneity among specimens and also were able to demonstrate statistically significant differences. This analysis was carried out in this study to confirm the presence of sclerotic dentin and ensure that the specimens of the group of natural NCCLs were in similar condition. These findings corroborate previous studies on the molecular/structural differences between the organic and inorganic phases of the dentin in the natural NCCLs and APDs by means of Raman spectroscopy[6] and FTIR-PAS.[30]

Due to the fact that the sclerotic dentin is hypermineralized, resulting in a substrate that is less favorable to bonding,[6] studies have recommended roughening of natural NCCLs surfaces.[18,19,31] Some studies have advocated removal of the superficial sclerotic layer to increase intratubular retention to the adhesive system.[5,18] However, according to Tay and Pashley,[7] removing the hypermineralized layer in the natural NCCLs before the adhesive procedure may not result in increased bond strength, as the sclerotic dentin may still contain crystallites capable of preventing the adhesive from infiltrating into the dentinal tubules. Moreover, in a recent systematic review of the literature, it was not possible to test the null hypothesis that there would be no difference in the survival rate of restorations placed in natural NCCLs submitted to different surface treatments, due to the reduced number of studies that compared the influence of dentin roughing on the level of retention of restorations in natural NCCLs.[32] On the other hand, a recent study demonstrated that the

adhesive performance of a self-etch adhesive system containing 10-MDP in the sclerotic dentin of bovine teeth (control group) was superior compared with the same surface prepared with diamond burs.[33]

In the present study, APDs were prepared in the control dentin with ultrasound diamond burs to obtain a smear layer-free surface. A recent study demonstrated that complete absence of the smear layer improved the effectiveness of the bond to dentin of moderate and ultra-moderate self-etch adhesive systems.[34] Despite this, in the present study, chemical bonding occurred with greater intensity in the sclerotic dentin in natural NCCLs than in that of the APDs. Taking into consideration that the adhesive system containing the functional monomer 10-MDP used in this study demonstrated chemical affinity for hydroxyapatite, removing the hypermineralized layer with burs or previous acid conditioning seems to be unnecessary, as this may decrease its chemical bonding potential.

In vitro studies have some limitations regarding the simulation of the real clinical condition. Moreover, there are differences in the composition and degree of mineralization among teeth. To minimize this condition and allow a more direct comparison of the tested groups, cavities were tested pairwise, ie, the APDs were prepared in the same teeth on the surface opposite to the natural NCCL.

CONCLUSION

The results demonstrated that chemical bonding of 10-MDP adhesive to natural NCCLs is more intense than to APDs, due to the hypermineralized surface, and suggests that it is unnecessary to remove the hypermineralized layer with burs, as this may decrease the chemical bonding potential of 10-MDP. Further studies are necessary to test other adhesive systems, with different 10-MDP concentrations (not only in natural NCCLs, but also in other types of substrates with inactive cavitated carious lesions).

Acknowledgements

The authors thank the Brazilian Funding Agencies Financiadora de Estudos e Projetos (FINEP), Coordenação de Aperfeiçoamento de Pessoal de Nível Superior (CAPES), Conselho Nacional de Desenvolvimento Científico e Tecnológico (CNPq), and Fundação Araucária for financial support.

Regulatory Statement

This study was conducted in accordance with all the provisions of the local human subjects oversight committee guidelines and policies of the Institutional Review Board of State University of Maringa. The approval code for this study is 25006614.3.0000.0104.

Conflict of Interest

The authors of this manuscript certify that they have no proprietary, financial, or other personal interest of any nature or kind in any product, service, and/or company that is presented in this article.

(Accepted 28 July 2016)

REFERENCES

1. Levitch LC, Bader JD, Shugars DA, & Heymann HO (1994) Non-carious cervical lesions *Journal of Dentistry* **22(4)** 195-207.
2. Perez CR, Gonzalez MR, Prado NA, de Miranda MS, Macêdo MA, & Fernandes BM (2012) Restoration of noncarious cervical lesions: When, why, and how *International Journal of Dentistry* 687058.
3. Grippo JO, Simring M, & Schreiner S (2004) Attrition, abrasion, corrosion and abfraction revisited: A new perspective on tooth surface lesions *Journal of the American Dental Association* **135(8)** 1109-1118.
4. Tay FR, Kwong SM, Itthagarun A, King NM, Yip HK, Moulding KM, & Pashley DH (2000) Bonding of a self-etching primer to non-carious cervical sclerotic dentin: Interfacial ultrastructure and microtensile bond strength evaluation *Journal of Adhesive Dentistry* **2(1)** 9-28.
5. Kwong SM, Cheung GS, Kei LH, Itthagarun A, Smales R, Tay FR, & Pashley DH (2002) Micro-tensile bond strengths to sclerotic dentin using a self-etching and a total-etching technique *Dental Materials* **18(5)** 359-369.
6. Xu C, Karan K, Yao X, & Wang Y (2009) Molecular structural analysis of noncarious cervical sclerotic dentin using Raman spectroscopy *Journal of Raman Spectroscopy* **40(12)** 1780-1785.
7. Tay FR, & Pashley DH (2004) Resin bonding to cervical sclerotic dentin: A review *Journal of Dentistry* **32(3)** 173-196.
8. Peumans M, De Munck J, Van Landuyt KL, Poitevin A, Lambrechts P, & Van Meerbeek B (2010) Eight-year clinical evaluation of a 2-step self-etch adhesive with and without selective enamel etching *Dental Materials* **26(12)** 1176-1184.
9. Van Meerbeek B, De Munck J, Yoshida Y, Inoue S, Vargas M, Vijay P, Van Landuyt K, Lambrechts P, & Vanherle G (2003) Buonocore memorial lecture. Adhesion to enamel and dentin: current status and future challenges *Operative Dentistry* **28(3)** 215-235.
10. Van Meerbeek B, Yoshihara K, Yoshida Y, Mine A, De Munck J, & Van Landuyt KL (2011) State of the art of self-etch adhesives *Dental Materials* **27(1)** 17-28.
11. Yoshida Y, Nagakane K, Fukuda R, Nakayama Y, Okazaki M, Shintani H, Inoue S, Tagawa Y, Suzuki K, De Munck J, & Van Meerbeek B (2004) Comparative study on adhesive performance of functional monomers *Journal of Dental Research* **83(6)** 454-458.
12. Yoshida Y, Van Meerbeek B, Nakayama Y, Snauwaert J, Hellemans L, Lambrechts P, Vanherle G, & Wakasa K

(2000) Evidence of chemical bonding at biomaterial-hard tissue interfaces *Journal of Dental Research* **79(2)** 709-714.

13. Carvalho RM, Manso AP, Geraldeli S, Tay FR, & Pashley DH (2012) Durability of bonds and clinical success of adhesive restorations *Dental Materials* **28(1)** 72-86.
14. Perdigão J (2010) Dentin bonding-variables related to the clinical situation and the substrate treatment *Dental Materials* **26(2)** e24-e37.
15. Yoshida Y, & Inoue S (2012) Chemical analyses in dental adhesive technology *Japanese Dental Science Review* **48(2)** 141-152.
16. Yoshida Y, Yoshihara K, Nagaoka N, Hayakawa S, Torii Y, & Ogawa T (2012) Self-assembled nano-layering at the adhesive interface *Journal of Dental Research* **91(4)** 376-381.
17. Yoshihara K, Yoshida Y, Nagaoka N, Fukegawa D, Hayakawa S, Mine A, Nakamura M, Minagi S, Osaka A, Suzuki K, & Van Meerbeek B (2010) Nano-controlled molecular interaction at adhesive interfaces for hard tissue reconstruction *Acta Biomateriallia* **6(9)** 3573-3582.
18. van Dijken JW (2010) A prospective 8-year evaluation of a mild two-step self-etching adhesive and a heavily filled two-step etch-and-rinse system in non-carious cervical lesions *Dental Materials* **26(9)** 940-946.
19. van Dijken JW (2013) A randomized controlled 5-year prospective study of two HEMA-free adhesives, a 1-step self etching and a 3-step etch-and-rinse, in non-carious cervical lesions *Dental Materials* **29(11)** e271-280.
20. Ritter AV, Heymann HO, Swift EJ, Sturdevant JR, & Wilder AD (2008) Clinical evaluation of an all-in-one adhesive in non-carious cervical lesions with different degrees of dentin sclerosis *Operative Dentistry* **33(4)** 370-278.
21. Peter, J (2011). *Infrared and Raman Spectroscopy: Principles and Spectral Interpretation* Elsevier, San Diego.
22. Magalhães MF, Neto Ferreira RA, Grossi PA, & de Andrade RM (2008) Measurement of thermophysical properties of human dentin: Effect of open porosity *Journal of Dentistry* **36(8)** 588-594.
23. Snook RD, Lowe RD, & Baesso ML (1998) Photothermal spectrometry for membrane and interfacial region studies *Analyst* **123(4)** 587-593.
24. Ubaldini AL, Baesso ML, Sehn E, Sato F, Benetti AR, & Pascotto RC (2012) Fourier transform infrared photoacoustic spectroscopy study of physicochemical interaction between human dentin and etch-&-rinse adhesives in a simulated moist bond technique *Journal of Biomedical Optics* **17(6)** 065002.
25. Yoshihara K, Yoshida Y, Nagaoka N, Hayakawa S, Okihara T, De Munck J, Maruo Y, Nishigawa G, Minagi S, Osaka A, & Van Meerbeek B (2013) Adhesive interfacial interaction affected by different carbon-chain monomers *Dental Materials* **29(8)** 888-897.
26. Spencer P, Byerley TJ, Eick JD, &Witt JD (1992) Chemical characterization of the dentin/adhesive interface by Fourier transform infrared photoacoustic spectroscopy *Dental Materials* **8(1)** 10-15.
27. Wang Y, Yao X, & Parthasarathy R (2009) Characterization of interfacial chemistry of adhesive/dentin bond using FTIR chemical imaging with univariate and multivariate data processing *Journal Biomedical Materials Research Part A* **91(1)** 251-262.
28. Yoshihara K, Yoshida Y, Hayakawa S, Nagaoka N, Irie M, Ogawa T, Van Landuyt K, Osaka A, Suzuki K, Miagi S, & Van Meerbeek B (2011) Nanolayering of phosphoric acid ester monomer on enamel and dentin *Acta Biomateriallia* **7(8)** 3187-3195.
29. Yoshida Y, Yoshihara K, Hayakawa S, Nagaoka N, Okihara T, Matsumoto T, Minagi S, Osaka A, Van Landuyt K, & Van Meerbeek B (2012) HEMA inhibits interfacial nano-layering of the functional monomer MDP *Journal of Dental Research* **91(11)** 1060-1065
30. Mixson JM, Spencer P, Moore DL, Chappell RP, & Adams S (1995) Surface morphology and chemical characterization of abrasion/erosion lesions *American Journal of Dentistry* **8(1)** 5-9.
31. Van Landuyt KL, Peumans M, De Munck J, Cardoso MV, Ermis B, & Van Meerbeek B (2011) Three-year clinical performance of a HEMA-free one-step self-etch adhesive in non-carious cervical lesions *European Journal Oral Science* **119(6)** 511-516.
32. Santos MJ, Ari N, Steele S, Costella J, & Banting D (2014) Retention of tooth-colored restorations in non-carious cervical lesions—A systematic review *Clinical Oral Investigations* **18(5)** 1369-1381.
33. Luque-Martinez IV, Mena-Serrano A, Muñoz MA, Hass V, Reis A, & Loguercio AD (2013) Effect of bur roughness on bond to sclerotic dentin with self-etch adhesive systems *Operative Dentistry* **38(1)** 39-47.
34. Suyama Y, Lührs AK, De Munck J, Mine A, Poitevin A, Yamada T, Van Meerbeek B, & Cardoso MV (2013) Potential smear layer interference with bonding of self-etching adhesives to dentin *Journal of Adhesive Dentistry* **15(4)** 317-324.

©Operative Dentistry, 2017, **42-4,** 367-374

Effect of Surface Treatment, Silane, and Universal Adhesive on Microshear Bond Strength of Nanofilled Composite Repairs

IA Fornazari • I Wille • EM Meda • RT Brum • EM Souza

Clinical Relevance

The use of a silane-containing universal adhesive eliminates the need to apply silane as a separate step in the clinical protocol for composite repair.

SUMMARY

Purpose: The aim of this study was to evaluate the effect of surface treatment and universal adhesive on the microshear bond strength of nanoparticle composite repairs.

Methods: One hundred and forty-four specimens were built with a nanofilled composite (Filtek Supreme Ultra, 3M ESPE). The surfaces of all the specimens were polished with SiC paper and stored in distilled water at 37°C for 14 days. Half of the specimens were then air abraded with Al_2O_3 particles and cleaned with phosphoric acid. Polished specimens (P) and polished and air-abraded specimens (A), respectively, were randomly divided into two sets of six groups (n=12) according to the following treatments: hydrophobic adhesive only (PH and AH, respectively), silane and hydrophobic adhesive (PCH, ACH), methacryloyloxydecyl dihydrogen phosphate (MDP)–containing silane and hydrophobic adhesive (PMH, AMH), universal adhesive only (PU, AU), silane and universal adhesive (PCU, ACU), and MDP-containing silane and universal adhesive (PMU, AMU). A cylinder with the same composite resin (1.1-mm diameter) was bonded to the treated surfaces to simulate the repair. After 48 hours, the specimens were subjected to microshear testing in a universal testing machine. The failure area was analyzed under an optical microscope at 50× magnification to identify the failure type, and the data were analyzed by three-way analysis of variance and the Games-Howell test (α=0.05).

Isabelle A Fornazari, DDS, MDS candidate, Graduate Program in Dentistry, Pontifícia Universidade Católica do Paraná, Curitiba, Brazil

Isadora Wille, DDS, School of Dentistry, Pontifícia Universidade Católica do Paraná, Curitiba, Brazil

Eduardo M Meda, DDS, MDS, PhD candidate, Graduate Program in Dentistry, Pontifícia Universidade Católica do Paraná, Curitiba, Brazil

Rafael T Brum, PhD, School of Dentistry, Pontifícia Universidade Católica do Paraná, Curitiba, Brazil

*Evelise M Souza, DDS, MSD, PhD, Graduate Program in Dentistry, Pontifícia Universidade Católica do Paraná, Curitiba, Brazil

*Corresponding author: Imaculada Conceição, 1155, Prado Velho, Curitiba, PR 80215-901, Brazil; e-mail: evesouza@yahoo.com

DOI: 10.2341/16-259-L

Results: The variables "surface treatment" and "adhesive" showed statistically significant differences for $p<0.05$. The highest mean shear bond strength was found in the ACU group but was not statistically different from the means for the other air-abraded groups except AH. All the polished groups except PU showed statistically significant differences compared with the air-abraded groups. The PU group had the highest mean among the polished groups. Cohesive failure was the most frequent failure mode in the air-abraded specimens, while mixed failure was the most common mode in the polished specimens.

Conclusions: While air abrasion with Al_2O_3 particles increased the repair bond strength of the nanoparticle composite, the use of MDP-containing silane did not lead to a statistically significant increase in bond strength. Silane-containing universal adhesive on its own was as effective as any combination of silane and adhesive, particularly when applied on air-abraded surfaces.

INTRODUCTION

Composite resins are now routinely used in dentistry because of their aesthetic and adhesive characteristics and their superior ability to preserve sound tooth structure.[1-3] However, conditions in the oral environment, such as temperature and pH changes, diet, and other factors, may cause resin composites to degrade.[4,5] *In vivo* degradation can lead to discoloration, microleakage, wear, chipping, and even fracture of the restoration.[6] Nevertheless, if the defects are minor, such as loss of anatomical shape and extrinsic discoloration, the restoration may not require total replacement.[7] In such situations, repair of the restoration is more appropriate, as it is minimally invasive and a fast, simple procedure.[8] Furthermore, composite repair has been reported to be as effective as total replacement and to cause less tooth structure removal, increasing restoration longevity and reducing the cost of treatment.[7-11]

The success of the repair procedure in composites depends on several factors, such as the characteristics of the surface, the wettability of the chemical bonding agents, and the chemical composition of the composite.[10,12,13] A rough surface is crucial in composite repair and can be achieved mechanically by the use of highly abrasive diamond burs, air abrasion with aluminum oxide particles, or chemically by hydrofluoric acid etching.[14] In addition to micromechanical retention, a chemical bond is desirable to enhance the bond strength of composite repairs. Dental composites usually consist of filler particles, such as silica, lithium aluminum silicates, hydroxyapatite, and boron silicates. The application of a silane agent can increase the bonding between the fillers and the organic resin matrix.[15-19] However, as some commercially available composites contain zirconia particles in addition to the traditional glass and ceramic fillers, further studies are required into the role of silane in the repair of these materials.

Adhesives also seem to exert an influence on composite repair bond strength. Their role is to increase the wettability of the mechanically treated, silanized surface.[20] Recently, a new category of adhesives called multimode or universal adhesives was launched. These contain a phosphate monomer (methacryloyloxydecyl dihydrogen phosphate [MDP]) and silane in addition to conventional functional monomers.[21] However, there is a dearth of studies in the literature on the impact of such adhesives on composite repair bond strength.[22,23]

This study therefore sought to analyze the effect of a universal adhesive used with and without a conventional and an MDP-containing silane agent on the repair bond strength of a silica/zirconia nanofilled composite. The null hypothesis was that there would not be any differences between the treatments when they were used to repair a nanofilled composite.

METHODS AND MATERIALS

A total of 144 truncated cone-shaped specimens (7.5-mm top diameter; 4.5-mm bottom diameter; 3-mm thickness) were built with an A2 enamel shade nanofilled resin composite (Filtek Supreme Ultra, 3M ESPE, St Paul, MN, USA). The specimens were built using a split metal mold placed between Mylar strips and two glass plates. The composites were packed into the mold in two increments and light cured for 20 seconds each with an LED light-curing unit (Bluephase, Ivoclar Vivadent, Schaan, Liechtenstein) at a light intensity of 800 to 1000 mW/cm^2. The intensity was measured with a radiometer after every five specimens cured.

The specimens were then embedded in self-cured acrylic resin in a plastic ring with at least 1 mm of their surface exposed. All the specimens were ground sequentially with 400- and 600-grit SiC paper under water cooling and then kept in distilled water at 37°C for 14 days.

Table 1: *Materials Used in the Study*

Materials	Manufacturer	Composition
Heliobond	Ivoclar Vivadent (Schaan, Liechtenstein)	Bis-GMA; TEGDMA; catalysts and stabilizers
Scotchbond Universal Adhesive	3M ESPE (St Paul, MN, USA)	Bis-GMA; HEMA; decamethylene dimethacrylate; ethanol; water; silane treated silica; 1,10-decanediol and phosphorous oxide; copolymer of acrylic and itaconic acid; dimethylaminobenzoate; camphorquinone; (dimethylamino) ethyl methacrylate; methyl ethyl ketone
Ceramic Primer	3M ESPE	Methacryloxypropyl trimethoxysilane; water; ethyl alcohol 3-(trimetoxysilyl methacrylate)
Monobond Plus	Ivoclar Vivadent	3-(trimethoxysilyl) propyl methacrylate; methacrylated phosphoric acid ester
Filtek Supreme Ultra Restorative Composite (A2 enamel shade)	3M ESPE	Silane-treated ceramic; silane-treated silica; UDMA; bisphenol A polyethylene glycol diether dimethacrylate; Bis-GMA; silane-treated zirconia; polyethylene glycol dimethacrylate; TEGDMA; 2,6-di-tert-butyl-p-cresol

Abbreviations: Bis-GMA, bisphenol A diglycidyl ether dimethacrylate; HEMA, 2-hydroxyethyl methacrylate; TEGDMA, triethylene glycol dimethacrylate; UDMA, urethane dimethacrylate.

Half of the specimens were air abraded for 10 seconds with 50-μm Al_2O_3 particles 10 mm from the surface under a pressure of 4 bar. The surfaces of all the specimens were then etched with 37% phosphoric acid for 30 seconds, washed with air/water spray for 60 seconds, and dried with a blast of air for 60 seconds.

Double-sided adhesive tape with a central orifice 1.2 mm in diameter was used to limit the bonding area on the composite surfaces that were to be repaired in all the specimens. Polished specimens (P) and polished and air-abraded specimens (A), respectively, were randomly divided into two sets of six groups (n=12) according to the bonding procedure. The materials used in the study and their respective compositions are shown in Table 1.

The specimens in groups AH and PH were treated only with a layer of hydrophobic adhesive (Heliobond, Ivoclar Vivadent) applied on the air-abraded or polished surface, respectively, and light cured for 20 seconds. Groups ACH and PCH were treated with a conventional silane (Ceramic Primer, 3M ESPE) for 60 seconds, and groups AMH and PMH were treated with MDP-containing silane (Monobond Plus, Ivoclar Vivadent) for the same amount of time. After application of the silane, an air jet was used to evaporate the solvent, and the same hydrophobic adhesive was applied as described above.

The specimens in groups AU and PU were treated with a layer of universal adhesive (Scotchbond Universal Adhesive, 3M ESPE) applied on the air-abraded or polished surface, respectively; air-dried for 20 seconds for the solvent to evaporate; and light cured for the same time. Groups ACU and PCU were treated with a conventional silane (Ceramic Primer, 3M ESPE), and groups AMU and PMU were treated with MDP-containing silane (Monobond Plus, Ivoclar Vivadent) for 60 seconds. After the silane had been applied, the solvent was evaporated with an air jet, and the same universal adhesive was applied as described above.

The composite repair was carried out by inserting the same composite into transparent tubes (1.1-mm diameter and 1 mm high) placed on the treated surfaces. The repair composite was light cured with the same LED-curing unit for 40 seconds, and the specimens were stored in distilled water at 37°C for 48 hours, after which the plastic tubes and tapes were removed carefully using a scalpel blade to expose the cylindrical composite repairs. These were then analyzed under an optical microscope (Olympus BX60, Olympus Corp, Tokyo, Japan) at 50× magnification to identify any interfacial flaws, gaps, bubbles, or other defects. Specimens with defects were excluded from the study. Microshear bond strength testing was performed in a universal testing machine (EMIC 2000, Instron, Illinois Tool Works Inc, Norwood, MA, USA) using a metal blade positioned at the repair interface at a crosshead speed of 0.5 mm/min until failure occurred.

The failure area was examined under an optical microscope (Olympus BX60, Olympus Corp) at 50× magnification to identify the failure type, which was classified as adhesive (adhesive interface), cohesive in the original composite resin, cohesive in the repair composite resin, or mixed (more than one type).

The data were analyzed descriptively to obtain the mean and standard deviation for each group. Three-way analysis of variance, Tukey Honestly Significant Difference and Games-Howell tests were performed to detect statistical differences between the variables and to compare the groups. All tests were performed

Table 2: *Mean ± Standard Deviation of Microshear Bond Strength (MPa) of the Study Groups*[a]

Group	Surface Treatment	Silane	Adhesive	Bond Strength	Significant Differences
AH	Al_2O_3 air abrasion	—	Heliobond	16.45 ± 4.04	BCD
ACH		Ceramic Primer	Heliobond	20.82 ± 4.89	AB
AMH		Monobond Plus	Heliobond	18.63 ± 3.66	AB
AU	Al_2O_3 air abrasion	—	SB Universal	19.58 ± 4.32	AB
ACU		Ceramic Primer	SB Universal	20.91 ± 4.23	A
AMU		Monobond Plus	SB Universal	17.46 ± 2.95	ABC
PH	Polishing	—	Heliobond	8.44 ± 2.14	F
PCH		Ceramic Primer	Heliobond	13.29 ± 2.87	DE
PMH		Monobond Plus	Heliobond	12.43 ± 2.54	DE
PU	Polishing	—	SB Universal	15.05 ± 3.75	BCD
PCU		Ceramic Primer	SB Universal	13.31 ± 3.88	CDE
PMU		Monobond Plus	SB Universal	10.79 ± 2.43	EF

[a] *Groups connected by the same letter in the same column are not significantly different ($p<0.05$).*

at a 5% significance level using the SPSS 20.0 statistical package (IBM Inc, Chicago, IL, USA).

RESULTS

The results for microshear bond strength are shown in Table 2 and Figure 1. The differences between the variables "adhesive" and "surface treatment" were statistically significant, as was the interaction between "adhesive" and "silane."

Air-abraded specimens treated with a conventional silane and universal adhesive (ACH) had the highest repair bond strength in the study. However, among the air-abraded specimens, this result was statistically different from the result only for specimens treated with hydrophobic adhesive alone (group AH).

In contrast, the polished specimens treated with hydrophobic adhesive (group PH) had the lowest

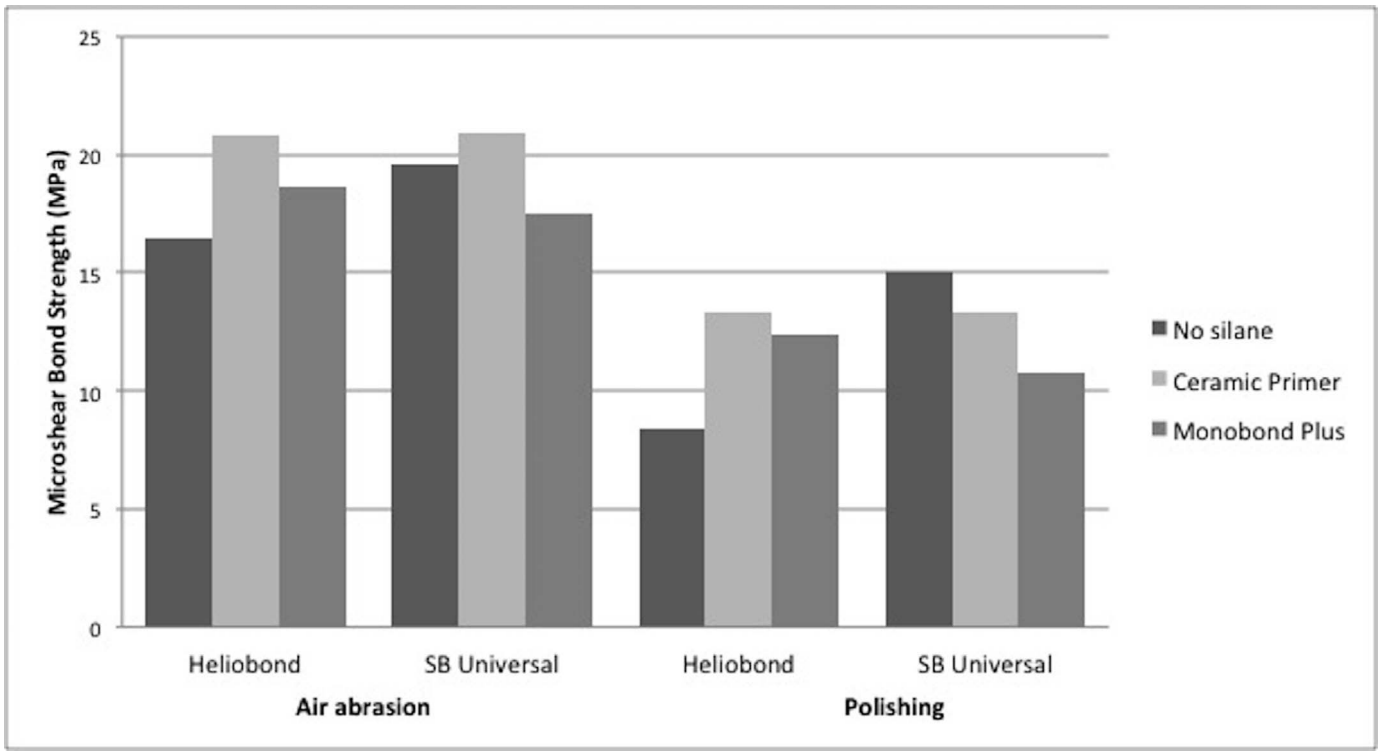

Figure 1. *Microshear bond strength (MPa) of the repaired groups according to surface treatment and type of silane.*

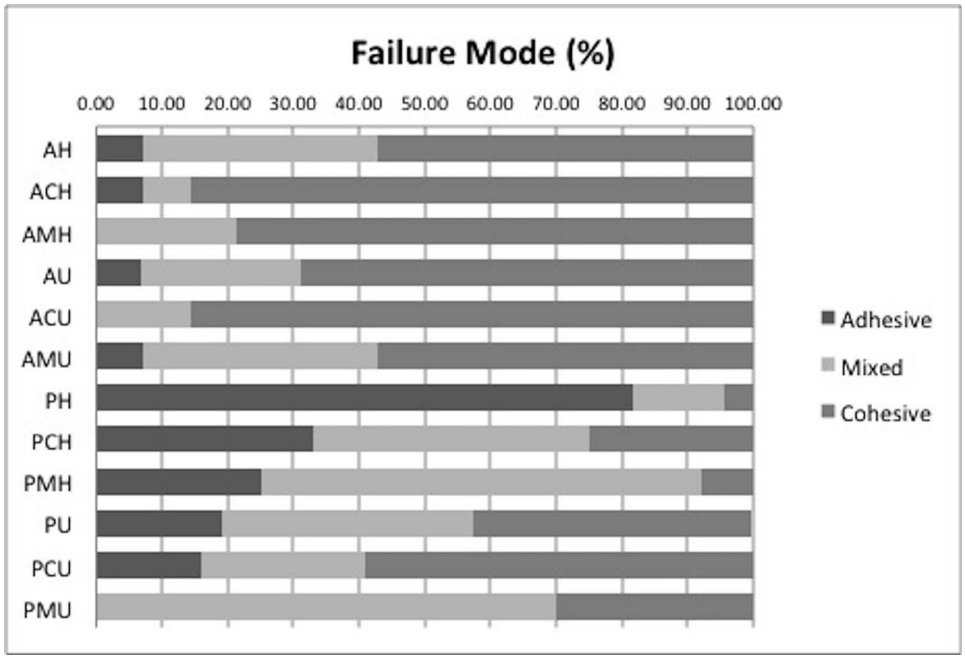

Figure 2. *Failure modes (%) of the evaluated groups.*

repair bond strength, although this result was not statistically different from the result for the group that received the same surface treatment followed by treatment with phosphate-containing silane and universal adhesive (PMU). In general, the polished specimens had lower shear bond strength than the air-abraded specimens. Interestingly, the results for bond strength in the PU group (polished surfaces treated with universal adhesive) were not statistically different from those for the air-abraded groups treated with hydrophobic adhesive (AH) alone, with hydrophobic adhesive and one type of silane (ACH and AMH), with universal adhesive alone (AU), or with universal adhesive and the phosphate-containing silane (AMU).

The failure modes of the specimens are shown in Figure 2. While most of the failures in the air-abraded specimens were cohesive in the composite repair, most of the failures were mixed in the polished specimens. In group PH (polished specimens treated with the hydrophobic adhesive), over 80% of the failures were adhesive.

DISCUSSION

This study evaluated the effect of different surface treatments and bonding materials on the bond strength of repairs in a nanofilled composite. The null hypothesis was rejected, as significant differences were found between the groups.

Filtek Supreme Ultra, the composite used in this study, is a nanocomposite with fillers that are a combination of nonagglomerated/nonaggregated 20-nm silica filler, nonagglomerated/nonaggregated 4- to 11-nm zirconia filler, and aggregated zirconia/silica cluster filler (comprised of 20-nm silica and 4- to 11-nm zirconia particles). The filler loading for nontranslucent shades is about 78.5% by weight and 63.3% by volume.[24] The inorganic portion consists of 60% to 80% ceramic and 1% to 10% silica/zirconia by weight. A previous study using the same composite found similar bond strengths when the oxygen-inhibited layer was maintained and when silane was applied before the adhesive in immediate repairs.[25] In the present study, bond strength was higher when conventional or MDP-containing silane was applied before the hydrophobic adhesive than when only the adhesive was applied. These results are probably due to the presence of exposed particles after air abrasion and the consequent good chemical bond between the resin matrix of the composite repair and exposed particles in the original resin.

Several studies have shown that application of a silane agent increases the wettability of the surface to be repaired, promoting a chemical bond between the resin matrix and the silica or glass filler particles.[25-29] Silane coupling agents are bifunctional, as they have not only a nonhydrolyzable functional group with a double carbon bond that reacts and can polymerize with monomers containing double bonds in the organic matrix of the resin composite but also hydrolyzable alkoxy groups that react with hydroxyl groups in the inorganic surface of silica-based materials forming oxygen bridges.[28]

Because of its highly crystalline, inert nature, zirconia can bond to resin-based materials to only a limited degree.[30] Different surface treatments, cleaning methods, and ceramic primers have been investigated in an attempt to overcome this limitation. The surface treatments most frequently used to improve mechanical retention to zirconia ceramic substrates are air abrasion with aluminum oxide particles and silica coating.[30-33] Recently, some studies have demonstrated that phosphate monomer–containing silanes can bond chemically to zirconia better than a conventional silane coupling agent.[31,32,34,35] Attia and Kern[33] compared the so-called universal primer Monobond Plus with a conventional silane applied to air-abraded or silica-coated zirconia ceramic. They used different cleaning methods and reported significantly higher long-term resin bonding to zirconia ceramic with the universal primer than with the conventional silane. However, to our knowledge, the present study is the first to investigate the efficacy of a phosphate monomer–containing silane in composite repairs. Our results show that Monobond Plus failed to produce a repair with higher bond strength than the conventional silane Ceramic Bond. This can be attributed to the low zirconia content of the nanofilled composite used here, around 10%.

The universal adhesive Scotchbond Universal contains, in addition to conventional methacrylate monomers, 10-MDP, a functional monomer known for its ability to bond chemically to calcium and make the adhesive interface more resistant to biodegradation.[36] Phosphate esters can also bond directly to the surface hydroxyl groups of non–silica-containing ceramics, such as zirconia, and enhance the hydrolytic stability of bonding more than silane coupling agents.[35] Furthermore, Scotchbond Universal adhesive contains prehydrolyzed silane, claimed by the manufacturer to be stable up to at least one year in storage.[21] A universal adhesive was investigated as a bonding agent for the repair of a nanofilled composite in a recent study in which air abrasion resulted in similar flexural bond strength to that achieved using phosphoric acid etching and unrepaired specimens (controls).[22] In another study, application of a universal adhesive was as effective as a conventional silane before application of a bonding agent in the repair of composites aged for three months and six years.[23] Our results show that the effectiveness of the universal adhesive was independent of the type of silane but that the repair bond strength increased when this type of adhesive was used with air abrasion as the surface treatment, probably because this resulted in a greater proportion of exposed ceramic fillers at the surface of the composite, increasing the surface area for bonding.

The use of an adhesive resin between the original and the repair composite increases the wettability of the surface as the resin penetrates and polymerizes into the prepared surface creating micromechanical retention.[6,7] A study comparing repair with and without application of adhesives in different composites concluded that their use increases bond strength for both immediate repairs and repairs of aged composites.[37] Since the aim of the present study was to evaluate the effect of different silanes and of air abrasion surface treatment, all specimens received an adhesive layer before the repair. However, the features of both adhesives evaluated are quite different in terms of viscosity, composition, and application mode. Although Heliobond is a Bis-GMA/TEGDMA–based material that is not expected to promote chemical bonding, air abrasion of the composite surface before Heliobond was applied resulted in greater repair bond strength.

After repair, the composite specimens in the present study were aged by storing them in distilled water for 14 days. Maximum water absorption occurs in the first week of storage, resulting in leaching of components and plasticization of the resin matrix.[38] Although some studies on repair bond strength use thermocycling as the aging process,[10,27,37] most use storage in water.[14,22,25,26,29] The latter method is sufficient to simulate clinical aging, as it causes water to be absorbed and consequent reduction of unreacted methacrylate carbon double bonds, which is required for the chemical bond with the repairing composite.[25]

While the most common test to evaluate the bonding effectiveness of composite repairs is the shear bond strength test,[7,25,23,27,37] this has frequently been criticized for its inhomogeneous stress distribution along the interface.[39] In the present study, air-abraded specimens had a higher percentage of cohesive fractures than polished specimens. This may be attributable to difficulties positioning the metal blade exactly at the specimen's interface, leading to dislocation of the stress toward the original composite. Adhesive failure was more common in the PH group, in which only the hydrophobic adhesive was used, resulting in the lowest bond strength in the study.

Composite repair is a minimally invasive technique that preserves sound tooth structure and

increases the longevity of restorations. However, the surface treatment and chemical bonding between the new and existing (aged) composite must be maximized to ensure an effective repair. Additional studies with different composites, bonding agents, and surface treatments should be performed to improve this technique and raise awareness of this treatment option among clinicians.

CONCLUSION

Within the limitations of this *in vitro* study, the following conclusions can be drawn. While air abrasion with Al_2O_3 particles increased the repair bond strength of the nanoparticle composite, the use of MDP-containing silane did not affect the results. The application of a silane-containing universal adhesive alone was as effective as any of the silane and adhesive combinations tested. The use of this material seems to be promising for the simplification of nanofilled composite repair.

Acknowledgement

The authors would like to acknowledge the National Counsel of Technological and Scientific Development (CNPq) for financial support.

Conflict of Interest

The authors of this article certify that they have no proprietary, financial, or other personal interest of any nature or kind in any product, service, and/or company that is presented in this article.

(Accepted 19 November 2016)

REFERENCES

1. Tyas MJ, Anusavice KJ, Frencken JE, & Mount GJ (2000) Minimal intervention dentistry: A review. FDI Commission Project 1-97 *International Dental Journal* **50(1)** 1-12.
2. White JM, & Eakle WS (2000) Rationale and treatment approach in minimally invasive dentistry *Journal of the American Dental Association* **(Supplement 131)** 13S-19S.
3. Murdoch-Kinch CA, & McLean ME (2003) Minimally invasive dentistry *Journal of the American Dental Association* **134(1)** 87-95.
4. Akova T, Ozkomur A, & Uysal H (2006) Effect of food-simulating liquids on the mechanical properties of provisional restorative materials *Dental Materials* **22(12)** 1130-1134.
5. Sarkar NK (2000) Internal corrosion in dental composite wear *Journal of Biomedical Materials Research* **53(4)** 371-380.
6. Rinastiti M, Özcan M, Siswomihardjo W, & Busscher HJ (2011) Effects of surface conditioning on repair bond strengths of non-aged and aged microhybrid, nanohybrid, and nanofilled composite resins *Clinical Oral Investigations* **15(5)** 625-633.
7. Rinastiti M, Özcan M, Siswomihardjo W, & Busscher HJ (2010) Immediate repair bond strengths of microhybrid, nanohybrid and nanofilled composites after different surface treatments *Journal of Dentistry* **38(1)** 29-38.
8. Fernández E, Martín J, Vildósola P, Oliveira Junior OB, Gordan V, Mjör I, Bersezio C, Estay J, de Andrade MF, & Moncada G (2015) Can repair increase the longevity of composite resins? Results of a 10-year clinical trial *Journal of Dentistry* **43(2)** 279-286.
9. Moncada G, Fernández E, Martín J, Arancibia C, Mjör IA, & Gordan VV (2008) Increasing the longevity of restorations by minimal intervention: A two-year clinical trial *Operative Dentistry* **33(3)** 258-264.
10. Loomans BA, Cardoso MV, Roeters FJ, Opdam NJ, De Munck J, Huysmans MC, & Van Meerbeek B (2011) Is there one optimal repair technique for all composites? *Dental Materials* **27(7)** 701-709.
11. Bacchi A, Consani RL, Sinhoreti MA, Feitosa VP, Cavalcante LM, Pfeifer CS, & Schneider LF (2013) Repair bond strength in aged methacrylate- and silorane-based composites *Journal of Adhesive Dentistry* **15(5)** 447-452.
12. Papacchini F, Dall'Oca S, Chieffi N, Goracci C, Sadek FT, Suh BI, Tay FR, & Ferrari M (2007) Composite-to-composite microtensile bond strength in the repair of a microfilled hybrid resin: Effect of surface treatment and oxygen inhibition *Journal of Adhesive Dentistry* **9(1)** 25-31.
13. Özcan M, Barbosa SH, Melo RM, Galhano GA, & Bottino MA (2007) Effect of surface conditioning methods on the microtensile bond strength of resin composite to composite after aging conditions *Dental Materials* **23(10)** 1276-1282.
14. Loomans BA, Cardoso MV, Opdam NJ, Roeters FJ, De Munck J, Huysmans MC, & Van Meerbeek B (2011) Surface roughness of etched composite resin in light of composite repair *Journal of Dentistry* **39(7)** 499-505.
15. Bouschlicher MR, Reinhardt JW, & Vargas MA (1997) Surface treatment techniques for resin composite repair *American Journal of Dentistry* **10(6)** 279-283.
16. Matinlinna JP, Lassila LV, Özcan M, Yli-Urpo A, & Vallittu PK (2004) An introduction to silanes and their clinical applications in dentistry *International Journal of Prosthodontics* **17(2)** 155-164.
17. Ferracane JL (2011) Resin composite: State of the art *Dental Materials* **27(1)** 29-38.
18. Lung CY, & Matinlinna JP (2012) Aspects of silane coupling agents and surface conditioning in dentistry: An overview *Dental Materials* **28(5)** 467-477.
19. Yesilyurt C, Kusgoz A, Bayram M, & Ulker M (2009) Initial repair bond strength of a nano-filled hybrid resin: Effect of surface treatments and bonding agents *Journal of Esthetic and Restorative Dentistry* **21(4)** 251-260.
20. Burtscher P (1993) Stability of radicals in cured composite materials *Dental Materials* **9(4)** 218-221.
21. 3M ESPE (2013) Scotchbond Universal Adhesive technical product profile. Retrieved online July 28, 2016 from:

http://multimedia.3m.com/mws/media/754751O/scotchbond-universal-adhesive-technical-product-profile

22. Tantbirojn D, Fernando C, & Versluis A (2015) Failure strengths of composite additions and repairs *Operative Dentistry* **40(4)** 364-371.
23. Staxrud F, & Dahl JE (2015) Silanising agents promote resin-composite repair *International Dental Journal* **65(6)** 311-315.
24. 3M ESPE (2010) Filtek Supreme Ultra technical product profile. Retrieved online July 28, 2016 from: http://multimedia.3m.com/mws/media/629066O/filtektm-supreme-ultrauniversal-restorative
25. Imbery TA, Gray T, DeLatour F, Boxx C, Best AM, & Moon PC (2014) Evaluation of flexural, diametral tensile, and shear bond strength of composite repairs *Operative Dentistry* **39(9)** E250-E260.
26. Maneenut C, Sakoolnamarka R, & Tyas MJ (2011) The repair potential of resin composite materials *Dental Materials* **27(2)** e20-ee27.
27. Joulaei M, Bahari M, Ahmadi A, & Savadi Oskoee S (2012) Effect of different surface treatments on repair micro-shear bond strength of silica- and zirconia-filled composite resins *Journal of Dental Research Dental Clinics Dental Prospects* **6(4)** 131-137.
28. Matinlinna JP, & Vallittu PK (2007) Bonding of resin composites to etchable ceramic surfaces—An insight review of the chemical aspects on surface conditioning *Journal of Oral Rehabilitation* **34(8)** 622-630.
29. Souza EM, Francischone CE, Powers JM, Rached RN, & Vieira S (2008) Effect of different surface treatments on the repair bond strength of indirect composites *American Journal of Dentistry* **21(2)** 93-96.
30. Thompson JY, Stoner BR, Piascik JR, & Smith R (2011) Adhesion/cementation to zirconia and other non-silicate ceramics: Where are we now? *Dental Materials* **27(1)** 71-82.
31. Yang B, Barloi A, & Kern M (2010) Influence of air-abrasion on zirconia ceramic bonding using an adhesive composite resin. *Dental Materials* **26(1)** 44-50.
32. Inokoshi M, Poitevin A, De Munck J, Minakuchi S, & Van Meerbeek B (2014) Bonding effectiveness to different chemically pre-treated dental zirconia *Clinical Oral Investigations* **18(7)** 1803-1812.
33. Attia A, & Kern M (2011) Long-term resin bonding to zirconia ceramic with a new universal primer *Journal of Prosthetic Dentistry* **106(5)** 319-327.
34. Inokoshi M, Kameyama A, De Munck J, Minakuchi S, & Van Meerbeek B (2013) Durable bonding to mechanically and/or chemically pre-treated dental zirconia *Journal of Dentistry* **41(2)** 170-179.
35. Kern M, & Wegner SM (1998) Bonding to zirconia ceramic: Adhesion methods and their durability *Dental Materials* **14(1)** 64-71.
36. Yoshida Y, Yoshihara K, Nagaoka N, Hayakawa S, Torii Y, Ogawa T, Osaka A, & Van Meerbeek B (2012) Self-assembled nano-layering at the adhesive interface *Journal of Dental Research* **91(4)** 376-381.
37. Staxrud F, & Dahl JE (2011) Role of bonding agents in the repair of composite resin restorations *European Journal of Oral Sciences* **119(4)** 316-322.
38. Biradar B, Biradar S, & Ms A (2012) Evaluation of the effect of water on three different light cured composite restorative materials stored in water: An in vitro study *International Journal of Dentistry* **2012** 640942.
39. Della Bona A, & Van Noort R (1995) Shear vs. tensile bond strength of resin composite bonded to ceramic *Journal of Dental Research* **74(9)** 1591-1596.

©Operative Dentistry, 2017, **42-4,** 375-386

Comparison of Polymerization Shrinkage, Physical Properties, and Marginal Adaptation of Flowable and Restorative Bulk Fill Resin-Based Composites

JH Jung • SH Park

Clinical Relevance

A sufficient light-curing time should be applied to bulk fill resin-based composites as the depth of cure is dependent on the material used.

SUMMARY

Purpose: The purpose of this study was to compare the marginal adaptation of two flowable bulk fill resin-based composites (FB-RBCs), two restorative bulk fill resin-based composites (RB-RBCs), and one regular incremental-fill RBC in MOD cavities *in vitro*. Additionally, the influence of linear polymerization shrinkage, shrinkage force, flexural modulus, and bottom/top surface hardness ratio on the marginal adaptation was evaluated. Methods: A Class II MOD cavity was prepared in 40 extracted sound lower molars. In group 1 (control group), the preparation was filled with Filtek Z350 (Z3, 3M ESPE, St Paul, MN, USA) using the incremental filling technique. The FB-RBCs, SDR (SD, group 2) (Dentsply Caulk, Milford, DE, USA) and Venus Bulk Fill (VB, group 3) (Heraeus Kulzer, Dormagen, Germany), were placed in the core portion of the cavity first, and Z350 was filled in the remaining cavity. The RB-RBCs, Tetric N-Ceram Bulkfill (TB, group 4) (Ivoclar Vivadent, Schaan, Liechtenstein) and SonicFill (SF, Group 5) (Kerr, West Collins, Orange, CA, USA), were bulk filled into the preparation. Images of the magnified marginal area were captured under 100× magnification before and after thermomechanical loading, and the percentage ratio of the imperfect margin (%IM_{whole}) was calculated. Gaps, cracks in the enamel layer, and chipping of composite, enamel, or dentin were all considered to be imperfect margins. Linear polymerization shrinkage, polymerization shrinkage force, flexural strength, flexural modulus, and bottom/top surface hardness ratio of were measured. Eight specimens were allocated for each material for each test. One-way analysis of variance with the Scheffé test

Ja-Hyun Jung, MS, Conservative Dentistry, Yonsei University, Seoul, Republic of Korea

*Sung-ho Park, PhD, Conservative Dentistry, Oral Science Research Center, Yonsei University, Seoul, Republic of Korea

*Corresponding author: 50, Yonsei-ro, Seodaemun-gu, Seoul 120-752, Republic of Korea; e-mail: sunghopark@yuhs.ac

DOI: 10.2341/16-254-L

was used to compare the groups at a 95% confidence level. Results: Before thermomechanical loading, $\%IM_{whole}$ was in the order of group 3 ≤ groups 2 and 5 ≤ groups 1 and 4 (p=0.011), whereas after loading, it was in the order of group 4 ≤ group 5 ≤ group 1 ≤ groups 2 and 3 (p<0.001). The order of materials were Z3 < TB and SF < SD and VB (p<0.001) in polymerization shrinkage; SF ≤ TB ≤ Z3 < SD < VB (p<0.001) in polymerization shrinkage force; VB < SD < TB ≤ Z3 ≤ SF (p<0.001) in flexural modulus; SD, VB, and TB < Z3 and SF (p<0.001) in flexural strtength; and SF< Z3 < TB < VB and SD (p<0.001) in bottom/top surface hardness ratio. The Pearson correlation constant between $\%IM_{whole}$ and polymerization shrinkage, shrinkage force, elastic modulus, and bottom/top surface hardness ratio was 0.697, 0.708, −0.373, and 0.353, respectively, after thermomechanical loading. Conclusion: Within the limitations of this study, RB-RBCs showed better marginal adaptation than FB- RBCs. The lower level of polymerization shrinkage and polymerization shrinkage stress in RB-RBCs seems to contribute to this finding because it would induce less polymerization shrinkage force at the margin. FB-RBCs with lower flexural modulus may not provide an effective buffer to occlusal stress when they are capped with regular RBCs.

INTRODUCTION

The use of a resin-based composite (RBC) as a direct restorative material is increasing due to improved esthetics and adhesion to tooth structure. However, the volumetric polymerization shrinkage of RBC, being in the range of 2% to 3%, could cause various problems and may result in gaps between the tooth and the restorative material.[1] Such gaps may contribute to the formation of secondary dental caries or pathologic changes in the dental pulp.[2]

Kim and Park[3] reported that placing a composite into Class II cavities leads to the inward deformation of the cusp, and this cusp deflection was caused by the composites' cure. It was reported that restoring a cavity with the single bulk filling technique using a regular RBC resulted in more marginal leakage but less cuspal deflection compared with the incremental cure technique because bulk filling may result in an incomplete cure.[4] On the other hand, it was reported that the bulk filling technique resulted in more cuspal deflection than the incremental technique when RBCs are sufficiently polymerized by increasing the curing time up to 180 seconds.[3] Therefore, various methods, such as the incremental filling technique,[5] changing the curing mode,[6] using a stress-absorbing intermediate layer,[7] and using a sandwich technique with glass-ionomer,[8] have been suggested to increase marginal adaptation.

Flowable bulk fill resin-based composites (FB-RBCs), such as SDR and Venus Bulk Fill, have come onto the market, which claim to fill up to 4 to 5 mm thicknesses at once by improving the depth to which the RBCs can be light activated. According to the manufacturers of FB-RBCs, it is recommended to complete the restoration with a capping layer made of a regular incremental-fill RBC. It was reported that this step is imperative due to the lower flexural modulus and hardness of FB-RBCs compared to those of regular incremental-fill RBCs.[9]

Czasch and Ilie[10] compared SDR and Venus Bulk Fill and reported that Venus Bulk Fill showed, at all depths, a higher degree of conversion but was significantly lower in other physical properties than SDR. However, both materials showed a depth of cure of at least 6 mm.[10] In addition, Roggendorf and others[11] analyzed the marginal adaptation of MOD restorations with different RBCs while using SDR as the base material. This work showed that SDR did not have any negative impact on the marginal adaptation when used as a 4-mm-thick base material. According to Moorthy and others,[12] restorations with SDR showed the same level of microleakage in the cervical areas and a lower level of cuspal deflection compared to restorations without SDR. Kim and Park[13] recently compared the internal adaptation between RBCs and the cavity floor and also compared the linear polymerization shrinkage and the shrinkage force of RBCs. They reported that the internal adaptation was better when the cavity was filled in 2-mm increments with regular incremental-fill RBCs than when it was bulk filled with FB-RBCs. When the internal adaptation was correlated with the linear polymerization shrinkage and shrinkage force, they showed a high correlation.

Recently, restorative bulk fill resin-based composites (RB-RBCs) have been introduced to the market. According to the manufacturers, RB-RBCs have lower polymerization shrinkage stress than FB-RBCs; they need not be covered with regular incremental-fill RBCs and can themselves be used as filling materials.

Table 1: *Composite Materials Used in This Study and Their Composition*[a]

Product	Code	Category	Manufacturer	Base Resin	Filler (wt/vol%)
Filtek Z350	Z3	R	3M ESPE, St Paul, MN, USA	Bis-GMA/EMA, UDMA	78.5/59.5
SDR	SD	FB-RBC	Dentsply Caulk, Milford, DE, USA	Modified urethane dimethacrylate EBPADMA/TEGDMA	68/44
Venus Bulk Fill	VB	FB-RBC	Heraeus Kulzer, Dormagen, Germany	UDMA, EBPDMA	65/38
Tetric N-ceram Bulkfill	TB	RB-RBC	Ivoclar Vivadent, Schaan, Liechtenstein	Bis-GMA, UDMA dimethacrylate co-monomers	78/55 (including prepolymer)
SonicFill	SF	RB-RBC	Kerr, West Collins, Orange, CA, USA	Bis-GMA, TEGDMA, EBPDMA	83.5/68

[a] *Composition of base resin and filler content are from manufacturer's information.*
Abbreviations: BIS-GMA, bisphenol A dimethacrylate; BIS-EMA, bisphenol A polyethylene glycol diether dimethacrylate; UDMA, urethane dimethacrylate; TEGDMA, triethyleneglycol dimethacrylate; EBPADMA, ethoxylated bisphenol A dimethacrylate; U, regular incremental fill resin-based composite; FB-RBC, flowable bulk filled resin-based composite; RB-RBC, restorative bulk filled resin-based composite.

It has been reported that flowable resins can be used as a stress-absorbing intermediate layer, which may result in the improved adhesion to dentin and absorb the stress of polymerization or functional loading.[14] According to Kwon and others,[15] the flexural modulus of base materials and the polymerization shrinkage of RBCs affect the marginal adaptation of the final restorations. The differences in the physical properties, polymerization shrinkage, and restoration technique between FB-RBCs and RB-RBCs likely affect the marginal adaptation differently. Clinicians would not be required to use the time-consuming layering technique if FB-RBCs or RB-RBCs functioned well. However, the scientific evidence of their function remains insufficient.

The purpose of this study was to compare the marginal adaptation of FB-RBCs, RB-RBCs, and regular incremental-fill RBCs in MOD cavities *in vitro*. Additionally, the influence of polymerization shrinkage (amount and force), flexural modulus, and bottom/top surface hardness ratio on the marginal adaptation was evaluated. The null hypothesis for this study was that there is no difference in the marginal adaptation of FB-RBCs, RB-RBCs, and regular incremental-fill RBCs.

METHODS AND MATERIALS

Materials

In this study, five different RBCs from different manufacturers were used. Filtek Z350 (3M ESPE, St Paul, MN, USA) was the regular incremental-fill RBC, SDR (Dentsply Caulk, Milford, DE, USA) and Venus Bulk Fill (Heraeus Kulzer, Dormagen, Germany) were the FB-RBCs, and Tetric N-Ceram Bulkfill (Ivoclar Vivadent, Schaan, Liechtenstein) and SonicFill (Kerr, West Collins, Orange, CA, USA) were the RB-RBCs. The types and composition of the RBCs used in this study are summarized in Table 1.

Measurement of the Linear Polymerization Shrinkage

Polymerization shrinkage was measured using a custom-made Linometer (R&B Inc, Daejon, Korea) following the previously described procedures by Kim and Park.[13] Glycerin gel was applied to a metallic disc and a piece of glass slide to prevent adhesion to the resin. RBCs were transferred to a Teflon mold to ensure that the same amount of composite was used for each linometer sample (39.25 mm^3). Then the RBC was placed on the thin metallic discs, covered with a 1-mm-thick glass slide, and, using a screw, positioned into place under constant pressure. An LED-type light-curing unit (Bluephase N, Ivoclar Vivadent) with a power density of 1140 mW/cm^2 was placed 1 mm above the glass slide, and the material was light cured for 30 seconds. The power density of the light-curing unit was calculated by dividing the integration power (mW) of the light-curing unit, measured using an integration sphere (Gigahertz-Optic GmbH, Puchheim, Germany), by the fiber bundle area (cm^2). As the RBC under the glass slide was cured, it moved the aluminum disk under the RBC upward. The amount of disk displacement, which was caused by the linear shrinkage of the RBC, was measured in μm using an eddy current sensor every 0.5 seconds for a period of 120 seconds, and the data were stored simultaneously in a computer. This was measured eight times for each material.

Measurement of the Polymerization Shrinkage Force

The polymerization shrinkage force of the RBC was measured using a custom-made device and software (R&B Inc) following the previously described procedures by Kim and Park.[13] The compliance of this device was 0.3 μm/N. The instrument was driven by a motor and was devised to move a tension rod up

and down. The RBC (145 mm^3) was transferred to an acrylic disc, and the upper tension rod, which was made of stainless steel and had a diameter of 8 mm, was set to ensure that the thickness of the specimen was 1 mm and the diameter was 8 mm. The c-factor was 4. The force between the tension rod and the RBC was set to zero using the software before light curing. Then the RBC was light cured with a light-curing unit (Bluephase N, Ivoclar Vivadent, 1140 mW/cm^2) for 30 seconds through the acrylic disc. The polymerization shrinkage force was measured in kgf using a load cell (model UM-K100,100-kgf capacity, Dacell, Chungcheongbuk-do, South Korea) connected to the tension rod, and the resulting data were stored in a computer every 0.5 seconds for a period of 180 seconds. This measurement was completed eight times for each material studied.

Measurement of Flexural Modulus

Specimens of each RBC were made using a metallic mold of $25 \times 2 \times 2$ mm in accordance with ISO 4049. The specimen was light cured along its length using a light-curing unit (Bluephase N, Ivoclar Vivadent, 1140 mW/cm^2) for three exposure times of 20 seconds for each surface. Thus, a 240-second curing time was needed for four surfaces. As the diameter of the curing tip was 9 mm, 2 mm of overlapping occurred during light curing. The specimens were stored in light-proof conditions for 24 hours. The specimens were slightly wet ground with 600-grit and 1200-grit SiCs on all four surfaces to remove flash. Then a universal testing machine (Instron, Norwood, MA, USA) was used to conduct three-point bending tests. Eight specimens were allocated for each material. The span length was 20 mm, and the crosshead speed was 0.75 mm/min. After the measurement, flexural moduli ($E_{flexural}$, flexural modulus) were calculated in GPa using the following equation. Deformation range between 0.6 and 1.0 mm was used for this calculation:

$$E_{flexural} = FL^3/4wh^3d$$

where F = maximum load, L = span length, w = width of the specimen, h = specimen height, and d = deflection.

Measurement of Microhardness and Calculating Bottom/Top Surface Hardness Ratio

An opaque polyacrylic mold (Dentsply Caulk), which had a hole 4 mm deep and 4 mm in diameter, was used to prepare the RBC specimens. After a glass slide and a celluloid strip were placed on a flat surface, the mold was placed on the top of the strip. RBCs were bulk filled into the mold for each material and covered with a celluloid strip and a glass slide. A slight digital force was applied to the glass slide to ensure that the celluloid covered the RBC surface tightly and to make the surface flat and smooth. The tip of the curing light was placed within 1 mm of the upper surface of the glass slide and then light cured for 30 seconds using a light-curing unit (Bluephase N, Ivoclar Vivadent, 1140 mW/cm^2). Eight specimens were allocated to each group. Each specimen was removed from the mold, and its upper and lower surfaces were slightly polished with 2000-grit SiC paper. The specimens were then stored in dark and dry conditions for 24 hours at room temperature. The Vickers microhardness of the top and bottom surfaces of each specimen was measured using a Micro Hardness Tester (HMV-2, Shimadzu, Kyoto, Japan). For these measurements, a 5-kgf force was applied for five seconds, and four points were measured for each surface. The bottom/top surface hardness ratio was calculated and compared.

Measurement of Marginal Adaptation

Preparation of the specimens—Human teeth, which were extracted for periodontal or orthodontic reasons within a month of the study, were collected and stored in distilled water. Forty lower molar teeth free of coronal cracks or caries were used as specimens. The bucco-lingual dimension of the specimens was between 10.1 and 10.6 mm, and the mesiodistal dimension was between 10.7 and 11.2 mm. Then a Class II preparation was made on each of the molar teeth using a high-speed diamond bur (959 KR 018, Komet GEBR Brasseler GmbH & Co KG, Lemgo, Germany), and the enamel margin was trimmed with a fine-grit diamond bur (862 EF +010, Komet GEBR Brasseler). The bur was replaced with a new one every 10 teeth. Measured from the central fossa, the depth of the cavity was 4.5 mm, and the bucco-lingual width was 3.5 mm. On one side of the proximal cavities, the cavity was extended just from the central cavity, and the cervical margin was located on the enamel (the shallow proximal box), while a box-shaped cavity was prepared on the other side, the cervical margin was located on the dentin 1 mm beneath the CEJ, and the cavity depth was 6.5 mm (the deep proximal box) (Figure 1).

The enamel and dentin of the specimens were etched with 34% phosphoric acid (Caulk 34% Tooth Conditioner, Dentsply Caulk) for 15 seconds and washed with distilled water. After blot drying the

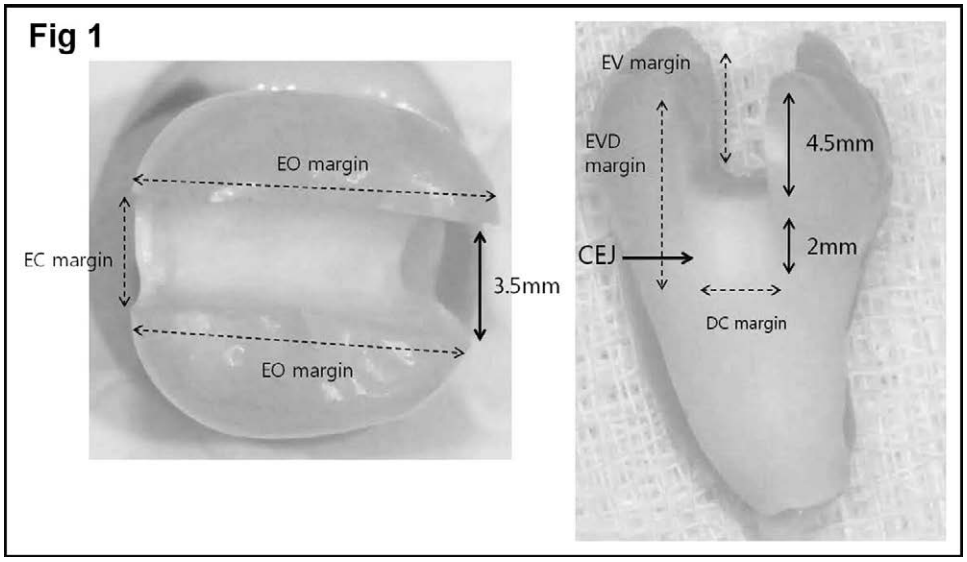

Figure 1. *Occlusal and proximal views of the cavity preparation.*

surface, the adhesive (XP Bond, Dentsply Caulk) was applied and light cured on the occlusal, mesial, and distal sides using an LED light-curing unit (Bluephase N, Ivoclar Vivadent, 1140 mW/cm^2) for 20 seconds at each position. The same curing light was used in the following curing process for the RBCs.

Forty specimens were randomly allocated into five groups. Then the cavities were filled and light cured as follows for each group:

• Control group (group 1)

After applying the Ivory retainer and matrix to the tooth specimen, the RBC (Z3) was applied. The first 2-mm increment was placed in the deep proximal box and was light cured for 20 seconds from the occlusal side. The second and third 2-mm increments were placed in the shallow to deep proximal side and light cured for 20 seconds each from the occlusal side. The fourth and fifth 2-mm increments were placed in the mesial and distal half of the remaining cavity and were light cured for 20 seconds each from the occlusal side. After removing the retainer and the matrix, additional light curing was applied from the buccal and lingual sides of the deep and shallow proximal cavities obliquely from the occlusal surface. Eighty seconds of additional light curing (20 seconds $\times$ 4) was applied in this process. Figure 2a shows a schematic diagram of the filling procedure.

• FB-RBCs: group 2 (SD + Z3) and group 3 (VB + Z3)

After applying an Ivory retainer and matrix to the tooth specimen, FB-RBCs (group 2: SD; group 3: VD) were placed in the core portion of the cavity. Then the FB-RBCs were light cured for 20 seconds from the occlusal direction. The thickness of the materials in the occlusal and deep proximal portions was calculated by subtracting the remaining depth of each portion after light curing from its original depth. Therefore, it was 3.5 and 5.5 mm in the occlusal and deep proximal portions, respectively. When the thickness of the material exceeded the criteria, the thickness was reduced using a high-speed fine-grit diamond bur (959 KREF 018, Komet GEBR Brasseler). In cases when the materials were not confined to the core portion and were not away from the margins, the extended portions were removed using a hand instrument. Z350 was added to the cavity (first in the deep proximal, then in the shallow proximal, then the mesial half, and then the distal half) and light cured for 20 seconds after each addition (Figure 2b). After removing the retainer and matrix, additional light curing was applied to the buccal and lingual sides of the deep and shallow proximal cavities obliquely from the occlusal surface; thus, a total of 80 seconds of additional light curing (20 seconds $\times$ 4) was applied.

• RB-RBCs: group 4 (TB) and group 5 (SF)

TB (group 4) and SF (group 5) were bulk filled in the cavity after applying the ivory retainer and matrix to the tooth specimen, followed by a 20-second photopolymerization. The filling process was carried out using hand instruments (group 4) or a sonically activated hand piece (group 5) as instructed by the manufacturer. After removing the retainer and matrix, additional light curing was applied from the buccal and lingual sides of the deep and shallow proximal cavity obliquely from the occlusal surface such that 80 seconds of additional light curing (20

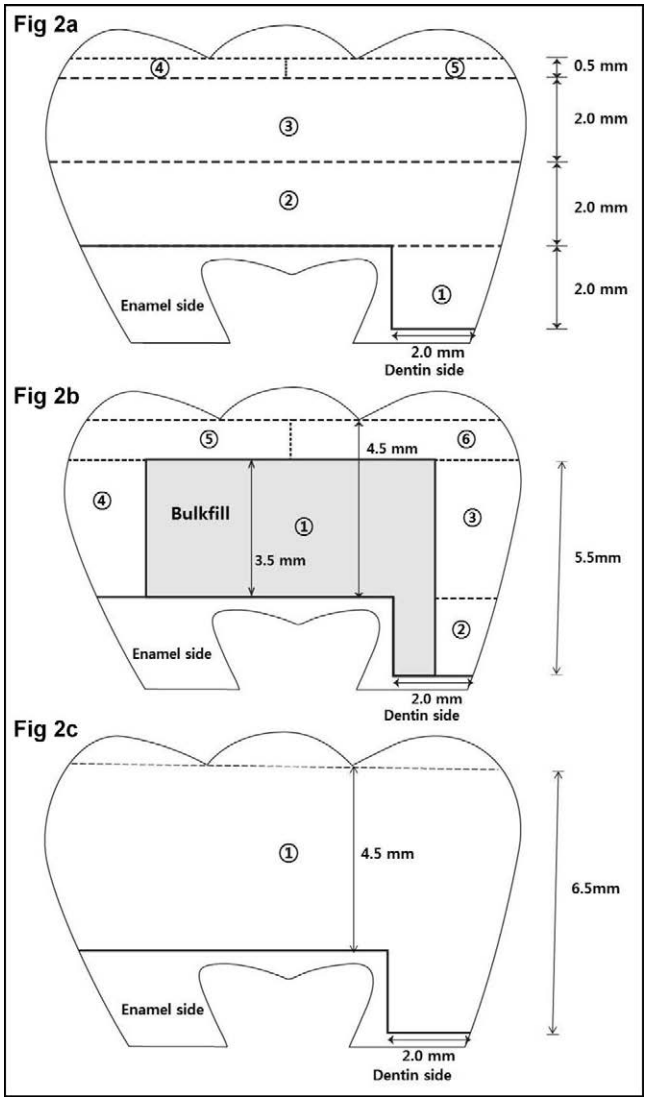

Figure 2a. *Schematic diagram of the resin placement of the control group (Z3).*
Figure 2b. *Schematic diagram of the bulk fill resin placement (SD, VB).*
Figure 2c. *Schematic diagram of the bulk fill resin placement (TB, SF).*

seconds × 4) was applied. Figure 2c shows a schematic diagram of this filling procedure. The calculated c-factor was about 2.1.

Stereomicroscope Imaging and Analysis of the Margin

All of the specimens were polished under a surgical microscope at 10× magnification (Carl Zeiss Surgical GmbH, Oberkochen, Germany) using a high-speed fine-grit diamond bur (863 EF, Komet GEBR Brasseler). Then they were polished with a flame-shaped silicone bur (Astropol F, P, and HP, Ivoclar Vivadent) in the order of Astropol F, P, and HP at 10,000 rpm.

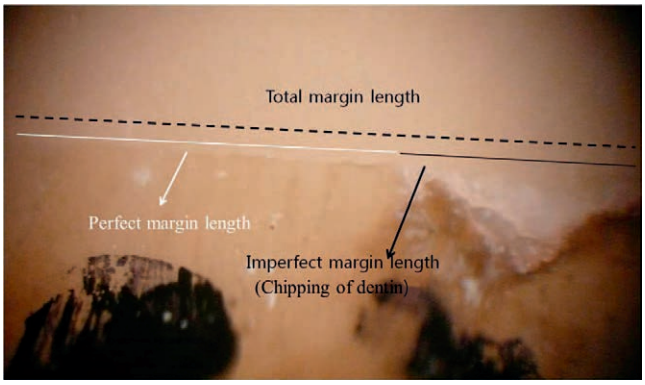

Figure 3. *Example of the margin analysis of the cavity.*

Finally, they were polished with a brush (Astrobrush, Ivoclar Vivadent) in which polishing paste was impregnated into the bristles. After polishing, the specimens were stored in 100% humidity for seven days. The specimens were positioned in a jig in which the specimens could be freely moved making it easy to observe the margin of the restoration. They were then observed using a stereomicroscope (Leica S8APO, Leica Microsystems, Wetzlar, Germany) at 100× magnification, and pictures of the whole margins were taken using a digital camera connected to the microscope. Using ImageJ software (version 1.46, National Institute of Mental Health, Bethesda, MD, USA), the lengths of the perfect and imperfect margins were calculated for each image. Adding the whole data of each image, the percentage of imperfect margin ($\%IM_{whole}$) (whole length of imperfect margin/[whole length of perfect margin + whole length of imperfect margin]×100) was calculated for each tooth specimen. Gaps between the restorations and cavity, cracks, and chippings of composites, enamel, or dentin were all considered to be imperfect margins (Figure 3). In addition, the cavity margins were categorized as the occlusal enamel margins (EO), the vertical enamel margins (EV), and the cervical enamel margins (EC) of the shallow proximal cavity as well as the vertical enamel margins (EVD) and the cervical dentin margins (DC) of the deep proximal cavity (Figure 1). The %IM was calculated in the EO, EV, EC, EVD, and DC as well.

Application of a Mechanical Load Using a Chewing Simulator

The CS-4.8 chewing simulator (SD Mechatronik, Feldkirchen-Westerham, Germany) was used under specific thermodynamic conditions to provide thermocycling (5°C to 55°C with a dwell-time of 60 seconds and a transfer time of 24 seconds) and mechanical load (49 N, 600,000 cycles, 1 Hz)

Table 2: *Polymerization Shrinkage, Shrinkage Force, Flexural Modulus, and Bottom/Top Surface Hardness Ratio*[a]

Materials	Linear Polymerization Shrinkage, μm / %	Polymerization Shrinkage Force, Kgf	Flexural Strength, MPa	Flexural Modulus, GPa	Bottom/Top Surface Hardness Value	
					VHN (Upper/Lower)	Ratio
Z3	11.98 (0.86) A /0.86	3.03 (0.16) B	128.05 (8.99) B	5.98 (0.66) CD	77.5/56.6	0.73 (0.03) B
SD	32.38 (1.27) C /2.31	4.00 (0.11) C	101.26 (11.39) A	3.29 (0.64) B	32.1/29.2	0.91 (0.02) D
VB	34.33 (3.14) C /2.45	4.94 (0.18) D	97.36 (5.63) A	2.35 (0.27) A	25.2/22.9	0.91 (0.02) D
TB	15.31 (0.86) B /1.09	3.01 (0.11) AB	100.21 (5.69) A	5.29 (0.41) C	49.3/40.4	0.82 (0.01) C
SF	16.43 (0.89) B /1.17	2.81 (0.19) A	136.67 (6.49) B	6.54 (0.50) D	70.5/47.94	0.68 (0.01) A

[a] *Different letters within a column indicate significantly different values* ($p<0.001$). *Figures in the parentheses are standard deviations.*

simultaneously. The specimens were embedded and fixed in chambers where thermocycling and mechanical loading were carried out. Chewing was simulated using a steel rod with a rounded conical end that pressed down on the center of the restorative material to apply a load from the top side. The rod moved 6 mm vertically and 0.3 mm horizontally. The rising speed was 55 mm/s, while the descending speed was 30 mm/s with a forward speed of 30 mm/s and a backward speed of 55 mm/s.

Analysis of the Marginal Adaptation

After mechanical loading, the margins of restorations were analyzed again, as described above.

Statistical Analysis

The linear polymerization shrinkage, the polymerization shrinkage force, the flexural modulus, and the bottom/top ratio of the microhardness of the RBCs were analyzed using one-way ANOVA, which was further verified using Tukey analysis at a 95% confidence interval. One-way ANOVA with Tukey was used to compare the $\%IM_{whole}$ of the groups at a 95% confidence interval. A paired *t*-test was used to compare the $\%IM_{whole}$ before and after thermomechanical loading in each group at a 95% confidence interval. The %IM between the groups at each part of the margins was analyzed using the Kruskal-Wallis and Mann-Whitney U-test method. Correlation analysis was performed to investigate the relationship between the %IM and linear polymerization shrinkage, shrinkage force, flexural modulus, and bottom/top surface hardness ratio.

RESULTS

Measurement of Polymerization Shrinkage

The linear polymerization shrinkage varied from 11.98 μm (Z3) to 34.33 μm (VB). The measured shrinkage levels were Z3 < TB and SF < SD and VB ($p<0.001$) (Table 2).

Measurement of the Polymerization Shrinkage Force

The polymerization shrinkage force was between 2.81 kgf (SF) and 4.94 kgf (VB). The measured levels were in the order of SF ≤ TB ≤ Z3 < SD < VB ($p<0.001$) (Table 2).

Measurement of the Flexural Strength and the Flexural Modulus

The flexural strength varied from 97.36 MPa (VB) to 136.67 MPa (SF). The measured values were in the order of VB, TB, and SD < Z3 and SF ($p<0.001$) (Table 2). The flexural modulus varied from 2.35 GPa (VB) to 6.54 GPa (SF). The measured values were in the order of VB < SD < TB ≤ Z3 ≤ SF ($p<0.001$) (Table 2).

Bottom/Top Surface Hardness Ratio

The bottom/top surface hardness ratio was between 0.68 (SF) and 0.91 (SD and VD). The measured values were in the order of SF < Z3 < TB < VB and SD ($p<0.001$) (Table 2).

$\%IM_{whole}$ and %IM

Before thermomechanical loading, $\%IM_{whole}$ was in the order of group 3 (VB + Z3) ≤ groups 2 (SD + Z3) and 5 (SF) ≤ groups 1 (Z3) and 4 (TB) ($p=0.011$), whereas after loading, it was in the order of group 4 (TB) ≤ group 5 (SF) ≤ group 1 (Z3) ≤ groups 2 (SD + Z3) and 3 (VB + Z3) ($p<0.001$). There were statistically significant differences between before and after mechanical loading in all groups ($p<0.001$) (Table 3). As for %IM in each cavity wall, no group showed a significant difference with the other groups in all of the margins before loading (Figure 4), whereas there was a significant difference between groups after thermomechanical loading. In EO and EV, %IM were group 5 (SF) ≤ groups 1 (Z3), 3 (VB + Z3), and 4 (TB) ≤ group 2 (SD + Z3) ($p = 0.044$ in EO, $p=0.015$ in EV) and group 5 (SF) ≤ groups 1 (Z3)

Table 3: *Mean Percentage of the Imperfect Margin Length to the Whole Cavity Margin Length (% IM) (Standard Deviation)*

Thermomechanical Loading Groups	$\%IM_{whole}$	
	Before	After
1	4.49 (2.92) B	20.44 (10.96) BC*
2	2.64 (1.62) AB	26.26 (5.24) C*
3	1.75 (1.51) A	22.05 (8.46) C*
4	4.07 (2.82) B	12.73 (3.94) A*
5	2.49 (1.83) AB	13.49 (1.87) AB*

*[a] Different letters indicate significantly different %IM levels among the different groups before ($p=0.011$) and after ($p<0.001$) thermomechanical loading. * indicates significant differences in the %IM between before and after thermomechanical loading ($p<0.001$). Group 1: Z3 (Control), Group 2: SD+Z3, Group 3: VB+Z3, Group 4: TB, Group 5: SF*

and 4 (TB) $\leq$ groups 2 (SD + Z3) and 3 (VB + Z3) in EC ($p=0.028$). There was no difference in %IM between the groups in DC and EDV (Figure 5).

Correlation Analysis

Before thermomechanical loading, the correlation coefficients (r) of the $\%IM_{whole}$ with linear polymerization shrinkage, shrinkage force, flexural modulus, and bottom/top surface hardness ratio were 0.362, 0.348, 0.360, and 0.285, respectively. After thermomechanical loading, they were 0.697, 0.708, −0.373, and 0.353, respectively.

DISCUSSION

The null hypothesis was partly rejected, as RB-RBCs showed better marginal adaptation than one of the two FB-RBCs following thermomechanical loading. RB-RBC showed smaller polymerization shrinkage and shrinkage force and higher flexural modulus than FB-RBC.

Gap formation in a restorative resin material was in proportion with the level of polymerization shrinkage.[16] A higher level of polymerization shrinkage stress may also result in a larger amount of microleakage.[17] In the present study, the correlation between $\%IM_{whole}$ and linear polymerization shrinkage and shrinkage stress was also relatively high. The %IM of RB-RBCs (TB and SF) was lower than FB- RBCs (SD and VB). This is consistent with a previous study.[18]

In this study, the correlation between $\%IM_{whole}$ and linear polymerization shrinkage and shrinkage

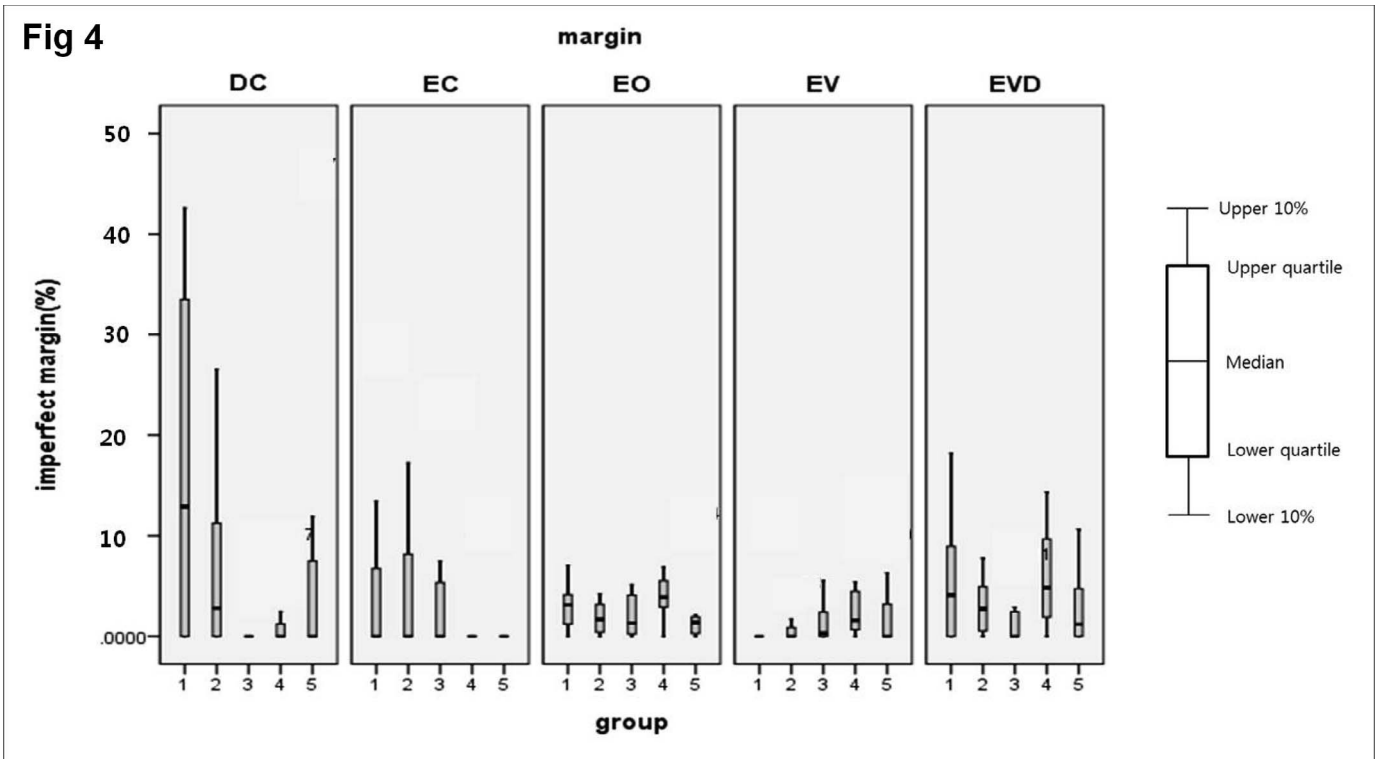

Figure 4. *The % ratio of the imperfect margin (%IM) in each tooth area before thermomechanical loading. EO, occlusal enamel margins; EV, vertical enamel margin; EC, cervical enamel margins of the shallow proximal cavity; EVD, vertical enamel margins; DC, cervical dentin margin of the deep proximal cavity. Group 1: Z3 (Control), Group 2: SD+Z3, Group 3: VB+Z3, Group 4: TB, Group 5: SF.*

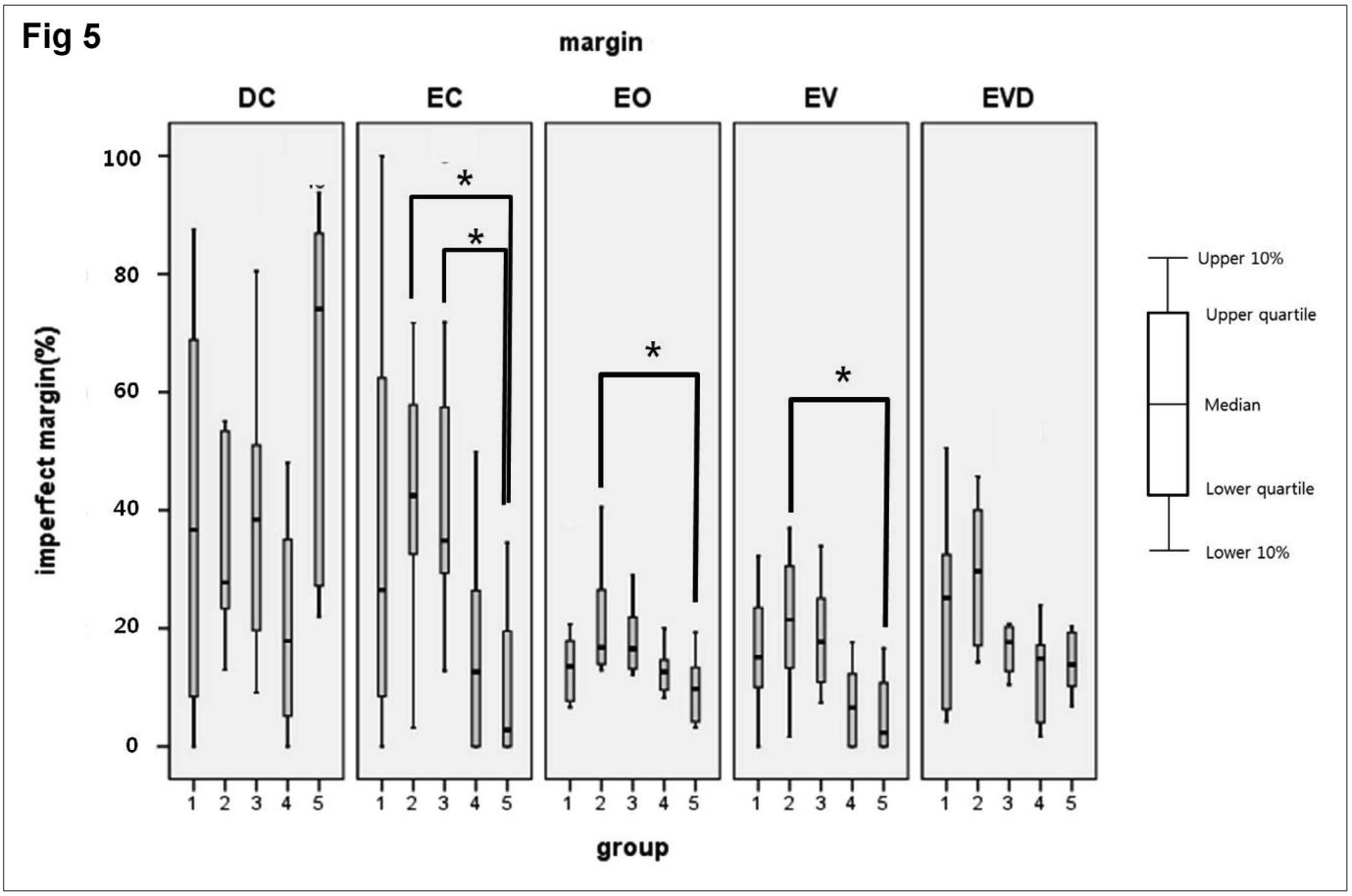

Figure 5. *The % ratio of the imperfect margin (%IM) in each tooth area after thermomechanical loading. * indicates significant differences in the %IM between groups (p = 0.028 in EC, 0.044 in EO, and 0.015 in EV). EO, occlusal enamel margins; EV, vertical enamel margin, EC: cervical enamel margins of the shallow proximal cavity, EVD, vertical enamel margins; DC, cervical dentin margins of the deep proximal cavity. Group 1: Z3 (Control), Group 2: SD+Z3, Group 3: VB+Z3, Group 4: TB, Group 5: SF.*

stress was higher in postloading (0.697 and 0.708) than in preloading (0.362 and 0348). In the preloading state, the influence of polymerization shrinkage and stress might be masked due to the tight bonding between the composites and the tooth, but their influence might remain in the margin as residual stresses. After loading, their influences might be shown more evidently when the bonding between composites and teeth is weakened through the loading process.

The higher volume percentage of the fillers RB-RBCs compared to FB-RBCs may affect the polymerization shrinkage, shrinkage stress, and flexural modulus. According to the manufacturer, the volume percentage of fillers in SD and VB are 44% and 38%, respectively, (Table 1), which are lower than those of TB and SF (55% and 68%, respectively). When the contents of the fillers increase, the contents of monomers decrease, resulting in a reduction of the total level of polymerization shrinkage and shrinkage stress and an increase in the flexural modulus of the material.[19,20]

FB-RBCs were placed only in a core portion of the cavity and Z3 was placed in the outer portion in groups 2 and 3. When the authors consider the core portion of this study as a base, they also consider that the flexural modulus of the core portion may affect the marginal adaptation. It was reported that base material with a lower flexural modulus, such as flowable resins, could absorb the impact that is applied during mechanical loading, and this may result in better marginal adaptation.[21,22] Kwon and others[15] reported that the marginal adaptation was different in the final restoration when the base or lining materials of a different flexural modulus were used. They reported that the optimal range of flexural modulus in flowable RBCs as base materials of 1 mm thick was 4 to 6 GPa, within which the base material can effectively buffer the occlusal stress, and that the moduli that were lower or higher than

this range resulted in a more imperfect margin. In their study, the flexural modulus of the experimental flowable RBC, which was 2 GPa, showed worse results than the other groups. In the present study, the flexural modulus in VB and SD was 2.35 and 3.29 GPa, respectively, and it seems that these low moduli negatively affect the marginal adaptation of the overlying final restoration. In addition, a relatively thick layer of core material was used in groups 2 and 3 (3.5 mm in the central area and 5.5 mm in the deep proximal area), and the thickness of Z3 was 1 mm or less in some areas due to the limitation of the cavity depth. The impact of thick, low modulus FB-RBCs under thin Z3 overlying restorations would be intensified to a greater degree.

According to research conducted by Watts and others,[23] an acceptable curing depth is achieved if the bottom hardness corresponds to at least 80% of the top surface hardness. In the present study, the bottom hardness exceeded 80% of surface hardness in all bulk fills except SF. This result is consistent with previous studies.[24,25] The lower bottom/top surface hardness ratio in SF may be related with its lower translucency than other bulk fill RBCs.[26] In the present study, the cavity depth was 6.5 mm in the deep proximal area. The relatively higher value in %IM in SF in the DC margin may be due to the insufficient cure of this material even though additional light curing was applied from the occlusal direction after the matrix band was removed from the proximal cavities. In clinical situations, care should be taken for the light-curing time in the deep proximal cavity, and additional light-curing time may be necessary. On the other hand, Alrahlah and others[27] reported that SF and TBF had higher depth of cure than VBF. Further studies are needed to clarify this.

It was reported that 30 seconds of curing time, which was longer than the manufacturer's recommendation for bulk fill RBCs (10 to 20 seconds), had positive effects on polymerization properties so that enhanced light curing of bulk fills in deep cavities was recommended.[28] In the present study, after 20 seconds of light curing for FB-RBC, 80 seconds of light curing was applied additionally for capping composite (groups 2 and 3). In groups 4 and 5, RB-RBCs were light cured for 20 seconds, and 80 seconds of additional light curing was applied after removing the retainer and matrix band. The sum of 100 seconds of light curing may have positive effects on the results of the present study.

According to the manufacturer, TB contains an initiator called Ivocerin. It is a germanium-based photoinitiator and has a higher photocuring activity than camphorquionone (CQ). It shows a higher absorption spectrum in the 350- to 470-nm range compared to CQ. It has the potential to reduce the curing time and increase the curing depth of composites.[29] As a result, it may enable even deeper polymerization in the present study, and it may be related to the higher bottom/top surface hardness ratio of TB (0.82) than SF (0.68) and Z3 (0.73) (Table 2). Ilie and others[30] reported that the influence of parameter irradiation time, distance away from the light tip, and depth on the elastic modulus, microhardness, and degree of conversion (DC) were material dependent. According to them, the strongest effect on all measured properties was exerted by the depth followed by irradiation time and distance away from light tip in TB.

Fok,[31] in his mathematical model, successfully predicted shrinkage stress's dependence on the interaction between the entire system's compliance and the material properties. In his model, the shrinkage stress decreased as the compliance of the system increased, and the faster the creep rate, the lower the shrinkage stress in zero compliance. When composites are cured in an MOD cavity, the cusps move inward and this cusp deflection could relieve shrinkage stress of composites in a cavity. Considering this, shrinkage force measurement allowing compliance of an instrument was recommended to simulate the situation in the MOD cavity.[32] In this study, the compliance of the testing machine for the shrinkage force measurement was 0.3 μm/N. As the recorded polymerization force was between 3 and 5 kgf in the present study, about 9 to 15 μm of movement of the testing machine occurred during measurement, which was consistent with the amount of cuspal deflection in the MOD cavity.[3]

In shrinkage force measurement, the c-factor is determined by the diameter and height of the specimens ($d/2h$, where d = diameter and h = height). In the present study, the c-factor of the composite specimens for shrinkage force measurement was 4, whereas it was 2.1 for the MOD restorations. It would have been more ideal if the former were 2.1, but the authors could not increase the height of the specimens as was wanted due to the flow of FB-RBC.

In a study using the Zurich wear testing method, a 5-kgf (49 N) load of 1,200,000 cycles and a themocycling of 5°C to 55°C was applied to mimic five years of service *in vivo*.[33] Considering the results of this study, the stress of thermomechanical loading of the present study would correspond to 2.5 years *in vivo*.

Traditionally, the marginal quality has been assessed with SEM at high magnification (200×).[34] However, stereomicroscopy has also been successfully used recently at lower magnification (6×, 20×, 40×, 100×).[15,35-38] It is simpler and easier to record. Heintze and others[38] pointed out that assessing the margin at 200× magnification would be clinically irrelevant because minor gaps of 2 to 5 μm and minor discrepancies would be recorded. They also indicated that semiquantitative evaluation by means of a stereomicroscope (6×) yielded a statistically significant lower defective margin value than did the SEM (200×) evaluation, but there was a strong correlation between the two evaluation methods. In the present study, 100× stereomicroscope was used according to the method by Kwon and others.[15] Further research is needed to determine clinical relevance.

CONCLUSION

Within the limitations of this study, RB-RBCs showed better marginal adaptation than FB-RBCs. The lower level of polymerization shrinkage and polymerization shrinkage stress in RB-RBCs seems to contribute to this finding because it would induce less polymerization shrinkage force at the margin. FB-RBCs with lower flexural modulus may not provide an effective buffer to occlusal stress when they are capped with regular RBCs.

Regulatory Statement

This study was conducted in accordance with all the provisions of the local human subjects oversight committee guidelines and policies of Yonsei University Dental Hospital. The approval code for this study is #12-0149.

Conflict of Interest

The authors of this article certify that they have no proprietary, financial, or other personal interest of any nature or kind in any product, service, and/or company that is presented in this article.

(Accepted 15 October 2016)

REFERENCES

1. Krejci I, Planinic M, Stavridakis M, & Bouillaguet S (2005) Resin composite shrinkage and marginal adaptation with different pulse-delay light curing protocols *European Journal of Oral Sciences* **113(6)** 531-536.
2. Jensen ME, & Chan DCN (1985) Polymerization shrinkage and microleakage In: Vanherle G, Smith DC (eds) *Posterior Composite Resin Dental Restorative Materials*. 3M Company, St Paul, MN 243-262.
3. Kim ME, & Park SH (2011) Comparison of premolar cuspal deflection in bulk or in incremental composite restoration methods *Operative Dentistry* **36(3)** 326-334.
4. Abbas G, Fleming GJ, Harrington E, Shortall AC, & Burke FJ (2003) Cuspal movement and microleakage in premolar teeth restored with a packable composite cured in bulk or in increments *Journal of Dentistry* **31(6)** 437-444.
5. Versluis A, Douglas WH, Cross M, & Sakaguchi RL (1996) Does an incremental filling technique reduce polymerization shrinkage stresses? *Journal of Dental Research* **75(3)** 871-878.
6. Hofmann N, Markert T, Hugo B, & Klaiber B (2003) Effect of high intensity vs. soft-start halogen irradiation on light-cured resin-based composites. Part I. Temperature rise and polymerization shrinkage *American Journal of Dentistry* **16(6)** 421-430.
7. Haak R, Wicht MJ, & Noack MJ (2003) Marginal and internal adaptation of extended Class I restorations lined with flowable composites *Journal of Dentistry* **31(4)** 231-239.
8. Dietrich T, Losche AC, Losche GM, & Roulet JF (1999) Marginal adaptation of direct composite and sandwich restorations in Class II cavities with cervical margins in dentine *Journal of Dentistry* **27(2)** 119-128.
9. Ilie N, Bucuta S, & Draenert M (2013) Bulk-fill resin-based composites: An in vitro assessment of their mechanical performance *Operative Dentistry* **38(6)** 618-625.
10. Czasch P, & Ilie N (2013) In vitro comparison of mechanical properties and degree of cure of bulk fill composites *Clinical Oral Investigations* **17(1)** 227-235.
11. Roggendorf MJ, Kramer N, Appelt A, Naumann M, & Frankenberger R (2011) Marginal quality of flowable 4-mm base vs. conventionally layered resin composite *Journal of Dentistry* **39(10)** 643-647.
12. Moorthy A, Hogg CH, Dowling AH, Grufferty BF, Benetti AR, & Fleming GJ (2012) Cuspal deflection and microleakage in premolar teeth restored with bulk-fill flowable resin-based composite base materials *Journal of Dentistry* **40(6)** 500-505.
13. Kim HJ, & Park SH (2014) Measurement of the internal adaptation of resin composites using micro-CT and its correlation with polymerization shrinkage *Operative Dentistry* **39(2)** E57-E70.
14. Chuang SF, Jin YT, Liu JK, Chang CH, & Shieh DB (2004) Influence of flowable composite lining thickness on Class II composite restorations *Operative Dentistry* **29(3)** 301-308.
15. Kwon OH, Kim DH, & Park SH (2010) The influence of elastic modulus of base material on the marginal adaptation of direct composite restoration *Operative Dentistry* **35(4)** 441-447.
16. Peutzfeldt A, & Asmussen E (2004) Determinants of in vitro gap formation of resin composites *Journal of Dentistry* **32(2)** 109-115.
17. Ferracane JL (2005) Developing a more complete understanding of stresses produced in dental composites during polymerization *Dental Materials* **21(1)** 36-42.

18. Poggio C, Chiesa M, Scribante A, Mekler J, & Colombo M (2013) Microleakage in Class II composite restorations with margins below the CEJ: In vitro evaluation of different restorative techniques *Medicina Oral, Patologia Oral y Cirugia Bucal* **18(5)** e793-e798.
19. Braga RR, Ballester RY, & Ferracane JL (2005) Factors involved in the development of polymerization shrinkage stress in resin-composites: A systematic review *Dental Materials* **21(10)** 962-970.
20. El-Damanhoury H, & Platt J (2014) Polymerization shrinkage stress kinetics and related properties of bulk-fill resin composites *Operative Dentistry* **39(4)** 374-382.
21. Kemp-Scholte CM, & Davidson CL (1990) Marginal integrity related to bond strength and strain capacity of composite resin restorative systems *Journal of Prosthetic Dentistry* **64(6)** 658-664.
22. Senawongse P, Pongprueksa P, & Tagami J (2010) The effect of the elastic modulus of low-viscosity resins on the microleakage of Class V resin composite restorations under occlusal loading *Dental Materials Journal* **29(3)** 324-329.
23. Watts DC, Amer O, & Combe EC (1984) Characteristics of visible-light-activated composite systems *British Dental Journal* **156(6)** 209-215.
24. Benetti AR, Havndrup-Pedersen C, Honore D, Pedersen MK, & Pallesen U (2015) Bulk-fill resin composites: Polymerization contraction, depth of cure, and gap formation *Operative Dentistry* **40(2)** 190-200.
25. Garcia D, Yaman P, Dennison J, & Neiva G (2014) Polymerization shrinkage and depth of cure of bulk fill flowable composite resins *Operative Dentistry* **39(4)** 441-448.
26. Bucuta S, & Ilie N (2014) Light transmittance and micro-mechanical properties of bulk fill vs. conventional resin based composites *Clinical Oral Investigations* **18(8)** 1991-2000.
27. Alrahlah A, Silikas N, & Watts DC (2014) Post-cure depth of cure of bulk fill dental resin-composites *Dental Materials* **30(2)** 149-154.
28. Zorzin J, Maier E, Harre S, Fey T, Belli R, Lohbauer U, Petschelt A, & Taschner M (2015) Bulk-fill resin composites: Polymerization properties and extended light curing *Dental Materials* **31(3)** 293-301.
29. Moszner N, Fischer UK, Ganster B, Liska R, & Rheinberger V (2008) Benzoyl germanium derivatives as novel visible light photoinitiators for dental materials *Dental Materials* **24(7)** 901-907.
30. Ilie N, Kessler A, & Durner J (2013) Influence of various irradiation processes on the mechanical properties and polymerisation kinetics of bulk-fill resin based composites *Journal of Dentistry* **41(8)** 695-702.
31. Fok AS (2013) Shrinkage stress development in dental composites—An analytical treatment *Dental Materials* **29(11)** 1108-1115.
32. Ferracane JL (2008) Buonocore Lecture. Placing dental composites—A stressful experience *Operative Dentistry* **33(3)** 247-257.
33. Heintze SD (2006) How to qualify and validate wear simulation devices and methods *Dental Materials* **22(8)** 712-734.
34. Roulet JF, Reich T, Blunck U, & Noack M (1989) Quantitative margin analysis in the scanning electron microscope *Scanning Microscopy* **3(1)** 147-158; discussion 158-149.
35. Keshvad A, Hooshmand T, Asefzadeh F, Khalilinejad F, Alihemmati M, & Van Noort R (2011) Marginal gap, internal fit, and fracture load of leucite-reinforced ceramic inlays fabricated by CEREC inLab and hot-pressed techniques *Journal of Prosthodontics* **20(7)** 535-540.
36. Korkut L, Cotert HS, & Kurtulmus H (2011) Marginal, internal fit and microleakage of zirconia infrastructures: An in-vitro study *Operative Dentistry* **36(1)** 72-79.
37. Tamac E, Toksavul S, & Toman M (2014) Clinical marginal and internal adaptation of CAD/CAM milling, laser sintering, and cast metal ceramic crowns *Journal of Prosthetic Dentistry* **112(4)** 909-913.
38. Heintze SD, Monreal D, & Peschke A (2015) Marginal quality of Class II composite restorations placed in bulk compared to an incremental technique: Evaluation with SEM and stereomicroscope *Journal of Adhesive Dentistry* **17(2)** 147-154.

©Operative Dentistry, 2017, **42-4,** 387-395

Masking Colored Substrates Using Monolithic and Bilayer CAD-CAM Ceramic Structures

GR Basso • AB Kodama • AH Pimentel • MR Kaizer • A Della Bona • RR Moraes • N Boscato

Clinical Relevance

Bilayer ceramic systems are viable options for challenging clinical situations where discolored teeth or metal abutments need to be masked. Although the monolithic lithium disilicate seems to be able to mask a C4-shaded substrate, thinner bilayer structures showed similar results.

SUMMARY

Objective: To evaluate the masking ability and translucency of monolithic and bilayer CAD-CAM ceramic structures.

Methods: Discs of high translucency (HT) and low translucency (LT) lithium disilicate–based ceramic (IPS e.max CAD) with different thicknesses (0.7, 1, 1.5, and 2 mm) were evaluated as a monolithic structure or combined (bilayer) with a 0.5-mm-thick zirconia framework (IPS e.max ZirCAD). The masking ability and translucency were calculated based on CIE L*a*b* color coordinates measured with a spectrophotometer (SP60, X-Rite). The translucency parameter (TP) was calculated using color coordinates measured over standard white-and-black backgrounds. The masking ability was calculated by CIEDE2000 color difference metric (ΔE_{00}) for each specimen measured over a tooth-colored substrate (shade A2) compared to three darker backgrounds (shade C4 and two metal substrates). Confidence intervals (CI) for the means (95% CI) were calculated for TP and ΔE_{00}. The Pearson correlation between ΔE_{00} and TP was investigated for monolithic and bilayer structures over all backgrounds.

Results: The thinner the lithium disilicate layer, the greater the translucency and the higher the ΔE_{00} values. The effect of ceramic thickness on both translucency and masking

Gabriela R Basso, DDS, MSc, PhD, postdoctoral fellow, Graduate Program in Dentistry, Federal University of Pelotas, Pelotas, Brazil

Ayumi B Kodama, DDS, master student, Graduate Program in Dentistry, Federal University of Pelotas, Pelotas, Brazil

Alice H Pimentel, DDS, private practice, Pelotas, Brazil

Marina R Kaizer, DDS, MSc, PhD, postdoctoral fellow, Graduate Program in Materials Science and Engineering, Federal University of Pelotas, Pelotas, Brazil

Alvaro Della Bona, DDS, MSc, PhD, senior professor and Dean, Dental School, Postgraduate Program in Dentistry, University of Passo Fundo, Passo Fundo, Brazil.

Rafael R Moraes, DDS, MSc, PhD, professor, Graduate Program in Dentistry, Federal University of Pelotas, Pelotas, Brazil

*Noéli Boscato, DDS, MSc, PhD, professor, Graduate Program in Dentistry, Federal University of Pelotas, Pelotas, Brazil

*Corresponding author: Gonçalves Chaves Street 457, CEP 96015-560, Pelotas, RS, Brazil; e-mail: noeliboscato@gmail.com

DOI: 10.2341/16-247-L

ability was more pronounced for the monolithic structures. In addition, monolayers always presented a greater color variation than their bilayer counterparts. The metallic background produced greater ΔE_{00} than the C4-shaded substrate.

Conclusion: Monolithic veneers were able to mask C4-shaded background but did not mask metallic backgrounds. Bilayer structures showed greater shade masking ability than monolithic structures.

INTRODUCTION

Dental esthetics complaints are often related to discolored teeth or restorations.[1,2] Achieving natural tooth-like restoration is an important aspect influencing the treatment success.[1,2] Restorative procedures that involve full-coverage ceramic restorations are often associated with intraradicular retainers.[3] Although glass-fiber posts have been widely used,[3-5] there are still clinical cases demanding esthetic restorations over metallic post and cores.[3-5] Masking metallic cores and discolored tooth substrates with all-ceramic restorations is still one of the greatest challenges for restorative dentistry.

A diversity of all-ceramic systems is currently available, attempting to cover distinct clinical scenarios by combining strength and esthetics. Another important aspect that differentiates the various ceramic systems is their fabrication technique. Restorations placed after a chair-side single visit have an appealing advantage over the traditional multistep laboratory fabrication: reduced time to complete the treatment. Glass ceramics are often used in chair-side CAD-CAM dental treatments. The lithium disilicate–based ceramic (eg, IPS e.max CAD, Ivoclar Vivadent, Schaan, Liechtenstein) is the strongest glass ceramic yet shows superior esthetic qualities in its monolithic presentation.[6] On the other hand, the traditional multistep lab technique offers the possibility to achieve excellent individualization of the restoration and the use of zirconia infrastructure. Zirconia is the strongest and toughest of the dental ceramics,[7-10] and its opaque appearance yields high masking ability.[11,12] But zirconia is not esthetically pleasant; thus, most restorations demand a second fabrication step: veneering with an esthetic ceramic to obtain an optical appearance similar to natural teeth.[13,14]

Combining a machined glass veneer with a machined zirconia framework is a new trend in all-ceramic systems. The bonding of the two pieces can be achieved by a fused glass layer (CAD-on system, Ivoclar Vivadent) or bonding with a composite resin (VITA Rapid Layer Technology, Vita Zahnfabrik, Bad Sackingen, Germany). Reported benefits of these systems include the use of a veneer ceramic[6,15,16] with lower porosity because of the CAD-CAM fabrication technology.[17-22] Yet there is no report on the optical characteristics of all-ceramic restorations fabricated by milling both the veneer and the framework structures.

Choosing a ceramic system for an esthetic restoration that demands masking ability is challenging. One may question whether a relatively easy-to-make monolithic glass-ceramic restoration is a suitable option or whether a thinner bilayer veneered zirconia restoration would present better masking ability, thus allowing the preservation of tooth structure. Therefore, the aim of this study was to evaluate the masking ability and translucency of CAD-CAM ceramic structures (monolayer and bilayer) with different thicknesses, testing the hypothesis that the masking ability is influenced by the thickness, translucency, and layering of the ceramic structure.

METHODS AND MATERIALS

Study Design

This *in vitro* study had a $2 \times 2 \times 4 \times 3$ factorial design (n=10), with the following factors under investigation: structural design (two levels: monolayer—CAD-CAM lithium disilicate; bilayer —CAD-CAM lithium disilicate veneer + zirconia framework), translucency of the veneer (two levels: high translucency [HT] and low translucency [LT]), thickness of the veneer layer (four levels: 0.7, 1.0, 1.5, and 2.0 mm), and background colored substrates (three levels: shade C4, coppery, and silvery). Figure 1 presents a diagram of the study design.

A lithium disilicate–based glass ceramic (IPS e.max CAD, Ivoclar Vivadent), clinically indicated for monolithic restorations or veneering material, and zirconia-based ceramic (IPS e.max ZirCAD, Ivoclar Vivadent), used as a framework material, were used in the present study. The response variables included the translucency parameter (TP) and the masking ability estimated by the CIEDE2000 color difference metric (ΔE_{00}) over a typical dental shade substrate (A2) and discolored backgrounds (shade C4, coppery, and silvery). The correlation between TP and ΔE_{00} was also investigated.

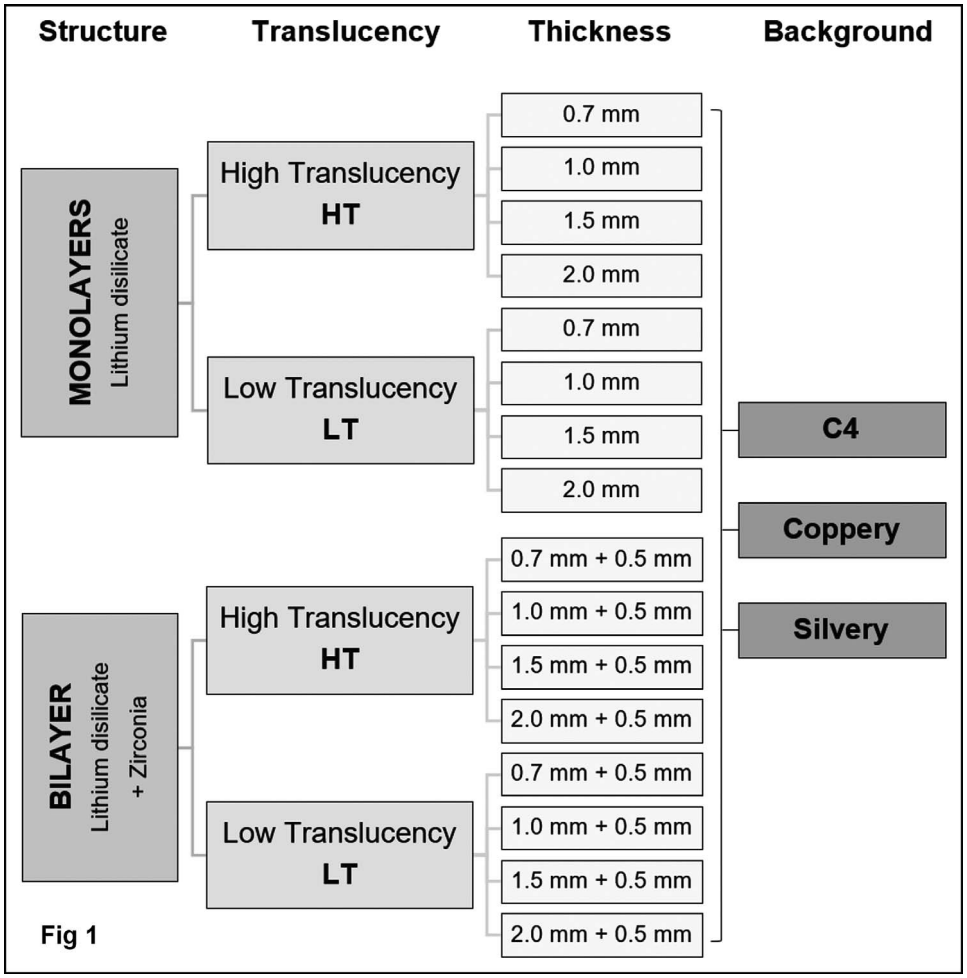

Figure 1. *Diagram of the experimental design.*

Preparation of Ceramic Structures

Discs (diameter 10 mm) from A1 shade of HT and LT IPS e.max CAD blocks were cut with thicknesses of 0.7, 1.0, 1.5, and 2.0 mm, simulating monolayer restorations. Additionally, 0.5-mm-thick zirconia discs were produced from IPS e.max ZirCAD blocks to simulate the framework of bilayer restorations. All discs had both sides polished to 1200-grit SiC paper under running water. For the bilayer structures, a drop of glycerin was placed between the glass-ceramic and the zirconia discs. Glycerin was also used between the ceramic structures and the background substrate. A liquid coupling medium, such as glycerin, is necessary to avoid undesirable effects of air on optical properties, thus minimizing light scattering due to different refractive indices (ie, air and ceramic).[23]

Preparation of Background Substrates

Tooth substrate was simulated with 2-mm-thick porcelain specimens (Vita VM7, dentin, Vita Zahnfabrik). Shades A2 (positive control) and C4 (dark substrate) were used as tooth-like substrates. Additionally, discs were fabricated from two metal alloys, with coppery (Pd-Cu, 79% Pd, Spartan Plus, Ivoclar Vivadent) and silvery (Ag-Pd, 80% Ag, Pratalloy, Dentsply Caulk, Milford, DE, USA) appearance. Fabrication procedures were carried out according to the manufacturers' recommendations. The background specimens were flattened with 600-grit SiC abrasive papers, and the top surface was polished to 1200-grit SiC abrasive papers, always under running water.

Measuring the Color Coordinates

The CIE L*a*b* color coordinates of monolithic and bilayer specimens were measured with a spectrophotometer (SP60, X-Rite, Grand Rapids, MI, USA). The spectrophotometer was plugged into a voltage stabilizer to avoid changes in light source intensity. The equipment was calibrated on the standard tiles provided by the manufacturer. The specimens were

Table 1: *Mean (95% confidence interval) Values for the Translucency Parameter (TP) of Monolayer (Lithium Disilicate–Based Ceramic) and Bilayer (Lithium Disilicate–Based Ceramic + 0.5-mm-Thick Zirconia Framework) Ceramic Structures.*

Veneer Ceramic[a]	TP Monolayer[b]	TP Bilayer[b]
HT0.7	44.9 (44.2-45.6) A	13.8 (13.5-14.1) A
HT1.0	37.3 (36.8-37.8) B	12.1 (11.8-12.4) C
HT1.5	29.4 (28.8-30.0) D	10.2 (9.9-10.5) E
HT2.0	22.9 (22.6-23.2) F	8.3 (7.9-8.7) F
LT0.7	34.4 (33.9-34.9) C	13.1 (12.8-13.4) B
LT1.0	27.3 (26.7-27.9) E	11.1 (10.7-11.5) D
LT1.5	22.2 (21.7-22.7) F	9.0 (8.7-9.3) F
LT2.0	15.5 (15.2-15.8) G	6.6 (6.4-6.8) G

[a] *HT, high translucency; LT, low translucency. The number represents the thickness of specimens.*
[b] *Different letters following the values in the same column indicate statistically significant differences.*

evaluated over white (L^*=93.1, a^*=1.3, b^*=5.3) and black (L^*=27.9, a^*=0.0, b^*=0.0) backgrounds as well as over simulated tooth substrates: shades A2 (L^*=88.1, a^*=4.9, b^*=16.3) and C4 (L^*=79.0, a^*=5.3, b^*=12.9). Simulated metal abutments were also used as background substrates: coppery (L^*=57.5, a^*=6.5, b^*=18.4) and silvery (L^*=57.1, a^*=1.7, b^*=5.0).

Evaluation of TP

TP was estimated by the difference between color coordinates measured over a white background (L^*_W, a^*_W, and b^*_W) and a black background (L^*_B, a^*_B, and b^*_B) using the following equation:[24]

$$TP = [(L*_W - L*_B)^2 + (a*_W - a*_B)^2 + (b*_W - b*_B)^2]^{1/2}$$

Evaluation of Masking Ability

The masking ability was estimated by calculating the CIEDE2000 color variation (ΔE_{00}) between each ceramic structure over a light tooth-colored substrate (A2) and over the dark backgrounds (C4, coppery, and silvery), according to the following equation:[24,25]

$$\Delta E_{00} = [(\Delta L'/K_L S_L)^2 + (\Delta C'/K_C S_C)^2 + (\Delta H'/K_H S_H)^2 + R_T(\Delta C'/K_C S_C)(\Delta H'/K_H S_H)]^{1/2}$$

where $\Delta L'$, $\Delta C'$, and $\Delta H'$ are the differences in lightness, chroma, and hue between two sets of color coordinates; R_T is the rotation function that accounts for the interaction between chroma and hue differences in the blue region; S_L, S_C, and S_H are the weighting functions used to adjust the total color difference for variation in perceived magnitude with variation in the location of the color coordinate difference between two color readings; and K_L, K_C, and K_H are the correction terms for the experimental conditions.

Clinical thresholds described by Paravina and others[26] were considered. The perceptibility and acceptability thresholds were set at $\Delta E_{00} = 0.8$ and $\Delta E_{00} = 1.8$, respectively.

Statistical Analysis

Confidence intervals (CI) for the means (95% CI) were calculated for TP and ΔE_{00}. Groups were considered significantly different when the 95% CI bounds did not overlap. A *post hoc* power analysis was carried out with TP and ΔE_{00} data. The Pearson test was used to investigate the correlation between ΔE_{00} and TP for monolithic and bilayer structures over all backgrounds, reporting the linear regression coefficients (R^2) and their respective p-values.

RESULTS

TP

Table 1 presents the TP values for all groups, showing that the presence of a 0.5-mm zirconia framework (bilayer) significantly increased the opacity compared to the monolayer counterparts. Even the thinner bilayers (0.7 mm veneer + 0.5 mm zirconia) were more opaque than the thicker monolayers (2 mm). Within HT and LT groups, a reduction in thickness resulted in an increase in translucency for monolayer and bilayer structures. The HT groups showed higher translucency values than LT structures with the same thickness regardless of the structural design (monolayer or bilayer). The power analysis indicated a beta = 1 (power = 100%) for TP data.

Masking Ability

Figure 2 presents the results of ΔE_{00} for the masking ability of discolored substrates. The color variation over metallic backgrounds was always significantly higher than over the C4 simulated tooth substrate. For all substrates, within the same translucency and veneer thickness, monolayer groups presented a lower masking ability than bilayer groups. Over C4 simulated tooth substrate, thinner bilayers (0.7 mm veneer + 0.5 mm zirconia) presented masking ability similar to that of thicker monolayers (2 mm).

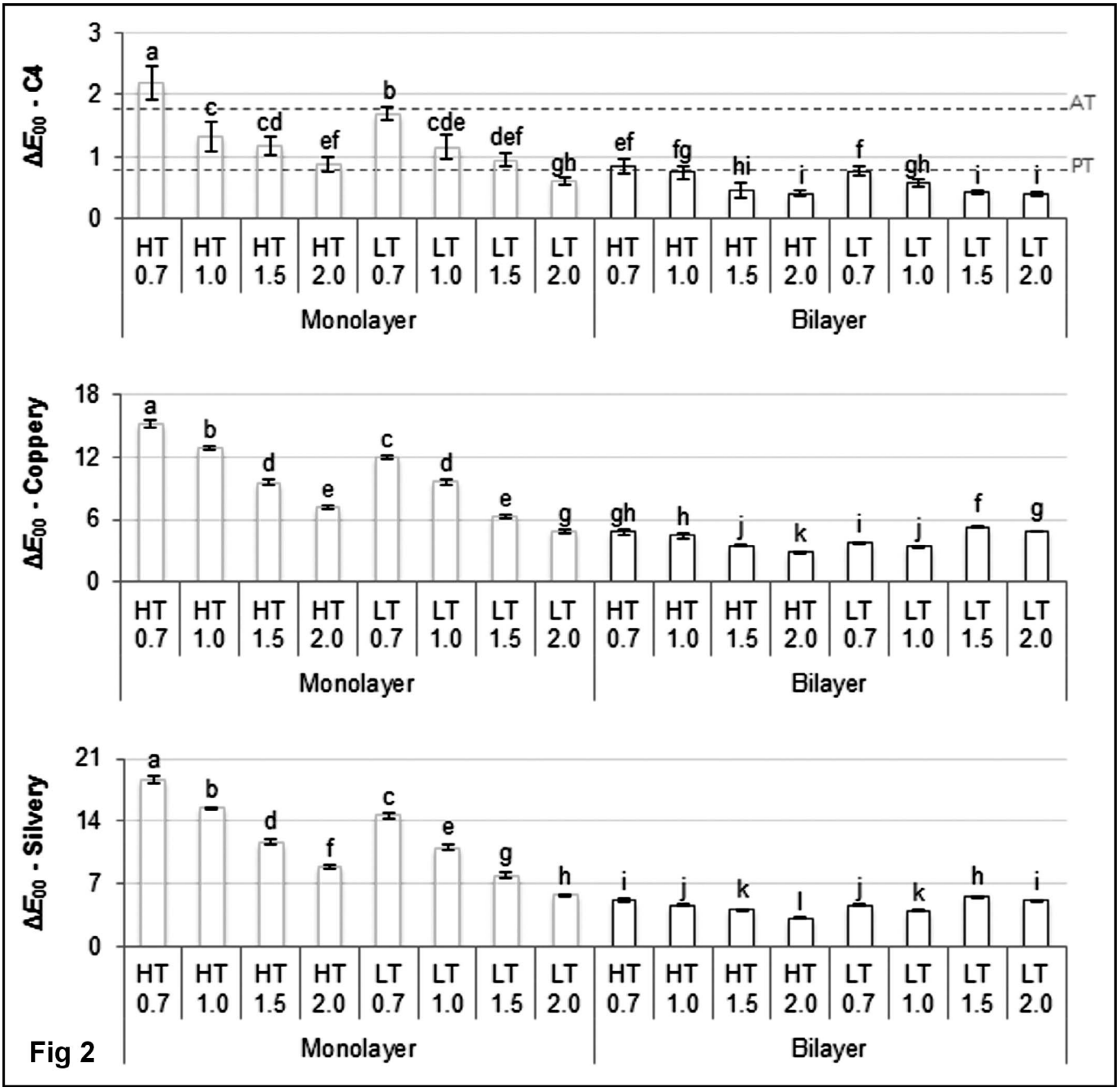

Figure 2. *Bar graph showing the mean and 95% confidence interval of color variations (ΔE_{00}) estimating the masking ability of monolayer and bilayer structures over discolored substrates (C4, coppery and silvery). The dashed lines seen in the C4 graph represent visual thresholds for 50%:50% perceptibility ($\Delta E_{00} = 0.8$) and acceptability ($\Delta E_{00} = 1.8$) of the color difference between two shades.[26] Those lines are not shown in the coppery and silvery charts because all groups had ΔE_{00} values above these thresholds. Different letters above columns in each graph indicate significance difference between groups.*

Nonetheless, over metallic backgrounds, thinner bilayers presented superior masking ability than thicker monolayers. For monolayers, regardless of the substrate, thinner ceramic structures produced lower masking ability. This effect was less evident for bilayers, especially when LT structures were used. For monolayer structures with the same thickness, HT ceramic most often showed a poorer masking ability than LT ceramic. On the other hand, the masking ability of bilayer structures of the same thickness was less sensitive to differences in ceramic translucency (HT or LT). The best masking ability

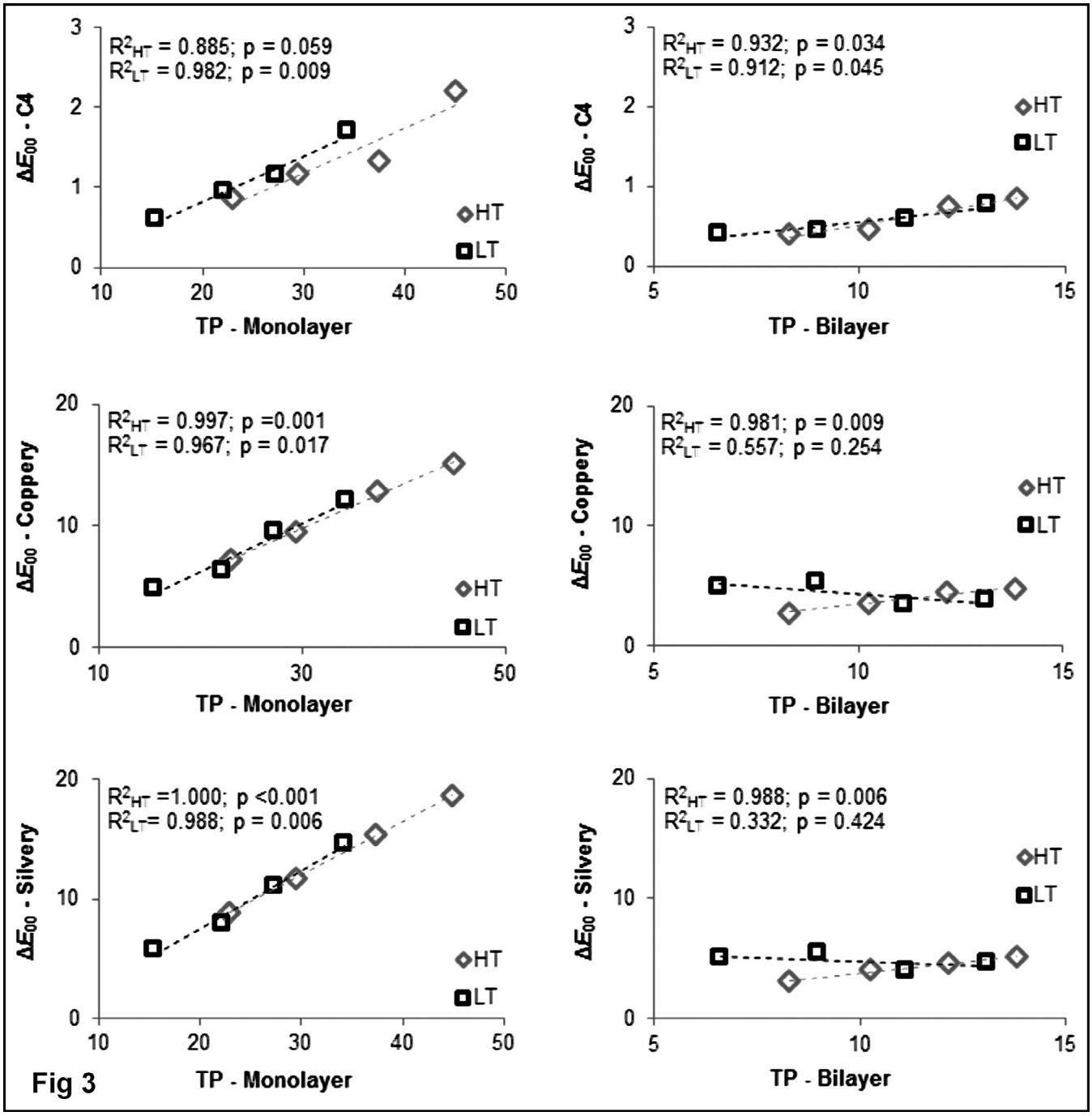

Figure 3. *Correlations between* ΔE_{00} *and TP for the monolayer and bilayer groups over the different backgrounds. Linear regression coefficients* (R^2) *and their respective* p*-values are shown for each correlation.*

for monolayers was achieved with LT2.0 (C4 ΔE_{00}=0.6, coppery ΔE_{00}=4.88, silvery ΔE_{00}=5.69). For the bilayers, HT2.0 showed the best masking ability (C4 ΔE_{00}=0.41, coppery ΔE_{00}=2.82, silvery ΔE_{00}=3.13), which was not statistically different from groups LT1.5 and LT2.0 over the C4 substrate. The power analysis indicated a beta = 1 (power =100%) for ΔE_{00} data.

Correlation Between TP and ΔE_{00}

Figure 3 shows the correlation between TP and ΔE_{00} for all groups evaluated over the three discolored

substrates (C4, coppery, and silvery). For all monolithic ceramic structures, the correlations were strong and positive for both ceramic translucencies (HT and LT) regardless of the color background (C4, coppery, or silvery). Similar correlations were also found for the bilayer structures over the C4 background. The bilayer structures placed over metallic substrates (coppery and silvery) showed similar correlations. For monolayer structures over metallic substrates, correlations were strong and positive for both HT and LT veneers. For bilayer structures over metallic substrates, strong and positive correlations were observed only when HT veneers were used. LT veneers resulted in no significant correlation between TP and ΔE_{00}.

DISCUSSION

The present study evaluated the masking ability and translucency of the CAD-CAM ceramic structures used as either a monolayer (lithium disilicate–based glass-ceramic) or a bilayer (lithium disilicate veneer with zirconia framework), confirming the hypothesis that the masking ability is influenced by the thickness, translucency, and layering of the ceramic structure. A ceramic veneer layer with lower translucency (LT material and/or greater thickness) and the presence of the zirconia framework greatly favored the masking of the discolored substrates. The ability of ceramic restorations to mask discolored backgrounds and their final esthetic appearance result from a complex balance of factors that are not restricted to those evaluated in this study and mentioned above.[11,27-29]

Concerning translucency, the present study showed that thinner ceramic specimens had higher TP values, which is in line with previous studies.[30,31] In addition, greater TP values were found for the thinnest HT glass-ceramic specimens (0.7 mm) of both monolayer and bilayer ceramic structures. Previous studies have shown that the color of restorations is significantly affected by ceramic thickness and substrate shade.[27,29-33] Therefore, the indication of translucent and thinner ceramic restorations should be restricted to substrates closely matching the desired final color of the restorations.

Furthermore, the findings of the present study showed that the bilayer structure (CAD/CAM fabricated zirconia-based ceramic framework veneered with a lithium disilicate–based glass ceramic) has a lower TP than the counterpart monolayer ceramic structure (monolithic CAD/CAM lithium disilicate–based glass ceramic). Even the thinner bilayer (0.7 mm veneer + 0.5 mm zirconia) was more opaque than the thicker monolayer (2 mm). This observation can be explained by the following: 1) the opacity of the dense zirconia framework, which hinders light transmittance through the bilayer restoration, and 2) the refractive index mismatch between glass ceramic and zirconia—the light beam is scattered while traveling across media with different refractive indexes.[23] Considering this rationale, it can be suggested that a bilayer structure allows the preservation of tooth structure by using a thinner restoration yet offers a better esthetic appearance than a monolithic ceramic structure to mask dark substrates.

All evaluated ceramic structures (except for the monolithic HT0.7) showed acceptable (AT) values for masking a simulated tooth-discolored C4 substrate. The best C4 substrate masking ability was obtained with LT2.0 monolayers and all bilayers, which stayed under the perceptibility threshold. With regard to color and appearance of dental restorations, thresholds for perceptible/acceptable color mismatch are constantly being revised in the literature.[26,34-36] Some color difference formulas using weighting factors, including CIEDE2000 (K_L:K_C:K_H), were developed to predict color differences.[37] The present study used the parametric factors $K_L = 1$, $K_C = 1$ and $K_H = 1$, which are used for the CIEDE2000 (1:1:1) color difference metric. Yet studies on visual judgments performed on the acceptability of dental ceramics[38] and the comparison of visual and instrumental shade matching in dentistry[37] showed that using CIEDE2000 (2:1:1), where $K_L = 2$, resulted in color differences that better correlated to visual observations from average observers. In addition, a recent worldwide multicenter study[26] reported that 50% of the observers perceive a color difference[24] that reaches $\Delta E_{00} > 0.8$ (PT), yet they will consider the color difference unacceptable only when it reaches values of $\Delta E_{00} > 1.8$ (AT). Such findings were considered for the ISO/DTR 28642 standard[39] and adopted in the present study.

Regarding the masking of simulated metal abutments (coppery and silvery backgrounds), none of the evaluated ceramic structures were able to yield $\Delta E_{00} < 1.8$,[26] which would correspond to a clinically acceptable color difference (AT) in comparison to the control, observed over the A2 simulated dental substrate. This observation held true regardless of the structural thickness or the presence of the zirconia framework, in agreement with other studies.[40,41]

The present study provided additional scientific support to overcome the clinical challenge of esthetically masking dark substrates, such as metal abutments, using all-ceramic restorations. Yet there still is a need for further investigation on whether increasing the thickness of the zirconia framework as well as the use of opaque cements and/or opaque pigments could offer acceptable masking of metal abutments. The use of glycerin as a coupling agent between the glass-ceramic and the zirconia discs may not replicate the optical effects of the fusing layer (glass or composite resin) and is a limitation of the present study. Nonetheless, it eliminates light scattering between the two ceramic layers.[23] Further investigation is needed to understand the optical effects of various fusing materials used to bond machined glass veneer to the machined zirconia framework.

CONCLUSIONS

Within the limitations of this *in vitro* study, the following conclusions can be drawn:

- Monolithic CAD-CAM lithium disilicate was able to mask a discolored tooth background but did not succeed in masking metallic substrates;
- Bilayer ceramic structures, associating a CAD-CAM zirconia framework with a CAD-CAM lithium disilicate veneer, improved masking over all evaluated substrates.

Conflict of Interest

The authors of this article certify that they have no proprietary, financial, or other personal interest of any nature or kind in any product, service, and/or company that is presented in this article.

(Accepted 14 November 2016)

REFERENCES

1. Land MF, & Hopp CD (2010) Survival rates of all-ceramic systems differ by clinical indication and fabrication method *Journal of Evidence-Based Dental Practice* **10(1)** 37-38, http://dx.doi.org/10.1016/j.jebdp.2009.11.013.
2. Larson TD (2003) 25 years of veneering: What have we learned? *Northwest Dentistry* **82(4)** 35-39.
3. Fernandes AS, Shetty S, & Coutinho I (2003) Factors determining post selection: A literature review *Journal of Prosthetic Dentistry* **90(6)** 556-562, http://dx.doi.org/10.1016/S002239130300622X.
4. Sarkis-Onofre R, Jacinto Rde C, Boscato N, Cenci MS, & Pereira-Cenci T (2014) Cast metal vs. glass fibre posts: A randomized controlled trial with up to 3 years of follow up *Journal of Dentistry* **42(5)** 582-587, http://dx.doi.org/10.1016/j.jdent.2014.02.003.
5. Soares CJ, Valdivia AD, da Silva GR, Santana FR, & Menezes Mde S (2012) Longitudinal clinical evaluation of post systems: A literature review *Brazilian Dental Journal* **23(2)** 135-140, http://dx.doi.org/10.1590/S0103-64402012000200008.
6. Pieger S, Salman A, & Bidra AS (2014) Clinical outcomes of lithium disilicate single crowns and partial fixed dental prostheses: A systematic review *Journal of Prosthetic Dentistry* **112(1)** 22-30, http://dx.doi.org/10.1016/j.prosdent.2014.01.005.
7. Al-Amleh B, Lyons K, & Swain M (2010) Clinical trials in zirconia: A systematic review *Journal of Oral Rehabilitation* **37(8)** 641-652, http://dx.doi.org/10.1111/j.1365-2842.2010.02094.x.
8. Denry I, & Kelly JR (2008) State of the art of zirconia for dental applications *Dental Materials* **24(3)** 299-307, http://dx.doi.org/10.1016/j.dental.2007.05.007.
9. Larsson C, & Wennerberg A (2014) The clinical success of zirconia-based crowns: A systematic review *International Journal of Prosthodontics* **27(1)** 33-43, http://dx.doi.org/10.11607/ijp.3647.
10. Lawn BR, Pajares A, Zhang Y, Deng Y, Polack MA, Lloyd IK, Rekow ED, & Thompson VP (2004) Materials design in the performance of all-ceramic crowns *Biomaterials* **25(14)** 2885-2892, http://dx.doi.org/10.1016/j.biomaterials.2003.09.050.
11. Choi YJ, & Razzoog ME (2013) Masking ability of zirconia with and without veneering porcelain *Journal of Prosthodontics-Implant Esthetic and Reconstructive Dentistry* **22(2)** 98-104, http://dx.doi.org/10.1111/j.1532-849X.2012.00915.x.
12. Zhang Y (2014) Making yttria-stabilized tetragonal zirconia translucent *Dental Materials* **30(10)** 1195-1203, http://dx.doi.org/10.1016/j.dental.2014.08.375.
13. Heffernan MJ, Aquilino SA, Diaz-Arnold AM, Haselton DR, Stanford CM, & Vargas MA (2002) Relative translucency of six all-ceramic systems. Part II: Core and veneer materials *Journal of Prosthetic Dentistry* **88(1)** 10-15, http://dx.doi.org/10.1067/mpr.2002.126795.
14. Heffernan MJ, Aquilino SA, Diaz-Arnold AM, Haselton DR, Stanford CM, & Vargas MA (2002) Relative translucency of six all-ceramic systems. Part I: Core materials *Journal of Prosthetic Dentistry* **88(1)** 4-9, http://dx.doi.org/10.1067/mpr.2002.126794.
15. Della Bona A, Nogueira AD, & Pecho OE (2014) Optical properties of CAD-CAM ceramic systems *Journal of Dentistry* **42(9)** 1202-1209, http://dx.doi.org/10.1016/j.jdent.2014.07.005.
16. Sulaiman TA, Delgado AJ, & Donovan TE (2015) Survival rate of lithium disilicate restorations at 4 years: A retrospective study *Journal of Prosthetic Dentistry* **114(3)** 364-366, http://dx.doi.org/10.1016/j.prosdent.2015.04.011.
17. Basso GR, Moraes RR, Borba M, Duan Y, Griggs JA, & Della Bona A (2016) Reliability and failure behavior of CAD-on fixed partial dentures *Dental Materials* **32(5)** 624-630, http://dx.doi.org/10.1016/j.dental.2016.01.013.
18. Basso GR, Moraes RR, Borba M, Griggs JA, & Della Bona A (2015) Flexural strength and reliability of monolithic and trilayer ceramic structures obtained by the CAD-on

technique *Dental Materials* **31(12)** 1453-1459, http://dx.doi.org/10.1016/j.dental.2015.09.013.

19. Griggs JA (2007) Recent advances in materials for all-ceramic restorations *Dental Clinics of North America* **51(3)** 713-727, http://dx.doi.org/10.1016/j.cden.2007.04.006.
20. Kanat B, Comlekoglu EM, Dundar-Comlekoglu M, Hakan B, Ozcan M, & Gungor MA (2014) Effect of various veneering techniques on mechanical strength of computer-controlled zirconia framework designs *Journal of Prosthodontics-Implant Esthetic and Reconstructive Dentistry* **23(6)** 445-455, http://dx.doi.org/10.1111/jopr.12130.
21. Schmitter M, Mueller D, & Rues S (2012) Chipping behaviour of all-ceramic crowns with zirconia framework and CAD/CAM manufactured veneer *Journal of Dentistry* **40(2)** 154-162, http://dx.doi.org/10.1016/j.jdent.2011.12.007.
22. Schmitter M, Mueller D, & Rues S (2013) In vitro chipping behaviour of all-ceramic crowns with a zirconia framework and feldspathic veneering: comparison of CAD/CAM-produced veneer with manually layered veneer *Journal of Oral Rehabilitation* **40(7)** 519-525, http://dx.doi.org/10.1111/joor.12061.
23. Nogueira AD, & Della Bona A (2013) The effect of a coupling medium on color and translucency of CAD-CAM ceramics *Journal of Dentistry* **41(Supplement 3)** e18-e23, http://dx.doi.org/10.1016/j.jdent.2013.02.005.
24. CIE Technical Committee (2004) Colorimetry, CIE pub no 15.3 *Vienna: CIE Central Bureau*.
25. Sharma G, Wu W, & Dalal EN (2005) The CIEDE2000 color-difference formula: Implementation notes, suplementary test data, and mathematical observations *Color Research and Application* **30** 21-30, http://dx.doi.org/10.1002/col.20070.
26. Paravina RD, Ghinea R, Herrera LJ, Della Bona A, Igiel C, Linninger M, Sakai M, Takahashi H, Tashkandi E, & Perez Mdel M (2015) Color difference thresholds in dentistry *Journal of Esthetic and Restorative Dentistry* **27(Supplement 1)** S1-S9, http://dx.doi.org/10.1111/jerd.12149.
27. Boscato N, Hauschild FG, Kaizer MR, & Moraes RR (2015) Effectiveness of combination of dentin and enamel layers on the masking ability of porcelain *Brazilian Dental Journal* **26(6)** 654-659, http://dx.doi.org/10.1590/0103-6440201300463.
28. Chaiyabutr Y, Kois JC, Lebeau D, & Nunokawa G (2011) Effect of abutment tooth color, cement color, and ceramic thickness on the resulting optical color of a CAD/CAM glass-ceramic lithium disilicate-reinforced crown *Journal of Prosthetic Dentistry* **105(2)** 83-90, http://dx.doi.org/10.1016/S0022-3913(11)60004-8.
29. Perroni AP, Amaral C, Kaizer MR, Moraes RR, & Boscato N (2016) Shade of resin-based luting agents and final color of porcelain veneers *Journal of Esthetic and Restorative Dentistry* **28(5)** 295-303, http://dx.doi.org/10.1111/jerd.12196.
30. Azer SS, Rosenstiel SF, Seghi RR, & Johnston WM (2011) Effect of substrate shades on the color of ceramic laminate veneers *Journal of Prosthetic Dentistry* **106(3)** 179-183, http://dx.doi.org/10.1016/S0022-3913(11)60117-0.
31. Bachhav VC, & Aras MA (2011) The effect of ceramic thickness and number of firings on the color of a zirconium oxide based all ceramic system fabricated using CAD/CAM technology *Journal of Advanced Prosthodontics* **3(2)** 57-62, http://dx.doi.org/10.4047/jap.2011.3.2.57.
32. de Azevedo Cubas GB, Camacho GB, Demarco FF, & Pereira-Cenci T (2011) The effect of luting agents and ceramic thickness on the color variation of different ceramics against a chromatic background *European Journal of Dentistry* **5(3)** 245-252.
33. Ozturk O, Uludag B, Usumez A, Sahin V, & Celik G (2008) The effect of ceramic thickness and number of firings on the color of two all-ceramic systems *Journal of Prosthetic Dentistry* **100(2)** 99-106, http://dx.doi.org/10.1016/S0022-3913(08)60156-0.
34. Ghinea R, Perez MM, Herrera LJ, Rivas MJ, Yebra A, & Paravina RD (2010) Color difference thresholds in dental ceramics *Journal of Dentistry* **38** E57-E64, http://dx.doi.org/10.1016/j.jdent.2010.07.008.
35. Johnston WM, & Kao EC (1989) Assessment of appearance match by visual observation and clinical colorimetry *Journal of Dental Research* **68(5)** 819-822.
36. Ragain JC, & Johnson WM (2000) Color acceptance of direct dental restorative materials by human observers *Color Research and Application* **25(4)** 278-285, http://dx.doi.org/10.1002/1520-6378(200008)25:4<278::Aid-Col8>3.0.Co;2-F.
37. Pecho OE, Ghinea R, Alessandretti R, Perez MM, & Della Bona A (2016) Visual and instrumental shade matching using CIELAB and CIEDE2000 color difference formulas *Dental Materials* **32(1)** 82-92, http://dx.doi.org/10.1016/j.dental.2015.10.015.
38. Perez MD, Ghinea R, Herrera LJ, Ionescu AM, Pomares H, Pulgar R, & Paravina RD (2011) Dental ceramics: A CIEDE2000 acceptability thresholds for lightness, chroma and hue differences *Journal of Dentistry* **39** E37-E44, http://dx.doi.org/10.1016/j.jdent.2011.09.007.
39. ISO/TR 28642:2011 (2011) Dentistry—Guidance on colour measurement, http://www.iso.org.
40. Della Bona A, Pecho OE, Ghinea R, Cardona JC, & Perez MM (2015) Colour parameters and shade correspondence of CAD-CAM ceramic systems *Journal of Dentistry* **43(6)** 726-734, http://dx.doi.org/10.1016/j.jdent.2015.02.015.
41. Kurklu D, Azer SS, Yilmaz B, & Johnston WM (2013) Porcelain thickness and cement shade effects on the colour and translucency of porcelain veneering materials *Journal of Dentistry* **41(11)** 1043-1050, http://dx.doi.org/10.1016/j.jdent.2013.08.017.

©Operative Dentistry, 2017, **42-4,** 396-406

Ferrule-Effect Dominates Over Use of a Fiber Post When Restoring Endodontically Treated Incisors: An *In Vitro* Study

P Magne • PC Lazari • MA Carvalho • T Johnson • AA Del Bel Cury

Clinical Relevance

The use of a post for the restoration of nonvital incisors with a ferrule is not necessary. The additional time, materials, and risk involved in the placement of the post do not provide an increase in mechanical resistance. Post placement can be correlated with unrestorable fractures.

ABSTRACT

Objectives: The aim of this study was to investigate the restoration of broken-down endodontically treated incisors with the ferrule effect using glass ceramic crowns bonded to composite resin core buildups with or without a fiber post. A no-ferrule group with post was also included for comparison.

Methods and Materials: Thirty decoronated endodontically treated bovine incisors with a 2-mm ferrule were restored with a direct buildup using a nanohybrid direct composite resin (Miris 2 and Optibond FL) with or without a glass-fiber–reinforced post. An additional group of 15 teeth without a ferrule were restored with buildup and a fiber post. All teeth were prepared to receive bonded glass ceramic crowns (e.max CAD luted with Variolink Esthetic DC) and were subjected to accelerated fatigue testing. Cyclic isometric loading was applied to the incisal edge at an angle of 30° and a frequency of 5 Hz, beginning with a load of 100 N (×5000 cycles). A 100 N load increase was applied each 15,000 cycles. Specimens were loaded until failure or to a maximum of 1000 N (×140,000 cycles). Groups were compared using the Kaplan Meier survival analysis (log rank test at $p=0.05$).

Results: None of the tested specimens withstood all 140,000 load cycles. Specimens with

*Pascal Magne, BSc, MSc, DMD, PhD, The Don & Sybil Harrington Professor of Esthetic Dentistry, Department of Restorative Sciences, Herman Ostrow School of Dentistry, University of Southern California, Los Angeles, CA, USA

Priscilla C Lazari, DDS, MS, Department of Prosthodontics and Periodontology, Piracicaba Dental School, University of Campinas, São Paulo,Brazil

Marco A Carvalho, DDS, MS, Department of Prosthodontics and Periodontology, Piracicaba Dental School, University of Campinas, São Paulo, Brazil

Taoheed Johnson, DMD, Advanced Specialty in Endodontics, Taoheed Johnson, DMD, Advanced Specialty in Endodontics, Herman Ostrow School of Dentistry, University of Southern California, Los Angeles, CA, USA

Altair A Del Bel Cury, DDS, PhD, professor, Department of Prosthodontics and Periodontology, Piracicaba Dental School, State University of Campinas, São Paulo, Brazil

*Corresponding author: 925 W 34th St, Los Angeles, CA 90089, USA; e-mail: magne@usc.edu

DOI: 10.2341/16-243-L

posts but without a ferrule were affected by an initial failure phenomenon (wide gap at the lingual margin between the buildup/crown assembly and the root). There was a significant difference in mean survived cycles between the ferrule groups (Fp=73,332× and FNp=73,244×) and the no-ferrule group (50,121×; p=0.001). The addition of a fiber post was not significant in the presence of the ferrule (p=0.884). In both groups with posts, 100% of failures were unrestorable. The no-post group had 47% of restorable and possibly restorable failures.

Conclusions: The survival of broken-down nonvital incisors was improved by the presence of the ferrule but not by the fiber-reinforced post. Fiber posts were always detrimental to the failure mode and were not able to compensate for the absence of a ferrule.

INTRODUCTION

The restoration of severely broken-down and endodontically treated incisors (ETI) is a major challenge in daily practice. Endodontically treated teeth have significantly different mechanical properties compared to vital teeth. The main modifications in the biomechanics of the tooth are attributable to the loss of tissue following caries lesion, fracture, or cavity preparation, including the access cavity before endodontic therapy.[1,2]

There is a general agreement that the ferrule is the most important mechanical factor[3-5] for the strength of ETI. The presence of an adequate ferrule decreases the impact of the post and core system, luting agents, and the final restoration on the performance of endodontically restored teeth.[3] Teeth prepared with a ferrule have a tendency to fail in a more favorable mode.[6] The amount of suggested ferrule varies from 1 mm[7] to 1.5 mm[8] up to 2 mm.[3] The resistance seems to increase significantly with an increased ferrule height,[9] and a better prognosis can be expected if the ferrule is circumferential.[10]

Traditionally, direct posts are used to retain adhesive core buildups in ETI. Hence, studies about ETI typically compare different types of buildup methods that usually include posts. When deciding to use a direct post, glass-fiber–reinforced (GFR) posts seem to have many benefits (adhesion, tooth-like flexibility, esthetics, etc.).[4,11,12] However, despite all the benefits of GFR posts, their selection and indication are still not fully understood. Earlier publications have reported loss of retention as a major mode of failure for glass-fiber posts luted with resin cements.[13-15] In addition, the preparation of an access channel, canal enlargement during endodontic procedures, and the use of specific chemicals as well as the post placement itself significantly reduce tooth strength.[2]

In posterior teeth, placement of a post has already proven not to significantly improve fracture resistance compared with composite resin core without extra retentive features.[16,17] Whenever a post is used, fewer restorable fractures are expected.[16,18] The uselessness of a post was even demonstrated on premolars[18] using restorative composite and a proven classic adhesive. Pereira and others[19] demonstrated the importance of the ferrule on canines, while Lima and others[20] showed the uselessness of posts in incisors; however, both studies used a single-load-to-failure experiment and metal crowns. Post insertion for teeth showing a minor substance loss should be critically reconsidered.[11] Thus, there is still a lack of scientific information about restoration of ETI with bonded ceramic crowns. Progress in dentin bonding and the so-called biomimetic approach[21] have triggered new ways of restoring ETI using adhesive ceramic crowns, and it has become more acceptable to restore ETI with extensive loss of coronal structure without a post.

Hence, the objective of the present study was to investigate the restoration of ETI with a ferrule using glass ceramic crowns bonded to composite resin core buildups with or without a fiber post. A no-ferrule group with a fiber post was also included for comparison.

The null hypotheses were that 1) the use of a GFR post and 2) the presence of ferrule would not influence the accelerated fatigue strength of ETI and that 3) the presence of a GFR post would not affect the failure mode of the restored ETI tested in this *in vitro* study.

METHODS AND MATERIALS

Tooth Preparation

Forty-five bovine incisors (n=15) with similar dimensions and pulp space were selected and stored in thymol-saturated solution (Thymol, Aqua Solutions Inc, Deer Park, TX, USA). The sample size was determined by a pilot study, without performing a power analysis, following similar experimental designs of previous studies.[16,18] All teeth were decoronated, up to either 15 mm (ferrule group) or 13 mm (no-ferrule group) from the apex, and subsequently separated into three groups: FP = ferrule with GFR

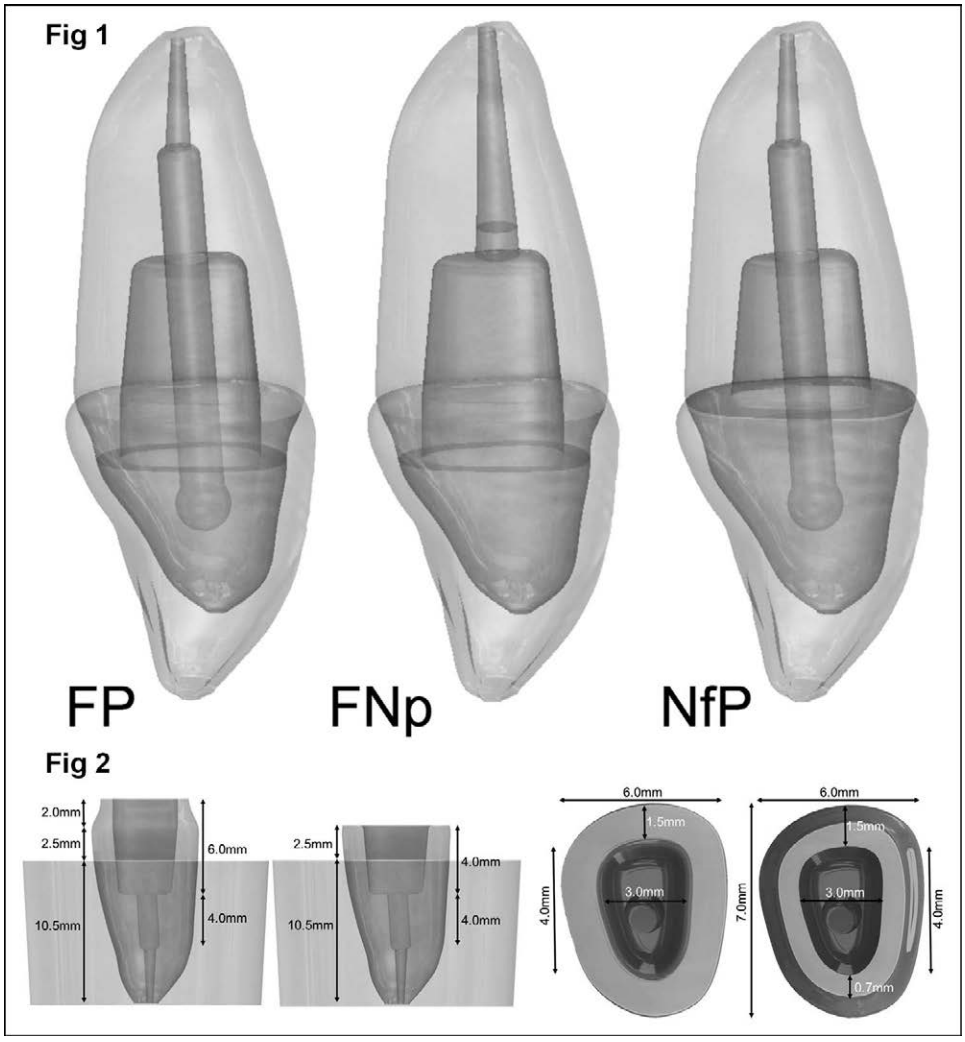

Figure 1. *Schematic views of restored endodontically treated incisors. (A): Group FP. (B): Group FNp. (C): Group NfP.*
Figure 2. *Schematic view of root dimensions before restoration.*

post and resin core buildup, FNp = ferrule and direct resin core buildup, or NfP = no ferrule with GFR post and resin core buildup (Figures 1 and 2). The specimens were mounted in a special positioning device with acrylic resin (Palapress Vario, Heraeus Kulzer, Armonk, NY, USA) embedding 11.5 mm of the root. For the ferrule groups, the specimens were prepared with a tapered round-ended diamond bur (Brasseler, Savannah, GA, USA), creating a 2-mm-high/1-mm-thick circular ferrule and a 0.8-mm horizontal circular chamfer (cervical limit). Table 1 presents the brand, company and qualitative composition information of materials used in the present study.

Endodontic Treatment

Standard chemomechanical endodontic protocol with ideal irrigants ensued.[22,23] The canals were instrumented to at least a size of 40/06 with K3XF rotary files (Sybron Endo, Orange, CA, USA) by crowning down and maintaining patency with a 10k file between rotary files. The canals were irrigated with 17% EDTA (Roydent, Johnson City, TN, USA) for one minute followed by 5.25% NaOCl (Chlorox, Oakland, CA, USA) for one minute as a final rinse.[24,25] The efficacy of irrigation was amplified by Endo Activator (Dentsply, Tulsa Dental Specialties, Tulsa, OK, USA) each with EDTA and NaOCl. After the canals were dried with paper points, one coat of Thermaseal Plus (Dentsply) was placed circumferentially around the lumen all the way to the working length with a 10 K-file. Then 0.6-taper K3XF gutta-percha cones (Sybron Endo) were coated with Thermaseal Plus and used for warm vertical obturation; the gutta-percha was thermoplasticized with a 0.6-taper Buchanan heated plugger (Sybron Endo) and then packed down with stainless-steel Buchanan hand pluggers (Sybron Endo).

Table 1: *Material Application, Brand Name, Composition, and Manufacturers of the Materials Used in the Study*

Application	Brand Name	Composition	Manufacturer
Acrylic resin for tooth mounting	Palapress Vario	*Powder*: methyl methacrylate copolymer	Hereaus Kulzer (Wehrheim, Germany)
		Liquid: methyl methacrylate, dimethacrylate	
Dual cure self-adhesive universal resin cement for post cementation	RelyX Unicem 2	*Base paste*: methacrylate monomers containing or not containing phosphoric acid groups, silanated fillers, initiator components stabilizers, rheological additives	3M ESPE (Seefeld, Germany)
		Catalyst paste: methacrylate monomers; alkaline (basic) fillers; silanated fillers; initiator components; stabilizers; pigments; rheological additives	
Fiber post	Parapost Fiber Lux	60% glass fiber, 40% resin	Coltène Whaledent (Altstätten, Switzerland)
Glass ionomer barrier	Vitrebond Plus	*Liquid*: resin-modified polyalkenoic acid, HEMA (2-hydroxyethymethacrylate), water and initiators (including camphorquinone)	3M ESPE
		Paste: HEMA, BIS-GMA, water, initiators, a radiopaque fluoroaluminosilicate glass	
Silicatization	Rocatec Soft	High-purity 30-μm aluminum oxide, modified with silica	3M ESPE
Total-etch adhesive system	Optibond FL	*Primer*: 2-hydroxyethyl methacrylate ethanol, 2-[2-(methacryloyloxy)ethoxycarbonyl]benzoic acid, glycerol phosphate dimethacrylate	Kerr (Orange, CA, USA)
		Adhesive: 2-hydroxyethyl methacrylate, 3-trimethoxysilylpropyl methacrylate, 2-hydroxy-1,3-propanediyl bismethacrylate, alkali fluorosilicates(Na)	
Composite resin for core/buildup	Miris 2	Methacrylate, barium glass, silanized, amorphous silica, hydrophobed	Coltène Whaledent
Silanization	Monobond Plus	Alcohol solution of silane methacrylate, phosphoric acid methacrylate, sulfide methacrylate.	Ivoclar Vivadent (Schaan, Liechtenstein)
Self-etch adhesive system	Adhese Universal	Phosphoric acid methacrylate, methacrylated carboxylic acid polymer, hydrophilic monofunctional methacrylate, hydrophilic/hydrophobic crosslinking dimethacrylate, hydrophobic crosslinking dimethacrylate	Ivoclar Vivadent
Resin cement for restoration luting	Variolink Esthetic Dual Cure	*Monomer matrix*: urethane dimethacrylate, inorganic fillers (ytterbium trifluoride and spheroid mixed oxide), initiators, stabilizers, pigments	Ivoclar Vivadent
Acid for ceramic surface treatment	IPS Ceramic Etching Gel	5% hydrofluoric acid	Ivoclar Vivadent
Glass ceramic for restoration	IPS e.max CAD	SiO_2, Li_2O, K_2O, P_2O_5, ZrO_2, ZnO, Al_2O_3, MgO, coloring oxides	Ivoclar Vivadent

Preparation of Root Canal and Internal Ferrule

For post groups, gutta-percha was removed 8 mm deep into the pulp chamber from the cervical limit with a Reamer pilot drill size no. 3 (Ivoclar Vivadent, Schaan, Liechtenstein) using a hand piece at 1000 to 2000 rpm. For all groups, a so-called internal ferrule was prepared in the form of a box using a conical-shaped bur 4 mm deep from the cervical limit of the crown preparation.

Post Groups Preparation

The post spaces were prepared with ParaPost drills specifically designed for the ParaPost Fiber

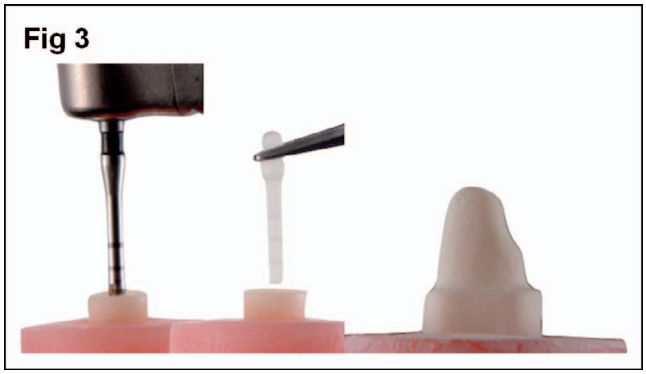

Figure 3. *Post insertion and buildup.*

Lux (no. 6, 1.5-mm diameter, Coltène Whaledent, Altstätten, Switzerland) (Figure 3). Using a cutting disc, the apical portion of the posts was removed to obtain a length of 11 mm (8 mm below and 3 mm above the cervical limit of the crown preparation). Prior to the luting procedure, the posts were cleaned with alcohol and air-dried. The post space walls were lightly coated with cement (RelyX Unicem 2 Automix, 3M ESPE, Seefeld, Germany), and the post was inserted. Cement excesses were cleaned, leaving 4 mm of post height in the cement. The cement system was light cured for 40 seconds (VALO Curing Light, Ultradent Products, Inc, South Jordan, UT, USA). After post cementation, the exposed dentin walls and the post were sandblasted with 30-μm silicated Al_2O_3 powder (Rocatec Soft, 3M ESPE). Silane (Ceramic Primer, 3M ESPE) was applied to the post head and air-dried. For dentin bonding purposes, 35% phosphoric acid (Ultra-Etch, Ultradent Products) was used for etching for 10 seconds, dentin walls and post rinsed and gently dried, followed by application of the adhesive system (Optibond FL Primer and Adhesive, Kerr, Orange, CA, USA) and light curing for 40 seconds (VALO Curing Light). All buildups were obtained with five to six 2-mm-thick increments of Miris 2 (Coltène Whaledent), each polymerized at 1000 mW/cm^2 (VALO Curing Light) for 40 seconds. An air-blocking barrier (KY Jelly, Johnson & Johnson Inc, Montreal, QC, Canada) was used to cover the preparation surface, and additional polymerization was carried out for 10 seconds per surface. Special care was taken to shape the Miris 2 buildup ideally in order to avoid any further corrections of the preparation surface and margins. All buildups were 11 mm high (4 mm internal and 7 mm above the cervical limit of the crown preparation).

No-Post Group Preparation

After internal ferrule preparation, a 1-mm-thick GI barrier (Vitrebond Plus, 3M ESPE) was placed followed by sandblasting (Rocatec Soft), acid etching of all exposed dentin (Ultra-Etch), and application of the adhesive system (Optibond FL Primer and Adhesive). The same buildup technique and materials were used as for the two post groups.

Design and Manufacturing of Restorations

All bonded ceramic crowns were fabricated using the Cerec 3 CAD/CAM system (Sirona Dental Systems GmbH, Bensheim, Germany). Digital impressions of the prepared teeth were performed with Cerec Blue Cam, using a contrast powder (IPS Contrast Spray Chairside, Ivoclar Vivadent). The specimens were fitted with a crown of standardized thickness and anatomy with 11-mm inciso-cervical length and 9-mm mesio-distal width. All crowns were milled in lithium disilicate ceramic (IPS e.max CAD, Ivoclar Vivadent) using the "crown mode" with the sprue located at the lingual surface. After milling, lithium disilicate restorations were glazed, crystallized, and fired according to the manufacturer's protocol (Programat CS, Ivoclar Vivadent) using IPS Object Fix Putty and IPS e.max CAD Crystall/Glaze Spray (Ivoclar Vivadent). The steps of digital design as well as the final restoration are presented in Figures 4 through 6.

Adhesive Luting of the Crowns

The dual-cure resin cement Variolink Esthetic DC (Ivoclar Vivadent) was used. Before luting, each restoration was fit on its respective tooth to check its marginal adaptation. All crowns were cleaned in an ultrasonic bath in distilled water followed by etching with 5% hydrofluoric acid (IPS ceramic etching gel, Ivoclar Vivadent) for 20 seconds and postetching cleaning for one minute in distilled water in an ultrasonic bath. Silane (Monobond Plus, Ivoclar Vivadent) was applied with a microbrush and heat dried at 100°C for five minutes in a minioven (D.I.-500, Coltène Whaledent).

The tooth preparation and buildups were sandblasted with 30-μm silicated Al_2O_3 powder (Rocatec Soft) and coated with Adhese Universal (Ivoclar Vivadent). Variolink Esthetic was then applied to the fitting surface of the crown and seated on the tooth with approximately 500*g* of pressure. Cement excesses were removed and followed by light polymerization three times for 20 seconds on each surface (buccal and lingual) with an LED light

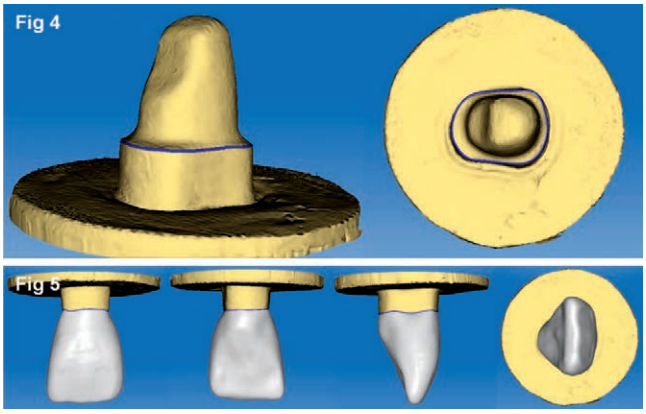

Figure 4. *CAD data set of preparation with preparation line.*
Figure 5. Standardization of crown design using Cerec software. All crowns were 11 mm high and 9 mm in mesial–distal width.

(VALO Curing Light). Air-blocking barrier (KY Jelly) and additional polymerization was carried out for 10 seconds per surface. The margins were finished with hand instruments (scalpel and scaler). The samples were stored in distilled water at room temperature (24°C) for a minimum of 24 hours following adhesive restoration placement and then subjected to accelerated fatigue testing.

Accelerated Fatigue Test

Masticatory forces were simulated in an artificial mouth using a closed-loop electrodynamic system (Acumen 3, MTS Systems, Eden Prairie, MN, USA). The chewing cycle was simulated by an isometric contraction (load control) applied through a flat composite resin antagonist (Z100, 3M ESPE). The force was applied at a palatal angle of 30° with the flat surface contacting three-fourths of the incisal edge (Figure 7). The load chamber was filled with distilled water to submerge the sample during testing. A cyclic load was applied at a frequency of 5 Hz, starting with a load of 100 N (warm-up of 5000 cycles), followed by stages of 200, 300, 400, 500, 600, 700, 800, 900, and 1000 N at a maximum of 15,000 cycles for each force. Samples were loaded until fracture or to a maximum of 140,000 cycles.

Analysis

All fatigue tests were monitored using a macro video camera and recorded continuously in order to determine the crack propagation mode (initial gap, root fracture, and final fracture). The numbers of endured cycles, load to failure, and failure mode of each specimen were recorded. After the test, each sample was evaluated by transillumination (Microlux, Addent, Danbury, CT, USA) and an optical

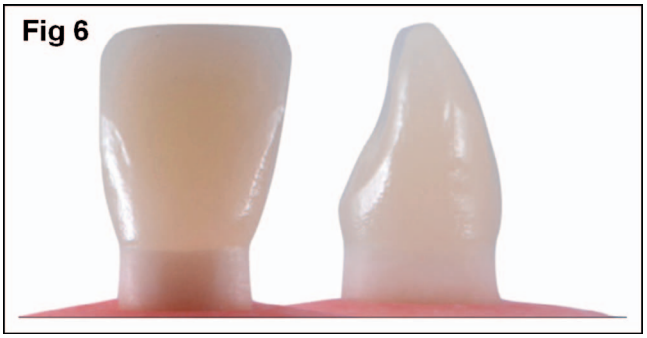

Figure 6. *Final assembly after cementation.*

microscope (Leica MZ 125, Leica Microsystems, Wetzlar, Germany) at 10:1 magnification. A visual distinction was made among three fracture modes, considering the reparability of the tooth: catastrophic, that is, root fracture that would require tooth extraction; possibly reparable, that is, cohesive/adhesive failure with fragment and minor damage, chip, or crack of underlying tooth structure; or reparable fracture, that is, cohesive or adhesive failure of restoration only.

The fatigue resistance of the groups was compared using the Kaplan-Meier survival table (for cycles). At each time interval (defined by each load step), the numbers of specimens intact at the interval and the number of specimens fracturing during the interval were counted, allowing the calculation of survival probability at each interval. A *post hoc* log rank test was used to analyze the influence of the ferrule, post system, and core buildup material on the fracture resistance of the ETI at a significance level of 0.05 (corrected for multiple comparisons when indicated).

Additionally, the fracture load and number of cycles at which the specimen failed was compared using one-way analysis of variance (ANOVA) fol-

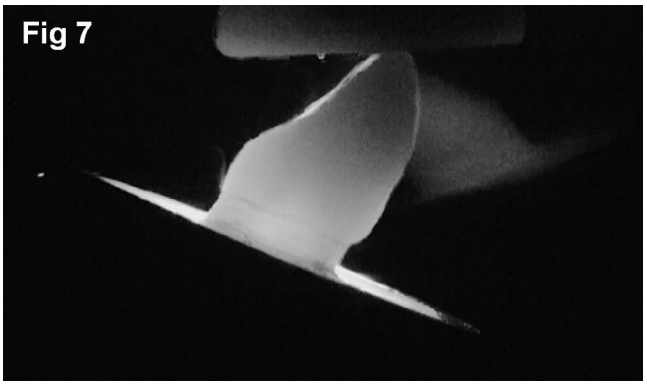

Figure 7. *Specimen in the load chamber. Cyclic isometric loading was applied to the incisal edge at an angle of 30°.*

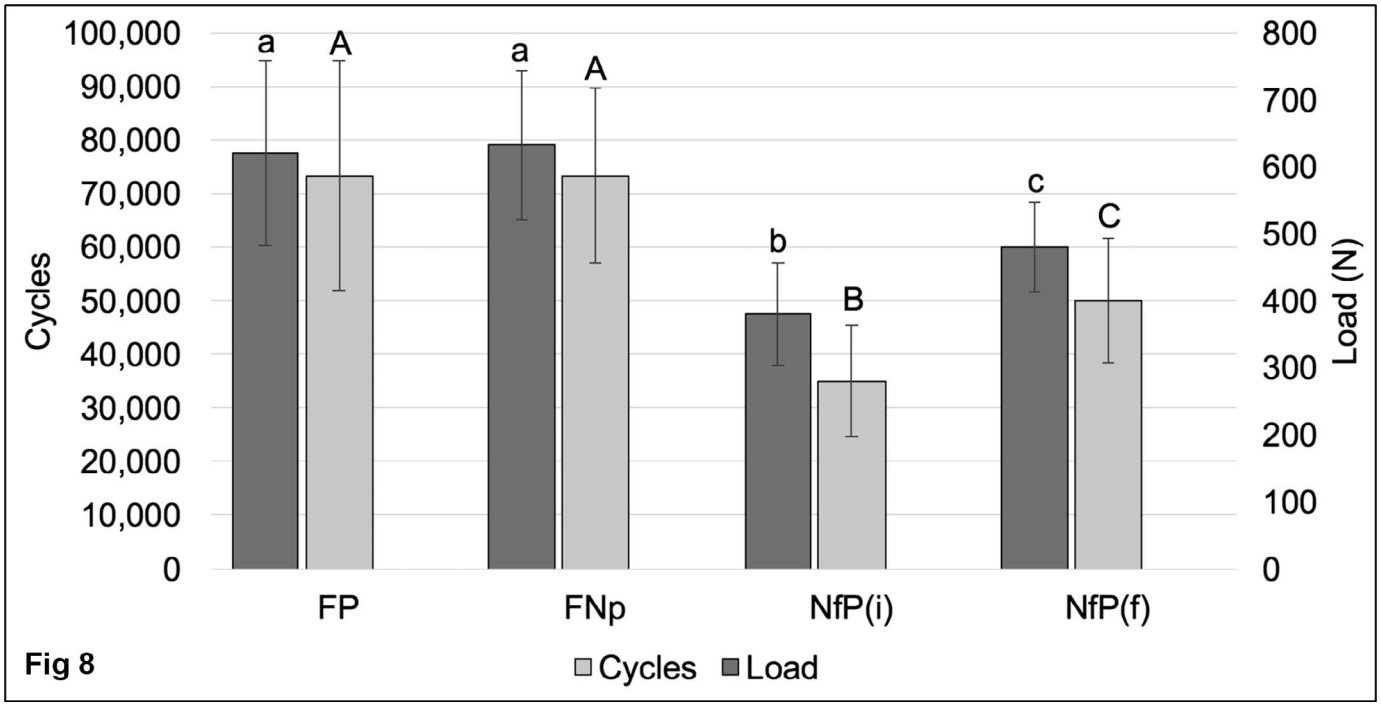

Figure 8. *Mean fracture loads (dark gray) and average number of survived load cycles (light gray) and their standard deviations, respectively.*

lowed by the Tukey test at a significance level of 0.05. For all statistical analyses, the level of significance was set at 95%. The data were analyzed with statistical software (SPSS 23, SPSS Inc, Chicago, IL, USA).

RESULTS

None of the specimens withstood all 140,000 load cycles. As all specimens fractured, the mean fracture load/cycles could be calculated (Figures 8 and 9). During cyclic loading, initial failures were detected in 81% (12/15) of the specimens in the no-ferrule group and 14% (2/15) and 7% (1/15) for a ferrule with a post and a ferrule without a post, respectively. The initial failure phenomenon can be described as the opening of a wide gap between the buildup/crown assembly and the root. The gap was always located at the lingual margin. Because clinical detection of such initial failures appears to be questionable, the analysis of survival was conducted for both the "final failure" (NfP[f]) and the "initial failure" (NfP[i]). The initial failure (i) values were recorded by reviewing the motion picture (high-definition macro mode) of the entire test for each specimen. Initial failure was easily detected by a significant high-pitched noise and simultaneous opening of a wide gap with emission of debris and air bubbles. The final failure (f) values were obtained by the testing machine when the sample completely fractured, causing the test to stop by activating the predetermined trigger parameters (axial displacement and axial acceleration).

The Kaplan-Meier survival graphs for all groups are displayed in Figure 9. The log-rank test showed significantly higher survival of groups with a ferrule

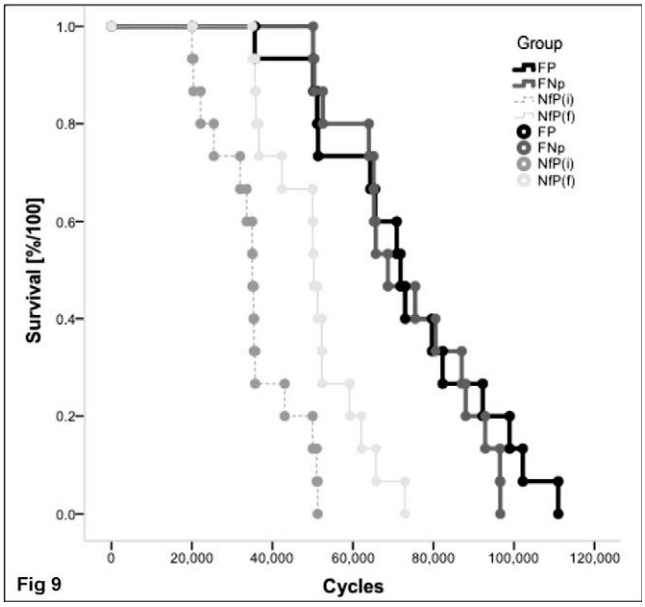

Figure 9. *Kaplan-Meier survival graphs for groups FFp, FNp, and NfFp. For better comparison, the survival graph of group NfFp was divided into initial failure and final failure.*

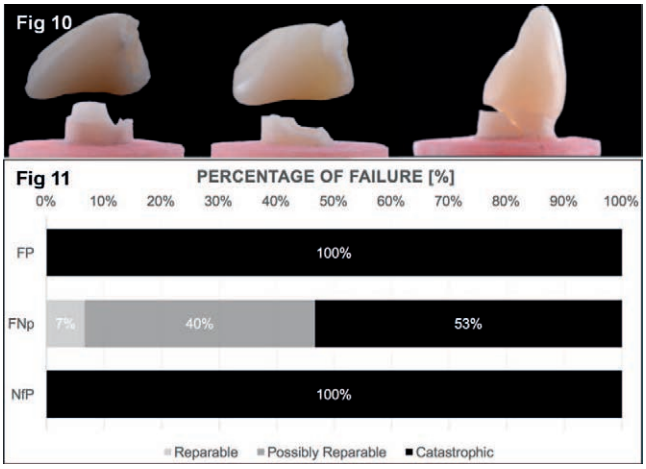

Figure 10. *All specimens were analyzed and classified in one of the three failure modes: "reparable" fracture (cohesive or cohesive/adhesive fracture of restoration only), "possibly reparable" (cohesive/adhesive failure with fragment and minor damage, chip, or crack, of underlying tooth structure) or "catastrophic" (tooth/root fracture that would require tooth extraction).*
Figure 11. Percentage of specimens per group for each fracture mode.

compared to groups without a ferrule ($p<0.001$). No difference could be found between groups with ferrule ($p=0.488$). Also when considering the initial failure, the log-rank test showed the same results; that is, a significantly higher survival of the ferrule group compared to the no-ferrule group ($p\leq0.001$) and no statistical difference between ferrule groups ($p=0.508$).

One-way ANOVA and the Tukey test revealed that the mean fracture load for the FP group (620.00±137.32 N; $p=0.984$) showed no statistical difference when compared with the FNp group (633.33±111.2697 N; $p=0.984$). Ferrule groups were significantly higher than the NfP group (380.00±77.4596 N [i], 480.00±67.6123 N [f]) considering the initial and final failure ($p<0.001$). The same results were found when the number of survived cycles was statistically compared (FP group to FNp group: $p=1.000$; FP group to NfP group: $p<0.01$; FNp group to NfP group: $p<0.01$). Figure 8 shows the mean values of fracture loads and survived cycles and their standard deviations, respectively.

Failure Mode Analysis

Groups with fiber post showed 100% catastrophic failures, while the no-post group presented 47% noncatastrophic failure. Possible fractures of the roots were made visible by transillumination in order to classify the specimen correctly (Figure 10). Figure 11 provides the number of specimens and percentage of each specific fracture mode for each group.

DISCUSSION

This study evaluated the effect of ferrule on the adhesive rehabilitation of ETI with glass ceramic crowns. A core buildup made with composite resin was compared with and without the use of a fiber-reinforced post system, and a no-ferrule group with fiber post was added for comparison. The first null hypothesis was accepted because there was no significant difference on fracture loads and survival rates when comparing ferrule groups with or without glass-fiber posts. The second null hypothesis was rejected because the presence of the ferrule increased the fatigue resistance of the ETI. Since the no-post group (FNp) presented 47% of noncatastrophic failures compared to 100% of catastrophic failure in both groups with post (FP and NfP), the third null hypothesis was also rejected.

Bovine teeth were used because of a lack of availability and large natural anatomic variations of extracted human teeth (age, size, and shape). Using standardized specimens is of paramount importance and allows minimizing confounding variables and gaining sensitivity in testing. Bovine dentin is often used for *in vitro* tests and is generally considered similar to human dentin in composition and geometric root configuration.[26,27] Because of the high standardization level that can be obtained using bovine roots and CAD/CAM technology, several confounding variables were avoided. However, the slight variations in internal dimensions (after internal ferrule preparation) of the root and the cementation process must still be considered as a possible limitation of this experiment.

All reviewed articles used single-rooted human or bovine teeth, and a constant load was applied at an angle to the long axis until fracture of the specimen occurred. Maximum loads that teeth could withstand and fracture patterns were analyzed and compared. However, the clinical significance of results obtained from *in vitro* static testing has been questioned[28] because a monostatic load does not represent the clinical situation in which repetitive mechanical loading and thermal changes are inherent. Therefore, in order to acquire more clinically relevant data with regard to the ferrule effect, the accelerated fatigue test was performed. This test consists of a stepped-load protocol, using a closed-loop electro-dynamic machine that allows a physiological representation of mastication.[30] This stepped-load protocol is a compromise

between the conventional load-to-failure protocol and the time-consuming low-load fatigue test.

The cyclic loads were phased, increasing the load in 100 N steps up to 1000 N at a frequency of 5 Hz. A flat composite resin surface was used as an antagonist instead of stainless steel, as suggested in other similar fatigue studies,[29,30] in order to prevent localized and intense point loads and unrealistic surface damage. Healthy humans exhibit maximal isometric bite forces in the incisor region ranging between 243 N (women) and 287 N (men).[31] Even higher forces may be encountered in bruxism, trauma (high extrinsic loads), or intrinsic masticatory accidents (under chewing loads but delivered to small area due to a hard foreign body, such as a stone or a seed). It is difficult, however, to draw direct correlations between the load range applied in this study and its significance *in vivo*. Due to the application of far higher forces in this study, it can be expected that an accelerated life cycle of the restored tooth may have been simulated.

In view of the present results, the use and effect of glass-fiber posts can be questioned. No significant difference could be observed between groups FP and FNp. These findings are in accordance with a previous study[20] in which fiber post insertion did not increase the fracture resistance of severely broken-down ETI with a ferrule. The results of this investigation confirm the general consensus that the presence of a ferrule (reminiscent of coronal dentin) is the most important factor and increases the resistance of the tooth.[32]

The combination of coronal dentin, shock-absorbing properties of the core buildup, and the use of a three-step etch-and-rinse adhesive appear to be the major advantages of this approach. It seems to more closely mimic the structure and biomechanical behavior of a natural tooth, in contrast to the concept of post-and-core buildups, in which a post is actually located at the position of the mechanically functionless pulp. Coronal dentin (ferrule) increases the intrinsic resistance of the core. Optimized approaches in bonding procedure, such as immediate dentin sealing and high strength of the nanohybrid composite resin, may have increased the assembly strength within the ferrule groups regardless of the presence of the post. All elements (crown, buildup, and tooth) have to form a cohesive assembly requiring a capable adhesive system and cement, which ideally mimics the properties of the dentin–enamel junction.

An initial failure phenomenon was observed essentially associated with the presence of a post without a ferrule. A sudden failure of the adhesion at the lingual margin could be easily observed thanks to high-definition video. It was immediately accompanied by the opening of a wide gap starting at the margin between the buildup/crown assembly and the root, intensifying and well preceding total failure. Such a phenomenon was also observed in other studies on endodontically treated molars restored with fiber posts.[16] From a clinical perspective, this type of failure is extremely critical because it is impossible to detect, can initiate bacterial contamination of the root-canal system (often referred to as "coronal leakage" or "coronal microleakage"), and can be a potential cause of periodontic and endodontic failure.[33] In addition, recurrent caries or fractured restorations may lead to recolonization of the root-canal system.[34] Schwartz and Robbins[34] concluded in their literature review that there are some questions about the flexibility of the glass-fiber post, suggesting that a flexible post allows too much movement of the core, resulting in increased microleakage under the crown. A reasonable explanation for the lack of initial failure on the FP group is the fact that the ferrule itself was responsible for increasing the resistance of the assembly and changing the bending behavior of the tooth/restoration. The absence of initial failure phenomenon in the ferrule groups is a significant advantage because patients would more rapidly consult in case of complication.

Fiber posts are popular because of their elastic modulus, similar to that of dentin,[35] which should improve the stress distribution within the root[36,37] and reduce the risk of vertical root fractures.[38] However, in view of the results in the present study, the use of a glass-fiber post should be questioned. In addition, the use of the fiber post was not able to compensate for the absence of a ferrule. A further problem with fiber posts was revealed with the rate of catastrophic failures (100% in FP and NfP compared to 53% in FNp). This result is in accordance with Zicari and others,[39] who stated that teeth restored with longer glass-fiber posts showed more nonrepairable failures.

Based on this preliminary study, there are several clinically relevant elements that can be drawn. Avoiding placement of a post significantly facilitates clinical procedures without interfering with longevity, as far as the right materials are selected. Anterior teeth with at least 2 mm of ferrule may be restored conservatively with a bonded restoration using a restorative composite resin as a core buildup, which should increase the chances for a restorable

failure without decreasing the resistance of the restored tooth. The amount of ferrule that is available to the clinician can vary substantially. The present data suggest that the operator should use the available tissue to provide a ferrule whenever possible. There is still a lack of data regarding the best treatment option in the absence of a ferrule. Before opting for crown lengthening or even extraction, the clinician should consider obtaining more coronal tooth structure through orthodontic extrusion when possible. However, further research will determine whether newer restoration designs, such as endocrowns, or new materials, such as fiber-reinforced composites, may be able to compensate for the absence of a ferrule and prevent more invasive surgical interventions.

CONCLUSIONS

Within the limitations of this *in vitro* study, the following conclusions can be drawn when restoring ETI:

1. Insertion of a fiber-reinforced post does not enhance the load-bearing capacity and survival of all-ceramic crowns.
2. In presence of a GFR post, catastrophic failure of the specimen was often preceded by the cyclic opening of a wide gap at the margin between the buildup/crown assembly and the root (initial failure). This significantly affected the survival rate.
3. The least amount of unrestorable failures was found with direct core buildups from a light-curing composite without a fiber-reinforced post.
4. The absence of a ferrule was not compensated for by the use of a fiber post.

Acknowledgements

The authors wish to express their gratitude to 3M ESPE (St Paul, MN, USA), Kerr (Orange, CA, USA), Ultradent (South Jordan, UT, USA), Heraeus Kulzer (Armonk, NY, USA), Coltène Whaledent (Altstätten, Switzerland), GC Corporation (Tokyo, Japan), Ivoclar Vivadent (Schaan, Liechtenstein), Sirona Dental Systems GmbH (Bensheim, Germany), Axis/Sybron Endo Kavo Kerr Group (Charlotte, NC, USA), Burbank Dental Lab (Los Angeles, CA, USA). This study was based on a thesis submitted to the University of Campinas in partial fulfillment of the requirements for the PhD degree. This investigation was supported in part by CAPES Foundation Brazil (PDSE: 99999.009625/2014-03).

Conflict of Interest

The authors of this article certify that they have no proprietary, financial, or other personal interest of any nature or kind in any product, service, and/or company that is presented in this article.

(Accepted 7 December 2016)

REFERENCES

1. Dietschi D, Duc O, Krejci I, & Sadan A (2008) Biomechanical considerations for the restoration of endodontically treated teeth: A systematic review of the literature—Part II. Evaluation of fatigue behavior, interfaces, and in vivo studies *Quintessence International* **39(2)** 117-129.
2. Dietschi D, Duc O, Krejci I, & Sadan A (2007) Biomechanical considerations for the restoration of endodontically treated teeth: A systematic review of the literature—Part 1. Composition and micro- and macrostructure alterations *Quintessence International* **38(9)** 733-743.
3. Juloski J, Radovic I, Goracci C, Vulicevic ZR, & Ferrari M (2012) Ferrule effect: A literature review *Journal of Endodontics* **38(1)** 11-19.
4. da Silva NR, Raposo LHA, Versluis A, Fernandes-Neto AJ, & Soares CJ (2010) The effect of post, core, crown type, and ferrule presence on the biomechanical behavior of endodontically treated bovine anterior teeth *Journal of Prosthetic Dentistry* **104(5)** 30-317.
5. Pereira JR, De Ornelas F, Rodrigues Conti PC, & Lins Do Valle A (2006) Effect of a crown ferrule on the fracture resistance of endodontically treated teeth restored with prefabricated posts. *Journal of Prosthetic Dentistry* **95(1)** 50-54.
6. Stankiewicz NR, & Wilson PR (2002) The ferrule effect: A literature review *International Endodontic Journal* **35(7)** 575-581.
7. Sorensen JA, & Engelman MJ (1990) Ferrule design and fracture resistance of endodontically treated teeth *Journal of Prosthetic Dentistry* **63(5)** 529-536.
8. Libman WJ, & Nicholls JI (1995) Load fatigue of teeth restored with cast posts and cores and complete crowns *International Journal of Prosthodontics* **8(2)** 155-161.
9. Isidor F, Brøndum K, & Ravnholt G (1999) The influence of post length and crown ferrule length on the resistance to cyclic loading of bovine teeth with prefabricated titanium posts *International Journal of Prosthodontics* **12(1)** 78-82.
10. Naumann M, Preuss A, & Rosentritt M (2006) Effect of incomplete crown ferrules on load capacity of endodontically treated maxillary incisors restored with fiber posts, composite build-ups, and all-ceramic crowns: An in vitro evaluation after chewing simulation *Acta Odontologica Scandinavica* **64(1)** 31-36.
11. Bitter K, Noetzel J, Stamm O, Vaudt J, Meyer-Lueckel H, Neumann K, & Kielbassa AM (2009) Randomized clinical trial comparing the effects of post placement on failure rate of postendodontic restorations: Preliminary results of a mean period of 32 months *Journal of Endodontics* **35(11)** 1477-1482.
12. Roscoe MG, Noritomi PY, Novais VR, & Soares CJ (2013) Influence of alveolar bone loss, post type, and ferrule presence on the biomechanical behavior of endodontically treated maxillary canines: Strain measurement and stress distribution *Journal of Prosthetic Dentistry* **110(2)** 116-126.

13. Theodosopoulou JN, & Chochlidakis KM (2009) A systematic review of dowel (post) and core materials and systems *Journal of Prosthodontics* **18(6)** 464-472.

14. Rasimick BJ, Wan J, Musikant BL, & Deutsch AS (2010) A review of failure modes in teeth restored with adhesively luted endodontic dowels *Journal of Prosthodontics* **19(8)** 639-646.

15. Sterzenbach G, Franke A, & Naumann M (2012) Rigid versus flexible dentine-like endodontic posts—Clinical testing of a biomechanical concept: Seven-year results of a randomized controlled clinical pilot trial on endodontically treated abutment teeth with severe hard tissue loss *Journal of Endodontics* **38(12)**1557-1563.

16. Magne P, Goldberg J, Edelhoff D, & Güth J-F (2016) Composite resin core buildups with and without post for the restoration of endodontically treated molars without ferrule *Operative Dentistry* **41(1)** 64-75.

17. Massa F, Dias C, & Blos CE (2010) Resistance to fracture of mandibular premolars restored using post-and-core systems *Quintessence International* **41(1)** 49-57.

18. Zicari F, Van Meerbeek B, Scotti R, & Naert I (2013) Effect of ferrule and post placement on fracture resistance of endodontically treated teeth after fatigue loading *Journal of Dentistry* **41(3)** 207-215.

19. Pereira JR, do Valle AL, Shiratori FK, Ghizoni JS, & de Melo MP (2009) Influence of intraradicular post and crown ferrule on the fracture strength of endodontically treated teeth *Brazilian Dental Journal* **20(4)** 297-302.

20. Lima AF De, Spazzin AO, Galafassi D, Correr-Sobrinho L, & Carlini-Júnior B (2010) Influence of ferrule preparation with or without glass fiber post on fracture resistance of endodontically treated teeth *Journal of Applied Oral Science* **18(4)** 360-363.

21. Magne P, & Douglas WH (1999) Rationalization of esthetic restorative dentistry based on biomimetics *Journal of Esthetic Dentistry* **11(1)** 5-15.

22. Torabinejad M, Handysides R, Khademi AA, & Bakland LK (2002) Clinical implications of the smear layer in endodontics: A review *Oral Surgery, Oral Medicine, Oral Pathology, Oral Radiology, and Endodontics* **94(6)** 658-666.

23. Siqueira JF, Rôças IN, Favieri A, & Lima KC (2000) Chemomechanical reduction of the bacterial population in the root canal after instrumentation and irrigation with 1%, 2.5%, and 5.25% sodium hypochlorite *Journal of Endodontics* **26(6)** 331-334.

24. Johnson WT, & Noblett WC (2009) *Cleaning and Shaping*. *Endodontics: Principles and Practice* **4th edition** Saunders, Philadelphia PA 258-286.

25. Paragliola R, Franco V, Fabiani C, Mazzoni A, Nato F, Tay FR, Breschi L, & Grandini S (2010) Final rinse optimization: Influence of different agitation protocols *Journal of Endodontics* **36(2)** 282-285.

26. Reis AF, Giannini M, Kavaguchi A, Soares CJ, & Line SRP (2004) Comparison of microtensile bond strength to enamel and dentin of human, bovine, and porcine teeth *Journal of Adhesive Dentistry* **6(2)** 117-121.

27. Fonseca RB, Haiter-Neto F, Carlo HL, Soares CJ, Sinhoreti MAC, Puppin-Rontani RM, & Correr-Sobrinho L (2008) Radiodensity and hardness of enamel and dentin of human and bovine teeth, varying bovine teeth age *Archives of Oral Biology* **53(11)** 1023-1029.

28. Kelly JR (1999) Clinically relevant approach to failure testing of all-ceramic restorations *Journal of Prosthetic Dentistry* **81(6)** 652-661.

29. Magne P, & Knezevic (2009) A Simulated fatigue resistance of composite resin versus porcelain CAD/CAM overlay restorations on endodontically treated molars *Quintessence International* **40(2)** 125-133.

30. Magne P, Oderich E, Boff LL, Cardoso AC, & Belser UC (2011) Fatigue resistance and failure mode of CAD/CAM composite resin implant abutments restored with type III composite resin and porcelain veneers *Clinical Oral Implants Research* **22(11)** 1275-1281.

31. Waltimo A, & Könönen M (1993) A novel bite force recorder and maximal isometric bite force values for healthy young adults *Scandinavian Journal of Dental Research* **101(3)** 171-175.

32. Tan PLB, Aquilino SA, Gratton DG, Stanford CM, Tan SC, Johnson WT, & Dawson D (2005) In vitro fracture resistance of endodontically treated central incisors with varying ferrule heights and configurations *Journal of Prosthetic Dentistry* **93** 331-336.

33. Saunders WP, & Saunders EM (1994) Coronal leakage as a cause of failure in root-canal therapy: A review *Endodontics and Dental Traumatology* **10(3)** 105-108.

34. Schwartz RS, & Robbins JW (2004) Post placement and restoration of endodontically treated teeth: A literature review *Journal of Endodontics* **30(5)** 289-301.

35. Plotino G, Grande NM, Bedini R, Pameijer CH, & Somma F (2007) Flexural properties of endodontic posts and human root dentin *Dental Materials* **23(9)** 1129-1135.

36. Mezzomo LA, Corso L, Marczak RJ, & Rivaldo EG (2011) Three-dimensional FEA of effects of two dowel-and-core approaches and effects of canal flaring on stress distribution in endodontically treated teeth *Journal of Prosthodontics* **20(2)** 120-129.

37. Watanabe MU, Anchieta RB, Rocha EP, Kina S, Almeida EO, Freitas AC, & Basting RT (2012) Influence of crown ferrule heights and dowel material selection on the mechanical behavior of root-filled teeth: A finite element analysis *Journal of Prosthodontics* **21(4)** 304-311.

38. Santos-Filho PCF, Veríssimo C, Soares PV, Saltarelo RC, Soares CJ, & Marcondes Martins LR (2014) Influence of ferrule, post system, and length on biomechanical behavior of endodontically treated anterior teeth *Journal of Endodontics* **40(1)** 119-123.

39. Zicari F, Van Meerbeek B, Scotti R, & Naert I (2012) Effect of fibre post length and adhesive strategy on fracture resistance of endodontically treated teeth after fatigue loading *Journal of Dentistry* **40(4)** 312-321.

©Operative Dentistry, 2017, **42-4,** 407-417

Characterization of a Diamond Ground Y-TZP and Reversion of the Tetragonal to Monoclinic Transformation

LM Candido • LMG Fais • EB Ferreira • SG Antonio • LAP Pinelli

Clinical Relevance

Surface characterization of Y-TZP frameworks provides a better understanding of why adjustments can weaken the interface between such structures and veneering porcelain. A heat treatment after grinding can reverse the transformation and potentially restore the protective toughening of the restoration.

SUMMARY

Purpose: To characterize the surface of an yttria-stabilized zirconia (Y-TZP) ceramic after diamond grinding in terms of its crystalline phase, morphology, mean roughness (*Ra*), and wettability as well as to determine a thermal treatment to reverse the resulting tetragonal to monoclinic (*t-m*) transformation.

Methods and Materials: Y-TZP specimens were distributed into different groups according to the actions (or no action) of grinding and irrigation. Grinding was accomplished using a diamond stone at a low speed. The samples were characterized by x-ray diffraction (XRD), scanning electron microscopy, goniometry, and profilometry. *In situ* high-temperature XRD was used to determine an annealing temperature to reverse the *t-m* transformation. *Ra* was submitted to the Kruskal-Wallis test, followed by the Dunn test (α=0.05). The volume fraction of the monoclinic phase and contact angle were submitted to one-way analysis of variance, followed by the Tukey test (α=0.05).

*Lucas Miguel Candido, DDS, MSD, PhD Student, Department of Dental Materials and Prosthodontics, Araraquara Dental School, Univ. Estadual Paulista UNESP, Araraquara, Brazil

Laiza Maria Grassi Fais, DDS, MSD, PhD, post-doctorate student, Department of Dental Materials and Prosthodontics, Araraquara Dental School, Univ. Estadual Paulista UNESP, Araraquara, Brazil

Eduardo Bellini Ferreira, MSD, PhD, associate professor, Department of Materials Engineering, Engineering School of Sao Carlos, Univ. São Paulo USP, Sao Carlos, Brazil

Selma Gutierrez Antonio, MSD, PhD, post-doctorate student, Department of Physical Chemistry, Araraquara Institute of Chemistry, Univ. Estadual Paulista UNESP, Araraquara, Brazil

Lígia Antunes Pereira Pinelli, DDS, MSD, PhD, assistant professor, Department of Dental Materials and Prosthodontics, Araraquara Dental School, Univ. Estadual Paulista UNESP, Araraquara, Brazil

*Corresponding author: Faculdade de Odontologia de Araraquara- UNESP, Rua Humaitá, 1680 CEP 14801-903, Araraquara, SP, Brazil; e-mail: candidomlucas@gmail.com

DOI: 10.2341/16-196-L

Results: Monoclinic zirconia was observed on the surface of samples after dry and wet grinding with a diamond stone. The volume fraction of the monoclinic phase was smaller on the dry ground samples (3.6%±0.3%) than on the wet ground samples (5.6%±0.3%). High-temperature XRD showed reversion of the *t-m* phase transformation, which started at 700°C and completed at 800°C in a conventional oven.

Conclusions: Grinding with a diamond stone partially transformed the crystalline phase on the surface of a Y-TZP ceramic from tetragonal to monoclinic zirconia while simultaneously increasing the surface roughness and wettability. The *t-m* transformation could be reversed by heat treatment at 800°C or 900°C for 60 minutes or 1000°C for 30 minutes.

INTRODUCTION

Yttria-stabilized tetragonal zirconia polycrystal (Y-TZP) is a polycrystalline material composed of the following three polymorphic phases: monoclinic (*m*), tetragonal (*t*), and cubic (*c*) zirconia; the proportions of these phases can vary by thermomechanical factors, rendering the material tougher. However, if the phase transformation is triggered during processing, the transformation might not result in beneficial properties.[1,2] In dentistry, Y-TZP has been widely used as a framework for metal-free crowns and fixed partial dentures, implants, abutments, and orthodontic brackets[1-6] because of its interesting optical and esthetic properties, high hardness, wear resistance, high flexural strength, and high resistance to fracture, inherent to the toughening process due to the tetragonal to monoclinic (*t-m*) transformation.[1-3,7]

However, aging, delamination, and chipping of veneering porcelain are problems often reported in the literature[4,5,8-11] associated with this type of material. Aging is connected to prolonged contact with an aqueous medium, which favors a slow phase *t-m* transformation on the material surface, which causes the loss of grains, increases in roughness, and the formation of microcracks as well as decreases in the hardness and strength of the material.[5,8] Delamination and chipping occur through different mechanisms, such as the mismatching of thermal expansion coefficients between the framework and the veneer ceramic, microstructural defects in the porcelain, porosity, surface defects, improper support frameworks, overload, fatigue, and low fracture resistance of the veneer ceramic.[4,10-13] While chipping results from the cohesive failure of the veneering porcelain, delamination arises from the adhesive failure between the zirconia framework and porcelain coverage.[4,11]

Attempts to improve the adhesion at the interface between zirconia and veneering porcelain have been undertaken. Different surface treatments, such as sandblasting, liner applying, polishing, grinding, etching, laser etching, and silicatization,[13-17] have been used to change the zirconia surface, increasing its roughness or its surface energy to improve wettability and, thus, favor adhesion.[13,16,17]

Special attention must be paid to grinding because, although it has been studied as a method to improve adhesion, it is often necessary during clinical trials to modify and adapt the sintered frameworks,[14,18-20] which can induce stresses promoting *t-m* transformation.[1,14,21,22] This transformation momentarily toughens the zirconia by local expansion and crack closing because the specific volume of the monoclinic phase is greater than the tetragonal phase; however, it can have a negative impact on the mechanical stability of fixed prostheses over time. After the *t-m* transformation, the material presents total or partial loss of the ability to prevent or to retard the propagation of cracks, and it can become critically friable.[14,23-26]

Given these contradictory results,[14,18,21,22,25,27-31] some authors have emphasized the importance of studying the effects of grinding with different types of instruments at high and low speeds.[1,20,30,32] Regardless of the method used for grinding, changes in the material surface can increase the surface roughness, induce defects, and activate the *t-m* transformation,[14,18,21,22,27,29-31] thereby increasing the volume percentage of monoclinic zirconia. Such phase transformation depends on the metastability of the conversion, the grinding severity, and the temperature at the site.[14,25,29,30] A higher content of monoclinic zirconia, together with greater roughness and a higher concentration of surface defects, renders the material more susceptible to long-term degradation and loss of mechanical strength.[3,5,8,21,23,26,30,33] Different grinding procedures have been studied in the literature,[19,22,24,25,32] but to the best of our knowledge, no one has examined whether grinding with a diamond stone is a less harmful technique for Y-TZP.

Considering the phase transformation and superficial defects induced by grinding, a heat treatment can be performed before application of a veneering porcelain.[5,19,32] It was suggested that the applied heat acts as a regenerative treatment,[13] reversing

Table 1: *Distribution of the Experimental Groups*

Group	Condition
C	Sintered without grinding, control
DG	Sintered and dry ground
WG	Sintered and wet ground

the monoclinic zirconia to the tetragonal phase, and thus returning the zirconia to a metastable tetragonal phase.[5,19] In addition to the reversing transformation, such regenerative thermal treatment is very interesting because it could also act to close the surface microcracks caused by grinding.[13] Such treatment would then reduce all of the aforementioned problems, making it extremely important for the durability of a prosthesis.[5,19,32]

In combination with a less invasive grinding technique, a protocol of heat treatment with appropriate parameters could render the prosthesis material more stable against fracture and degradation. Although several authors have studied the application of heat treatment after the grinding procedure,[5,13,14,19,23,28,32] there is still no consensus in the literature on whether [5,19,32] or not[13,14,23,28] such a treatment should be performed, which could be related to the use of inappropriate parameters of temperature and time. It is essential to determine the effect of stone grinding and to elaborate a protocol of regenerative heat treatment for Y-TZP.

Thus, the aims of the present study were to characterize the crystalline phases, surface morphology, roughness, and wettability of the surfaces of Y-TZP specimens after grinding with a diamond stone with or without irrigation and to determine the time and temperature to reverse the *t-m* transformation to establish a protocol for regenerative heat treatment (annealing) of ground Y-TZP. The null hypothesis was that grinding with a diamond stone would not change the crystallographic phases, morphology, roughness, or wettability of the surface of a Y-TZP ceramic.

METHODS AND MATERIALS

Specimen Preparation

Blocks of Y-TZP zirconia (Lava Frame Zirconia, 3M ESPE AG, Seefeld, Germany) were sectioned into pre-sintered specimens using a high precision cutoff machine (ISOMET 1000, Buehler, Lake Bluff, IL, USA) with a diamond disc (Series Diamond 15LC, Buehler) under water irrigation. The samples were cut into two different sizes as follows: 10 mm × 10 mm × 1.5 mm for non-ground specimens and 10 mm × 10 mm × 1.9 mm for ground specimens.

Irregularities at the specimen edges were removed with silicone tips (Exa-cerapol, Edenta, Labordental, Hauptstrasse, Switzerland). The upper surfaces of the specimens were sequentially polished with #1200, #1500, and #2000 silicon carbide sandpaper (401Q, 3M ESPE, Sumaré, Brazil). The final dimensions were measured using digital calipers (500-144B, Mitutoyo Sul Americana, Suzano, Brazil). Sintering was accomplished with a heat treatment program of 8 hours at a maximum temperature of 1500°C, following the manufacturer's instructions (Lava Furnace 200, Dekema Dental-Keramiköfen, Freilassing, Germany). The specimens were divided into three groups according to the experimental procedures (Table 1).

Zirconia Grinding

A homemade device (Figure 1a) was developed at the Araraquara Dental School, UNESP, to standardize the amount of longitudinal grinding. It was used to remove 0.3 mm from the surfaces of zirconia samples with and without irrigation (groups WG and DG, respectively). The sample grinding was performed with a diamond stone (MasterCeram, MCE 133 104, Eurodental Commercial Importer Ltd, São Paulo, Brazil) in a low-speed electric handpiece (Micro Electric Motor Bench for Prosthetics LB 100, Beltec, Araraquara, Brazil) at 20,000 rpm. During grinding, the long axis of the diamond stone was set parallel to the long axis of the sample (Figure 1b), which remained static while the electric low-speed handpiece moved with the aid of a tailstock. The WG specimens were ground under water flowing from a triple syringe (Figure 1c).

Surface Properties

X-Ray Diffraction (XRD)—XRD was used to identify the Y-TZP crystalline phases with an x-ray diffractometer D8 Advance (Bruker, Karlsruhe, Germany) using the following settings: a Cu $K\alpha_1$ wavelength = 1.5406 Å and a $K\alpha_2$ wavelength = 1.5444 Å, an intensity ratio of $I_{k\alpha 2}/I_{k\alpha 1} = 0.5$, 2θ between 20° to 80°, an angular step of 0.02°, the use of continuous mode, a step time of 3 seconds, and a sample size of n = 3. The monoclinic and tetragonal phases were identified by comparison with the crystal structures described in Gualtieri and others[34] and Bondars and others.[35]

Scanning Electron Microscopy (SEM)—Specimens (n=2) were covered with carbon, and their surfaces

Figure 1. *(a): Grinding device. (b): Dry grinding. (c): Wet grinding.*

were examined using a scanning electron microscope (Inspect F50, FEI, Achtseweg Noord 5, Eindhoven, Netherlands).

Mean Roughness—The mean roughness of specimens (*Ra*, μm; n=10) was measured using a profilometer (Mitutoyo SJ 400, Mitutoyo Corporation, Yokohama, Japan) with a reading accuracy of 0.01 μm, a read length of 2.5 mm, an active tip speed of 0.5 mm/s, and an active tip radius of 5 μm. Three measurements were obtained for each surface, and the average was calculated. For the G groups, the measurements were performed in the opposite direction of the grinding lines.

Wettability—Wettability (n=5) was determined by measuring the static contact angle of a sessile drop of distilled water in an automatic goniometer (Dataphysics, OCA20, Filderstadt, Baden-Württemberg, Germany). The wettability measurement was performed at a controlled temperature (20°C) and after a settling time of 20 seconds for a distilled water drop (15 μL). The average contact angle was calculated from three readings performed on the surface of each sample.

High-Temperature In Situ XRD—To set the parameters for establishing a protocol for regenerative heat treatment (annealing), the specimen that presented the largest fraction of monoclinic phase identified by room temperature XRD (group WG) was submitted to an *in situ* high-temperature XRD analysis (n=3). For this analysis, a heating chamber was coupled to the same XRD equipment described previously. The XRD patterns were measured at a step size of 2.7° and a step time of 0.5 seconds in continuous mode at temperatures of 25°C, 100°C, 200°C, 300°C, 400°C, 500°C, 600°C, 700°C, 800°C, and 900°C. The sample was heated at 10°C/min up to the set temperatures, and the temperature was maintained for 5 minutes for stabilization before each analysis. The analyses were performed in a unique sequence, and it took 10 minutes to complete the analysis at each temperature step.

Annealing—The specimens with the highest amount of monoclinic zirconia after grinding (group WG) were heat treated at different temperatures and for different time periods to study the possibility of reversion of the *t-m* transformation. Isothermal heat treatments were performed in a lab furnace (AluminiPress, EDG Equipamentos e Controles Ltda, São Carlos, Brazil) at 700°C, 800°C, 900°C, and 1000°C for 30 and 60 minutes (N=8, one specimen per temperature and time). The samples were placed in the preheated furnace, which was already at the treatment temperature. After heat treatment, the specimens were removed from the furnace and cooled to room temperature. The crystalline phases on the previously ground and annealed surfaces were then characterized by conventional XRD.

Statistical Analysis

The SEM results were submitted to descriptive analysis, and the conventional and high-temperature XRD patterns were analyzed using the Rietveld method. The normality of the mean roughness (*Ra*), contact angle, and amount of monoclinic phase

Table 2: *Average Volume Fraction (%) and Standard Deviations of the Monoclinic Phase in Y-TZP*

Group	Monoclinic Fraction (%)*
C	0.0 ± 0.0[a]
DG	3.6 ± 0.3[b]
WG	5.6 ± 0.3[c]

** Different superscript letters indicate statistical difference ($p<0.01$).*

obtained by conventional XRD was verified by the Shapiro-Wilk test ($\alpha=0.05$). *Ra* was submitted to the Kruskal-Wallis test followed by the Dunn test ($\alpha=0.05$). The contact angle and amount of monoclinic phase were submitted to one-way analysis of variance, followed by the Tukey test ($\alpha=0.05$).

RESULTS

X-Ray Diffraction

The results of XRD are shown in Table 2. The presence of monoclinic zirconia was observed in both G groups (DG and WG). The volume fraction of monoclinic zirconia in the group ground with irrigation (WG, 5.6%±0.3%) was statistically higher ($p<0.01$) than that in the DG group (3.6%±0.3%).

Scanning Electron Microscopy

Figures 2 through 5 show SEM micrographs of the specimens in which one can observe the grinding

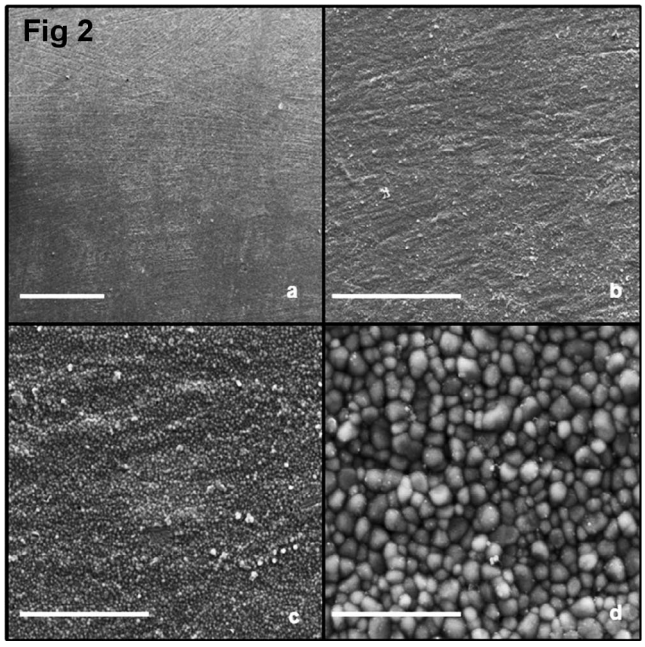

Figure 2. *Surface topography of sintered Y-TZP (C) without grinding at different magnifications. Scale bars correspond to (a): 500 μm, (b): 100 μm, (c): 20 μm and (d): 4 μm.*

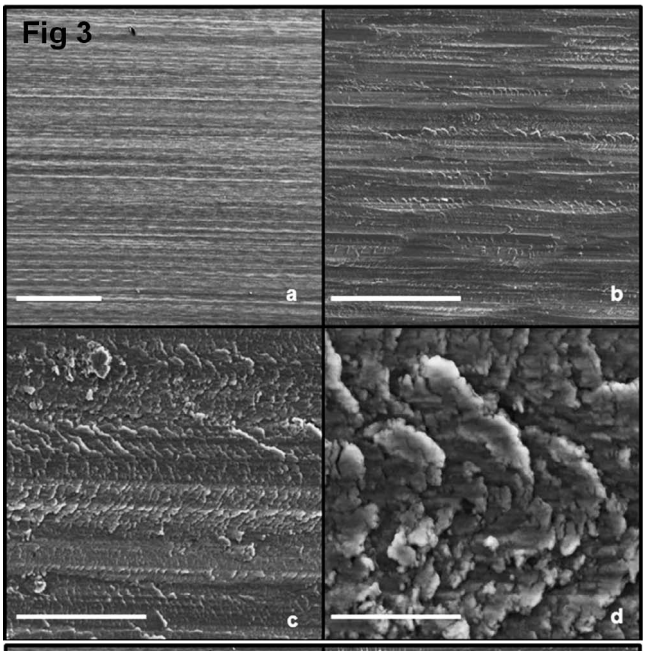

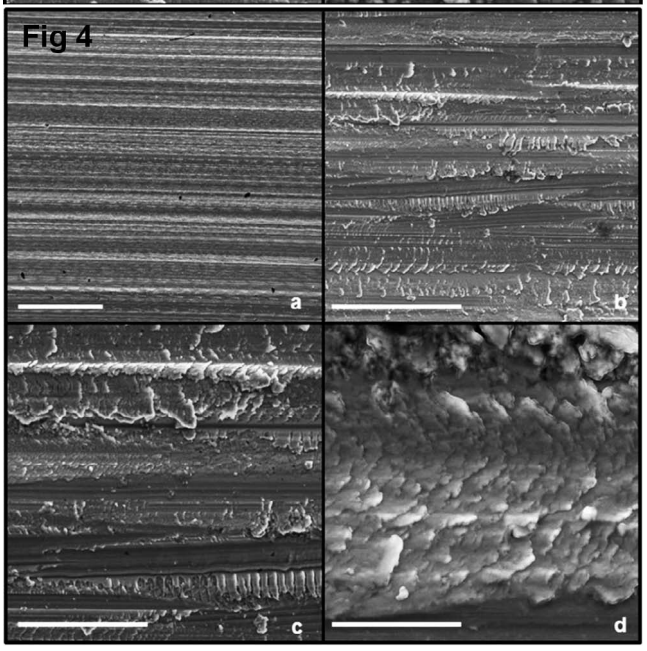

Figure 3. *Surface topography of sintered and dry ground Y-TZP (DG) at different magnifications. Scale bars correspond to (a): 500 μm, (b): 100 μm, (c): 20 μm, and (d): 4 μm.*

Figure 4. *Surface topography of sintered and wet ground zirconia (WG) at different magnifications. Scale bars correspond to (a): 500 μm, (b): 100 μm, (c): 20 μm, and (d): 4 μm.*

effects on the material surface. For groups DG (Figure 3) and WG (Figure 4), grinding produced scratches, which were parallel to the direction of longitudinal movement of the diamond stone. After roughening the sample surface with a diamond stone, the heterogeneous wear hid the grain microstructure under the microscope. By observing the

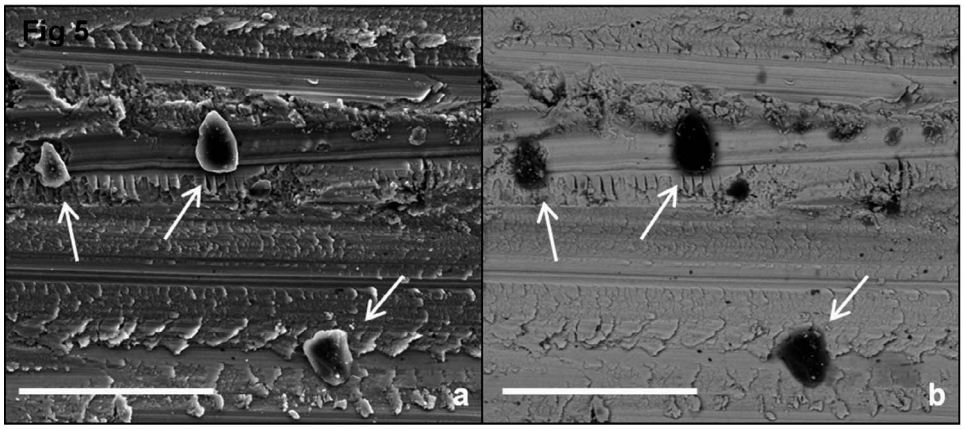

Figure 5. *Surface topography of a WG sample observed by SEM with (a): secondary electrons, and (b): backscattered electrons. Arrows indicate particles compatible with diamond stone. Bar corresponds to 20 μm.*

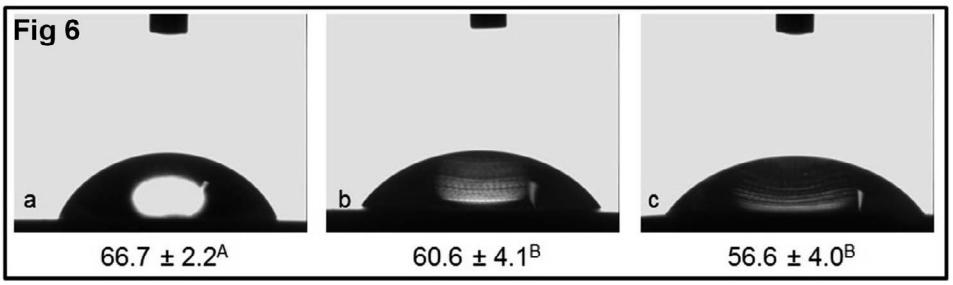

Figure 6. *Spreading of a distilled water drop with contact angle mean values and standard deviations. (a): C group, (b): DG group, and (c): WG group.*

grinding patterns at the same magnification in the SEM, one could observe that some grinding lines in Figure 4a were darker than those in Figure 3a, showing that the scratch valleys were deeper in group WG than in group DG (confirmed subsequently with profilometry), which, together with a more splintered surface, indicated that wet grinding was more severe. Figure 5 shows particles on the surface of one such sample after grinding. Using SEM/BSE (backscattered electrons), one could observe that these particles had a composition different from (lighter than) zirconia, likely because of the presence of fragments of diamond stone.

Mean Roughness (Ra)

The medians and standard deviations of *Ra* from all of the groups are shown in Table 3. Statistically significant differences were observed among all of the groups ($p<0.01$). Group WG was rougher than the others.

Table 3: *Medians and Standard Deviations of* Ra *(μm) of Specimens From All of the Groups*

Group	*Ra**
C	0.14 ± 0.02^{a}
DG	1.44 ± 0.13^{b}
WG	3.24 ± 0.75^{c}

** Different superscript letters indicate statistical difference (p<0.01).*

Wettability

The images of the contact angles and the averages and standard deviations of the specimens are shown in Figure 6. Statistically significant differences were observed between the contact angles ($p<0.01$). The ground specimens presented average contact angles smaller than the controls ($p<0.01$), but there was no significant difference between the WG and DG groups.

In Situ High-Temperature XRD

Table 4 shows the percentages of tetragonal and monoclinic zirconia obtained by *in situ* high-temperature XRD. As shown in Table 4, one could observe that annealing at 700°C under the conditions of high-temperature XRD could totally reverse the monoclinic zirconia to the tetragonal phase.

Annealing

Table 5 shows the volume fraction of tetragonal and monoclinic zirconia as a function of the time and temperature of isothermal heat treatments. It could be observed that in the lab furnace the *m-t* transformation was complete after 800°C for 60 minutes. At 900°C, the entire transformation also occurred in 60 minutes, and at 1000°C, the monoclinic zirconia was totally eliminated in 30 minutes.

Table 4: *Volume Fraction of Tetragonal and Monoclinic Zirconia on the Specimen Surface Depending on Temperature in the* In Situ *High-Temperature X-Ray Diffraction*

Temperature	Tetragonal (%)	Monoclinic (%)
25°C	94.6 ± 0.3	5.4 ± 0.3
100°C	95.2 ± 1.7	4.8 ± 1.7
200°C	91.6 ± 4.0	8.4 ± 4.0
300°C	92.1 ± 2.4	7.9 ± 2.4
400°C	91.6 ± 2.0	8.4 ± 2.0
500°C	94.4 ± 1.5	5.6 ± 1.5
600°C	96.0 ± 0.4	4.0 ± 0.4
700°C	100.0 ± 0.0	0.0 ± 0.0
800°C	100.0 ± 0.0	0.0 ± 0.0
900°C	100.0 ± 0.0	0.0 ± 0.0

Table 5: *Volume Fraction of Tetragonal and Monoclinic Zirconia as a Function of Time and Temperature of the Heat Treatment*

Temperature	Time (min)	Tetragonal (%)	Monoclinic (%)
700°C	30	98.3	1.7
	60	99.2	0.8
800°C	30	99.0	1.0
	60	100.0	0.0
900°C	30	99.5	0.5
	60	100.0	0.0
1000°C	30	100.0	0.0
	60	100.0	0.0

DISCUSSION

Although zirconia frameworks are obtained using CAD-CAM (computer-aided design/computer-aided manufacturing) systems, there is often a need for grinding, whether in the clinic or prosthetic laboratory.[18,19] While most of the available studies have evaluated the effects of grinding with diamond burs,[22,24,27] other methods, such as diamond stones at low speed, have not been studied in the literature, but such grinding can cause different changes on the Y-TZP surface.

Therefore, the present study evaluated the effects of grinding the surface of a Y-TZP ceramic with a diamond stone, with and without water irrigation, by characterizing the resulting superficial crystalline phases, morphology, roughness, and wettability and by determining the time and temperature to reverse the *t-m* transformation to establish a protocol for a regenerative heat treatment (annealing) of diamond-ground Y-TZP. The null hypothesis (grinding with diamond stone would not change the crystallographic phases, roughness, or wettability of the surface of a Y-TZP ceramic) was not supported.

As observed in the present study, grinding with a diamond stone led to significant changes in the material. After grinding, one could observe changes in the surface amount of monoclinic and tetragonal zirconia, morphology, roughness, and wettability. In the literature,[19,22,24,26,27] factors such as the abrasive grain size, wear time, load pressure, tool efficiency, and temperature of grinding could cause changes in the material associated with the polymorphic transformation of the tetragonal zirconia to the monoclinic phase (*t-m*).

The *t-m* phase transformation produced a toughening effect in which zirconia grains increased in size by becoming monoclinic. Grinding, sandblasting, and/or chemical etching[24,25,32] induce crack nucleation and growth on the surface. In turn, this action causes pressure release in the microstructure around the metastable tetragonal grains, subsequently causing the tetragonal to monoclinic transformation and forcing cracks to close. This transformation can increase the flexural strength of the material,[19] but it can also cause the loss of the ability to prevent the spread of cracks,[30,36] it might favor long-term degradation,[8,5,14] and it can damage the adhesion of the veneering porcelain.[4,12,13,22,25]

Grinding with diamond stone with (WG) or without (DG) irrigation induced the *t-m* phase transformation, as evidenced in Table 2. Grinding under water (WG) produced larger amounts of transformation and monoclinic phase, which is in accordance with some authors' results showing that grinding led to higher monoclinic content.[19,24,25,32] However, in these studies, grinding was performed using diamond burs, while in the present study, it was conducted with a diamond stone at a lower speed.

The differences relative to the amount of change measured in the DG and WG groups could be attributed to the cutting power of the diamond stone in these different situations because the grinding severity was directly related to the amount of *t-m* transformation.[1,29] It was observed during grinding with irrigation that water served as a cleaning agent, removing the stone powder, increasing the cutting capacity, and therefore providing more severe grinding. According to Wang and others,[37] grinding power increases due to irrigation, making

the cutting instrument more efficient. Moreover, the lack of lubrication of the stone during dry grinding (DG group) contributed to the impregnation of zirconia powder in the tool, a phenomenon described as "slurrying" in engineering,[38] and in this case, the diamond stone produced less severe grinding, resulting in a polished surface.

The effect of grinding on the ceramic material's surface was demonstrated by SEM images. It was observed for groups DG and WG that grinding produced scratches parallel to the direction of longitudinal movement of the diamond stone on the ceramic surface and a more irregular structure, with the presence of chips and concealment of the structure of the grains (Figures 3 and 4). In group WG, the wear valleys (Figure 4) were deeper than in group DG, and particles that had possibly detached from the diamond stone (Figure 5) were observed on the worn surface. BSE SEM showed that the composition of these fragments was lower in atomic weight than that of zirconia because of the darker glow.

The results of roughness (Table 3) were in agreement with the SEM images. The samples ground under irrigation showed higher *Ra* values ($p<0.05$). These results corroborated the micrograph results, which showed the influence of the deep valleys and particle deposition from the diamond stone on this surface. Grinding without irrigation yielded a less uneven surface and a lower phase transformation due to polishing afforded by the cutting tool, as described previously. The function of the polishing tool used in this study was studied by Chavali and others,[39] who observed a good polishing effect with the stone at a rotation of approximately 15,000 rpm with no irrigation.

Grinding increased the specimens' wettability (Figure 6) ($p<0.05$); however, there was no difference in the water drop spreading after grinding with and without irrigation, unlike what occurred with the roughness of the specimens. The *Ra* difference between the DG and WG groups was not sufficient to modify the wetting behavior of zirconia by water. This wettability difference between the worn groups, even with a major variation in roughness, might be related to the surface pattern and not only to the numerical value of *Ra*. Among the grinding groups, even at a larger value of *Ra*, the change in the surface pattern was smaller than the change observed between the ground groups and controls.

According to Noro and others,[40] in addition to surface morphology, the physical chemistry of the material also affects the wettability; therefore, beyond the standard roughness, the contamination of samples from the surfaces of the WG group by particles belonging to the diamond stone (Figure 5) and possibly the presence of natural hydrocarbons in the atmosphere[41] might have caused the drop spreading to be similar between the DG and WG groups. Even the samples cleaned by ultrasound had compounds that might have penetrated into the deepest valleys observed in group WG. It has been observed that chemical compounds consisting of carbon decrease the wettability of the surface of Y-TZP.[40,41]

As already mentioned, monoclinic grains can impair the long-term degradation of Y-TZP. Some manufacturers and researchers have suggested that an annealing process can reverse the *t-m* phase transformation caused by grinding. Such reverse transformation produces a tougher microstructure, minimizing the problems previously reported, which include degradation and the loss of adhesion of the veneering porcelain.[19,23,30]

The suggestion to heat-treat the material after grinding is not new. Denry and Holloway[23] fully reversed the phase transformation, that is, promoted the *m-t* reaction after heat treatment at 1000°C for 1 hour. However, various suggestions for treatment temperatures and times have emerged, with time periods varying between 15 minutes and 2 hour and temperatures between 500°C and 1200°C.[13,14,23,28,29]

In the present study, using high-temperature XRD, it was possible to more precisely observe the temperature at which the tetragonal to monoclinic phase transformation reversed in a commercial Y-TZP after grinding (Table 4). It was observed in specimens from the WG group that at temperatures greater than 700°C the *m-t* transformation occurred completely after the heat treatment schedule of the *in situ* high-temperature XRD, suggesting a temperature at this level for the reverse heat treatment. Thus, the temperature of 700°C served as a guide in the study of a heat treatment protocol.

Heat treatments were thus performed in a lab furnace at 700°C, 800°C, 900°C and 1000°C for 30 and 60 minutes. Table 5 shows that monoclinic zirconia remained on the surface of a WG sample after isothermal heat treatments at 700°C for 30 and 60 minutes. The ZrO_2-Y_2O_3 phase equilibrium diagram[42] shows a eutectoid reaction of $m+c \rightarrow t$ (by heating) at approximately 565°C and 2.5% Y_2O_3 (mole). At temperatures greater than ~565°C and with a typical molar composition of ZrO_2-3% Y_2O_3, the overall monoclinic phase vanishes, giving rise to

tetragonal and cubic zirconia when equilibrium is reached. In the cooling path, tetragonal zirconia can subsist in a metastable form, constrained by the neighboring cubic matrix. Thus, the reversal caused by annealing treatment must be suitable to convert the monoclinic to tetragonal zirconia at the same time that it retains the tetragonal form during cooling to room temperature. The nonexistence of the monoclinic phase after annealing at 700°C in the *in situ* high-temperature XRD could be explained by the longer heating time (~ 3 hours) and repetitive dwelling at different temperatures before reaching this temperature. In general, time periods longer than 1 hour would not be feasible for prosthetic preparation. In a conventional oven, with isothermal heat treatments, the total reversal of the monoclinic phase to tetragonal zirconia was obtained at 800°C after 60 minutes (Table 5), which was a lower temperature than those found in the literature.[13,14,23] At 900°C, the total reversal was observed in 60 minutes, corroborating the study of Kosmac and others.[14] This temperature level is less than that proposed by Denry and Holloway[23] and Fischer and others[13] of 1000°C for 15 minutes. For Denry and Holloway,[23] temperatures less than 1000°C were not sufficient to reverse the monoclinic to the tetragonal phase, whereas for Fischer and others,[13] the monoclinic phase could be transformed into the tetragonal at 1000°C, but microcracks in the material surface would not close, suggesting the need for further studies. The present study suggested that, together with the reversal of the *t-m* polymorphic transformation at temperatures greater than 800°C, a mechanism of crack healing must be active to constrain the transformed grains of t-ZrO_2 in the cubic matrix, retaining it in the metastable tetragonal form at room temperature. Nevertheless, further studies are necessary to confirm this hypothesis.

According to the manufacturer, the diamond stone used in the present work is recommended for use without irrigation, but it was tested here with irrigation in an attempt to promote a less aggressive procedure, following studies that suggested that refrigerated grinding caused fewer surface defects and produced an adequate compressive layer on the surface of Y-TZP.[1,14] However, in the present study, grinding with water caused greater damage to zirconia, with the MasterCeram diamond stone indicated for grinding without irrigation at approximately 20,000 rpm. Furthermore, to reverse the *t-m* transformation after diamond grinding, it is appropriate to perform a regenerative heat treatment at 800°C or 900°C for 60 minutes or 1000°C for 30 minutes.

CONCLUSIONS

Grinding with a diamond stone transformed part of the tetragonal crystallographic phase on the surface of Y-TZP ceramics into monoclinic zirconia and increased the surface roughness and wettability. Dry grinding with a diamond stone was less prejudicial to the zirconia. Heating at 800°C or 900°C for 60 minutes or at 1000°C for 30 minutes was an efficient treatment for the total reversion of the *t-m* phase transformation.

Acknowledgements

The authors wish to thank Mr Wagner Rafael Correr, Professor Alexandre Cuin, Mr Rodolfo Debone Piazza, and Professor Rodrigo Fernando Costa Marques for their contributions to this research. This work was supported by FAPESP (grant number 2015/04552-3). Eduardo Bellini Ferreira wishes also to thank FAPESP for the research funding through CeRTEV (grant number 2013/07793-6).

Conflict of Interest

The authors of this manuscript certify that they have no proprietary, financial, or other personal interest of any nature or kind in any product, service, and/or company that is presented in this article.

(Accepted 19 September 2016)

REFERENCES

1. Vagkopoulou T, Koutayas SO, Koidis P, & Strub JR (2009) Zirconia in dentistry: Part 1. Discovering the nature of an upcoming bioceramic *European Journal of Esthetic Dentistry* **4(2)** 130-151.
2. Piconi C, & Maccauro G (1999) Zirconia as a ceramic biomaterial *Biomaterials* **20(1)** 1-25.
3. Denry I, & Kelly JR (2008) State of the art of zirconia for dental applications *Dental Materials* **24(3)** 299-307.
4. Sailer I, Pjetursson BE, Zwahlen M, & Hämmerle CH (2007) A systematic review of the survival and complication rates of all-ceramic and metal-ceramic reconstructions after an observation period of at least 3 years. Part II: Fixed dental prostheses *Clinical Oral Implants Research* **18(3)** 86-96.
5. Lee TH, Lee SH, Her SB, Chang WG, & Lim BS (2012) Effects of surface treatments on the susceptibilities of low temperature degradation by autoclaving in zirconia *Journal of Biomedical Materials Research Part B Applied Biomaterials* **100(5)** 1334-1343.
6. Studart AR, Filser F, Kocher P, & Gauckler LJ (2007) In vitro lifetime of dental ceramics under cyclic loading in water *Biomaterials* **28(17)** 2695-2705.
7. Garvie RC, & Nicholson PS (1972) Structure and thermomechanical properties of partially stabilized zirconia in CaO-ZrO_2 system *Journal of the American Ceramic Society* **55** 152-157.

8. Chevalier J (2006) What future for zirconia as a biomaterial? *Biomaterials* **27(4)** 535-543.
9. Larsson C, & Wennerberg A (2014) The clinical success of zirconia-based crowns: A systematic review *International Journal of Prosthodontics* **27(1)** 33-43.
10. Sonza QN, Della Bona A, & Borba M (2014) Effect of the infrastructure material on the failure behavior of prosthetic crowns *Dental Materials* **30(5)** 578-585
11. Anusavice KJ (2012) Standardizing failure, success, and survival decisions in clinical studies of ceramic and metal-ceramic fixed dental prostheses *Dental Materials* **28(1)** 102-111.
12. Al-Amleh B, Neil Waddell J, Lyons K, & Swain MV (2014) Influence of veneering porcelain thickness and cooling rate on residual stresses in zirconia molar crowns *Dental Materials* **30(3)** 271-280.
13. Fischer J, Grohmann P, & Stawarczyk B (2008) Effect of zirconia surface treatments on the shear strength of zirconia/veneering ceramic composites *Dental Materials Journal* **27(3)** 448-454
14. Kosmac T, Oblak C, Jevnikar P, Funduk N, & Marion L (2000) Strength and reliability of surface treated Y-TZP dental ceramics *Journal of Biomedical Materials Research* **53(4)** 304-313.
15. Komine F, Fushiki R, Koizuka M, Taguchi K, Kamio S, & Matsumura H (2012) Effect of surface treatment on bond strength between an indirect composite material and a zirconia framework *Journal of Oral Science* **54(1)** 39-46.
16. Liu D, Matinlinna JP, Tsoi JK, Pow EH, Miyazaki T, Shibata Y, & Kan CW (2013) A new modified laser pretreatment for porcelain zirconia bonding *Dental Materials* **29(5)** 559-565.
17. Queiroz JR, Benetti P, Massi M, Junior LN, & Della Bona A (2012) Effect of multiple firing and silica deposition on the zirconia-porcelain interfacial bond strength *Dental Materials* **28(7)** 763-768.
18. Canneto JJ, Cattani-Lorente M, Durual S, Wiskott AH, & Scherrer SS (2016) Grinding damage assessment on four high-strength ceramics *Dental Materials* **32(2)** 171-182.
19. Ramos GF, Pereira GK, Amaral M, Valandro LF, & Bottino MA. (2016) Effect of grinding and heat treatment on the mechanical behavior of zirconia ceramic *Brazilian Oral Research* **30(1)** 1-8.
20. Nakamura K, Kanno T, Milleding P, & Ortengren U (2010) Zirconia as a dental implant abutment material: A systematic review *International Journal of Prosthodontics* **23(4)** 299-309.
21. Amaral M, Valandro LF, Bottino MA, & Souza RO (2013) Low-temperature degradation of a Y-TZP ceramic after surface treatments *Journal of Biomedical Materials Research Part B Applied Biomaterials* **101(8)**1387-1392.
22. Pereira GK, Amaral M, Simoneti R, Rocha GC, Cesar PF, & Valandro LF (2014) Effect of grinding with diamond-disc and -bur on the mechanical behavior of a Y-TZP ceramic *Journal of the Mechanical Behavior of Biomedical Materials* **37(September)** 133-134.
23. Denry IL, & Holloway JA (2006) Microstructural and crystallographic surface changes after grinding zirconia-based dental ceramics *Journal of Biomedical Materials Research Part B Applied Biomaterials* **76(2)** 440-448.
24. Güngör BM, Yılmaz H, Karakoca Nemli S, Turhan Bal B, & Aydın C (2015) Effect of surface treatments on the biaxial flexural strength, phase transformation, and surface roughness of bilayered porcelain/zirconia dental ceramics *Journal of Prosthetic Dentistry* **113(6)** 585-595.
25. Karakoca S, & Yilmaz H (2009) Influence of surface treatments on surface roughness, phase transformation, and biaxial flexural strength of Y-TZP ceramics *Journal of Biomedical Materials Research Part B Applied Biomaterials* **91(2)** 930-937.
26. Kim JW, Covel NS, Guess PC, Rekow ED, & Zhang Y (2010). Concerns of hydrothermal degradation in CAD/CAM zirconia *Journal of Dental Research* **89(1)** 91-95.
27. Aboushelib MN, & Wang H (2010) Effect of surface treatment on flexural strength of zirconia bars *Journal of Prosthetic Dentistry* **104(2)** 98-104.
28. Fonseca RG, Abi-Rached Fde O, da Silva FS, Henriques BA, & Pinelli LA (2014) Effect of surface and heat treatments on the biaxial flexural strength and phase transformation of a Y-TZP ceramic *Journal of Adhesive Dentistry* **16(5)** 451-458.
29. Guazzato M, Quach L, Albakry M, & Swain MV (2005) Influence of surface and heat treatments on the flexural strength of Y-TZP dental ceramic *Journal of Dentistry* **33(1)** 9-18.
30. Işeri U, Ozkurt Z, Yalnız A, & Kazazoğlu E (2012) Comparison of different grinding procedures on the flexural strength of zirconia *Journal of Prosthetic Dentistry* **107(5)** 309-315.
31. Qeblawi DM, Munoz CA, Brewer JD, & Monaco EA (2010) The effect of zirconia surface treatment on flexural strength and shear bond strength to a resin cement *Journal of Prosthetic Dentistry* **103(4)** 210-220.
32. Subaşı MG, Demir N, Kara Ö, Ozturk AN, & Özel F (2014) Mechanical properties of zirconia after different surface treatments and repeated firings *Journal of Advanced Prosthodontics* **6(6)** 462-467.
33. Monaco C, Tucci A, Esposito L, & Scotti R (2013) Microstructural changes produced by abrading Y-TZP in presintered and sintered conditions *Journal of Dentistry* **41(2)** 121-126.
34. Gualtieri A, Norby P, Hanson J, & Hriljac (1996) Rietveld refinement using synchrotron X-ray powder diffraction data collected in transmission geometry using an imaging-plate detector: application to standard m-ZrO_2 *Journal of Applied Crystallography* **29(6)** 707-713.
35. Bondars B, Heidemane G, & Grabis J (1995) Powder diffraction investigations of plasma sprayed zirconia *Journal of Materials Science* **30(6)** 1621-1625.
36. Preis V, Behr M, Hahnel S, Handel G, & Rosentritt M (2012) In vitro failure and fracture resistance of veneered and full-contour zirconia restorations *Journal of Dentistry* **40(11)** 921-928.
37. Wang Z, Willet P, Deaguiar PR, & Webster J (2001) Neural network detection of grinding burn from acoustic emission *International Journal of Machine Tools and Manufacture* **41(2)** 283-309.

38. Cameron A, Bauer R, & Warkentin A (2010) An investigation of the effects of wheel-cleaning parameters in creep-feed grinding *International Journal of Machine Tools and Manufacture* **50(1)** 126-130.

39. Chavali R, Lin CP, & Lawson NC (2015) Evaluation of different polishing systems and speeds for dental zirconia *Journal of Prosthodontics* epub ahead of print http://dx.doi.org/10.1111/jopr.12396.

40. Noro A, Kaneko M, Murata I, & Yoshinari M (2013) Influence of surface topography and surface physicochemistry on wettability of zirconia (tetragonal zirconia polycrystal) *Journal of Biomedical Materials Research Part B Applied Biomaterials* **101(2)** 355-63.

41. Rupp F, Scheideler L, Olshanska N, de Wild M, Wieland M, & Geis-Gerstorfer J (2006) Enhancing surface free energy and hydrophilicity through chemical modification of microstructured titanium implant surfaces *Journal of Biomedical Materials Research* **76(2)** 323-334.

42. Scott HG (1975) Phase relationships in the zirconia-yttria system *Journal of Materials Science* **10(9)** 1527-35.

©Operative Dentistry, 2017, **42-4,** 418-427

Light-emitting Diode Beam Profile and Spectral Output Influence on the Degree of Conversion of Bulk Fill Composites

MG Rocha • DCRS de Oliveira • IC Correa • L Correr-Sobrinho
MAC Sinhoreti • JL Ferracane • AB Correr

Clinical Relevance

The nonuniform emission of light-emitting diodes (LEDs) may provide a similar degree of conversion (DC) of a bulk fill composite with camphorquinone (CQ). However, the bulk fill composite with CQ and alternative photoinitiators may have a lower DC in depth as a result of lower wavelength absorption of alternative photoinitiators.

SUMMARY

Objectives: To evaluate the beam profile and the spectral output of monowave and polywave light-emitting diodes (LEDs) and their influence on the degree of conversion (DC) of bulk fill composites.

Methods: A monowave LED (Smartlite Focus, Dentsply) and a polywave LED (Valo Cordless, Ultradent) were characterized using a resin calibrator and a laser beam profile analyzer. Two bulk fill composites, Sonic Fill 2 (SF) containing camphorquinone (CQ) and Tetric EvoCeram Bulk Fill (TEB) containing CQ associated with alternative photoinitiators, were placed in custom-designed molds (n=3) and photoactivated by the monowave or polywave LED with 20 J/cm^2. To map the DC, longitudinal cross sections (0.5 mm thick) from the center of the restoration were evaluated using FT-NIR microscopy. SF and TEB light transmittances (n=3) through 4-mm-thick speci-

*Mateus Garcia Rocha, DDS, MSc, Piracicaba Dental School, State University of Campinas, Restorative Dentistry, Piracicaba, SP, Brazil

Dayane CRS de Oliveira, DDS, MS, PhD, Piracicaba Dental School, State University of Campinas, Restorative Dentistry, Piracicaba, SP, Brazil

Ivo Carlos Correa, DDS, MSc, PhD, Federal University of Rio de Janeiro, Prosthesis and Dental Materials, Rio de Janeiro, RJ, Brazil

Lourenco Correr-Sobrinho, DDS, MS, PhD, Piracicaba Dental School, University of Campinas, Restorative Dentistry, Piracicaba, SP, Brazil

Mario Alexandre C Sinhoreti, PhD, Piracicaba School of Dentistry, Department of Restorative Dentistry, Piracicaba, SP, Brazil

Jack L Ferracane, PhD, Oregon Health & Science University, Restorative Dentistry, Portland, OR, USA

Américo Bortolazzo Correr, DDS, Piracicaba Dental School, University of Campinas, Restorative Dentistry, Piracicaba, SP, Brazil

*Corresponding author: Av. Limeira 901, Piracicaba, São Paulo 13414-903, Brazil; e-mail: mateus_garcia@globo.com

DOI: 10.2341/16-164-L

mens were evaluated during curing. Data were analyzed using a split-plot analysis of variance and Tukey test (α=0.05; β=0.2).

Results: The monowave LED had a radiant emittance of 20 ± 0.5 J/cm^2 over 420-495 nm, and the polywave LED had an emittance of 15.5 ± 0.4 J/cm^2 over 420-495 nm and of 4.5 ± 0.2 J/cm^2 over 380-420 nm. The total radiant exposure at the bottom of TEB was 2.2 ± 0.2 J/cm^2 with the monowave LED and 1.6 ± 0.3 J/cm^2 with the polywave LED, and for SF it was 0.4 ± 0.1 J/cm^2 for both LEDs. There were no differences in the curing profiles produced either by the monowave or the polywave LED (p=0.9), according to the regions under influence of blue and/or violet emission at the same depth. There was no statistical difference in the DC for SF using the monowave or polywave LED at any depth (p=0.29). TEB had a higher DC at up to 2 mm in depth when the polywave LED was used (p<0.004), but no differences were found when starting at 2.5 mm.

Conclusions: Monowave and polywave LEDs emitted nonhomogeneous light beams, but this did not affect the DC homogeneity of bulk fill composites. For composites containing CQ associated with alternative photoinitiators, polywave LEDs had a higher DC, but only at the top part of the restoration; lower wavelength absorption photoinitiators were ineffective in deeper areas.

INTRODUCTION

The photoactivation of resin-based materials is always an important step in dentistry and still involves a concern for bulk fill composites.[1,2] An adequate radiant exposure is essential to produce biocompatible resin-based restorations with adequate physical properties to ensure clinical longevity.[2-4] However, the efficiency of photoactivation decreases with thickness as the radiant emittance is reduced because of the absorption and scattering of light within the composite.[5-7] The light attenuation is higher for the lower wavelengths (nm), such as violet (380-420 nm), in comparison to the higher blue wavelengths (420-495 nm) needed to activate the camphorquinone (CQ) photoinitiator used in all dental composites.

CQ has been partially substituted in some commercial products with alternative photoinitiators, such as diphenyl (2,4,6-trimethylbenzoyl) phosphine oxide (TPO), that are less yellow and have absorption peaks at wavelengths less than 420 nm.[8] As a result, polywave light-curing units with multiple light-emitting diodes (LEDs) possessing different wavelength range outputs (blue and violet) were designed.[9-11] However, the nonhomogeneity of the light beam emitted from these polywave units may affect the uniformity of the breadth and depth of the degree of conversion (DC) of resin-based materials, especially when CQ is used as the unique photoinitiator system.[12-14] Moreover, monowave units that emit only blue light may also be less efficient for curing resin-based materials containing CQ and alternative photoinitiators as a result of the absence of the appropriate wavelengths.[15-17]

A correlation between the nonhomogeneity of the emitted light and spatial variations in the microhardness of conventional resin-based composites (RBCs) up to 1.2 mm in thickness has been demonstrated.[13,18] However, a recent study on certain bulk fill composites did not show an influence of beam homogeneity on the cure's efficiency throughout the entire restoration.[8,12] In addition, monowave and polywave LEDs have different beam profiles and they might influence the DC of bulk fill composites that contain different photoinitiators. This could produce regions within the restoration with varied DCs and properties and may affect the clinical performance of bulk fill composites.

Thus, the aim of this study was to evaluate the influence of the beam profile of monowave and polywave LEDs on the degree of conversion of bulk fill composites containing only CQ or CQ associated with alternative photoinitiators. The hypotheses to be tested were that 1) monowave and polywave LEDs emit nonhomogeneous light beams, and 2) the beam profile of the monowave and polywave LEDs affects the homogeneity of the DC of bulk fill composites.

METHODS AND MATERIALS

Light-curing Unit Characterization

The mean radiant emittance (mW/cm^2) of a monowave LED (Smartlite Focus, Dentsply, York, PA, USA) and a polywave LED (Valo Cordless, Ultradent, South Jordan, UT, USA) were measured using a portable spectrometer-based instrument (CheckMARC, BlueLight Analytics, Nova Scotia, Canada) in order to calculate the photoactivation time needed to produce a radiant exposure of 20 J/cm^2.

The radiant exposure in the violet range (380-420 nm), blue range (420-495 nm), and overall range (380-495 nm) for each LED was obtained by integrating the irradiance vs the wavelength obtained with a spectrometer (MARC Resin Calibrator,

Table 1: *Manufacturer, Photoinitiator System, and Composition of Each Bulk fill Composite Evaluated*

Code	Bulk Fill Composite (Shade/Lot No.)	Manufacturer	Photoinitiator System	Resin Composition	Filler Amount (wt%/vol%)	Depth of Cure, mm[a]
SF	Sonic Fill 2 (A2/ 4427398)	Kerr, Orange, CA, USA	CQ, EDMAB	EPO, TEGDMA	Glass, SiO_2, oxide (84/66)	5
TEB	Tetric EvoCeram Bulk Fill (IVA/ P84136)	Ivoclar Vivadent, Schaan, Liechtenstein	CQ, EDMAB, TPO, Ivocerin	Bis-GMA, Bis-EMA, UDMA	Barium glass, YbF_3, oxide, PPF (81/61)	4

Abbreviations: Bis-EMA, ethoxylated Bis-phenol A methacrylate; Bis-GMA, bisphenol A glycidyl methacrylate; CQ, camphorquinone; EPO, poly(oxy-1,2-ethanediyl); PPF, prepolymerized fillers; TEGDMA, triethylene glycol dimethacrylate; TPO, diphenyl(2,4,6-trimethylbenzoyl)phosphine oxide; UDMA, urethane dimethacrylate; YbF_3, ytterbium trifluoride

[a] *According to the manufacturer.*

BlueLight Analytics). The Resin Calibrator has a cosine-corrected input sensor with a 4-mm-diameter aperture that receives light from 180°, and the light tips of the Valo Cordless and Smartlite Focus are 14 and 10 mm in diameter, respectively.

To determine the beam profile of each LED, radiant exposure distribution across the light tip was measured at the emitting surface using a laser beam analyzer (Model SP503U, Ophir-Spiricon, Logan, UT, USA). The resulting light from the LED was projected onto a diffusive surface of a frosted quartz target (DG2X21500, Thor Laboratories, Newton, NJ, USA), and the resulting image was recorded with the optical analysis software. Subsequently, narrow-bandpass filters with the full width at half-maximum of 10 nm (FWHM=10) (Thor Laboratories) were used to differentiate the spectral output at violet and blue wavelength peak regions, 400-410 nm and 455-465 nm, respectively. These were calibrated on separate images, and these images were plotted in color-coded maps in two-dimensional (2D) and three-dimensional (3D) views according to the maximum radiant emittance detected. The areas with higher and lower radiant emittance were determined in standard areas of 0.126 cm^2 in the regions of maximum and minimum radiant emittance detected.

Radiant Emittance Transmitted

Table 1 lists the bulk fill composites evaluated. Light transmittance through each composite was recorded during curing using Smartlite Focus and Valo Cordless LEDs. Samples of each bulk fill composite (n=3) were placed in Delrin molds (Ø=6 mm × 4 mm thick), which were placed on the bottom sensor (Ø=4 mm) of the Resin Calibrator with Mylar strips covering the top and bottom surfaces of the samples. The spectral radiant power and the radiant exposure transmitted through the bulk fill composite were calculated by integrating the irradiance over the different wavelength ranges from the graph of radiant emittance vs the wavelength obtained with the Resin Calibrator.

Mapping of the Degree of Conversion

Class I restorations (6×6 mm, 4 mm deep) of each bulk fill composite (n=3) were produced in a custom-designed transparent polymethylmethacrylate (PMMA) mold (Figure 1A-C).[8,12] The photoactivation was performed using each LED with 20 J/cm^2. A jig was made to position the LED reproducibly in order to establish the regions of the restoration exposed to the light emitted from the blue and violet LEDs and also the overlapping region in between from the polywave LED (Figure 1D). After 24 hours of dark, dry storage at 37°C, cross-section specimens (6 mm × 4 mm × 0.5 mm thick) from the center of the restoration, perpendicular to the top surface and parallel to the long axis of the block (Figure 1E), were obtained using an automated water-cooled, low-speed diamond saw (Isomet 1000, Buehler Ltd, Lake Bluff, IL, USA). The specimens were fixed onto a glass slab and placed over an automated x-y axis microscope platform. The DC was mapped along the cross section (width: 6 mm; depth: 4 mm) using a FT-NIR Microscope (Nicolet Continuum, Thermo Scientific, Waltham, MA, USA) coupled to a FT-NIR spectrometer (Nicolet Nexus 6700, Thermo Scientific) (Figure 1F). Every 500 μm in width and depth, an infrared spectrum was collected, resulting in 117 measuring points for each cross section. The measurements started 300 μm below the top surface in order to avoid the area of oxygen inhibition. At each measurement position, the specimens' NIR spectrums were collected in transmission mode with 50 scans at 4 cm^{-1} of resolution and a detector aperture size of 50. Spectra of uncured specimens (n=3) collected with the same settings were used as a reference to measure the peak area ratio corresponding to the aromatic and vinyl stretching absorptions. The DC (in %) was calculated as follows:

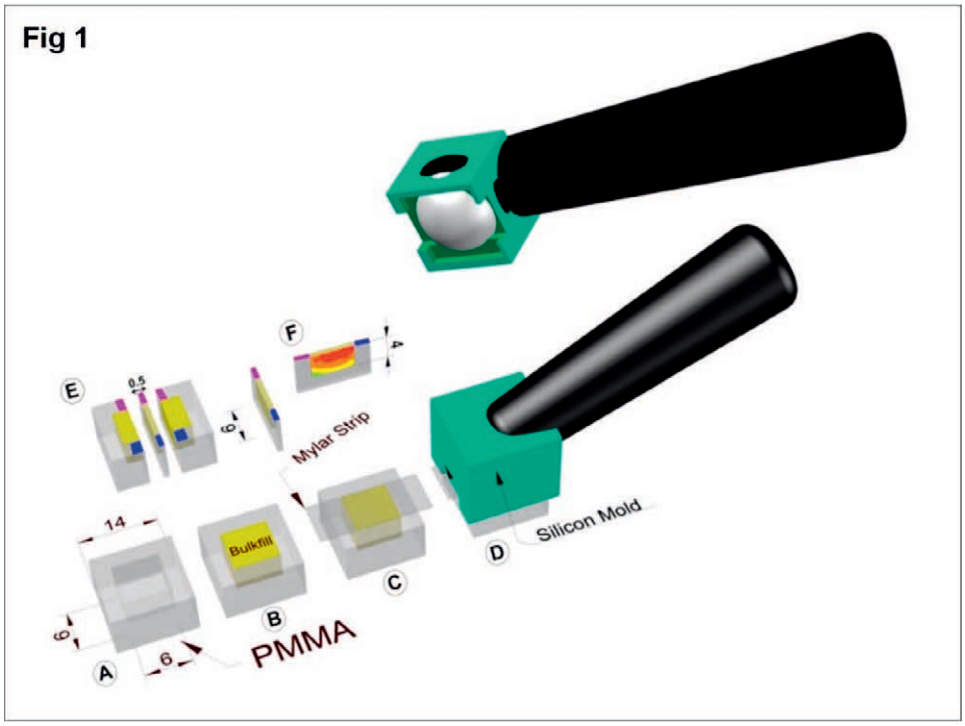

Figure 1. *Schematic design of the experimental setup. (A) PMMA mold with 6 × 6 × 4-mm cavity; (B) Bulk fill insertion into the PMMA mold; (C) Mylar strip covering the surface; (D) Light cured with 20 J/cm^2 using the LED positioned with a silicon jig mold; (E) Cross section of the center of the restoration with blue and violet LED emittance regions established; (F) Mapping of the DC using a FT-NIR microscope.*

$$DC = \{1 - [(\text{vinyl peak area pol}/\text{aromatic peak area pol})/(\text{vinyl peak area non pol}/\text{aromatic peak area non pol})]\} \times 100$$

where *pol* and *non pol* correspond to the area of the methacrylate peak for the polymeric and monomeric states, respectively.

The results were exported into mapping software (OriginPro 2015, OriginLab Co, Northampton, MA, USA). Color-coded maps were created to describe the DC as a function of position under the light beam in width (0-6 mm) and in depth (0-4 mm). For the polywave LED, the regions under the influence of the blue LED chips were set from 0 to 2 mm wide, the overlap in between the blue and violet LED chips were set from 2.5 to 4 mm wide, and the regions under the influence of the violet LED chips were set from 4.5 to 6 mm wide. Also, the map scales were set to indicate the maximum DC achieved with the bulk fill composites and a reduction of 10% of the maximum DC in each color-coded area.

Statistical Analysis

A split-plot analysis of variance was used for the statistical analysis of the DC values. The Tukey test was applied for multiple comparisons (α=0.05) for each of the different bulk fill composites (SF and TEB). The independent variables were set as between-subject groups for the LEDs (monowave or polywave) and as within-subject groups for the LED emittance regions in width (0, 0.5, 1, 1.5, 2, 2.5, 3, 3.5, 4, 4.5, 5, 5.5, and 6 mm) and depth (0, 0.5, 1, 1.5, 2, 2.5, 3, 3.5, and 4 mm) below the tip of the LED. For the polywave LED, the regions under the influence of the blue LED chips were set as the mean of points from 0 to 2 mm wide, the overlap in between blue and violet LEDs chips were set as the mean of points from 2.5 to 4 mm wide, and the regions under the influence of the violet LED chips were set as the mean of points from 4.5 to 6 mm wide. Power analysis was conducted to determine the sample size for each experiment to provide a power of at least 0.8 at a significance level of 0.05 (β=0.2).

RESULTS

Table 2 shows the mean radiant emittance and the total radiant exposure within each wavelength range for each LED. Figure 2 illustrates the beam profile of both LED units in 2D and 3D of 400-410-nm and 455-465-nm wavelength ranges. Smartlite Focus had an active area of emission of 0.352 cm^2 and a maximum radiant emittance of 1850 mW/cm^2, but

Table 2: *Light-emitting Diode (LED) Units: Mean Radiant Emittance (mW/cm^2) and Radiant Exposure (J/cm^2) According to the Different Wavelength Ranges*

Light-curing Unit	Mean Radiant Emittance, mW/cm^2	Time of Exposure, s	Wavelength Ranges, nm	Radiant Exposure, J/cm^2
Smartlite Focus	1000	20	420-495	20 ± 0.5
VALO Cordless	954	21	380-420	4.5 ± 0.2
			420-495	15.5 ± 0.4

the radiant emittance was not homogeneously distributed across the tip. A high emission (1082 mW/cm^2) was localized in a small area (0.126 cm^2) at the center of the light tip (red dash circle). An area of lower radiant emittance (534 mW/cm^2) was localized at the periphery of the light tip (blue dash circle). Valo Cordless had an active area of emisson of 0.750 cm^2 and a maximum radiant emittance of 1449 mW/cm^2, but the radiant emittance and the wavelength emission were not homogeneously distributed across the tip. For the blue wavelength emisson, localized standard areas of a higher radiant emittance of 1085 mW/cm^2 and a lower radiant emittance of 397.5 mW/cm^2 were seen. For the violet wavelength emission, localized areas of a higher radiant emmitance of 431 mW/cm^2 and a lower radiant emittance of 50 mW/cm^2 were seen.

Figure 3 illustrates the radiant emittance vs wavelength of each LED on the top surface of the specimen and through each bulk fill composite. Smartlite Focus had a peak emission at 470 nm; Valo Cordless had three peaks of emission at 400, 440, and 460 nm. The radiant exposure at the bottom (4 mm) of TEB was 2.2 ± 0.2 J/cm^2 with the Smartlite Focus and 1.6 ± 0.3 J/cm^2 with the Valo Cordless. For SF, the radiant exposure was 0.4 ± 0.1 J/cm^2 for both LEDs.

Figure 4 shows the mean (± standard deviation [SD]) DC in depth of each bulk fill composite according to each LED. For SF, there was no statistical difference in the DC using the Smartlite Focus or Valo Cordless LED (df=1; F=1.2; p=0.28) at any depth. However, TEB showed a higher DC for Valo Cordless than for Smartlite Focus up to 2 mm in depth (df=1; F=4.9; p=0.04). Starting at 2.5 mm there was no statistical difference between Valo Cordless and Smartlite Focus.

Figure 5 illustrates the mapping of the DC of each bulk fill composite according to the different LEDs. Comparing the width point by point throughout the sample, Smartlite Focus showed no statistical difference in the DC for both SF (df=16; F=0.5; p=0.93) and TEB (df=16; F=0.1; p=0.9) at any depth. Also, Valo Cordless showed no statistical difference among the blue, violet, and overlapping regions for both SF (df=16; F=0.6; p=0.86) and TEB (df=16; F=0.12; p=0.9). In addition, there was no statistical difference between Smartlite Focus and Valo Cordless in the same region (width and depth) of the sample for

Fig 2

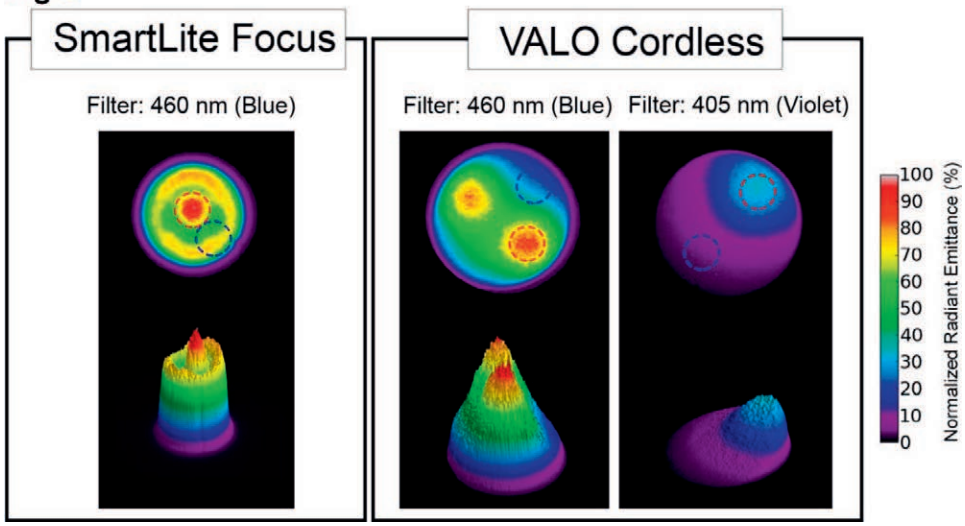

Figure 2. *Beam profile images of LED units (2D and 3D views) within 455-465-nm (blue) and 400-410-nm (violet) wavelength ranges. Red dash circles indicate area of higher radiant emittance, and blue dash circles indicate area of lower radiant emittance. One hundred percent normalized radiant emittance values were 1850 mW/cm^2 for Smartlite Focus and 1449 mW/cm^2 for Valo Cordless.*

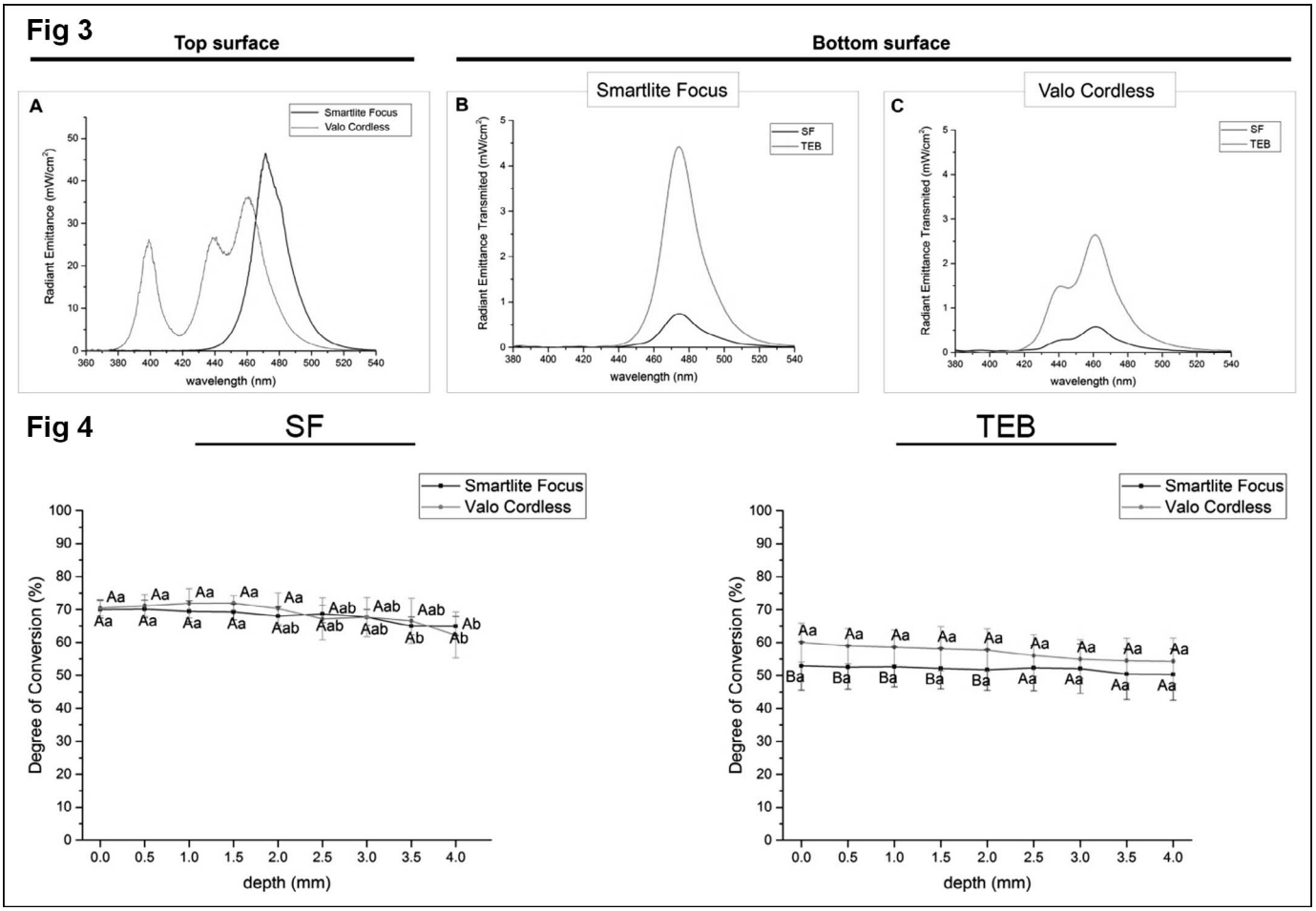

Figure 3. *Absolute irradiance (mW/cm²/nm) × wavelength (nm) for bulk fill composite cured with each LED unit. (A) Smartlite Focus and Valo Cordless at 0 mm, (B) Smartlite Focus through 4-mm thickness of SF and TEB, and (C) Valo Cordless through 4-mm thickness of SF and TEB.*
Figure 4. *Mean DC (%) at 0 to 4 mm in depth of each bulk fill composite according to the different LED unit.*

SF (df=32; F=0.57; p=0.96) and TEB (df=32; F=0.1; p=0.99).

DISCUSSION

An important step before the photoactivation of RBCs is the assessment of the light-curing unit (LCU), because the energy delivered to the surface of the RBCs should be sufficient to provide an adequate cure of the material.[2,3] This is necessary because while the same radiant exposure may be emitted by two different LCUs, the spectral power distribution could be completely different.[3,10,14]

Table 2 shows the same total radiant exposure (±20 J/cm^2) for the Smartlite Focus and the Valo Cordless. Since Smartlite Focus is a monowave LED and emits only a single narrow Gaussian band with a wavelength peak at 470 nm, the radiant exposure emitted by this light is all within the blue range. In contrast, Valo Cordless is a polywave LED with three emission peaks at 400, 440, and 460 nm; thus, some of the spectral power is emitted in the violet region (4.5 J/cm^2), while the majority of it is emitted in the blue region (15.5 J/cm^2).

This study verified that monowave and polywave LEDs have differences in their radiant emittance and wavelength distribution across the light tip, as demonstrated in the beam profile images (Figure 2).[13,14] The monowave LED has one LED chip localized at the center of the tip; thus, an area of higher radiant emittance is clear near this region. The polywave LED has four LED chips, and the beam profile results corroborate that the different LED chips are widely spatially separated.[10,19] However, narrow band-pass filters (FWHM=10 nm) have to be used sequentially to determine the different wavelength outputs, and they might only detect part of the beam profile image for the polywave LED. Only the output emissions from two 460-nm chips

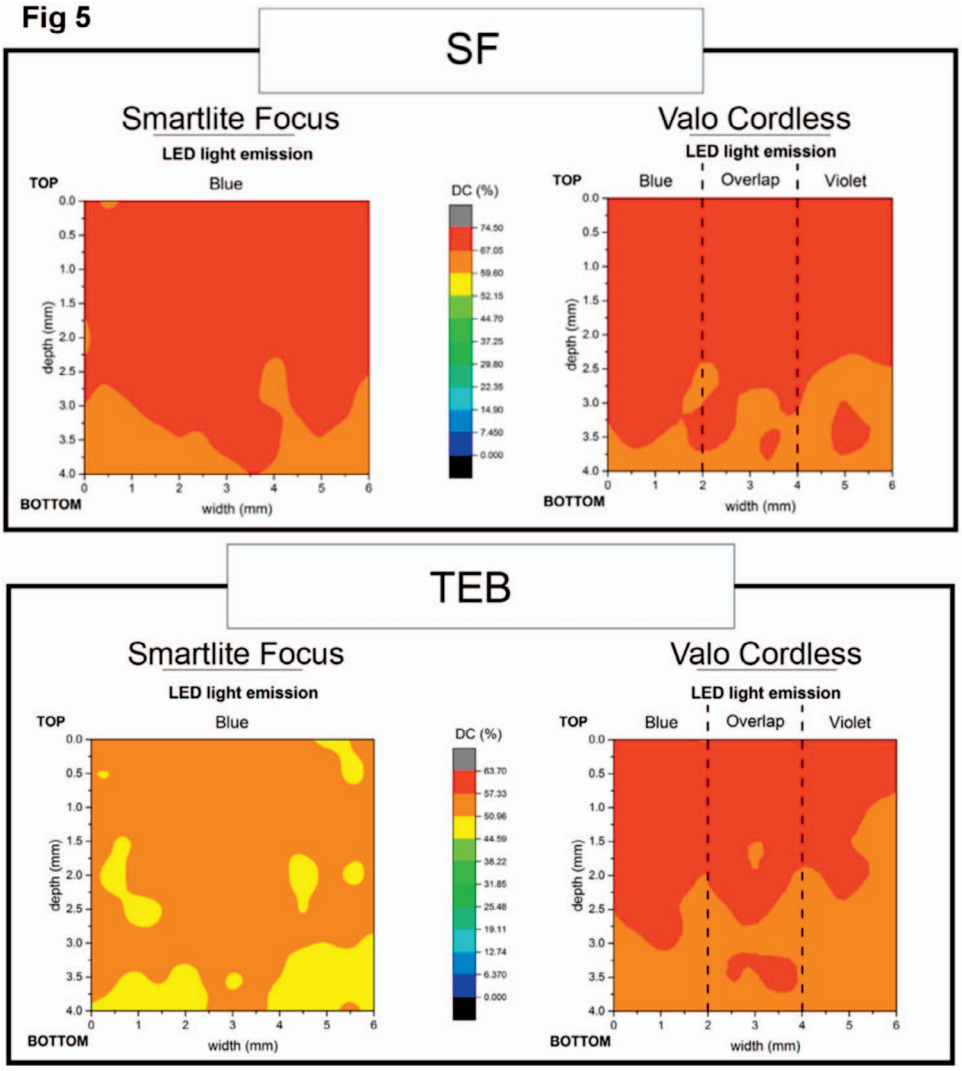

Figure 5. *Mapping of the DC (%) of bulk fill composites according to the different LED emittance regions (blue, violet, and the overlap in between blue and violet) of LED units.*

and the single 405-nm chip were detected; that of the 440-nm chip (which is located diagonally opposite to the 405-nm chip in the rectangular four-chip array) was not.[10] Thus, the first research hypothesis, that monowave and polywave LEDs emit a nonhomogeneous light beam, could be accepted. Polywave LEDs have previously been identified[14,18,19] as having a nonuniform spectral distribution across their light end tip at the violet and blue emission wavelengths. Local differences in irradiance distribution and spectral homogeneity could affect the extent or quality of the cure across the RBC specimen's surfaces and in its depth. The significance of these findings has yet to be widely appreciated, but the general impact of wide differences in the polywave LED's performance and the clinical factors related to the restoration's longevity are considered to be significant. Clinically, this means that the orientation and positioning of the LED might affect both the irradiance and wavelength received by different locations within the restoration.[13,14,18]

Despite the nonhomogeneous light beam emitted by both LEDs, the results showed that the curing profile of each bulk fill composite was similar for both LEDs. The distances in width and depth from the position of the LED chips of the monowave and polywave LEDs have no influence on the DC at any depth for SF or TEB. High-viscosity bulk fill composites such as SF and TEB are highly filled materials that contain 84/66 wt%/vol% and 81/61 wt%/vol%, respectively, of filler particles, as shown in Table 1. The mismatch between the refractive index of the filler particles and the organic matrix causes light scattering.[20] Thus, the light emitted by LEDs is scattered through the composite, and a diffuse reflection likely spreads light throughout the sample. Although the nonhomogeneous radiant

emittance emitted by the LEDs is over the top of the sample, the light scattering promoted inside the bulk fill composites spreads light within the sample. This could have provided a more homogeneous DC.[6,7] Therefore, the second research hypothesis, that the beam profile of the monowave and polywave LEDs affects the homogeneity of the DC of bulk fill composites, was rejected.

Despite the beam profile of the monowave and polywave LEDs having had no influence on the DC, the spectral output of the LEDs had a significant impact on the DC in depth for bulk fill composites containing CQ associated with alternative photoinitiators, such as TEB. The mean DC for TEB using the monowave LED was lower than that achieved with the polywave LED. This can be explained by the radiant emittance of the monowave LED and photoinitiator systems used in TEB. TEB has a combination of three photoinitiator systems: a Norrish type II photoinitiator system, CQ associated with EDMAB (tertiary amine); and two Norrish type I photoinitiator systems, TPO and a benzoyl germanium (Ivocerin). CQ and the EDMAB photoinitiator system absorb light in the blue range from 420 to 495 nm, with a peak absorption at 470 nm.[8,21] Ivocerin absorbs light in the violet and blue ranges from 370 to 510 nm, with a peak absorption at 418 nm.[17] TPO absorbs light in the violet range from 350 to 420 nm, with a peak absorption at 370 nm.[8,21] Smartlite Focus only emitted light within the blue range from 440 to 495 nm, where CQ heavily absorbs, and light at these wavelengths was able to penetrate through a 4-mm thickness of the composite (Figure 3). Thus, only CQ and the EDMAB photoinitiator system were excited by the LED emission and generated free radicals to initiate the polymerization throughout the restoration. Therefore, once the spectral output of the LED did not correspond with spectral absorption of all photoinitiator systems in the composition, the monowave LED was not efficient in curing TEB. When the narrow spectrum emission of the monowave LED is used instead of the broad spectrum of the polywave LED, there might be a reduction in DC for TEB.

Despite the higher mean DC for TEB using the polywave LED rather than the monowave LED, this difference was not significant at all depths. As shown in Figure 4, from the top surface (0 mm) to 2 mm in depth, TEB had a higher DC when cured using the polywave LED, but beyond 2.5 mm no statistical difference was found between the two LEDs. Valo Cordless emits light that can be absorbed by CQ, TPO, and Ivocerin. A higher DC might be expected as a result of these photoinitiator systems in the TEB composition working in synergism, generating more free radicals than CQ alone.[8] However, only blue light was capable of penetrating through the 4-mm-thick composite, and then only CQ and Ivocerin would be excited by the polywave LED emission at deeper portions.[22,23] This means that TEB combines three photoinitiators with three absorption peaks that should work in synergism to ensure adequate cure of the composite. However, this photoinitiator combination was effective just at the top part of the restoration up to 2 mm. Therefore, photoinitiator systems with a lower wavelength absorption than that of blue did not improve the DC at greater depths because the light that activates these photoinitiators are attenuated through the RBC and could not reach deeper areas of the restoration.

When TEB was cured with Smartlite Focus, the color-coded map of the DC showed areas in yellow that correspond to less than 80% of the maximum DC achieved for this composite. Previous studies[5,24] have suggested that a hardness or DC of at least 80% of the maximum attainable is considered to be adequately cured, but the statistical analyses used in this study showed no significant difference for these areas. Despite no differences for the same point in the graph (width and depth) between Smartlite Focus and Valo Cordless, when the mean of the points of all areas of the map is considered, Smartlite Focus has a lower DC than Valo Cordless.

For SF, no differences were found in the DC values between the two LEDs at any depth. SF has only CQ and EDMAB as the photoinitiator system, which is heavily absorbed at the blue wavelength range. Although the monowave LED emitted higher radiant exposure within the blue range from 420 to 495 nm over the top of the samples, the same radiant exposure (0.4 J/cm^2) was transmitted through the samples during curing, and this might explain the similarity in the DCs of this composite.

Thus, for bulk fill composites containing only CQ as the photoinitiator system, the use of either a monowave or polywave LED did not affect the DC or homogeneity of the cure. However, for bulk fill composites containing CQ associated with other photoinitiators with lower wavelength absorption, the use of a monowave LED resulted in a reduced DC. Further studies are being conducted in order to evaluate if the same behavior will occur in Class II restorations as a result of the presence of a dentin

barrier between the overlapping of blue and violet emittance from a polywave LED.

CONCLUSIONS

The monowave and polywave LEDs used in this study emitted nonhomogeneous light profiles, but the nonhomogeneity of the light beam did not affect the homogeneity of the DC of the bulk fill composites tested. For bulk fill composites containing only CQ as a photoinitiator, the monowave and polywave LEDs had the same efficiency. For composites containing CQ associated with alternative photoinitiators, the polywave LED had a higher DC, but only at the top part of the restoration and up to 2 mm in depth. Lower wavelength absorption photoinitiators were ineffective in deeper areas.

Acknowledgements

This study was supported by the FAPESP (grant 2016/06019-3) and the CNPq (grant 140965/2016-5). DO is a PhD Researcher at FAPESP (grant 2013/04241-2) and BEPE (grant 03028-6). We would like to acknowledge BlueLight Analytics for donating a MARC Resin Calibrator to the School of Dentistry of Oregon and Health and Science University and for producing the beam profile images used in this study and Dr Carmem Pfeifer for helping to develop the method used in this study.

Conflict of Interest

The authors of this manuscript certify that they have no proprietary, financial, or other personal interest of any nature or kind in any product, service, and/or company that is presented in this article.

(Accepted 19 September 2016)

REFERENCES

1. Zorzin J, Maier E, Harre S, Fey T, Belli R, Lohbauer U, Petschelt A, & Taschner M (2015) Bulk-fill resin composites: Polymerization properties and extended light curing *Dental Materials* **31(3)** 293-301.
2. Price RB, Shortall AC, & Palin WM (2014) Contemporary issues in light curing *Operative Dentistry* **39(1)** 4-14.
3. Price RB, Ferracane JL, & Shortall AC (2015) Light-curing units: A review of what we need to know *Journal of Dental Research* **94(9)** 1179-1186.
4. Ilie N, Kessler A, & Durner J (2013) Influence of various irradiation processes on the mechanical properties and polymerisation kinetics of bulk-fill resin based composites *Journal of Dentistry* **41(8)** 695-702.
5. Leprince JG, Leveque P, Nysten B, Gallez B, Devaux J, & Leloup G (2012) New insight into the "depth of cure" of dimethacrylate-based dental composites *Dental Materials* **28(5)** 512-520.
6. Shortall AC, Palin WM, & Burtscher P (2008) Refractive index mismatch and monomer reactivity influence composite curing depth *Journal of Dental Research* **87(1)** 84-88.
7. dos Santos GB, Alto RV, Filho HR, da Silva EM, & Fellows CE (2008) Light transmission on dental resin composites *Dental Materials* **24(5)** 571-576.
8. de Oliveira DC, Rocha MG, Correa IC, Correr AB, Ferracane JL, & Sinhoreti MA (2016) The effect of combining photoinitiator systems on the color and curing profile of resin-based composites *Dental Materials* **32(10)** 1209-1217.
9. Leprince JG, Palin WM, Hadis MA, Devaux J, & Leloup G (2013) Progress in dimethacrylate-based dental composite technology and curing efficiency *Dental Materials* **29(2)** 139-156.
10. Shortall AC, Felix CJ, & Watts DC (2015) Robust spectrometer-based methods for characterizing radiant exitance of dental LED light curing units *Dental Materials* **31(4)** 339-350.
11. Jandt KD, & Mills RW (2013) A brief history of LED photopolymerization *Dental Materials* **29(6)** 605-617.
12. Li X, Pongprueksa P, Van Meerbeek B, & De Munck J (2015) Curing profile of bulk-fill resin-based composites *Journal of Dentistry* **43(6)** 664-672.
13. Haenel T, Hausnerova B, Steinhaus J, Price RB, Sullivan B, & Moeginger B (2015) Effect of the irradiance distribution from light curing units on the local microhardness of the surface of dental resins *Dental Materials* **31(2)** 93-104.
14. Michaud PL, Price RB, Labrie D, Rueggeberg FA, & Sullivan B (2014) Localised irradiance distribution found in dental light curing units *Journal of Dentistry* **42(2)** 129-139.
15. Schneider LF, Cavalcante LM, Prahl SA, Pfeifer CS, & Ferracane JL (2012) Curing efficiency of dental resin composites formulated with camphorquinone or trimethylbenzoyl-diphenyl-phosphine oxide *Dental Materials* **28(4)** 392-397.
16. Schneider LF, Pfeifer CS, Consani S, Prahl SA, & Ferracane JL (2008) Influence of photoinitiator type on the rate of polymerization, degree of conversion, hardness and yellowing of dental resin composites *Dental Materials* **24(9)** 1169-1177.
17. Moszner N, Fischer UK, Ganster B, Liska R, & Rheinberger V (2008) Benzoyl germanium derivatives as novel visible light photoinitiators for dental materials *Dental Materials* **24(7)** 901-907.
18. Price RB, Labrie D, Rueggeberg FA, Sullivan B, Kostylev I, & Fahey J (2014) Correlation between the beam profile from a curing light and the microhardness of four resins *Dental Materials* **30(12)** 1345-1357.
19. Price RB, Labrie D, Rueggeberg FA, & Felix CM (2010) Irradiance differences in the violet (405 nm) and blue (460 nm) spectral ranges among dental light-curing units *Journal of Esthetic and Restorative Dentistry* **22(6)** 363-377.
20. de Oliveira DC, de Menezes LR, Gatti A, Correr Sobrinho L, Ferracane JL, & Sinhoreti MA (2016) Effect of nanofiller loading on cure efficiency and potential color

change of model composites *Journal of Esthetic and Restorative Dentistry* **28(3)** 171-177.

21. Neumann MG, Miranda WG Jr, Schmitt CC, Rueggeberg FA, & Correa IC (2005) Molar extinction coefficients and the photon absorption efficiency of dental photoinitiators and light curing units *Journal of Dentistry* **33(6)** 525-532.
22. Harlow JE, Rueggeberg FA, Labrie D, Sullivan B, & Price RB (2016) Transmission of violet and blue light through conventional (layered) and bulk cured resin-based composites *Journal of Dentistry* **53** 44-50.
23. Hadis MA, Shortall AC, & Palin WM (2012) Specimen aspect ratio and light transmission in photoactive dental resins *Dental Materials* **28(11)** 1154-1161.
24. Flury S, Hayoz S, Peutzfeldt A, Husler J, & Lussi A (2012) Depth of cure of resin composites: Is the ISO 4049 method suitable for bulk fill materials? *Dental Materials* **28(5)** 521-528.

©Operative Dentistry, 2017, **42-4,** 428-435

Microhardness and Roughness of Infiltrated White Spot Lesions Submitted to Different Challenges

ÉY Neres • MD Moda • EK Chiba • ALF Briso
JP Pessan • TC Fagundes

Clinical Relevance

Infiltrated white spot lesions seem to resist mechanical abrasion and artificial accelerated aging, but they are not resistant to a new cariogenic challenge.

SUMMARY

A white spot lesion is the first clinical sign of a caries lesion and represents mineral loss from the enamel subsurface. The purpose of this study was to evaluate the microhardness and surface roughness of white spot lesions after application of a resin infiltrant and subjection to different challenges. Caries-like lesions were induced in bovine enamel discs (n=50), and the specimens were randomly divided into five study groups (n=10): demineralized enamel (negative control, G1), infiltrated enamel (G2), infiltrated enamel submitted to brushing (G3), infiltrated enamel submitted to pH cycling (G4), and infiltrated enamel submitted to artificial aging (G5). Half of each enamel surface was used as its own positive control. Roughness data were analyzed using the Kruskal-Wallis test followed by the Dunn test. Results from microhardness were analyzed by two-way analysis of variance, followed by the Tukey test for multiple comparisons. The level of significance was set at 5%. Microhardness and roughness values obtained from the test side of the specimens were significantly lower compared with the sound enamel for all groups. Microhardness values obtained for G2, G3, and G5 were not significantly different. Values found for G1 were significantly lower compared with those for G2, G3, and G5. The lowest microhardness values were observed for G4, which was significantly different from

Émerson Yoshio Neres, DDS, Department of Restorative Dentistry, São Paulo State University (Unesp), School of Dentistry, Araçatuba, Brazil

Mariana Moda, DDS, PhD student, Department of Restorative Dentistry, Araçatuba Dental School, UNESP – Univ Estadual Paulista, Araçatuba, Brazil

Erika Kiyoko Chiba, undergraduate student, Department of Restorative Dentistry, São Paulo State University (Unesp), School of Dentistry, Araçatuba, Brazil

André Luis Fraga Briso, DDS, MS, PhD, associate professor, Department of Restorative Dentistry, São Paulo State University (Unesp), School of Dentistry, Araçatuba, Brazil

Juliano Pelim Pessan, DDS, MS, PhD, assistant professor, Department of Pediatric Dentistry and Public Health, São Paulo State University (Unesp), School of Dentistry, Araçatuba, Brazil

*Ticiane Cestari Fagundes, DDS, MS, PhD, assistant professor, Department of Restorative Dentistry, São Paulo State University (Unesp), School of Dentistry, Araçatuba, Brazil

*Corresponding author: R. José Bonifácio, 1193, Araçatuba, SP, 16015-050, Brazil; e-mail: ticiane@foa.unesp.br

DOI: 10.2341/16-144-L

the other groups. Surface roughness was not significantly different between G2 and G3. The resin infiltrant presented superiority over the unprotected white spot lesions, as they were more resistant to mechanical and aging challenges. However, resin infiltration was not able to reestablish the properties of sound enamel and was not resistant to a new cariogenic challenge.

INTRODUCTION

White spots are recognized as initial carious lesions, which could develop into cavities. Different management approaches have been applied to treat white spot lesions on smooth surfaces, as early as possible, to avoid invasive treatment with cavity preparation.[1] These include remineralization of the lesion with topically applied fluoride products[2] or use of a microabrasion technique, which is especially indicated for remineralized superficial lesions.[3] Although microabrasion is an effective method for eliminating a white spot lesion, minimal wear occurs in healthy tissues.[3]

More recently, a noninvasive alternative treatment was proposed, based on caries infiltration with a hydrophobic resin, which has a refractive index close to that of sound enamel, therefore masking the white spot by infiltrating the porous enamel.[4] This treatment has also been proposed to inhibit demineralization because the diffusion pathways for cariogenic acids are blocked, therefore sealing the white spot lesions.[4] The infiltrant resin is a product that allows for the treatment of carious lesions in early stages without invasive measures.[5]

However, the oral environment is constantly under mechanical and chemical challenges that may affect the tooth structure or restorative materials. Toothbrushing is a mechanical challenge for the prevention and control of oral diseases, such as dental caries and periodontal disease. Nevertheless, there is increased wear during brushing compared with sound enamel in demineralized enamel.[6,7] In this regard, *in vitro* toothbrushing has been a useful tool for testing the resistance to wear of sealant materials.[6,7] Moreover, pH cycling models are also used to evaluate treatment options for white spot lesions, since these models mimic pH alterations of the oral environment.[8] Additionally, artificial accelerated aging systems have been used to simulate aging of the tooth structure and/or restorative materials because it simulates the chemical and physical environments that could partially replace the oral cavity conditions.[9]

Considering the scarce literature on studies evaluating the effect of resin infiltrants applied on white spot lesions submitted to different challenges, this study evaluated the microhardness and surface roughness of infiltrated white spot lesions after exposure to toothbrushing, a pH cycling regimen, and artificial aging. The null hypothesis was that the type of challenge does not influence the microhardness and surface roughness of white spot lesions and infiltrated enamel.

METHODS AND MATERIALS

Sample Preparation

This study was previously approved by the local animal ethical committee (protocol #2014-01115). Sound permanent bovine incisors obtained from steers aged 24 to 30 months old were collected and stored in 0.1% thymol solution. Specimens without white spots, cracks, or any other defect were selected and then cleaned using slurry pumice and brush. The tooth roots were removed under abundant water irrigation. The crowns were then mounted in a cutting machine using a cylindrical diamond tip (Dinser Ferramentas Diamantadas, São Paulo, Brazil). Discs containing enamel and dentin were cut, each with a 5.7-mm diameter, from the middle third of the buccal surface of each tooth.

The specimens were fixed on an acrylic base, and the dentin surfaces were flattened using a polishing machine (Arotec, Cotia, Brazil) with 320-grit aluminum oxide sandpaper (Buehler Ltd, Lake Bluff, IL, USA) under water cooling at low speed (100 rpm) until a 2.2-mm thickness was obtained. Then, the enamel surfaces were flattened and polished using 400-, 600-, 800-, and 1200-grit sandpaper, reaching enamel thickness of 1.3 mm. Final polishing was performed with felt disks and 1 μm diamond paste (Extec Corp, Enfield, CT, USA) for 3 minutes.

Analysis of Surface Microhardness

Baseline surface microhardness was determined by the mean of five indentations produced 100 μm apart from each other in the center of the specimen with a Knoop (KHN) diamond indenter and a load of 25 g and dwell time of 10 seconds, using a microhardness meter durometer (Buehler 5114, Buehler) and specific software for image analysis (OmniMet, Buehler). Only specimens with baseline values between 300 and 380 KHN were selected for the study.

Table 1: *Composition and Application Steps of Resin Infiltrant (Icon, DMG, Hamburg, Germany) According to the Manufacturer's Instructions*

Composition	Application Steps	Batch No.
Icon-etch: (HCl 15%) pyrogenic silicic acid, surface-active substances	Apply Icon-Etch. Let set for 2 min. Rinse off with water for 30 s. Air dry.	711766/ 708255/ 702131
Icon-dry: 99% ethanol	Apply Icon-Dry. Let set for 30 s. Air dry.	
Icon-infiltrant: methacrylate-based resin matrix, initiators, and additives	Apply Icon-Infiltrant. Let set for 3 min. Light-cure for 40 s. Apply Icon-Infiltrant. Let set for 1 min. Light-cure for 40 s.	

Induction of White Spot Lesions

Prior to the experiment, two layers of acid-resistant nail varnish (Risqué, Barueri, São Paulo, Brazil) were applied on half of the enamel surface. This protected surface served as sound enamel (positive control). Each specimen was immersed in 32 mL of a demineralizing solution containing 50 mM acetate buffer solution and 1.28 mM $Ca(NO_3)_2\_4H_2O$, 0.74 mM $(NaH_2PO_4)\cdot 2H_2O$, and 0.03 ppm F at pH 5.0,[10] for 24 hours at 37 °C. Subsequently, specimens were removed from the solution and thoroughly washed with deionized water. This treatment produced white spot lesions on the enamel surface.

Experimental Groups

The 50 specimens were divided into five groups (n=10) as follows: negative control (not treated, G1), infiltrated enamel (G2), infiltrated enamel submitted to brushing (G3), infiltrated enamel submitted to pH cycling (G4), and infiltrated enamel submitted to artificial aging (G5).

Resin infiltrant (Icon, DMG, Hamburg, Germany) was applied on the specimens of G2, G3, G4, and G5 and light cured at 1100 mW/cm^2 using a light-emitting diode device (Kavo, Poly Wireless, Joinville, Brazil), following the manufacturer's instructions. Composition and manufacturer's instructions are shown in Table 1. Then, specimens were polished using medium, fine, and superfine aluminum oxide abrasive Sof-Lex discs (3M-ESPE Dental Products, St Paul, MN, USA) in a low-speed hand piece under air cooling for 20 seconds. All specimens were stored for 7 days at 37 °C and 100% relative humidity. After this period, specimens from G1 and G2 were analyzed for microhardness and surface roughness, and specimens from G3, G4, and G5 were subjected to challenges.

Toothbrushing

Toothbrushing was performed on half of the surface of discs of G3 using a mechanical brushing machine (150 g axial load, 5 strokes/s; Elquip Maq Escovação, São Carlos, Brazil) with slurries of dentifrices and water (1:3 w/w, Colgate Total 12, Colgate-Palmolive, São Paulo, Brazil, 1450 ppm as NaF).[6] The specimens were submitted to 10,000 strokes of toothbrushing, over a total of 45 minutes. Specimens were removed and ultrasonically cleaned with water for 10 minutes.

pH-Cycling Model

Ten discs were individually submitted to a pH cycling model at 37 °C over 7 days. The pH cycling consisted of immersing the specimens in 35.5 mL of demineralizing solution: (2.0 mmol/ L Ca, 2.0 mmol/ L P, 0.075 mol/ L acetate buffer, 2.22 mL/ mm^2 of enamel surface) for 6 hours, alternated with immersion in 17.75 mL of remineralizing solution: (1.5 mmol/ L Ca, 0.9 mmol/ L P, 0.15 mol/ L KCl, 0.02 mol/ L cacodylate buffer, pH 7.0, 0.25 mL/mm^2) for 18 hours for 5 days. Then, specimens were kept for 2 more days in a fresh remineralizing solution, completing 7 days of treatment.[11] Specimens were washed in deionized water for 30 seconds between demineralizing and remineralizing cycles.

Accelerated Artificial Aging

The accelerated artificial aging process was performed in an ultraviolet (UV) accelerated aging chamber (EQUV, Equilam Ind Com Ltda, Diadema, Brazil), according to ASTM G154. The accelerated aging process consisted of alternating periods of UV light (8 hours) and condensation (4 hours), under heat (65 °C±3 °C or 45 °C±3 °C) and 100% humidity. Specimens were subjected to a total of 252 hours of aging and 168 hours of UV-B irradiation with a 313-nm emission peak.[9]

Measurement of Microhardness and Surface Roughness of Enamel Surface

After challenges, a final microhardness measurement on the test side of each specimen was performed as previously described.

Table 2: *Means ± Standard Deviations Surface Microhardness (KHN – kg/mm^2) of Enamel Discs According to Treatment Group (1 to 5) and Area of the Specimen (Control or Test)*[a]

Groups	Control	Test
1: Not treated	345.0 ± 32.7^{Aa}	117.8 ± 13.4^{Bb}
2: Infiltrated	351.2 ± 22.6^{Aa}	228.3 ± 15.4^{Ba}
3: Infiltrated and brushing	341.3 ± 20.6^{Aa}	227.2 ± 10.9^{Ba}
4: Infiltrated and pH cycling	352.7 ± 23.0^{Aa}	30.9 ± 3.8^{Bc}
5: infiltrated and artificial aging	344.1 ± 14.8^{Aa}	237.3 ± 19.0^{Ba}

[a] *Capital superscript letters indicate significant differences between control and test areas; lowercase superscript letters represent significant differences among treatment groups in each column (Tukey test, p<0.05).*

Table 3: *Means ± Standard Deviations Surface Roughness (Ra μm) of Enamel Discs According to Treatment Group (1 to 5) and Area of the Specimen (Control or Test)* [a]

Groups	Control	Test
1: Not treated	0.03 ± 0.005^{Aa}	0.05 ± 0.03^{Ba}
2: Infiltrated	0.03 ± 0.007^{Aa}	0.12 ± 0.05^{Ba,b}
3: Infiltrated and brushing	0.04 ± 0.009^{Aa}	0.22 ± 0.08^{Bb}
4: Infiltrated and pH cycling	0.03 ± 0.015^{Aa}	0.65 ± 0.30^{Bc}
5: Infiltrated and artificial aging	0.04 ± 0.026^{Aa}	0.09 ± 0.02^{Ba}

[a] *Capital superscript letters indicate significant differences between control and test areas; lowercase superscript letters represent significant differences among treatment groups in each column (Dunn test, p<0.05).*

The nail varnish on the enamel surfaces was carefully removed using acetone-soaked cotton wool. Surface roughness was characterized by the average roughness (Ra), which represents the arithmetic mean value of all absolute distances of the roughness profile from the center line within the measuring length. Three measurements were recorded on half of each surface using a roughness meter Surftest SJ 400 – Mitutoyo (Mitutoyo American Corporation, Kanagawa, Japan). The cutoff value (distance traversed by the stylus over which the data were collected) for surface roughness was 0.25 mm.

Scanning Electronic Microscopy (SEM) Analysis

Two specimens of each material were mounted on aluminum stubs, sputter-coated with gold (Balzers SCD-050 sputter coater, OC Oerlikon Corporation AG, Pfäffikon, Switzerland) and submitted to SEM analysis (Evo LS15, Carl Zeiss, Oberkochen, Germany) at 70× magnification of the most representative center area of the specimen.

Statistical Analysis

The software StatView version 5.0 (SAS Institute, Cary, NC, USA) was used for the statistical analysis. The assumptions of equality of variances and normal distribution of data were checked using the Bartlett and Shapiro-Wilk tests, respectively. The microhardness results were analyzed using two-way analysis of variance, followed by the Tukey test for multiple comparisons. Since homogeneity was not achieved, the roughness data were analyzed using the Kruskal-Wallis test, followed by the Dunn test. The level of significance was set at 5%.

RESULTS

Microhardness and surface roughness values of the test groups (G1–G5) were significantly lower compared with those obtained for sound enamel ($p<0.05$). Microhardness of G1 (no treated white spot lesion) was significantly lower compared with G2, G3, and G5 ($p<0.05$). The lowest microhardness values were observed for G4 (submitted to pH cycling), which was significantly different from all other groups ($p<0.05$). The mean (standard deviation [SD]) microhardness for all groups is presented in Table 2.

Regarding surface roughness, G4 (pH cycling) presented the highest values, which was significantly different compared with the other groups ($p<0.05$). The mean (SD) surface roughness is displayed in Table 3.

SEM images (Figures 1 through 5) showed major differences between sound enamel and test groups, mainly for the group that was infiltrated and submitted to pH cycling (Figure 4). In contrast, a similar appearance was found for groups only infiltrated and infiltrated with brushing (Figures 2 and 3).

DISCUSSION

Changes in microhardness and surface roughness in direct restorative materials, especially resin-based materials, have a direct influence on the longevity of a restoration.[9] When such changes occur in white spot lesions infiltrated by resin infiltrant, the loss of strength and smoothness of the material can leave such surfaces unprotected and favor the development of new caries lesions.[6,12] The null hypothesis was partially rejected, since the resin infiltrant increased the microhardness of white spot lesions, except after pH cycling. Additionally, the highest surface roughness was also found after pH cycling.

Previous studies have used test methodologies similar to those used in this work to evaluate the surface of infiltrated enamel.[13-15] The present data

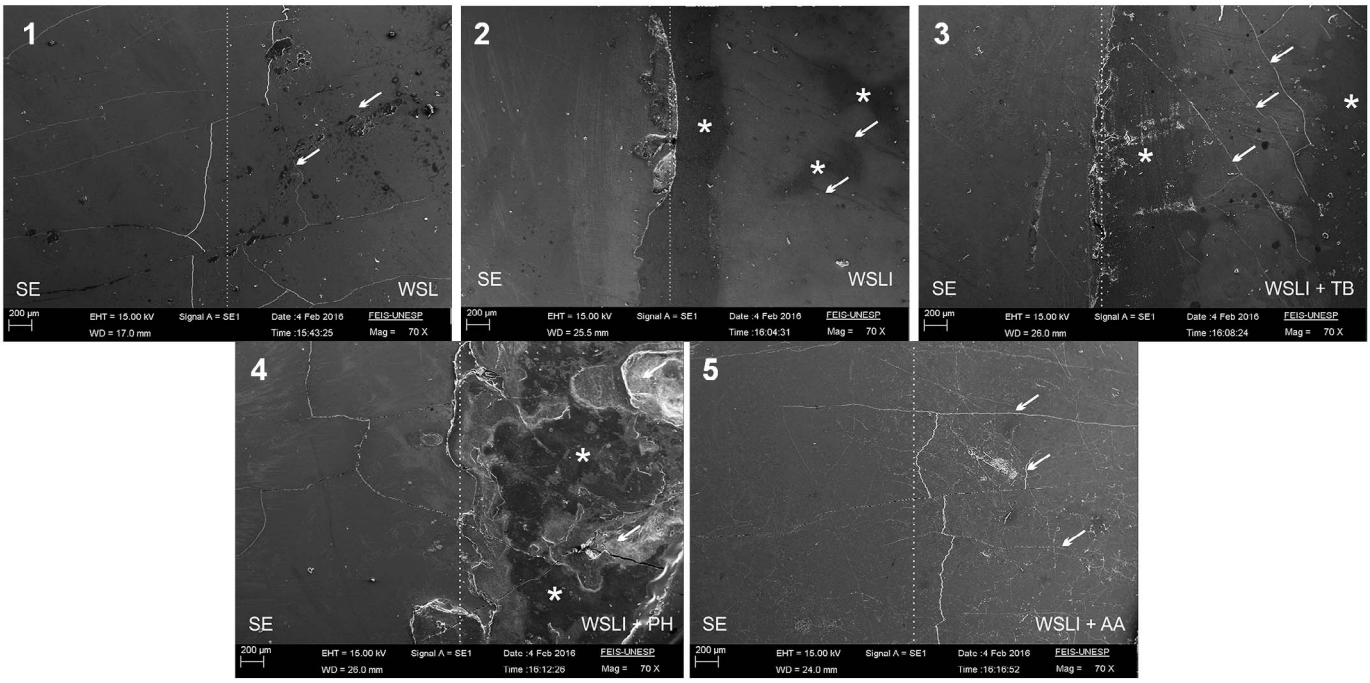

Figure 1. *SEM image from G1. Right side represents the white spot lesion. Left side is sound enamel. A similar appearance between the two sides may be observed, although a few irregular areas are observed on the surface (arrows). Abbreviations: SE, sound enamel; WSL, white spot lesion.*
Figure 2. *SEM image from G2. Right side represents the white spot lesion after resin infiltrant application. Left side is sound enamel. Irregularities in the test surface were observed when compared with sound enamel (arrows), and areas with resin infiltrant may be observed (asterisk). Abbreviations: SE, sound enamel; WSLI, white spot lesion infiltrated.*
Figure 3. *SEM image from G3. Right side represents the white spot lesion after resin infiltrant application and brushing. Left side is sound enamel. Large areas with resin infiltrant may be observed (asterisk) associated with areas of cracks (arrows). Abbreviations: SE, sound enamel; WSLI + TB, white spot lesion infiltrated and toothbrushing.*
Figure 4. *SEM image from G4. Right side presents the white spot lesion after resin infiltrant application and pH cycling. Sound enamel is observed on the left side. A great difference between sound enamel and the test side is seen. Islands of infiltrant material can be observed in darker areas (asterisk). Modified areas of enamel surface may be observed, evidence of an aggressive challenge. Abbreviations: SE, sound enamel; WSLI + PH, white spot lesion infiltrated and pH cycling.*
Figure 5. *SEM image from G5. Right side presents the white spot lesion after resin infiltrant application and artificial aging. Left side is sound enamel. Many cracks are seen on the test side compared with sound enamel (arrows). Abbreviations: SE, sound enamel; WSLI + AA, white spot lesion infiltrated and artificial aging.*

are in line with previous studies reporting lower microhardness values in artificial white spot lesions treated with a resin infiltrant compared with sound enamel.[13-15] This fact may be associated with characteristics of the resin infiltrant organic matrix, mainly composed of triethylene glycol dimethacrylate (TEGDMA).[6,12,13,16] This monomer has a high degree of conversion; however, formation of the polymer chain does not always occur.[17] Moreover, the absence of strong intermolecular secondary bonds, as well as aromatic rings, results in mechanical properties inferior to those of other monomers.[17] Furthermore, material shrinkage during polymerization leaves some regions of noninfiltrated demineralized enamel, which may also contribute to the decrease in surface microhardness compared with sound enamel.[14,15]

Despite the aforementioned disadvantages, the great penetration capacity of resin infiltrant may be due to the low viscosity presented by TEGDMA as well as its low molecular weight, allowing greater penetration of infiltrant compared with other materials, such as sealants and adhesives.[12,15,18,19] In this sense, although the mechanical properties of TEGDMA-infiltrated and sound enamel are different, significantly higher microhardness values were observed for groups with white spot lesions treated with resin infiltrant (G2, G3, and G5) compared with artificial white spot lesions (G1), demonstrating that the resin infiltrant was able to penetrate the lesion body. A confocal microscopic study showed higher penetration of Icon resin infiltrant than other resin-based materials into initial erosion lesions.[20]

An increase in surface roughness of infiltrated groups was observed in the present study compared with sound enamel. Demineralized prismatic areas not filled by the infiltrant, either by polymerization shrinkage or by interference of ethanol in the

polymerization, could contribute to this increase in roughness.[15,21] Conditioning with hydrochloric acid may also have contributed to this phenomenon, since Yim and others,[22] when comparing the effectiveness of enamel conditioning with 15% hydrochloric acid (120 seconds) and 37% phosphoric acid (5 seconds), observed that hydrochloric acid produced grooves and cracks in enamel, which would result in higher surface roughness, even though it promoted better penetration of the resin infiltrant due to its high demineralizing capacity. Irregularities in test surfaces were observed compared with sound enamel in Figures 2, through 5, in which resin infiltrant was used.

The protective capacity of resin was also shown to significantly increase Vickers microhardness when the infiltrant was applied in two layers instead of a single application, even after a new cariogenic challenge.[13] The protective effect of this infiltrant was also assessed by transverse microradiography and confocal microscopy, demonstrating that the infiltrant was able to resist to new cariogenic challenges, especially when used in combination with a fluoride gel.[23] Thereby, the resin material acts as a physical barrier to new acidic attacks and fluoride catalyzes calcium, allowing enamel remineralization by saliva.[23] Moreover, the same resin infiltrant was also able to protect the enamel surface from erosive challenges, regardless of etching with 15% HCl gel.[19] It has been suggested that the presence of resin infiltrant in the lesion subsurface has a protective effect on enamel because it acts as a barrier, occluding the pores formed by a white spot lesion, which then becomes more resistant to new cariogenic attacks.[14] Based on this information, the results of the present study were somehow unexpected, since the resin infiltrant was unable to protect enamel from pH cycling. The discrepant results may be due to differences in pH cycling models for *in vitro* evaluations.[8] In this sense, it is noteworthy that the majority of studies cited earlier used long-term (50 day) pH cycling models under weaker challenge conditions,[13,23] which is very different from the short-term protocol used in the present study. Another reason might be due to the excess removal done during the polishing procedure after infiltrant application, since it was found that resin-based materials are able to protect enamel against erosion only when they are present over enamel as a physical barrier.[24] Nonetheless, the different results obtained in this study and those previously reported indicate that further investigations are still needed in this field.

Increased porosity of the resin infiltrant due to its low wear resistance against acid challenge has also been shown.[13] This low wear resistance may be related to the polymer chain conformation and weak secondary bonds present in the TEGDMA molecule, as previously described.[17] Furthermore, TEGDMA may be released from homopolymers or copolymers, forming a polymer chain prone to chemical degradation, especially in acidic environments.[15] After pH cycling, there were perceptible changes on the specimen surface (Figure 4), being heterogeneous with the majority of the resin infiltrant removed by the acid attack and revealing only small islands of infiltrants that resisted the acidic stress. These observations were also noted in an *in vitro* study on the resistance of light-cured sealants to acidic soft drinks.[7]

Regarding resistance to abrasion, the challenge adopted in the present study (10,000 brushing cycles) was unable to remove the infiltrant (Figure 3), as noted in previous studies in which the resin infiltrant resisted up to 20,000 cycles, as shown by profilometric and confocal microscopy data.[6,19] Abrasion resistance has been related to the thick layer of material, since two layers of resin infiltrant are necessary according to the manufacturer's instructions.[19] However, resin infiltrant was not resistant when submitted to erosive and abrasive challenges by 15 cycles of acidic beverages and toothbrushing.[25]

As for the accelerated aging assay, similar results were obtained for groups in which this challenge was used. This accelerated aging system simulates the destructive environmental capacity and predicts the relative durability of materials, simulating the chemical and physical challenges. Saliva is simulated by conditions of 100% humidity and a condensation process using distilled water saturated with oxygen. Light is simulated by sources of UV-B light. The specimens were positioned on the machine's fixing plates for automatically repeated and alternating cycles of UV-B light and condensation.[9] This type of irradiation has the potential for photo-oxidation that induces breaks of single or double carbon bonds.[9] These chemical bonds have an important function in the configuration of polymer chains present in the organic matrix of resin-based materials.[9] No influence in microhardness and roughness was observed on the resin infiltrant surface after this challenge, although many cracks might be seen on the test side under SEM evaluation (Figure 5). This type of challenge might impact other characteristics, such as color alteration.

Despite the limitations of an *in vitro* study, the objective was to simulate some of the clinical conditions to which the material would be subjected. In the present study, the infiltrant was not effective against a new acid challenge, which may impose some limitations regarding individuals at high caries risk because some aspects of caries progress may not be under control. However, further clinical studies are needed since the conditions described in this present study differ from *in vivo* conditions, considering that some clinical circumstances, such as the roles of saliva and resin expansion or shrinkage by thermal cycling, were not evaluated.

CONCLUSION

The resin infiltrant was not able to reestablish sound enamel properties and was not resistant to a new cariogenic challenge. However, it presented superiority over unprotected white spot lesions, resisting the challenges of mechanical abrasion and artificial accelerated aging.

Acknowledgement

This study was financially supported by FAPESP - São Paulo Research Foundation (2014/25760-0).

Regulatory Statement

This study was conducted in accordance with all the provisions of the local human subjects oversight committee guidelines and policies of the FOA UNESP animal ethical committee. The approval code for this study is protocol #2014-01115.

Conflict of Interest

The authors of this manuscript certify that they have no proprietary, financial, or other personal interest of any nature or kind in any product, service, and/or company that is presented in this article.

(Accepted 9 September 2016)

REFERENCES

1. Tinanoff N, Coll JA, Dhar V, Maas WR, Chhibber S, & Zokaei L (2015) Evidence-based update of pediatric dental restorative procedures: preventive strategies *Journal of Clinical Pediatric Dentistry* **39(3)** 193-197.
2. Buzalaf MA, Pessan JP, Honório HM, & Ten Cate JM (2011) Mechanisms of action of fluoride for caries control *Monographs in Oral Science* **22** 97-114.
3. Sundfeld RH, Sundfeld-Neto D, Machado LS, Franco LM, Fagundes TC, & Briso AL (2014) Microabrasion in tooth enamel discoloration defects: three cases with long-term follow-ups *Journal of Applied Oral Science* **22(4)** 347-354.
4. Lacerda AJ, Ávila DM, Borges AB, Pucci CR, & Rocha Gomes Torres C (2016) Adhesive systems as an alternative material for color masking of white spot lesions: do they work? *Journal of Adhesive Dentistry* **18(1)** 43-50.
5. Meyer-Lueckel H, & Paris S (2008) Improved resin infiltration of natural caries lesions. *Journal of Dental Research* **87(12)** 1112-1116.
6. Belli R, Rahiotis C, Schubert EW, Baratieri LN, Petschelt A, & Lohbauer U (2011) Wear and morphology of infiltrated white spot lesions *Journal of Dentistry* **39(5)** 376-385.
7. Korbmacher-Steiner HM, Schilling AF, Huck LG, Kahl-Nieke B, & Amling M (2013) Laboratory evaluation of toothbrush/toothpaste abrasion resistance after smooth enamel surface sealing *Clinical Oral Investigations* **17(3)** 765-774.
8. Buzalaf MA, Hannas AR, Magalhães AC, Rios D, Honório HM, & Delbem AC (2010) pH-cycling models for in vitro evaluation of the efficacy of fluoridated dentifrices for caries control: strengths and limitations. *Journal of Applied Oral Science* **18(4)** 316-334.
9. Catelan A, Briso AL, Sundfeld RH, & Dos Santos PH (2010) Effect of artificial aging on the roughness and microhardness of sealed composites *Journal of Esthetic and Restorative Dentistry* **22(5)** 324-330.
10. Queiroz CS, Hara AT, Paes Leme AF, & Cury JA (2008) pH-cycling models to evaluate the effect of low fluoride dentifrice on enamel de- and remineralization. *Brazilian Dental Journal* **19(1)** 21-27.
11. Vieira AE, Delbem AC, Sassaki KT, Rodrigues E, Cury JA, & Cunha RF (2005) Fluoride dose response in pH-cycling models using bovine enamel *Caries Research* **39(6)** 514-520.
12. Paris S, Lausch J, Selje T, Dörfer CE, & Meyer-Lueckel H (2014) Comparison of sealant and infiltrant penetration into pit and fissure caries lesions in vitro *Journal of Dentistry* **42(4)** 432-438.
13. Paris S, Schwendicke F, Seddig S, Müller WD, Dörfer C, & Meyer-Lueckel H (2013) Micro-hardness and mineral loss of enamel lesions after infiltration with various resins: influence of infiltrant composition and application frequency in vitro. *Journal of Dentistry* **41(6)** 543-548.
14. Taher NM, Alkhamis HA, & Dowaidi SM (2012) The influence of resin infiltration system on enamel micro-hardness and surface roughness: an in vitro study *Saudi Dental Journal* **24(2)** 79-84.
15. Torres CR, Rosa PC, Ferreira NS, & Borges AB (2012) Effect of caries infiltration technique and fluoride therapy on microhardness of enamel carious lesions. *Operative Dentistry* **37(4)** 363-369.
16. Ulrich I, Mueller J, Wolgin M, Frank W, & Kielbassa AM (2015) Tridimensional surface roughness analysis after resin infiltration of deproteinized natural subsurface carious lesions *Clinical Oral Investigations* **19(6)** 1473-1483.
17. Gajewski VE, Pfeifer CS, Fróes-Salgado NR, Boaro LC, & Braga RR (2012) Monomers used in resin composites: degree of conversion, mechanical properties and water sorption/solubility *Brazilian Dental Journal* **23(5)** 508-514.

18. Min JH, Inaba D, Kwon HK, Chung JH, & Kim BI (2015) Evaluation of penetration effect of resin infiltrant using optical coherence tomography *Journal of Dentistry* **43(6)** 720-725.

19. Oliveira GC, Boteon AP, Ionta FQ, Moretto MJ, Honório HM, Wang L, & Rios D (2015) In vitro effects of resin infiltration on enamel erosion inhibition *Operative Dentistry* **40(5)** 492-502.

20. Ionta FQ, Boteon AP, Moretto MJ, Júnior OB, Honório HM, Silva TC, & Rios D (2016) Penetration of resin-based materials into initial erosion lesion: a confocal microscopic study *Microscopy Research and Technique* **79(2)** 72-80.

21. Askar H, Lausch J, Dörfer CE, Meyer-Lueckel H, & Paris S (2015) Penetration of micro-filled infiltrant resins into artificial caries lesions *Journal of Dentistry* **43(7)** 832-838.

22. Yim HK, Min JH, Kwon HK, & Kim BI (2014) Modification of surface pretreatment of white spot lesions to improve the safety and efficacy of resin infiltration *Korean Journal of Orthodontics* **44(4)** 195-202.

23. Gelani R, Zandona AF, Lippert F, Kamocka MM, & Eckert G (2014) In vitro progression of artificial white spot lesions sealed with an infiltrant resin *Operative Dentistry* **39(5)** 481-488.

24. Tereza GP, Oliveira GC, Andrade Moreira Machado MA, Oliveira TM, Silva TC, & Rios D (2016) Influence of removing excess of resin-based materials applied to eroded enamel on the resistance to erosive challenge *Journal of Dentistry* **47** 49-54.

25. Zhao X, Pan J, Zhang S, Malmstrom HS, & Ren YF (2017) Effectiveness of resin-based materials against erosive and abrasive enamel wear *Clinical Oral Investigations* **21(1)** 463-468.

©Operative Dentistry, 2017, **42-4,** 436-444

Different Methods for Inlay Production: Effect on Internal and Marginal Adaptation, Adjustment Time, and Contact Point

MP Rippe • C Monaco • L Volpe • MA Bottino • R Scotti • LF Valandro

Clinical Relevance

Digital impressions and milling by a CAD-CAM system appear to be appropriate techniques since they promote similar marginal and internal adaptations when compared to the conventional impression and lost wax technique using pressed ceramic.

SUMMARY

The aim of this study was to evaluate the effect of different production methods of resin and ceramic inlays on marginal and internal adaptation, adjustment time, and proximal contacts. Forty premolars were selected, embedded (their roots), and prepared to receive inlays that were made as follows (n=10): LaRe—digital impression with a Lava C.O.S. scanner, followed by milling of Lava Ultimate block (composite resin) in a milling center; CeRe—digital impression with a Cerec 3D Bluecam scanner, followed by milling of Lava Ultimate block in Cerec; CeDis—digital impression with a Cerec 3D Bluecam scanner, followed by milling of IPS e.max CAD block (lithium disilicate) in Cerec; and PresDis—impression with polyvinyl siloxane, inlay made using the lost wax technique and IPS e.max Press pressed ceramic (lithium disilicate). Marginal and internal adaptations were measured using the replica technique. The inlay adjustments were performed using diamond burs in a contra-angle hand piece, and the time for adjustment was recorded using a timer, in seconds. The tightness of the proxi-

*Marília Pivetta Rippe, DDS, MSD, PhD, adjunct professor, Division of Prosthodontics, Department of Restorative Dentistry, Federal University of Santa Maria, Santa Maria, Brazil

Carlo Monaco, DDS, PhD, assistant professor and researcher, Department of Biomedical Sciences and Neuromotor, Division of Prosthodontics, Alma Mater Studiorum University of Bologna, Bologna, Italy

Lucia Volpe, DDS, MSD, Department of Biomedical Sciences and Neuromotor, Division of Prosthodontics, Alma Mater Studiorum University of Bologna, Bologna, Italy

Marco Antonio Bottino, DDS, PhD, professor, Dental Materials and Prosthodontics, São Paulo State University, São José dos Campos, Brazil

Roberto Scotti, professor, Department of Biomedical Sciences and Neuromotor, Division of Prosthodontics, Alma Mater Studiorum University of Bologna, Bologna, Italy

Luiz Felipe Valandro, DDS, MSD, PhD, associate professor, Division of Prosthodontics, Department of Restorative Dentistry, Federal University of Santa Maria, Santa Maria, Brazil

*Corresponding author: 1184 Floriano Peixoto, Santa Maria, RS 97015-372, Brazil; e-mail: mariliarip@hotmail.com

DOI: 10.2341/16-093-L

mal contact was measured using standardized metal blades. The statistical analyses for marginal fit data showed that at the cervical edge, CeDis (177.8 μm) had greater misfit than CeRe (116.7 μm), while all the groups had similar adaptation at the occlusal edge. The groups had similar internal fit at the pulpal wall, while LaRe (104.7 μm) > CeDis (66.7 μm) = CeRe (76.7 μm) at the axial wall. The groups restored with lithium disilicate ceramic took more time for adjustment when compared to the resin restorative material. The lowest proximal contact, in micrometers, was seen in the CeRe group (8.8 μm).

INTRODUCTION

Apart from fracture resistance and esthetics, marginal accuracy is one of the most important criteria for the clinical success of all-ceramic restorations.[1,2] Poor marginal adaptation of restorations increases plaque retention inducing the onset of periodontal disease[3] and can lead to microleakage resulting in endodontic inflammation[4] and secondary caries.[5] After a five-year study conducted on more than 1000 restorations,[6] it was concluded that 120 μm was the maximum tolerable marginal opening. However, another study[7] considered a 150 μm gap to be clinically acceptable. These data indicate lack of consensus on the maximum value of the marginal gap. Marginal fit is influenced by several factors, such as finish line configuration, size of cement space, restoration production method, and cementation of the restorations.[8]

A good final marginal adaptation is possible only if an accurate impression is obtained. Hence, the accuracy of the impression is essential for the success of the restoration. Currently, the conventional impression technique using elastomeric materials or digital impressions can be used. Syrek and others[7] showed that the digital impression promoted better marginal fit of all-ceramic crowns when compared to conventional two-step impressions. According to those authors, this might be explained by the traditional work flow, where a master model is created for fabrication of the crown, while the crown coping is designed directly from the intraoral scan without creating an intermediate model or die in the digital work flow.

The computer-aided design/computer-aided manufacturing (CAD/CAM) system enables two types of scans: the direct, or chair-side model and the indirect, or lab model. In the first model, the dentist performs the "impression" of the preparation using an intraoral scanner, and the restoration is designed and milled in the dentist's office independent of the laboratory. In the indirect model, the dentist makes a conventional impression with an elastomeric material and sends the impression to the laboratory, where the impression is poured and a model is scanned using an extraoral scanner. Subsequently, the restoration is designed and milled by the technician via a CAD-CAM system. Although the accuracy of the extraoral scanning is satisfactory, the conventional impression can deform due to the contraction or expansion from impression materials and plaster, according to Ting-shu and Jian.[9] Furthermore, Mously and others[10] showed that different manufacturing techniques have affected the marginal and internal adaptation of ceramic crown restorations. Hamza and others[11] also showed that different CAD/CAM systems and different ceramic types and their interactions presented a statistically significant effect on the marginal fit.

Neves and others[12] evaluated marginal adaptation of lithium disilicate crowns manufactured from different CAD/CAM systems: the microcomputed (CEREC or E4D) technique and the ceramic pressed technique. They observed that lithium disilicate crowns fabricated using the CAD/CAM Cerec Bluecam system 3D scanner or the pressed technique had a significantly lower marginal leakage when compared to crowns manufactured using a laser scanner system/CAM E4D CAD.

Another alternative material for making inlays in CAD/CAM is the composite resin. Currently, resin nanoceramic blocks (LAVA Ultimate, 3M ESPE, St Paul, MN, USA) are available on the market. This material contains nanometers and nanoclusters of silica and zirconia, constituting a total of 80% of the weight of the nanoceramic.[13]

Inlays are quite feasible for clinical practice in the chair-side model. However, it is unclear whether this method would be advantageous for the clinician, considering the time consumed with the adjustment of the restoration. Furthermore, it is not known whether the interproximal contact of the CAD/CAM model is better than the conventional model using the pressed technique.

Thus, the aim of this study was to assess the different methods of inlay production using different materials in relation to marginal and internal adaptation, adjustment time, and proximal contact tightness. The null hypothesis was that there is no difference among the different inlay production methods and the material in relation to 1) marginal

Table 1: *Experimental Design*

Groups' Codes	Model	Impression Technique	Manufacture Inlays	Material	Ceramic Composition
LaRe	Lab-side	Intraoral dental scanner Lava C.O.S. (3M ESPE, St Paul, MN, USA) with titanium dioxide powder (Cerec Propellant, VITA, Bad Säckingen, Germany)	Center milling—the scans were immediately sent via the Internet to the dental laboratory (45-μm cement space according to the manufacturer's instruction)	Composite resin	About 80% weight nanoceramic and about 20% weight resin
CeRe	Chair-side	Intraoral dental scanner Bluecam (Sirona) with powder (Optispray, Sirona Dental Systems, Bensheim, Germany)	Milling: Cerec MC XL (40-μm cement space)[a]		
CeDis	Chair-side	Intraoral dental scanner Bluecam (Sirona) with powder (Optispray, Sirona Dental Systems)	Milling: Cerec MC XL (40-μm cement space)[a]	Lithium disilicate	SiO_2 57 to 80; Li_2O 11 to 19; K_2O 0 to 1; 3 P_2O_5 0 to 11; ZrO_2 0 to 8; ZnO 0 to 8; Al_2O_3 0 to 5; MgO 0 to 5; coloring oxides 0 to 8 (in% by weight)
PresDis	Lab-side	Conventional impression—one-step technique with polyvinyl siloxane	Lost wax technique with pressed ceramic. The investment ring was removed by using a separating disk and glass polishing beads and using IPS e.max Press Invex Liquid (Ivoclar Vivadent, Schaan, Liechtenstein). The ceramic inlays were cleaned in an ultrasonic cleaner and airborne-particle abraded.		

[a] *It was not possible to use 45 μm in that software.*

adaptation, 2) internal adaptation, 3) time for adjustment, and 4) proximal contact.

METHODS AND MATERIALS

This study was approved by the Committee of Ethics in Research of the Federal University of Santa Maria (UFSM), and the teeth were donated by the Human Teeth Bank of UFSM.

Sample size calculation for the marginal and internal fit outcome was based on the Tukey (5%) pairwise comparison after one-way analysis of variance (ANOVA) (http://www.stat.uiowa.edu/~rlenth/Power) to demonstrate a 30-μm[7] difference in mean maximum marginal and internal gap between the four groups. The sample size was calculated as 10 teeth per group, based on a significance level of 0.05, a power of 80%, and a standard deviation of 20 μm.[7]

Forty human maxillary premolars were selected according to the inclusion criteria of there being no cracks in the tooth and according to its vestibular-lingual dimensions. The teeth were numbered and, using a computer program (http://www.randomizer.org), randomly allocated into four testing groups (Table 1).

Embedding the Teeth in a Model

The premolars were embedded between two molars in a cylinder filled with polyurethane resin in order to simulate the interproximal contact of the inlay with the other teeth. To accomplish positioning of the teeth in the resin, the occlusal surface of each tooth was glued to an adapted surveyor with the crown perpendicular to the x-axis (ground); the teeth were embedded in a cylinder containing polyurethane resin (F16 Polyol, Axson Technologies, St Ouen I'Aumône, France) up to 3 mm below the cemento-enamel junction, with the occlusal surface parallel to the horizontal plane.

Cavity Preparation

Standardized MOD inlay cavity preparations were performed on all premolars using a conical trunk diamond bur with rounded angles (KG Sorensen 3131, Barueri, Brazil). The burs were mounted in a high-speed hand piece and fixed to a modified optic microscope that enabled reductions to be obtained as parallel as possible to the long axis of the tooth. The preparations had the convergence of the bur (±10°) and the following dimensions: buccal-lingual width,

3 mm; occlusal box depth, 3 mm; and rounded internal line angles. Each diamond bur was used to prepare five teeth, and all preparations were polished using the same bur (# 3131, KG Sorensen, Cotia, Brazil) with a grain size of 25 μm.

Impressions and Inlay Manufacturing

LaRe—The impressions were made using the Lava C.O.S. scanner, which is a 3D-in-motion technology that captures 3D data in a video sequence and models the data in real time (Table 1), and the restorations were prepared using composite resin blocks (Lava Ultimate, 3M ESPE) in a milling center.

CeRe and CeDis—The impressions were made using the CEREC AC with a Bluecam scanner, which is a camera that has a blue light–emitting diode with a specific wavelength (Table 1). Half of the restorations were prepared using composite resin blocks (Lava Ultimate, 3M ESPE), and the other half was prepared using lithium disilicate blocks (Ivoclar Vivadent, Schaan, Liechtenstein). After milling, the lithium disilicate inlays were sintered according to the manufacturer's recommendation.

PresDis—A conventional impression was performed for each prepared tooth using polyvinyl siloxane (Elite HD + Regular Body, Zhermack, Badia Polesine, Italy) and the one-step technique. The mold was poured with type IV plaster one hour after removal. The fabrication of the lithium disilicate inlays was performed in accordance with the manufacturer's recommendations (IPS e.max Press, Ivoclar Vivadent). The inlays were waxed on a die for each tooth using three coats of die spacer (about 30 μm) (Yeti die spacer, Yeti Dental Products GmbH, Engen, Germany) according to the instructions of the ceramic manufacturer. All wax patterns were invested and pressed by a single dental laboratory technician (Table 1).

Adjustment Time

After manufacturing, the inlays were put inside the prepared teeth, and the interproximal contact between the inlay and each adjacent tooth was adjusted with the aid of an occlusal marker, AccuFilm II (Parkell, Edgewood, NY, USA), which is 21 μm thick. The adjustments were performed using diamond burs with a grain size of 25 μm for the resin inlays and a grain size of 40 μm for the lithium disilicate inlays using a slow-speed motor associated with a contra-angle hand piece up to 30,000 rpm for lithium disilicate and up to 6000 rpm for resin. The adjustment of the proximal inlays was performed with fine-grain diamond burs in order to avoid polishing, which might lead to additional wear. The time of adjustment was recorded using a timer in seconds.

Proximal Contact

The tightness of the interproximal contact was verified using metal strips of 8, 30, and 50 microns (Shimstock-Folie, Coltene, Altstätten, Switzerland) placed between the inlay and the molar on both sides of the inlay. This procedure was performed by the same operator without the application of force. A mean of the two proximal contacts was performed for each inlay.

Internal and Marginal Fitting

After inlay production, replicas were made of the intermediate space between the inner surface of the inlay and the tooth cavity. This was achieved by coating the tooth cavity walls with a thin layer of light-body additional silicone material, followed by seating the inlay into the cavity and applying a force of 750*g* on the inlay.

The inlay was removed after setting of the impression material, leaving a thin film of light-body material adhering to the cavity that represented the discrepancy between the inlay and the tooth cavity. For the purpose of stabilization, a medium-body material was applied that adhered to the light-body film in the cavity. This procedure enabled the removal and handling of the "cement replica" made from the light-body material. The points measured from the replica are shown in Figure 1.

The replica was cut in the middle, and the parts were observed in a stereomicroscope in order to measure the thickness of the light-body silicone, which corresponds to the internal and marginal fit, according to Figure 2. Three replicas of the cement replica were made for each tooth, and a mean was calculated from the three replicas.

Data Analysis

The data measured from the marginal and internal adaptation (marginal fit: occlusal and cervical edges; internal fit: pulp and axial walls) and adjustment time were analyzed using the one-way ANOVA and the Tukey test ($p=0.05$). The proximal contact data were analyzed using the Kruskal-Wallis test.

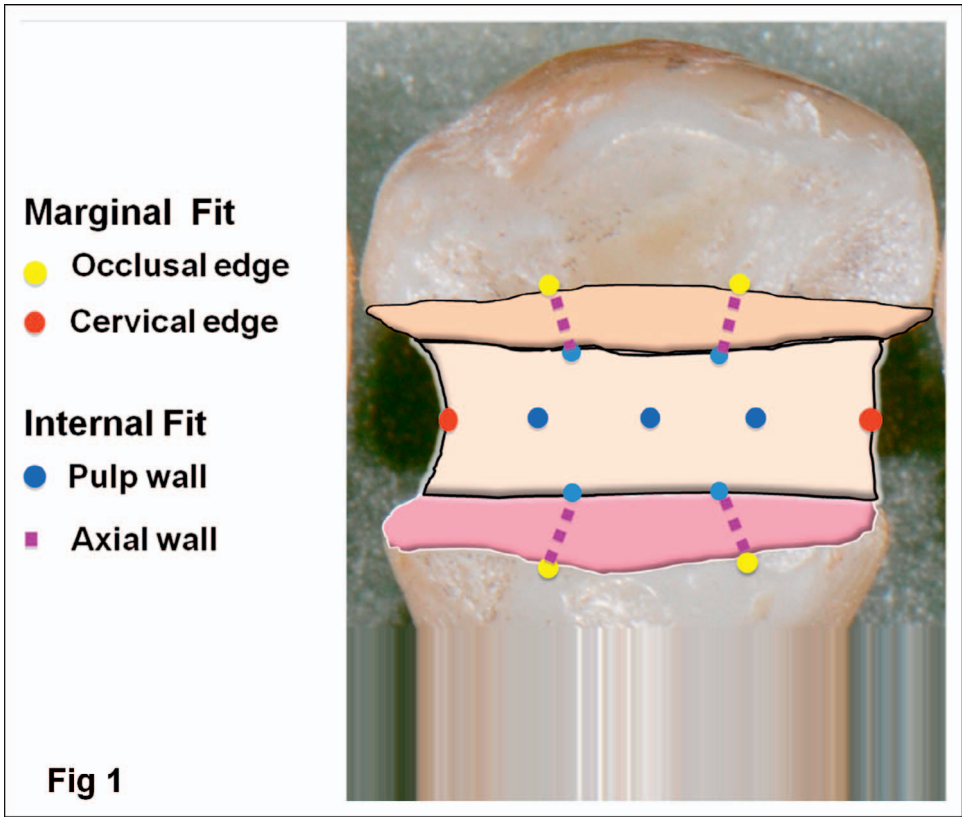

Figure 1. *Location of the points where the fit were measured.*

RESULTS

The Cerec system with the lithium disilicate group had higher marginal misfit at the cervical edge when compared to the Cerec system with the composite resin (p=0.03), while the occlusal edge presented no statistical differences (p=0.21) (Table 2).

For internal fit, statistical differences were noted for the axial wall (LaRe > CeDis = CeRe) (p=0.0007) (Table 2), while no significant differences were found among groups when considering the pulp wall (p=0.08).

The smallest adjustment time (p=0.01) occurred for the Cerec system and composite resin group, but it was not statistically different from the Lava C.O.S. scanner with composite resin (Table 3). The best proximal contact was observed with the Cerec system and composite resin group, and the worst was with the Cerec system and lithium disilicate group (Table 3).

DISCUSSION

The first null hypothesis (no difference among the inlay production methods and materials for marginal adaptation) was rejected since the Cerec system with composite resin and lithium disilicate groups had statistically different marginal fit at the cervical edge. The second hypothesis (no difference among the inlay production methods and materials for internal adaptation) was also rejected since the Lava C.O.S. scanner with the composite resin group and Cerec system with lithium disilicate and composite resin groups presented different internal fits at the axial wall. The Lava C.O.S. scanner with the composite resin group presented the largest misfit at the internal axial wall but the smallest misfit at the marginal occlusal edge. However, there was no statistical difference between the groups. On the other hand, the Cerec system with the lithium disilicate group presented the largest misfit at the marginal occlusal and pulp edge and the smallest misfit at the internal axial wall.

This difference of adaptation between composite resin and lithium disilicate might have occurred due to the composition of the material. Lithium disilicate has a high modulus of elasticity around 95 GPa, while the modulus of the studied resin is 12 GPa. The high modulus of the lithium disilicate may hinder milling, making its surface more irregular and decreasing its marginal accuracy. This relationship between high modulus of the ceramic and less accuracy in the Cerec system has also been demon-

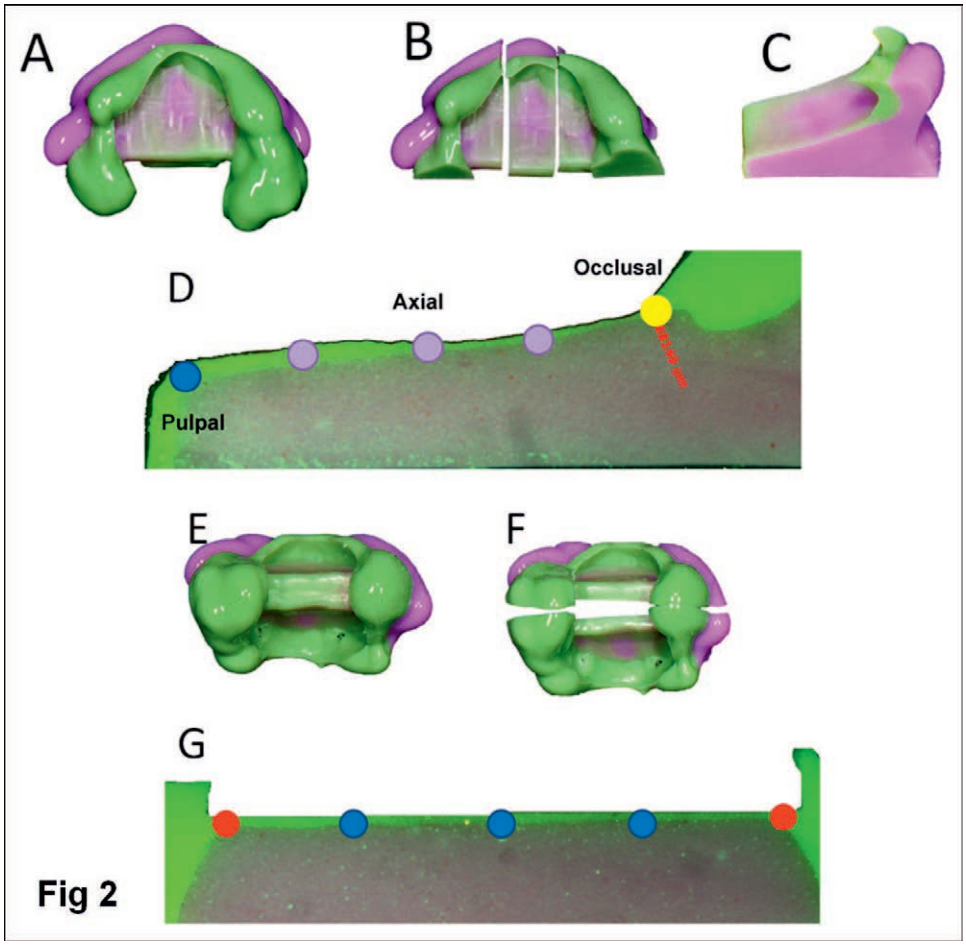

Figure 2. *Replica cuts and measures (μm). A: replica from the vestibular side. B: Cuts were performed in both vestibular and palatal sides. C: internal side after the cut was performed . D: stereomicrograph of section shown in C showing the measurement points of the green silicone. E: replica from the pulp side. F: cut performed of the pulp side. G: stereomicrograph of the internal side of the cut shown in "F" showing measurement points of the green silicone. The yellow ball corresponds with the occlusal edge and the red ones with the cervical edge. Violet balls correspond to the axial wall and blue ones to the pulp wall.*

strated in other studies, such as Bottino and others[14] and Hamza and others.[11] Furthermore, Awada and Nathanson[15] reported that the material factor had a significant effect on the mean flexural strength, flexural modulus, modulus of resilience, and roughness of the margin edge for restorations. Those authors also showed that crowns milled from the new resin-based blocks seemed to have visibly smoother margins when compared with ceramic materials. It is likely more difficult to reproduce details at the margin when milling ceramic materials compared to polymeric materials due to the fact that the edge of the ceramic is thinner despite its greater strength and also to the fact that the lithium disilicate is more friable; consequently, their milling becomes more critical. In cases of inlays, the composite resin has some additional advantages since crystallization before cementation is not necessary, unlike the lithium disilicate. This makes the resin more practical for the chair-side system and cheaper since it makes a furnace in the office unnecessary.

In relation to internal adaptation, according to Hoop and Land,[16] the relatively large internal gap may allow restorations to seat further, effectively

Table 2: *Mean and Standard Deviation (in Parentheses) Values of Marginal and Internal Fit (μm)*[a]

Groups	Marginal Fit (μm)		Internal Fit (μm)	
	Occlusal Edge	Cervical Edge	Pulp Wall	Axial Wall
LaRe	105.9 (±40.3) A	130.9 (±38.4) AB	233.8 (±80.5) A	104.7 (±13.9) A
CeRe	145.3 (±106.5) A	116.7 (±42.1) B	227.5 (±94.2) A	76.7 (±24.6) B
CeDis	171.8 (±56.6) A	177.8 (±68.9) A	207.2 (±61.3) A	66.7 (±19.9) B
PresDis	132.0 (±54.8) A	149.5 (±27.6) AB	156.0 (±44) A	87.0 (±16.5) AB

[a] *Different letters indicate a significant difference ($p<0.05$) between the groups (column).*

Table 3: *Mean (Standard Deviation) Adjustment Time and Proximal Contact*[a]

Groups	Adjustment Time (s)	Proximal Contact (μm)
LaRe	322 (±263.8) AB	21.2 AB
CeRe	189.4 (±167.4) B	8.8 B
CeDis	497.8 (±276.5) A	29.2 A
PresDis	471.5 (±194.7) A	10.9 AB

[a] *Different letters indicate a significant difference ($p<0.05$) between the groups (column).*

reducing the marginal gap widths in inlays. According to Ender and Mehl,[17] Lava C.O.S. provides an accuracy of 45.8 μm with the scanning protocol recommended from the manufacturer, while Cerec Bluecam provides an accuracy of 23.3 μm. The difference of accuracy between these scanners can be explained due to the difference of the working principles and different light sources of the two scanners.

The Bluecam scanner works on the principle of stripe light projection, combined with active triangulation through the short wavelength of blue light. According to Sirona (the manufacturers of the Bluecam scanner), a pattern of parallel lines is projected onto the tooth, and these lines are distorted by the tooth contours. The distortions can be viewed from an angle (triangulation) that delivers information on the various elevations of the tooth. If the line pattern is shifted by moving the grid during the exposure, the measuring points can be clearly assigned. The Lava C.O.S. scanner is based on the principle of active (optical) wavefront sampling, which obtains 3D information from a single lens imaging system by measuring depth based on the defocus of the primary optical system. This device has three sensors that capture the surface to be scanned from different perspectives. With these three images captured at the same time, 3D surface patches are generated by proprietary image processing algorithms using the in-focus and out-of-focus information (Lava Chairside Oral Scanner C.O.S., 3M ESPE technical datasheet, 2009). However, it is important to consider that the cement and internal space for the Lava with the composite resin group was slightly greater than the other groups.

Moreover, the preparation might have influenced the quality of the image captured. All preparations were standardized through the use of one type of bur, regardless of the type of scanner or material of the inlay. Renne and others[18] showed that the preparation quality has a significant impact on marginal gap for crowns fabricated with a CAD/CAM system. According to Hoop and Land,[16] the inlay preparation for CAD/CAM should present 1.5 to 2 mm of pulpal floor depth, and the box walls should diverge in an occlusal direction by approximately 10° or more, which makes optical capture easier and reduces the risk of excessive binding during seating for the initial evaluation. In this study, the preparation had a convergence of 10° but was a little deeper (3 mm) in order to simulate the worst-case scenario.

In the present study, the digital intraoral impression and CAD/CAM systems, regardless of the type of scanner, did not show superior accuracy when compared to the conventional impression and press ceramic technique. This result is in agreement with Addi and others,[19] who reported that after luting there were only slight differences of fit between the restorations fabricated using three different manufacturing techniques and ceramics and that long-term follow-up studies would be necessary to assess the clinical significance of the slight differences between the systems. According to Neves and others,[12] lithium disilicate crowns fabricated using the Cerec 3D Bluecam scanner CAD/CAM system or the heat-pressing technique had similar vertical misfit. Bindl and Mormann[4] also evaluated the marginal and internal fit of all-ceramic molar crown copings made from CAD/CAM and conventional techniques (pressed technique), and they demonstrated the same accuracy of fit between the two models.

The literature is controversial regarding the clinically acceptable thickness of the marginal gap. According to Holmes and others,[20] a marginal gap of 100 to 120 μm is acceptable for avoiding potential degradation or dissolution problems that can contribute to cement loss. However, many other studies[10,21,22] consider marginal gap values of 100 to 200 μm to be clinically acceptable for cemented restorations. Another important consideration is that the marginal gap measurements used in the present study were the absolute marginal discrepancy,[8] which can provide larger values than actual marginal gap measurements.

In relation to the proximal contact and adjustment time, hypotheses 3 and 4 were rejected. As shown in Table 3, longer adjustment times led to less tight proximal contacts. The Cerec system with the lithium disilicate group presented the longest adjustment times and the less tight proximal contacts, which was statistically different from the Cerec system with the composite resin group, which

presented the shortest adjustment time and the tightest proximal contact. These comparisons show that these differences among the groups produced from the Cerec system seem to have occurred due to the difference between the materials and not due to the inlay production method, as lab-side and chair-side models, because pressed lithium disilicate and the Lava C.O.S. scanner with composite resin groups were not statistically different from the Cerec system with lithium disilicate and composite resin, respectively. Despite the fact that the lithium disilicate is harder than the resin, care was taken in relation to the use of the bur with greater grit and more rpm for the lithium disilicate when compared to the resin.

Another factor to consider is that the thickness of the occlusal marker (21 μm) used to adjust the interproximal contact was larger than the mean of the contact point for the Cerec system with composite and pressed lithium disilicate groups. It shows that a slight adjustment was made in these groups; however, the pressed lithium disilicate group might have been slower due to the hardness of the lithium disilicate in relation to resin.

Dorfer and others[23] quantified the proximal contact strength *in vivo* by the creation of interproximal frictional forces during the removal of a 50-μm-thick metal strip. Those authors concluded that the contact point might be significantly influenced by location, tooth type, chewing, variations in the time of the day, and periodontal condition of the tooth. Therefore, the interproximal contact of the present study can be considered satisfactory for all groups since the least tight contact point measured was 29.2 μm, which was much less than the metal strip of 50 μm used to quantify the proximal contact strength.

A limitation of this study was the use of few types of ceramics since the feldspathic and other resin and ceramics could have been investigated, although it was not possible to fabricate lithium disilicate inlays using the lab model with the Lava system. Using other types of restorative materials would have been interesting for more comparisons in relation to marginal and internal fitting, time of adjustment and tightness of the interproximal contact; however, the main purpose of the present research was highlighted the different methods of inlay production.

Further studies should be conducted with other parameters and other types of materials indicated for inlay production. It would be interesting to evaluate other types of scanners with or without powder as well as to verify whether these different methods of inlay production influence the bond strength and fatigue loading conditions.

CONCLUSION

- For marginal fit at the cervical edge, the composite resin material presents a better fit than the lithium disilicate with the CEREC system, while there is no difference among the material/methods for inlay production at the occlusal edge.
- For the internal fit at the axial wall, the Lava C.O.S. presents a worse fit than the CEREC system but was similar to pressed ceramic. Additionally, there was no difference among the different inlay production methods when considering the pulp wall.
- All of the inlay production methods promoted acceptable interproximal contacts.
- The groups restored with lithium disilicate ceramic took more time for adjustment when compared to the resin restorative material.

Acknowledgments

This study was supported by FAPESP Grant (Fundação de Amparo à Pesquisa do Estado de São Paulo). The authors thank the Mignani Laboratory for inlay production.

Regulatory Statement

This study was conducted in accordance with all the provisions of the local human subjects oversight committee guidelines and policies of Federal University of Santa Maria. The approval code for this study is 52827416.1.0000.5346.

Conflict of Interest

The authors of this article certify that they have no proprietary, financial, or other personal interest of any nature or kind in any product, service, and/or company that is presented in this article.

(Accepted 17 November 2016)

REFERENCES

1. Pera P, Gilodi S, Bassi F, & Carossa S (1994) In vitro marginal adaptation of alumina porcelain ceramic crowns *Journal of Prosthetic Dentistry* **72(6)** 585-590.
2. Rinke S, Huls A, & Jahn L (1995) Marginal accuracy and fracture strength of conventional and copy milled all-ceramic crowns *International Journal of Prosthodontics* **8(4)** 303-310.
3. Valderhaug J, & Heloe LA (1977) Oral hygiene in a group of supervised patients with fixed prostheses *Journal of Periodontology* **48(4)** 221-224.
4. Bindl A, & Mormann WH (2005) Marginal and internal fit of all-ceramic CAD/CAM crown-copings on chamfer

preparations *Journal of Oral Rehabilitation* **32(6)** 441-447.

5. Kokubo Y, Ohkubo C, Tsumita M, Miyashita A, Vult von Steyern P, & Fukushima S (2005) Clinical marginal and internal gaps of Procera AllCeram crowns *Journal of Oral Rehabilitation* **32(7)** 526-530.
6. McLean JW, & von Fraunhofer JA (1971) The estimation of cement film thickness by an in vivo technique *Brazilian Dental Journal* **131(3)** 107-111.
7. Syrek A, Reich G, Ranftl D, Klein C, Cerny B, & Brodesser J (2010) Clinical evaluation of all-ceramic crowns fabricated from intraoral digital impressions based on the principle of active wavefront sampling *Journal of Dentistry* **38(7)** 553-559.
8. Contrepois M, Soenen A, Bartala M, & Laviole O (2013) Marginal adaptation of ceramic crowns: A systematic review *Journal of Prosthetic Dentistry* **110(6)** 447-454.
9. Ting-shu S, & Jian S (2015) Intraoral digital impression technique: A review *Journal of Prosthodontics* **24(4)** 313-321.
10. Mously HA, Finkelman M, Zandparsa R, & Hirayama H (2014) Marginal and internal adaptation of ceramic crown restorations fabricated with CAD/CAM technology and the heat-press technique *Journal of Prosthetic Dentistry* **112(2)** 249-256.
11. Hamza TA, Ezzat HA, El-Hossary MMK, Katamish HAEM, Shokry TE, & Rosenstiel SF (2013) Accuracy of ceramic restorations made with two CAD/CAM systems *Journal of Prosthetic Dentistry* **109(2)** 83-87.
12. Neves FD, Prado CJ, Prudente MS, Carneiro TA, Zancopé K, Davi LR, Mendonça G, Cooper LF, & Soares CJ (2014) Micro-computed tomography evaluation of marginal fit of lithium disilicate crowns fabricated by using chairside CAD/CAM systems or the heat-pressing technique *Journal of Prosthetic Dentistry* **112(5)** 1134-1140.
13. Stawarczyk B, Krawczuk A, & Ilie N (2015) Tensile bond strength of resin composite repair in vitro using different surface preparation conditionings to an aged CAD/CAM resin nanoceramic *Clinical Oral Investigation* **19(2)** 299-308.
14. Bottino MA, Campos F, Ramos NC, Rippe MP, Valandro LF, & Melo RM (2015) Inlays made from a hybrid material: Adaptation and bond strengths *Operative Dentistry* **40(3)** E83-E91.
15. Awada A, & Nathanson D (2015) Mechanical properties of resin-ceramic CAD/CAM restorative materials *Journal of Prosthetic Dentistry* **114(4)** 587-593.
16. Hoop CD, & Land MF (2013) Considerations for ceramic inlays in posterior teeth: A review *Clinical, Cosmetic and Investigational Dentistry* **18(5)** 21-32.
17. Ender A, & Mehl A (2013) Influence of scanning strategies on the accuracy of digital intraoral scanning systems *International Journal of Computerized Dentistry* **16(1)** 11-21.
18. Renne W, McGill ST, Forshee KV, DeFee MR, & Mennito AS (2012) Predicting marginal fit of CAD/CAM crowns based on the presence or absence of common preparation errors *Journal of Prosthetic Dentistry* **108(5)** 310-315.
19. Addi S, Hedayati-Khams A, Poya A, & Sjogren G (2002) Interface gap size of manually and CAD/CAM manufactured ceramic inlay/onlays in vitro *Journal of Dentistry* **30(1)** 53-58.
20. Holmes JR, Sulik WD, Holland GA, & Bayne SC (1992) Marginal fit of castable ceramic crowns *Journal of Prosthetic Dentistry* **67(5)** 594-599.
21. Boening KW, Wolf BH, Schmidt AE, Kästner K, & Walter MH (2000) Clinical fit of Procera AllCeram crowns *Journal of Prosthetic Dentistry* **84(4)** 419-424.
22. Pelekanos S, Koumanou M, Koutayas SO, Zinelis S, & Eliades G (2009) Micro-CT evaluation of the marginal fit of different In-Ceram alumina copings *European Journal of Esthetic Dentistry* **4(3)** 278-292.
23. Dörfer CE, von Bethlenfalvy ER, Staehle HJ, & Pioch T (2000) Factors influencing proximal dental contact strengths *European Journal of Oral Science* **108(5)** 368-377.

©Operative Dentistry, 2017, **42-4,** 445-455

Characterization of Inorganic Filler Content, Mechanical Properties, and Light Transmission of Bulk-fill Resin Composites

BM Fronza • APA Ayres • RR Pacheco • FA Rueggeberg • CTS Dias • M Giannini

Clinical Relevance

Light attenuation at greater depths did not influence flexural strength of bulk-fill composites, which can be applied in a 4-mm thickness. Some of these materials present inferior mechanical properties compared with conventional composite.

SUMMARY

Objectives: The aims of this study were to characterize inorganic content (IC), light transmission (LT), biaxial flexural strength (BFS), and flexural modulus (FM) of one conventional (layered) and four bulk-fill composites at different depths.

Methods: Bulk-fill composites tested were Surefil SDR flow (SDR), Filtek Bulk Fill (FBF), Tetric EvoCeram Bulk Fill (TEC), and EverX Posterior (EXP). Herculite Classic (HER) was used as a control. Energy dispersive x-ray analysis and scanning electron microscopy were used to characterize filler particle composition and morphology. The LT through different composite thicknesses (1, 2, 3, and 4 mm) was measured using a laboratory-grade spectral radiometer system (n=5). For the BFS and FM tests, sets of eight stacked composite discs (0.5-mm thick) were prepared simulating bulk filling of a 4-mm-thick increment (n=8).

Results: SDR demonstrated larger, irregular particles than those observed in TEC or HER. Filler particles in FBF were spherical, while those in EXP were composed of fiberglass strands. The LT decreased with increased composite thickness for all materials. Bulk-fill composites allowed higher LT than the HER. Furthermore, HER proved to be the unique material, having lower BFS values at deeper

*Bruna Marin Fronza, DDS, MSc, PhD student. Department of Restorative Dentistry, Piracicaba Dental School, State University of Campinas, Piracicaba, Brazil

Ana Paula Almeida Ayres, DDS, MSc, PhD student. Department of Restorative Dentistry, Piracicaba Dental School, State University of Campinas, Piracicaba, Brazil

Rafael Rocha Pacheco, DDS, MSc, assistant professor, University of Detroit Mercy, School of Dentistry, Detroit, USA.

Frederick Rueggeberg, DDS, MSc, professor, Dental Materials Section, Department of Restorative Sciences, Dental College of Georgia, Augusta University. Augusta, GA, USA.

Carlos Tadeu dos Santos Dias, MSc, PhD, full professor, Exact Sciences Department, Luiz de Queiroz College of Agriculture, University of São Paulo, Piracicaba, Brazil

Marcelo Giannini, DDS, MSc, PhD, associate professor, Department of Restorative Dentistry, Piracicaba Dental School, State University of Campinas, Piracicaba, Brazil

*Corresponding author: Av. Limeira, 901. Piracicaba, SP, 13414-903, Brazil; e-mail: bruna.fronza@hotmail.com

DOI: 10.2341/16-024-L

regions. SDR, FBF, and TEC bulk-fill composites presented reduced FM with increasing composite depth.

Conclusions: The bulk-fill composites investigated exhibited higher LT, independent of different filler content and characteristics. Although an increase in composite thickness reduced LT, the BFS of bulk-fill composites at deeper layers was not compromised.

INTRODUCTION

Development of dental resin-based composites began with use of a bisphenol-A glycidyl methacrylate monomer (Bis-GMA) combined with glass filler particles created by Bowen in 1958.[1] Since that time, the composition of composite resins has evolved significantly. The basic formulation of composite resins is methacrylate monomeric mixtures and inorganic fillers coated with a silane coupling agent, along with photoinitiator systems that promote polymerization when the material is light activated, to form a highly cross-linked network with high mechanical properties.[2-4] Most improvements to composites have involved the inorganic fillers that have been reduced in size to produce materials with greater surface gloss retention and wear resistance.[3,5]

However, concerns related to aspects of the organic resin matrix remain, such as the extent of monomer conversion into polymer, which provides materials with high modulus and strength.[4,6] Also, polymerization shrinkage, caused by monomer approximation during the curing reaction, and the stress generated along with modulus development may negatively impact the clinical performance of bonded restorations.[7,8] Incremental filling techniques for composites have been suggested to minimize polymerization shrinkage stress and ensure efficient polymerization.[9-11] The average maximum thickness recommended for each increment of regular composites is 2 mm, and depending on the composite resin formulation, light irradiation is recommended to last from 10 to 40 seconds. Thus, restorations involving large cavity preparation volumes are time consuming for the operator and inconvenient for the patient.[12]

Bulk-fill composites activated by light have recently been introduced, using new composite resin formulations. According to the manufacturers, these new materials enable depths of cure up to 4 or 5 mm with minimal polymerization shrinkage stress. Successful resin composite restorations require an efficient polymerization process to enhance mechanical properties and biocompatibility and offer the potential for long-term success.[6] One approach to improve curing depth of bulk-fill composites is to increase material translucency, thereby allowing more light to pass through to deeper levels of the material, which provides a more uniform monomer conversion with depth.[13]

The optical properties of resin composites and their light-activated polymerization reactions are interdependent: a higher radiant exposure yields a higher degree of conversion, which leads to enhanced physical properties.[14] Light transmission (LT) is affected by material composition. Filler particles hinder LT due to scattering, which is dependent on filler particle size and related to the incident wavelength of the curing light. The refractive indices of fillers and resin matrix in a composite, as well as the mismatch between them, also influence light refraction and, thus, light penetration depth. Other components, such as pigments and photoinitiators, absorb light and result in a decrease in depth of cure.[6,15,16]

There are differences among bulk-fill composites with respect to filler loading and resin matrix composition. Some products have a flowable consistency, while other materials have a high filler content or feature glass fibers for reinforcement and are thus more viscous.[17] Consequently, the mechanical properties of these materials are expected to present variations among brands. Because fracture of composite resin restorations remains a major cause of clinical failure,[18,19] laboratory evaluation of composite properties and the factors influencing their physical behaviour are needed to better predict the clinical outcomes of direct restorations. Specifically, flexural strength and modulus of composites have been shown to correlate with clinical performance.[20] Furthermore, LT through composites plays an important role in the polymerization process and, thus, in determining the final mechanical properties of restorations.[19]

The purposes of this study were to characterize the morphology and composition of filler particles and their influence on LT and on the biaxial flexural strength (BFS) and flexural modulus (FM) of a variety of commercially available bulk-fill composites at selected depths. One conventional, layered, microhybrid composite was used as a control. The following hypotheses were tested: (1) differences in filler particle characteristics will be observed between bulk-fill and conventional composites; (2) LT will be higher in bulk-fill composites compared with

Table 1: *Materials Evaluated and Respective Manufacturers' Information*

Abbreviation Used in Text	Brand Name	Manufacturer (Lot Number)	Matrix Composition*	Filler Type[a]	Filler Loading[a] (%, by Volume)	Shade
HER	Herculite Classic	Kerr Co, Orange, CA, USA (4009366)	Bis-GMA, TEGDMA	Borosilicate-aluminum glass	59	A2
SDR	Surefill SDR flow	Dentsply Caulk, Mildford, DE, USA (08153)	Modified UDMA, TEGDMA, EBPDMA	Barium-aluminofluoro-borosilicate glass, strontium-aluminofluoro-borosilicate glass	44	Universal
FBF	Filtek Bulk Fill	3M ESPE, St Paul, MN, USA (402919)	Bis-GMA, Bis-EMA, UDMA, TEGDMA, Procrylat resins	Zirconia/silica, ytterbium trifluoride	42.5	A2
TEC	Tetric EvoCeram Bulk Fill	Ivoclar Vivadent, AG, Schaan, Liechtenstein (R04686)	Bis-GMA, UDMA	Barium glass, ytterbium trifluoride, oxides and pre-polymers	60 (17% pre-polymers)	IVA
EXP	EverX Posterior	GC Corporation, Tokyo, Japan (1401152)	Bis-GMA, TEGDMA, PMMA	Hybrid filler fractions and E-glass fibers	57	Universal

Abbreviations: Bis-GMA, bisphenol-A diglycidyl ether dimethacrylate; Bis-EMA, ethoxylated bisphenol-A dimethacrylate; EPDMA, ethoxylated bisphenol-A dimethacrylate; PMMA, polymethyl methacrylate; TEGDMA, triethylenegycol dimethacrylate; UDMA, urethane dimethacrylate.
[a] *Information supplied by manufacturer.*

a conventional, layered composite, and (3) there will be no significant difference in mechanical properties among the bulk-fill composites at similar depths, while properties will be reduced with increasing composite depth.

METHODS AND MATERIALS

Five resin-based composites were investigated: one conventional, incrementally layered material used as a control (Herculite Classic [HER]); two high-viscosity, bulk-fill composites (Tetric EvoCeram Bulk Fill [TEC] and EverX Posterior [EXP]); and two flowable bulk-fill composites (Surefil SDR flow [SDR] and Filtek Bulk Fill [FBF]). The compositions, lot numbers, and manufacturer information for these products are presented in Table 1.

Filler Content and Characterization

Approximately 1 g of unpolymerized composite was washed in 6 mL of acetone (99.5%, Merck KGA, Darmstadt, Germany) and centrifuged at 1000 rpm for 5 minutes (Excelsa, model 206, FANEM, São Paulo, Brazil). This procedure was repeated until the entire organic matrix was dissolved, as evidenced by clarity of the supernatant fluid.[19] Chloroform (99.8%, Merck KGA) was then used in the same manner. The remaining content of fillers was then immersed in 6 mL of absolute ethanol (Merck KGA) for 24 hours followed by drying at 37°C in an incubator (FANEM). The recovered filler particles were then placed on plastic stubs and sputter-coated with carbon (MED 010 Baltec, Balzers, Liechtenstein) before examination using energy-dispersive x-ray (EDX) spectrometry analysis, or placed on metallic stubs and sputter-coated with gold (MED 010 Baltec) before scanning electron microscopy (SEM) observation. EDX analysis (Vantage, NORAN Instruments, Middleton, WI, USA) coupled to a scanning electron microscope (JEOL, JSM-5600LV, Tokyo, Japan) was performed to identify the elemental composition of the recovered insoluble filler particles. Each spectrum was acquired for 100 seconds (voltage 15 kV, dead time 20% to 25%, working distance 20 mm). Images showing the identified chemical elements and their relative concentration were obtained from five different analyses of each material at different locations on a stub.

For filler particle morphologic characterization, specimens were examined using SEM (voltage 15 kV, beam width 25–30 nm, working distance 10–15 mm) at 50×, 1000×, and 5000× magnifications. Representative images at different magnifications were obtained for each material and were used for qualitative analysis and particle-size comparison using software analysis of the recorded images (ImageJ, 1.6.0_24, National Institutes of Health, Bethesda, MD, USA).

Light Transmission Through Cured Composite

Composite discs (n=5) of each material at four different thicknesses were fabricated to evaluate LT. Silicon molds (6 mm in diameter) were used to

fabricate discs with thicknesses of 1, 2, 3, and 4 mm. Each material was light-activated using a polywave light-emitting diode curing unit (LCU; VALO, Ultradent Products Inc, South Jordan, UT, USA) for the exposure duration recommended by the manufacturer (20 seconds for the bulk-fill composites and 40 seconds for the conventional composite) with the emitting end of the light source as close to the upper composite surface as possible without actually touching it.

The irradiance of the LCU and the light transmittance were determined using a laboratory-grade spectral radiometer (USB 2000, Ocean Optics, Dunedin, FL, USA) attached to a 7.62-cm-diameter integrating sphere (CTSM-LSM-60-SF, Labsphere Inc, Sutton, NH, USA) associated with specific software (Spectra Suite version 5.1, Ocean Optics Inc, Dunedin, FL, USA). A mean value of 1153 mW/cm^2 was obtained for the total irradiance of LCU (100%; without interposing disc) between 350 and 550 nm. To measure LT, each composite disc was positioned between the integrating sphere aperture and the curing unit tip. The light source was positioned such that the tip remained parallel to the specimen surface and just slightly touched it.

Each spectrum was obtained during the first 5 seconds of light irradiation. The transmittance value for each sample was calculated as a percentage by dividing the irradiance value measured through each specimen by the average curing light irradiance with no interposing disc.

The data demonstrated asymmetrical distribution. Adjustments were performed using a generalized linear model considering the gamma distribution (asymmetric mode) according to a two-way design. Software (GENMOD, SAS/STAT 9.3, Cary, NC, USA) was applied to analyze the data. Multiple comparisons of the results among the different composite depths were performed using a feature of that software (DIFF). All statistical testing was performed at a pre-set alpha of 0.05.

Biaxial Flexural Strength and Modulus

Disc-shaped specimens (n=8) approximately 0.5 mm thick and 6.0 mm in diameter were fabricated using a set of eight Teflon molds that were stacked on each other. A metal device was used to hold the eight composite-filled Teflon molds together. For each 0.5-mm-thick specimen, an acetate strip was positioned on the bench top, and the empty mold was placed on top. The mold was slightly overfilled with uncured composite paste and then covered with a second acetate strip. Vertical pressure was applied to force the material to conform to the confines of the mold dimensions and to extrude excess material. The filled Teflon mold was then placed into the holding jig, using the two vertical metal guides to precisely position it. A second mold was then placed on top of the acetate strip of the previously filled specimen and filled with composite; another acetate sheet was then placed, and vertical pressure was applied. This process was continued until a total of eight such molds had been stacked, with a total thickness of 4 mm, but such that the cylinder could be disassembled after light curing from the top into separate 0.5-mm-thick increments. Once all the wafers were stacked, the composite stack was photocured using the LCU with the distal end of the light guide touching the acetate-covered surface of the top-most wafer. This process is similar to that performed in other work.[21] Specimen fabrication was performed in a light-proof room with a controlled temperature: 21°C.

After irradiation, the composite specimens were removed from the molds and their dimensions were measured using a digital micrometer (six-digit precision, MDC-Lite, Mitutoyo Corporation, Kanagawa, Japan). The discs were stored in the dark, in an incubator maintained at 37°C ± 1°C at a relative humidity for one week prior to BFS determination.

For BFS testing, each disc was individually placed into a custom-made jig and subjected to the piston-on-ring biaxial test,[21,22] using a universal testing machine (Model 5844, Instron Corporation, Canton, MA, USA), at a crosshead speed of 1.27 mm/min, until failure. The maximum load at failure was recorded for each specimen, and the flexural modulus (FM) was determined from the linear portion of each stress/strain curve. The following formula was used to obtain the BFS data:

$$\mathrm{BFS} = -0.238 \times 7\mathrm{P}(\mathrm{X} - \mathrm{Y})/\mathrm{b}^2,$$

where BFS is the maximum tensile stress (MPa), P is the total load at fracture (N), b is the specimen thickness (mm) and

$$\mathrm{X} = (1+v)ln(r2/r3)^2 + [(1-v)/2](r2/r3)^2,$$

$$\mathrm{Y} = (1+v)[1+ln(r1/r3)^2] + [(1-v)(r1/r3)^2],$$

where v is Poisson's ratio (0.25), $r1$ is the radius of the support circle (mm), $r2$ is the radius of the loaded area (mm), and $r3$ is the radius of the disc (mm).

The BFS and FM values were calculated using software (SRS Biaxial Testing Software, Instron

Corp. and were expressed in megapascals and gigapascals, respectively. Exploratory analysis of data suggested logarithmic transformation with base 10 for both BFS and FM data. Data were subjected to split-plot two-way (material and depth) analysis of variance using SAS/STAT 9.3 software. Tukey post hoc tests were performed to detect significant differences among the groups using a preset alpha of 0.05.

RESULTS

Filler Content and Characterization

The elemental composition of HER revealed the presence of aluminium, silicon, and barium (Figure 1A). The SEM micrograph showed irregularly shaped particles ranging from 0.5 to 2.2 μm in diameter (Figures 1B,C). The inorganic elements in SDR were found to include aluminium, silicon, barium, and a minor amount of fluoride (Figure 2A). This material consisted mainly of irregular particles of two distinct sizes: larger particles approximately 20 μm and smaller particles ranging from 0.5 to 1 μm (Figures 2B,C). The TEC composite had a composition and morphology similar to that of HER, consisting of aluminium, silicon, and barium with particles ranging in size from 0.4 to 2.2 μm (Figures 3A through C). EDX analysis revealed that FBF contained aluminium, silicon, and zirconium (Figure 4A), consisting only of spherical particles with diameters ranging from 0.1 to 4.0 μm (Figures 4B,C). The filler particles in EXP were basically fiberglass consisting of aluminium, silicon, barium, fluoride, and calcium (Figure 5A) with lengths up to 1 mm and a diameter of approximately 15 μm (Figures 5B,C). However, small particles with a diameter of 1 μm were also observed.

Light Transmission Through Cured Composite

Table 2 presents the mean values for the percentage of light passing through each composite. Statistical results indicated that both material ($p<0.0001$) and depth ($p<0.0001$) significantly influenced LT. The interaction between factors was statistically significant ($p<0.0001$). In general, the HER material had a lower LT, while SDR presented higher LT for all depths evaluated. However, all of the composites exhibited a similar trend for light transmittance to decrease with respect to increase in sample depth.

Biaxial Flexural Strength and Modulus

Average BFS and FM values for the composites are presented in Tables 3 and 4, respectively. Statistical analyses indicated that both material ($p<0.0001$) and depth ($p=0.0022$) significantly influenced BFS results. Regarding factorial model, no significant interaction between factors was identified ($p=0.2741$). Considering this global analysis regarding the depths of all materials together, 0.5-mm, 1.5-mm, and 2.0-mm depths had significantly higher BFS than the 4.0-mm depth. Although the factorial model did not present significant interaction between factors (materials and depths), when an interaction slice was performed it detected a significant difference among depths only for HER ($p<0.0001$). For this conventional material, the BFS at a depth of 0.5 to 2 mm was higher compared with a depth 4 mm. The bulk-fill composites did not show significant difference among depths ($p<0.05$) (Table 3). When data obtained at different depths for a given material were pooled, significant differences were found among materials. In general, HER, SDR, and FBF demonstrated higher BFS values, followed by EXP and TEC, which had the lowest values.

For FM data, statistically significant differences were also observed among the materials ($p<0.0001$) and depths (p=0.0002), again with no significant interaction between them ($p=0.0865$). In this global factorial model and considering all materials together, FM was significantly higher at 0.5-mm and 2.0-mm depths compared with the 4.0-mm depth. Meanwhile, the slice of interaction demonstrated that there were significant differences in FM among depths for SDR, FBF, and TEC ($p=0.0004$, $p=0.0116$, and $p=0.0048$, respectively) (Table 4). Regarding the comparison of materials, HER and SDR demonstrated the highest and lowest moduli, respectively. The products EXP, FBF, and TEC showed intermediate FM values, with EXP demonstrating a higher value than both FBF and TEC, which had moduli that were not statistically different.

DISCUSSION

The first hypothesis, stating that there will be qualitative differences in filler particle characteristics between bulk-fill and conventional composites was observed in this investigation. While the shapes of the filler particles in SDR, FBF, and, EXP (Figures 2, 4, and 5) were different and larger than the particles in the HER composite (Figure 1), particles in the TEC composite (Figure 3) were of similar shape and size to those in HER. Furthermore, LT through the composites was similar for all materials for a given depth, although SDR exhibited higher LT, and HER had the lowest LT percentages of all materials (Table 2). Thus, the second hypoth-

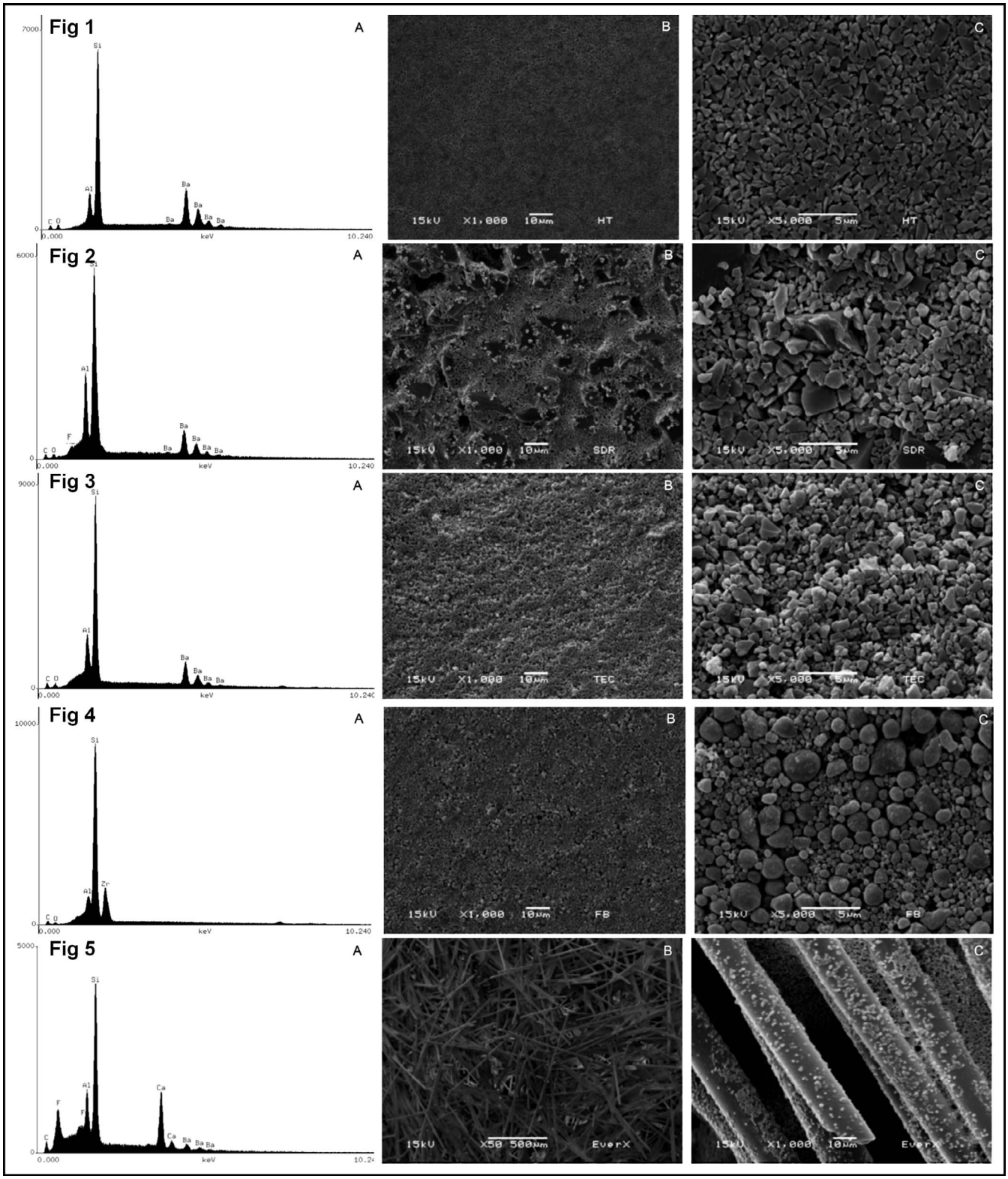

Figure 1. *Elements identified by EDX analysis for HER (A) and SEM micrographs: original magnification 1000× (B) and 5000× (C).*
Figure 2. *Elements identified by EDX analysis for SDR (A) and SEM micrographs: original magnification 1000× (B) and 5000× (C).*
Figure 3. *Elements identified by EDX analysis for TEC (A) and SEM micrographs: original magnification 1000× (B) and 5000× (C).*
Figure 4. *Elements identified by EDX analysis for FBF (A) and SEM micrographs: original magnification 1000× (B) and 5000× (C).*
Figure 5. *Elements identified by EDX analysis for EXP (A) and SEM micrographs: original magnification 50× (B) and 1000× (C).*

Table 2: *Mean (Standard Deviation) for Light Transmission (%)*[a]

Depth (mm)	Material				
	Layered	Bulk-Fill			
		Flowable		Viscous Paste	
	HER	SDR	FBF	TEC	EXP
1	21.1 (0.4) Da	38.6 (1.1) Aa	31.3 (0.5) Ba	27.3 (0.6) Ca	27.1 (4.7) Ca
2	11.1 (0.4) Db	23.3 (0.1) Ab	16.4 (1.2) Bb	15.2 (0.6) Cb	16.5 (0.9) Bb
3	5.5 (0.3) Cc	15.5 (0.3) Ac	8.5 (0.2) Bc	8.9 (0.3) Bc	8.7 (0.3) Bc
4	2.5 (0.1) Cd	9.1 (0.4) Ad	4.3 (0.3) Bd	4.4 (0.1) Bd	4.9 (0.5) Bd

Abbreviations: EXP, EverX Posterior; FBF, Filtek Bulk Fill; HER, Herculite Classic; SDR, Surefil SDR flow; TEC, Tetric EvoCeram Bulk Fill.
[a] Means (n=5) followed by the same letter (uppercase compare columns (materials), lowercase compare rows (depths)) are not statistically different (p>0.05).

Table 3: *Mean (Standard Deviation) Biaxial Flexural Strength (MPa) With Composite Depth* [a]

Depth (mm)	Material					Tukey
	Layered	Bulk-Fiill				
		Flowable		Viscous Paste		
	HER	SDR	FBF	TEC	EXP	
0.5	173.9 (31.7) *a*	148.8 (12.3) *a*	171.3 (24.8) *a*	76.3 (9.6) *a*	103.4 (8.0) *a*	**a**
1.0	165.3 (35.9) *ab*	149.5 (22.4) *a*	171.9 (17.1) *a*	77.3 (14.4) *a*	102.6 (14.0) *a*	**ab**
1.5	175 (31.4) *a*	152.3 (14.8) *a*	170.5 (23.8) *a*	78.5 (12.8) *a*	106.8 (10.7) *a*	**a**
2.0	167.6 (31.8) *ab*	148.9 (13.3) *a*	169.5 (22.5) *a*	79.7 (8.7) *a*	107.0 (7.6) *a*	**a**
2.5	141.5 (27.7) *abc*	151.9 (25.1) *a*	157.0 (28.3) *a*	79.4 (3.8) *a*	103.5 (14.2) *a*	**ab**
3.0	137.0 (26.4) *bc*	148.4 (9.9) *a*	157.8 (24.8) *a*	77.2 (11.0) *a*	104.3 (9.8) *a*	**ab**
3.5	147.7 (33.2) *abc*	152.2 (15.7) *a*	151.0 (27.2) *a*	75.1 (8.2) *a*	103.9 (14.3) *a*	**ab**
4.0	124.2 (22.9) *c*	146.0 (16.2) *a*	143.2 (22.7) *a*	76.2 (11.0) *a*	104.2 (12.0) *a*	**b**
Tukey	**A**	**A**	**A**	**C**	**B**	

Abbreviations: EXP, EverX Posterior; FBF, Filtek Bulk Fill; HER, Herculite Classic; SDR, Surefil SDR flow; TEC, Tetric EvoCeram Bulk Fill.
[a] Means (n=8) followed by the same bold uppercase letter (columns comparing materials) are not statistically different (p>0.05). Bold lowercase letters (outside the table) are related to global factorial model (all materials together) that compares depths (rows). The italic lowercase letters (inside the table) represent the slice of interaction and also compare depths, but within the same material.

Table 4: *Mean (Standard Deviation) Flexural Modulus (GPa) With Composite Depth* [a]

Depth (mm)	Material					Tukey
	Layered	Bulk-Fill				
		Flowable		Viscous Paste		
	HER	SDR	FBF	TEC	EXP	
0.5	5.0 (1.4) *a*	3.2 (0.5) *a*	3.8 (0.7) *a*	3.7 (0.5) *ab*	4.6 (1.0) *a*	**a**
1.0	4.9 (0.5) *a*	2.6 (0.3) *ab*	3.8 (0.7) *a*	3.9 (1.0) *ab*	4.5 (1.2) *a*	**abc**
1.5	5.1 (1.2) *a*	2.6 (0.5) *ab*	3.4 (0.3) *ab*	4.2 (1.1) *a*	4.4 (0.9) *a*	**abc**
2.0	5.3 (1.3) *a*	2.5 (0.5) *ab*	3.9 (0.9) *a*	3.7 (0.2) *ab*	4.5 (0.6) *a*	**ab**
2.5	4.9 (0.8) *a*	2.4 (0.3) *ab*	3.0 (0.7) *ab*	3.5 (1.0) *ab*	4.7 (1.0) *a*	**abc**
3.0	5.2 (0.8) *a*	2.2 (0.2) *b*	3.1 (1.4) *ab*	3.3 (0.8) *ab*	4.5 (1.1) *a*	**bc**
3.5	5.3 (1.1) *a*	2.2 (0.5) *b*	2.9 (0.8) *ab*	3.1 (0.9) *ab*	4.6 (0.7) *a*	**bc**
4.0	5.2 (0.5) *a*	2.3 (0.2) *ab*	2.7 (0.3) *b*	2.8 (0.5) *b*	4.5 (1.1) *a*	**c**
Tukey	**A**	**D**	**C**	**C**	**B**	

Abbreviations: EXP, EverX Posterior; FBF, Filtek Bulk Fill; HER, Herculite Classic; SDR, Surefil SDR flow; TEC, Tetric EvoCeram Bulk Fill.
[a] Means (n=8) followed by the same bold uppercase letter (columns comparing materials) are not statistically different (p>0.05). Bold lowercase letters (outside the table) are related to global factorial model (all materials together) that compares depths (rows). The italic lowercase letters (inside the table) represent the slice of interaction and also compare depths, but within the same material.

esis, that LT will be higher in bulk-fill composites compared with a conventional, layered composite was accepted.

Light transmission through a resin composite depends on light reflection, scattering, and absorption, which vary according to the material composition. Filler particles with diameters approaching half the wavelength of light used for curing increase light scattering, and thus light transmittance tends to increase with increasing filler size because scattering is decreased. Studies have also shown that increasing the size of silica particles reduces the extent of polymerization at greater depths for experimental and commercial composites.[6,23,24] Furthermore, not only the size of the particles but also the amount of filler loading influence LT. Higher filler content tends to reduce LT due to the increased probability of light refraction at the interfaces between the filler particles and the resin due to differences in their refractive indices.[6,13]

The lower filler loading for SDR explains its higher LT compared with that of HER (Table 1) as well as the larger particle size (approximately 20 μm) of the fillers (Figures 1 and 3). FBF also has low filler content, yet the presence of zirconium (Figure 2) may influence the LT behavior because this material has a higher refractive index, which explains the similar results compared with TEC and EXP.[25] Both TEC and EXP composites also exhibited higher LT than the conventional, layered control material: HER. Given that the inorganic content and morphologic characteristics of the fillers in TEC and HER were very similar, this finding may be attributed to the different compositions and shapes of the filler particles and the different monomers used in these composites.[6] Meanwhile, the higher transmittance of EXP, despite its high filler loading, may be due to the fiberglass filler, which may be effective in transmitting light inside the material.[26]

A study compared light transmittance through nanohybrid, flowable, and bulk-fill composites at 2-mm, 4-mm, and, 6-mm incremental thickness.[13] Bulk-fill composites used in that study, including several used in the current project (SDR, FBF, and TEC) demonstrated higher translucency than regular composites resin. In that study, measurements were made during real-time polymerization, different from this study, which evaluated LT through pre-polymerized composite cylinders. The authors reported that light transmittance increased as the polymerization reaction progressed. As polymer cross-linking starts, the density and refractive index of the polymer matrix increases, approaching the refractive index of the fillers, resulting in a reduction of scattering and an increase in LT.[13] It is therefore possible that LT values may be overestimated in the present study due to an increase in the effect of using pre-polymerized composites.

The third hypothesis, that there will be no significant difference in mechanical properties among bulk-fill composites at similar depths, while properties will be reduced with increasing composite depth, was partially accepted. For the BFS test, when the global analysis was considered, all materials had a decrease in flexural strength at the 4-mm layer. However, when interaction slice was performed, this effect was only observed in the HER conventional composite (Table 3). For the FM test, reduced values were also observed with increasing composite depth in global analysis. This was detected mainly in SDR, FBF and TEC, which also had significantly lower FM when materials were compared (Table 4).

Resin composite viscosity has been shown to be an important parameter affecting the polymerization kinetics and final degree of conversion of dimethacrylate monomers because it influences monomer mobility and reactivity. In turn, the rheologic properties of composite resins depend on monomer composition and filler content.[4,27] In general, higher BFS values indicate higher monomer conversion. In the present study, the conventional composite (HER) and two bulk-fill composites (SDR and FBF) exhibited higher BFS values despite differences in their filler contents. The good mechanical properties of HER can be attributed to the high filler loading (approximately 59% by volume).[28]

The products SDR and FBF are flowable composites and theoretically should undergo a higher degree of conversion than composites with regular viscosities.[29] SDR contains triethylenegycol dimethacrylate (TEGDMA), ethoxylated bisphenol-A dimethacrylate (EBPDMA), and urethane dimethacrylate (UDMA) modified by chain modulators: chemical moieties in the resin backbone that increase flexibility.[30] As a consequence, this material has the lowest FM values (Table 4). The monomers bisphenol-A diglycidyl ether dimethacrylate (Bis-GMA), ethoxylated bisphenol-A dimethacrylate (Bis-EMA), TEGDMA, UDMA, and procrylat are present in FBF. Bis-EMA has a high molecular weight but does not contain pendant hydroxyl groups and, thus, has a lower viscosity than does Bis-GMA.[12] Although the FM of composite resins may be affected by the mass fraction,[28,31] this behavior was not observed for EXP and TEC

composites and was in agreement with results obtained in other studies,[12,17,26,32] suggesting that a higher filler percentage only does not necessarily reflect superior mechanical properties. The increasing polymer network density, stress transfer between the filler particles and the resin matrix, and adhesion between these components also influence the polymerization reaction and final properties.[29]

Although the bulk-fill composite TEC has higher filler loading (approximately 60%), it exhibited one of the lowest BFS values. Use of pre-polymerized filler particles, such as in this material, has previously been shown to result in poorer mechanical properties.[33] Conversely, the photoinitiator Ivocerin, a derivative of dibenzoyl germanium, is incorporated in TEC, in addition to the camphorquinone/amine initiator system. Ivocerin is excited by shortwave visible light (380–450 nm) and is a more efficient free-radical generator than camphorquinone, leading to rapid polymerization and high monomer conversion.[34] Interestingly, although short wavelength visible light has a high dispersion effect and low penetration,[35] TEC exhibited uniform BFS values from depths of 0.5 to 4 mm, suggesting a great depth of cure, perhaps as a result of incorporation of Ivocerin.

The mechanical performance of EXP was intermediate compared with that of the other materials and was not expected because the use of fiberglass is known to provide material reinforcement.[36] Therefore, other factors, such as filler volume and their orientation and distribution may have contributed to this result. In the present study, thin specimens (0.5 mm) were used to test the mechanical properties, and it is likely that the fibers were aligned perpendicular to the applied load, which significantly reduced their reinforcement capability.[37]

Many researchers have investigated the mechanical properties of bulk-fill composites, but most often flexural strength has been evaluated using the three-point bending test, according to the ISO 4049 standard.[17,28,30,32,38,39] This method requires overlapping light exposures of the specimen to yield a specimen length greater than the tip diameter of the light guide. Use of such overlapping exposures may result in higher monomer conversion which may directly affect mechanical properties. Using this method, SDR was found to have a higher BFS than TEC[32,29] and a similar value to that of FBF,[28,38] which is in agreement with the results of the present study. Conversely, EXP has been reported to have a higher BFS than SDR,[17] and FBF and TEC were reported to have higher BFS values than SDR in one study,[29,38] while SDR was found to have a BFS similar to that of TEC in a different investigation.[28] Furthermore, in the present study, using the piston-ring biaxial test, the BFS of HER was determined to be higher than those of TEC and EXP but similar to those of the bulk-fill flowable composites SDR and FBF. Furthermore, the FM of the regular composite was found to be higher than those of the bulk-fill composites. The relationship between the LT findings and the BFS results are very interesting. All of the bulk-fill resin composites exhibited uniform BFS values at depths ranging from 0.5 mm to 4 mm, while the BFS values of HER composite decreased as the depth surpassed 2 mm (Table 3), although light attenuation was noted for all composites (Table 2). Monomer conversion, and consequently the mechanical properties, at a specific depth is not only dependent on the light reaching this particular layer but also on the initiation of the polymerization process of the layers above propagating in depth.[13] Depth of cure depends on filler characteristics, monomer composition, initiator concentration, shade and translucency of the material, and irradiance of the light source.[26,35]

When the effects of polymerization characteristics on mechanical properties are studied, tests in which single-shot curing protocols for making specimens are applicable, and biaxial flexure strength values are indicated.[6,12,39] BFS of two bulk-fill composites (X-tra base, Voco; and SDR, Dentsply) was evaluated at different depths up to 8 mm. Literature values found for SDR were in agreement with the results obtained in the present study because no statistically significant differences were found at depths up to 4 mm. At a depth of 8 mm, however, a measurable difference in the BFS value was noted compared with that obtained at 1 mm. These findings were also supported by monomer conversion analyses conducted by the same authors, which revealed no significant difference from depths of 1 mm to 4 mm.[12]

The present results suggest that the biaxial flexural test can be used as an indirect method for evaluating the depth of cure and comparing curing protocols for materials that may be used in a clinical setting. It must be noted, however, that the biaxial flexural test may not provide reliable data for elastic modulus determination.[6] In clinical situations, light can be easily attenuated by tip-to-target distance and by the angle between the tip of the light curing unit and the composite surface. In the present study, these factors were minimized by placement of the tip directly on the resin composite surface. Therefore, further studies that better simulate

clinical situations with different types of curing units and possibly clinical studies are required to ensure the adequate clinical performance of bulk-fill composites.

CONCLUSION

Within the limitations imposed by this in vitro study, the following conclusions may be made:

1. Different inorganic filler content characteristics were found among the composite resins. Irregular, spherical and cylindrical shapes were observed with sizes varying from 0.1 μm to 1 mm. Aluminium, barium, and silicon were present in all of the fillers.
2. LT decreased as composite thickness increased for both the regular and bulk-fill materials. However, the conventional composite HER demonstrated lower LT than the bulk-fill materials, among which SDR had the highest LT.
3. Light attenuation did not influence BFS of bulk-fill composites, while HER presented decreased BFS at greater depths. FM for SDR, FBF and TEC bulk-fill composites was reduced with increasing composite depth.

Acknowledgements

The authors acknowledge the State of São Paulo Research Foundation (FAPESP) for financial support (#2013/05247-4) of this study. The technical contributions of Adriano Martins and Donald Mettenburg are greatly appreciated.

Conflict of Interest

The authors of this manuscript certify that they have no proprietary, financial, or other personal interest of any nature or kind in any product, service, and/or company that is presented in this article.

(Accepted 19 September 2016)

REFERENCES

1. Bowen RL (1958) Synthesis of a silica-resin direct filling material: progress report *Journal of Dental Research* **37** 90-91.
2. Chen MH (2010) Update on dental nanocomposites *Journal of Dental Research* **89(6) 5**49-560.
3. Ferracane JL (2011) Resin composite—state of the art *Dental Materials* **27(1)** 29-38.
4. Stansbury JW (2012) Dimethacrylate network formation and polymer property evolution as determined by the selection of monomers and curing conditions *Dental Materials* **28(1)** 13-22.
5. Klapdohr S, & Moszner N (2005) New inorganic components for dental filling composites *Monatshefte Fur Chemie* **136** 21-45.
6. Leprince JG, Palin WM, Hadis MA, Devaux J, & Leloup G (2013) Progress in dimethacrylate-based dental composite technology and curing efficiency *Dental Materials* **29(2) 1**39-156.
7. Bowen RL (1967) Adhesive bonding of various materials to hard tooth tissues. VI. Forces developing in direct-filling materials during hardening *Journal of the American Dental Association* **74(3)** 439-445.
8. Braga RR, Ballester RY, & Ferracane JL (2005) Factors involved in the development of polymerization shrinkage stress in resin-composites: a systematic review *Dental Materials* **21(10)** 962-970.
9. Lutz E, Krejci I, & Oldenburg TR (1986) Elimination of polymerization stresses at the margins of posterior composite resin restorations: a new restorative technique *Quintessence International* **17(12)** 777-784.
10. Pollack BF (1987) Class II composites: 1987 thoughts and techniques *NY State Dental Journal* **53(5)** 25-27.
11. Hilton TJ, & Ferracane JL (1999) Cavity preparation factors and microleakage of Class II composite restorations filled at intraoral temperatures *American Journal of Dentistry* **12(3)** 123-130.
12. Finan L, Palin WM, Moskwa N, McGinley EL, & Fleming GJ (2013) The influence of irradiation potential on the degree of conversion and mechanical properties of two bulk-fill flowable RBC base materials *Dental Materials* **29(8)** 906-912.
13. Bucuta S, & Ilie N (2014) Light transmittance and micromechanical properties of bulk fill vs. conventional resin based composites *Clinical Oral Investigation* **18(8)**1991-2000.
14. Musanje L, & Darvell BW (2003) Polymerization of resin composite restorative materials: exposure reciprocity *Dental Materials* **19(6)** 531-541.
15. Turssi CP, Ferracane JL, & Vogel K (2005) Filler features and their effects on wear and degree of conversion of particulate dental resin composites *Biomaterials* **26(24)** 4932-4937.
16. Tarle Z, Attin T, Marovic D, Andermatt L, Ristic M, & Tauböck TT (2015) Influence of irradiation time on subsurface degree of conversion and microhardness of high-viscosity bulk-fill resin composites *Clinical Oral Investigation* **19(4)** 831-840.
17. Goracci C, Cadenaro M, Fontanive L, Giangrosso G, Juloski J, Vichi A, & Ferrari M (2014) Polymerization efficiency and flexural strength of low-stress restorative composites *Dental Materials* **30(6)** 688-694.
18. Roulet JF (1988) The problems associated with substituting composite resins for amalgam: a status report on posterior composites *Journal of Dentistry* **16(3)** 101-113.
19. Aguiar TR, Di Francescantonio M, Bedran-Russo AK, & Giannini M (2012) Inorganic composition and filler particles morphology of conventional and self-adhesive resin cements by SEM/EDX *Microscopy Research and Technique* **75(10)** 1348-1352.
20. Thomaidis S, Kakaboura A, Mueller WD, & Zinelis S (2013) Mechanical properties of contemporary composite

resins and their interrelations *Dental Materials* **29(8)** e132-e141.

21. Rueggeberg FA, Cole MA, Looney SW, Vickers A, & Swift EJ (2009) Comparison of manufacturer-recommended exposure durations with those determined using biaxial flexure strength and scraped composite thickness among a variety of light-curing units *Journal of Esthetic and Restorative Dentistry* **21(1)** 43-61.
22. Giannini M, Mettenburg D, Arrais CA, & Rueggeberg FA (2011) The effect of filler addition on biaxial flexure strength and modulus of commercial dentin bonding systems *Quintessence International* **42(2)** e39-e43.
23. Arikawa H, Kanie T, Fujii K, Takahashi H, & Ban S (2007) Effect of filler properties in composite resins on light transmittance characteristics and color *Dental Materials Journal* **26(1)** 38-44.
24. Fujita K, Ikemi T, & Nishiyama N (2011) Effects of particle size of silica filler on polymerization conversion in a light-curing resin composite *Dental Materials* **27(11)** 1079-1085.
25. Guo G, Fan Y, Zhang JF, Hagan JL, & Xu X (2012) Novel dental composites reinforced with zirconia-silica ceramic nanofibers *Dental Materials* **28(4)** 360-368.
26. Le Bell AM, Tanner J, Lassila LV, Kangasniemi I, & Vallittu PK (2003) Depth of light-initiated polymerization of glass fiber-reinforced composite in a simulated root canal *International Journal of Prosthodontics* **16(4)** 403-408.
27. Lovell LG, Newman SM, & Bowman CN (1999) The effects of light intensity, temperature, and comonomer composition on the polymerization behavior of dimethacrylate dental resins *Journal of Dental Research* **78(8)** 1469-1476.
28. Leprince JG, Palin WM, Vanacker J, Sabbagh J, Devaux J, & Leloup G (2014) Physico-mechanical characteristics of commercially available bulk-fill composites *Journal of Dentistry* **42(8)** 993-1000.
29. Sideridou I, Tserki V, & Papanastasiou G (2002) Effect of chemical structure on degree of conversion in light-cured dimethacrylate-based dental resins *Biomaterials* **23(8)** 1819-1829.
30. Czasch P, & Ilie N (2013) In vitro comparison of mechanical properties and degree of cure of bulk fill composites *Clinical Oral Investigation* **17(1)** 227-235.
31. Sabbagh J, Vreven J, & Leloup G (2002) Dynamic and static moduli of elasticity of resin-based materials *Dental Materials* **18(1)** 64-71.
32. Garoushi S, Säilynoja E, Vallittu PK, & Lassila L (2013) Physical properties and depth of cure of a new short fiber reinforced composite *Dental Materials* **29(8)** 835-841
33. Beun S, Glorieux T, Devaux J, Vreven J, & Leloup G (2007) Characterization of nanofilled compared to universal and microfilled composites *Dental Materials* **23(1)** 51-59.
34. Moszner N, Fischer UK, Ganster B, Liska R, & Rheinberger V (2008) Benzoyl germanium derivatives as novel visible light photoinitiators for dental materials *Dental Materials* **24(7) 9**01-907.
35. Miles RB, Lempert WR, & Forkey JN (2001) Laser Rayleigh scattering *Measurement Science & Technology* **12** 33-51.
36. Khan AS, Azam MT, Khan M, Mian SA, & Rehman IU (2015) An update on glass fiber dental restorative composites: a systematic review. *Materials Science and Engineering C: Materials for Biological Applications* **47(C)** 26-39.
37. Dyer SR, Lassila LV, Jokinen M, & Vallittu PK (2004) Effect of fiber position and orientation on fracture load of fiber-reinforced composite *Dental Materials* **20(10)** 947-955.
38. Ilie N, Bauer H, Draenert M, & Hickel R (2013) Resin-based composite light-cured properties assessed by laboratory standards and simulated clinical conditions *Operative Dentistry* **38(2)** 159-167.
39. El-Damanhoury H, & Platt J (2014) Polymerization shrinkage stress kinetics and related properties of bulk-fill resin composites *Operative Dentistry* **39(4)** 374-382.

Online Only Articles

On occasion we receive manuscripts that we would like to publish, but do not have the page room to include in the print journal. For the full article, please go to www.jopdentonline.org or enter the provided address into your address bar.

Clinical Evaluation of a Silorane- and a Methacrylate-Based Resin Composite in Class II Restorations: 24-Month Results

E Karaman • AR Yazici • G Ozgunaltay • I Ustunkol • A Berber

Clinical Relevance: This clinical study found that both silorane- and methacrylate-based resin composite restorations showed clinically acceptable performance after 24 months in class II slot restorations.

doi: http://dx/doi.org/10.2341/15-286-C

Clinical Performance of Different Solvent-based Dentin Adhesives With Nanofill or Nanohybrid Composites in Class III Restorations: Five Year Results

M Demirci • S Tuncer • HS Sancaklı • N Tekçe • C Baydemir

Clinical Relevance: The clinical performance of different solvent-based dentin adhesives with nanofill or nanohybrid composites in Class III restorations was satisfactory. Marginal discoloration and marginal integrity deterioration were reasons for the failure of the self-etch adhesive systems in Class III cavities.

doi: http://dx/doi.org/10.2341/16-326-C

©Operative Dentistry, 2017, **42-4,** E102-E110

Clinical Evaluation of a Silorane- and a Methacrylate-Based Resin Composite in Class II Restorations: 24-Month Results

E Karaman • AR Yazici • G Ozgunaltay • I Ustunkol • A Berber

Clinical Relevance

This clinical study found that both silorane- and methacrylate-based resin composite restorations showed clinically acceptable performance after 24 months in class II slot restorations.

SUMMARY

Objective: To compare the 24-month clinical performance of two different resin composites in class II slot restorations.

Methods and Materials: Thirty-seven patients having at least two approximal carious lesions were enrolled in the study. A total of 116 teeth (58 pairs) were restored with either a silorane-based composite (Filtek Silorane) and its self-etch adhesive (Silorane Adhesive System, 3M ESPE) or a methacrylate-based packable resin composite (X-tra Fil) and its self-etch adhesive (Futurabond NR, VOCO GmbH) according to the toss of a coin. The restorations were evaluated at baseline and at six-, 12-, and 24-month recalls by two calibrated examiners according to the modified US Public Health Service criteria. The comparison of the two restorative materials for each category was performed with the Pearson chi-square test. Within group differences of the materials at different recall times were compared using the Cochran Q and Friedman tests. Bonferroni-adjusted McNemar test was used when significant difference was found ($p<0.05$).

Results: After 24 months, no statistically significant differences were found between the two restorative materials for the criteria evaluated.

Conclusions: Both silorane- and methacrylate-based resin composites showed clinically acceptable performance in class II slot restorations after 24 months.

*Emel Karaman, DDS, PhD, Faculty of Dentistry, Department of Restorative Dentistry, Ondokuz Mayis University, Samsun, Turkey

A. Rüya Yazici, DDS, PhD, Faculty of Dentistry, Department of Restorative Dentistry, , Hacettepe University, Ankara, Turkey

Gul Ozgunaltay, DDS, PhD, Faculty of Dentistry, Department of Restorative Dentistry

Hacettepe University, Ankara, Turkey

Ildem Ustunkol, Izmir Oral and Tooth Health Center, Izmir, Turkey

Asli Berber, Mamak Oral and Tooth Health Center, Ankara, Turkey

*Corresponding author: Faculty of Dentistry, Department of Restorative Dentistry, Ondokuz Mayis University, Samsun 55139, Turkey; e-mail dtemelc@yahoo.com

DOI: 10.2341/15-286-C

INTRODUCTION

Today, resin composites have become one of the most popular esthetic restorative materials, even for posterior regions. However, several drawbacks of these materials, such as difficulty in placement due to their sticky nature and shrinkage during polymerization, are still major concerns for dentists placing direct composite restorations in posterior teeth. Polymerization shrinkage has been shown to cause several clinical problems, such as loss of marginal integrity, microleakage, marginal discoloration, postoperative sensitivity, cuspal deflection, and gap formation.[1,2]

Several different restoratives with improved mechanical and physical properties have been proposed to overcome these drawbacks. Manufacturers have developed "packable" or "condensable" composites by densely loading fillers into hybrid composites with improved mechanical properties, such as decreased wear, increased packability and depth of cure, and reduced polymerization shrinkage achieved through increased filler loading.[3]

Another approach to overcome polymerization shrinkage is the introduction of a different type of resin composite with a novel monomer technology, Filtek Silorane, which is a low-shrink posterior restorative that has a matrix derived from a molecule-dominated silorane instead of the conventional methacrylate-based organic matrix. During polymerization of silorane-based composite, ring-opening monomers connect by opening, flattening, and extending toward each other. This polymerization mechanism results in lower volumetric shrinkage than experienced with methacrylate-based ones.[4] *In vitro* studies have reported promising results for Filtek Silorane, including lower polymerization shrinkage[5,6] and cuspal deflection,[7] effective bonding to tooth tissues, and marginal adaptation.[8-13] Although the successful results obtained in *in vitro* studies done with Filtek Silorane were not clinically validated, many *in vivo* studies showed a similar but not superior clinical performance of Filtek Silorane compared with methacrylate-based composites,[14-19] while one clinical study showed lower clinical performance of Filtek Silorane in terms of marginal adaptation.[20]

The aim of the present clinical study was to compare the clinical performance of a silorane-based resin composite, Filtek Silorane, with that of a methacrylate-based resin composite, X-tra Fil, in class II slot restorations over 24 months. The null hypothesis tested was that there would be no difference in clinical performance between the two different restorative resins tested after 24 months.

METHODS AND MATERIALS

Patient Selection

The protocol and consent form for this randomized controlled clinical study were previously reviewed and approved by the University Human Ethics Committee (HEK 10/35). Before participating in the study, all patients read and signed these written informed consent forms.

A total of 37 patients (27 female and 10 male) who were seeking routine dental care at the restorative dentistry clinics at the University School of Dentistry were selected. Patients having at least two similar-sized approximal carious lesions were included in this study. Their mean age was 29 years, ranging from 18 to 52 years.

Patients with poor oral hygiene, severe medical complications, rampant caries or severe chronic periodontitis, and a history of severe active bruxism and xerostomia were excluded from the study. Permanent premolars and molars with primary caries lesions and without any restorations were included in the study. All teeth included in the study had neighboring teeth and were in occlusion with antagonist teeth.

Clinical Procedures

To detect a difference between the restoration groups according to the retention rate of 30%, with 90% power and 5% type I error rate, it was found that at least 47 teeth should be taken in each group. A total of 116 teeth (58 pairs) were restored with either a silorane-based low-shrinkage resin composite, Filtek Silorane, and its self-etch adhesive, Silorane Adhesive System (3M ESPE, St Paul, MN, USA), or a methacrylate-based packable resin composite, X-tra Fil, and its self-etch adhesive, Futurabond NR (VOCO GmbH, Cuxhaven, Germany), according to the toss of a coin (Table 1). Table 2 shows the distribution of restorations with regard to maxilla/mandibule, premolar/molar, and MO/DO.

Bitewing radiographs of the teeth to be restored were taken preoperatively. The lesion depth of the teeth to be restored was the middle or beyond the middle third of the dentin. Cavities were prepared using diamond burs (Diatech, Heerbrugg, Switzerland) under water cooling with no intentional bevels on enamel cavosurface margins and limited to removal of carious tissue. Hand instruments and low-speed steel burs were used to remove the carious

Table 1: *Resins Composites and Adhesive Systems Used in This Study*

Product	Type	Composition	Manufacturer
X-tra Fil	Packable hybrid composite resin	Bis-GMA, UDMA, and TEGDMA with 70.1 vol% bariumboroaluminiumsilicate filler	VOCO GmbH (Cuxhaven, Germany)
Filtek Silorane	Low-shrinkage composite resin	3,4-Epoxycyclohexylethylcyclopolymethylsiloxane, bis-3,4-epoxycyclohexylethylphenylmethylsilane, yttrium fluoride (15%), camphorquinone, iodum salt, stabilizers, pigments, silanized quartz particles	3M ESPE (St Paul, MN, USA)
Futura Bond NR	One-step self-etch adhesive	Bis-GMA, HEMA, BHT, ethanol, organic acids, fluorides	VOCO
Silorane System Adhesive	Two-step self-etch adhesive	Primer: phosphorylated methacrylates, bis-GMA, HEMA, water, ethanol, silane-treated silica filler, Vitrebond copolymer, initiators, stabilizers; adhesive: hydrophobic DMA, phosphorylated methacrylates, TEGDMA, silane-treated silica filler, initiators, stabilizers	3M ESPE

Abbreviations: Bis-GMA, bis-phenol A diglycidylmethacrylate; UDMA, urethane dimethacrylate; TEGDMA, triethylene glycol dimethacrylate; HEMA, 2-hydroxyethyl methacrylate; BHT, butylated hydroxytoluene.

tissue. The excavated preparation floor was checked by probing with a sharp explorer and visual inspection. Local anesthesia was applied if necessary. Isolation was accomplished by cotton rolls and a suction device. For all cavities, a metallic matrix was used, and careful wedging was performed with wooden wedges. All materials were used according to the manufacturers' instructions. Filtek Silorane and X-tra Fil resin composites were placed in oblique increments not exceeding 2 mm in thickness. Composite layers were light cured for 40 seconds with a halogen light-curing unit (Hi-Lux Ultra, Benlioglu, Ankara, Turkey) with a minimum light output of 550 mW/cm^2. Using a radiometer (Curing Radiometer Model 100, Demetron Corp, Orange, CA, USA), the light output of the curing unit was monitored periodically. After polymerization, the occlusion/articulation was checked with articulating papers, and restorations were finished under water cooling with fine diamond burs (Diatech) and polished with rubber polishing kits. Finishing strips (GC, Tokyo, Japan) were used for finishing and polishing of the proximal surfaces. Interproximal contacts were checked with dental floss. All of the restorative procedures were performed by the same operator (EK) with 10 years of clinical experience.

Clinical Evaluation Procedure

This study was double-blinded, as neither the patients nor the evaluators were aware of which resin composite had been used. Two calibrated examiners (GO and RY) independently evaluated the restorations with the aid of a dental explorer and an intraoral mirror. At the beginning of the study, these examiners were calibrated by rating 20 high-resolution clinical photographs of posterior composite restorations that were representative of each score for each criterion. In the case of disagreement during evaluations, both re-examined the restorations and arrived at a final joint decision in order to obtain only one score for each restoration. The intra- and interexaminer Cohen kappa statistic was high ($>$0.90). The same evaluators evaluated the restorations during the 24-month period.

All restorations were evaluated after one week (baseline), and six, 12, and 24 months using modified US Public Health Service (USPHS) criteria for the following characteristics: retention, anatomical form, marginal adaptation, color matching, marginal discoloration, surface texture, and secondary caries (Table 3).[21] Bitewing radiographs were taken at all recall times. The restorations were scored as follows: Alpha represented the ideal clinical situation, Bravo was clinically acceptable, and Charlie represented a clin-

Table 2: *Distribution of Restorations*

	Filtek Silorane		X-tra Fil		
	OM	OD	OM	OD	Total
Maxilla					
Premolar	11	17	9	19	56
Molar	9	5	10	2	26
Mandibule					
Premolar	1	9	3	10	23
Molar	4	2	2	3	11
Total	25	33	24	34	116

Table 3: *Modified US Public Health Service Evaluation Criteria*[21]

Characteristic	Evaluation Criteria
Retention	Alpha: The restoration is present.
	Charlie: The restoration is absent.
Marginal discoloration	Alpha: There is no visual evidence of marginal discoloration different from the color of the restorative material and from the color of the adjacent tooth structure.
	Bravo: There is visual evidence of marginal discoloration at the junction of the tooth structure and the restoration that has not penetrated along the restoration in a pulpal direction.
	Charlie: There is visual evidence of marginal discoloration at the junction of the tooth structure and the restoration, but the discoloration has penetrated along the restoration in a pulpal direction.
Marginal adaptation	Alpha: Restoration is closely adapted to the tooth. The explorer does not catch when drawn across the surface of the restoration toward the tooth structure, or, if the explorer does catch, there is no visible crevice along the periphery of the restoration.
	Bravo: The explorer catches and there is visible evidence of a crevice, which the explorer penetrates, indicating that the edge of the restoration does not adapt closely to the tooth structure. The dentin and/or the base are not exposed and the restoration is not mobile.
	Charlie: The explorer penetrates a crevice defect that extends to the dentino-enamel junction.
Color match	Alpha: Restoration matches the shade and translucency of adjacent tooth structure.
	Bravo: Restoration does not match the shade and translucency of adjacent tooth structure, but the mismatch is within the normal range of tooth shades.
	Charlie: Restoration does not match the shade and translucency of adjacent tooth structure, and the mismatch is outside the normal range of tooth shades and translucency.
Surface texture	Alpha: Surface texture is similar to polished enamel as determined by means of a sharp explorer.
	Bravo: Surface texture is gritty or similar to a surface subject to a white stone or rougher than the adjacent tooth structure.
	Charlie: Surface pitting is sufficiently coarse to inhibit the continuous movement of an explorer across the surface.
Anatomic form	Alpha: Restoration is continuous with existing anatomic form.
	Bravo: Restoration is discontinuous with existing anatomic form, but missing material is not sufficient to expose dentin or base.
	Charlie: Sufficient material is lost to expose dentin or base.
Secondary caries	Alpha: No caries are present.
	Charlie: Caries are present.

ically unacceptable situation. In the case of disagreements, the restorations were re-evaluated, and a consensus was reached.

Postoperative sensitivity was assessed by air and/or tactile contact and was recorded as absent, mild, or severe. Sensitivity to air was assessed by blowing a stream of compressed air for five seconds while shielding the neighboring teeth with the fingers. Sensitivity to tactile contact was assessed by moving a probe over the restored tooth surface. Subjects were also questioned regarding sensitivity to cold/hot or other stimuli.

Statistical Evaluation

The comparison of the two restorative materials for each category was performed with the Pearson chi-square test at a significance level of 0.05. Within group differences of the materials at different recall times were compared using the Cochran Q and Friedman tests. Bonferroni-adjusted McNemar test was used when significant difference was found ($p<0.05$). All data were analyzed by means of SPSS version 20.0 for Windows (SPSS Inc, Chicago, IL, USA).

RESULTS

All patients were evaluated at the six-month recall (recall rate=100%). At the 12-month recall, three patients did not attend (recall rate=91.8%). After 24 months, 30 patients (92 of 116 restorations) were evaluated (recall rate=81.0%). Seven patients were lost to follow-up due to moving to another town.

Table 4 presents the data of clinical evaluation of the materials used in this study over 24 months.

Retention

A 100% retention rate was recorded for Silorane and X-tra Fil restorations at the six- and 12-month recalls. At the end of 24 months, one restoration

Table 4: *Clinical Evaluation of the Materials Used in This Study Over 24 Months*

	Filtek Silorane				X-tra Fil				Between-Group *p*
	n	A (%)	B (%)	C (%)	n	A (%)	B (%)	C (%)	
Retention									
Baseline	58	58 (100)	—	0 (0.0)	58	58 (100)	—	0 (0.0)	—
Six-month	58	58 (100)	—	0 (0.0)	58	58 (100)	—	0 (0.0)	—
12-month	51	51 (100)	—	0 (0.0)	52	52 (100)	—	0 (0.0)	—
24-month	46	45 (97.8)	—	1 (2.1)	46	45 (97.8)	—	1 (2.1)	1.000
Within-group *p*			0.392				0.392		
Marginal discoloration									
Baseline	58	58 (100)	0 (0.0)	0 (0.0)	58	58 (100)	0 (0.0)	0 (0.0)	—
Six -month	58	56 (96.5)	1 (1.7)	1 (1.7)	58	58 (100)	0 (0.0)	0 (0.0)	0.246
12-month	51	50 (98)	1 (1.9)	0 (0.0)	52	52 (100)	0 (0.0)	0 (0.0)	0.495
24-month	46	44 (95.6)	0 (0.0)	2 (4.3)	46	46 (100)	0 (0.0)	0 (0.0)	0.133
Within-group *p*			0.029				1.000		
Marginal adaptation									
Baseline	58	58 (100)	0 (0.0)	0 (0.0)	58	58 (100)	0 (0.0)	0 (0.0)	—
Six-month	58	58 (100)	0 (0.0)	0 (0.0)	58	55 (94.8)	3 (5.1)	0 (0.0)	0.243
12-month	51	48 (94.1)	3 (5.8)	0 (0.0)	52	42 (80.7)	9 (17.3)	1 (1.9)	0.086
24-month	46	39 (84.7)	6 (13)	1 (2.1)	46	35 (76)	10 (21.7)	1 (2.1)	0.544
Within-group *p*			0.002				0.001		
Color match									
Baseline	58	57 (98.2)	1 (1.7)	0 (0.0)	58	55 (94.8)	3 (5.1)	0 (0.0)	—
Six-month	58	57 (98.2)	1 (1.7)	0 (0.0)	58	55 (94.8)	3 (5.1)	0 (0.0)	—
12-month	51	49 (96.0)	2 (3.9)	0 (0.0)	52	48 (92.3)	4 (7.6)	0 (0.0)	—
24-month	46	44 (95.6)	2 (4.3)	0 (0.0)	46	44 (95.6)	2 (4.3)	0 (0.0)	—
Within-group *p*			0.392				0.261		
Surface texture									
Baseline	58	58 (100)	0 (0.0)	0 (0.0)	58	58 (100)	0 (0.0)	0 (0.0)	—
Six-month	58	57 (98.2)	1 (1.7)	0 (0.0)	58	57 (98.2)	1 (1.7)	0 (0.0)	1.000
12-month	51	50 (98.0)	1 (1.9)	0 (0.0)	52	51 (98.0)	1 (1.9)	0 (0.0)	1.000
24-month	46	45 (97.8)	1 (2.1)	0 (0.0)	46	45 (97.8)	1 (2.1)	0 (0.0)	0.422
Within-group *p*			0.368				1.000		
Anatomic form									
Baseline	58	58 (100)	0 (0.0)	0 (0.0)	58	58 (100)	0 (0.0)	0 (0.0)	—
Six-month	58	58 (100)	0 (0.0)	0 (0.0)	58	58 (100)	0 (0.0)	0 (0.0)	—
12-month	51	51 (100)	0 (0.0)	0 (0.0)	52	52 (100)	0 (0.0)	0 (0.0)	—
24-month	46	46 (100)	0 (0.0)	0 (0.0)	46	46 (100)	0 (0.0)	0 (0.0)	—
Within-group *p*	—				—				
Secondary caries									
Baseline	58	58 (100)	—	0 (0.0)	58	58 (100)	—	0 (0.0)	—
Six-month	58	58 (100)	—	0 (0.0)	58	58 (100)	—	0 (0.0)	—
12-month	51	51 (100)	—	0 (0.0)	52	52 (100)	—	0 (0.0)	—
24-month	46	46 (100)	—	0 (0.0)	46	46 (100)	—	0 (0.0)	—
Within-group *p*	—				—				

Abbreviations: A, Alpha; B, Bravo; C, Charlie.

from the Silorane group and one from the X-tra Fil group were missing. No statistically significant differences were found between the two materials' retention rates ($p>0.05$).

Marginal Discoloration

At the six-month recall, one restoration received a Bravo score and one a Charlie score from the Silorane group in terms of marginal discoloration.

At the 12-month recall, one Silorane restoration had a Bravo score, while two Silorane restorations received Charlie scores at the 24-month recall. The marginal discoloration results were statistically significant within the Silorane group ($p=0.029$). None of the X-tra Fil restorations showed marginal discoloration during the 24-month period. There was no statistically significant difference between Silorane and X-tra Fil restorations ($p>0.05$).

Marginal Adaptation

At 12 and 24 months, three and six restorations, respectively, received Bravo scores, and one restoration received a Charlie score for marginal adaptation in the Silorane group. The numbers of Bravo scores for the X-tra Fil restorations were three, nine, and 10 at the six-, 12-, and 24-month recalls, respectively. At 12 and 24 months, one restoration received a Charlie score.

The results for intragroup comparisons were statistically significant for both groups ($p=0.002$ for Silorane and $p=0.001$ for X-tra Fil), while no statistically significant differences were found between restorative materials at the end of 24 months ($p>0.05$).

Color Match

In terms of color match, one Silorane restoration and three X-tra Fil restorations received Bravo scores at baseline and at the six-month recall. At the 12-month recall, two of the 51 Silorane restorations and four of the 52 X-tra Fil restorations were rated Bravo. At the end of the study, two restorations were rated as Bravo in each group. There was no statistically significant difference between the groups during the 24 months ($p>0.05$).

Surface Texture

At the six-, 12-, and 24-month recalls, only one restoration's surface texture from each group was gritty and rated as Bravo ($p>0.05$).

During the 24-month period, all evaluated restorations were continuous with existing anatomic form, and no secondary carries were detected. None of the patients reported postoperative sensitivity.

DISCUSSION

In the present study, silorane- and methacrylate-based restorative materials' clinical performance was compared and resulted in similar clinical outcomes after 24 months, so the null hypothesis was accepted.

Since the introduction of Filtek Silorane, several *in vitro* studies with contradictory findings have been conducted to evaluate its performance.[8,22] In a recent *in vitro* study, marginal adaptation and bonding effectiveness of a silorane- (Filtek Silorane) and a methacrylate-based packable composite (Filtek P60) were found to be similar.[8] On the other hand, another *in vitro* study reported better marginal adaptation with a silorane- than with a methacrylate-based composite.[22] In a further *in vitro* study, Sampaio and others[23] evaluated the resin/dentin interface created by a silorane- and three different methacrylate-based composites and found similar microtensile bond strength values at 24 hours and six months. In an *in vivo* study, Schmidt and others[20] evaluated the marginal adaptation of Filtek Silorane and CeramX (methacrylate-based composite) for one year and reported that the methacrylate-based one exhibited better performance.

Polymerization shrinkage and the adhesive systems used are known to be important factors that influence the marginal adaptation of composite resins.[24] Releasing stresses onto the adhesive interface as a result of polymerization shrinkage impairs the marginal integrity of restorations and shortens the clinical longevity of direct resin restorations.[25] Although *in vitro* studies confirm that a silorane-based composite has a lower volumetric shrinkage (less than 1.0%) than methacrylate-based ones[5] and causes less cuspal deflection[7,26] and microleakage,[10,11] the results of this study showed that reduced polymerization shrinkage yielded no detectable clinical performance improvement. The changes in composite viscoelastic behavior that occur during polymerization, from predominantly viscous to mostly elastic, make polymerization stress development a quite complex event. In accordance with our findings, in a five-year clinical study Schmidt and others[14] and in a three-year clinical study Mahmoud and others[16] also found similar marginal adaptation in class II restorations restored with silorane- and methacrylate-based composites. Yazici and others[17] evaluated the clinical performance of Filtek Silorane, Filtek P60 (packable resin composite), and Filtek Supreme (nanofilled resin composite) in class I restorations and found similar clinical performance over three years. However, contrary to our findings, they found statistically significant differences between Filtek Silorane and a packable resin composite, Filtek P60, in terms of marginal adaptation.

It has been reported that during the polymerization of the predominantly elastic-viscous material,

the viscoelastic properties of silorane change and the low initial flow of base resin restricts the flow of silorane, and this results in increased stresses.[6] Weinmann and others[4] also reported high initial flexural modulus shown by Silorane, which may explain its high polymerization stress value in spite of the low volumetric shrinkage (both postgel and total). Similar marginal adaptation results of silorane resin composite, despite its low polymerization shrinkage, might be explained in this way.

Another factor that may influence the marginal adaptation of composite restorations is the adhesive system. In the current study, both composite resins were used with their respective adhesive systems from the same manufacturer. Silorane System Adhesive is a two-step self-etch system with a pH of about 2.7, while Futura Bond NR has a pH of about 1.4. The acidity of the adhesives has been reported to interfere with demineralization and adhesion to tooth structures;[27] however, this was not confirmed in our study because there was no statistically significant difference in terms of marginal adaptation. In accordance with our findings, Barraco and others[15] found similar clinical performance of Filtek Silorane applied with its respective adhesive system and Filtek Z250 applied with a two-step etch-and-rinse adhesive (Adper Scotchbond 1 XT, 3M ESPE) and a two-step self-etch adhesive (Adper Scotchbond SE) at the end of two years.

The cavity configuration is also a factor affecting the transmission of polymerization shrinkage stress[28], but in our study the C factor had no influence since all of the cavities evaluated were class II slot cavities with a similar C factor.

In the present study, the incidence and extent of marginal discoloration of Silorane restorations increased over 24 months, while none of the X-tra Fil restorations showed marginal discoloration. However, there were no differences between the different recall times in terms of marginal discoloration in Silorane and X-tra Fil restorations. It is known that marginal discoloration is one of the first signs of a composite resin's clinical failure and is related to microleakage. Several *in vitro* studies[11-13] have proven that silorane-based composites improve marginal adaptation due to their reduced shrinkage, thereby decreasing the residual stress at the adhesive-tooth interface, and show less microleakage than methacrylate-based ones. Contradicting the idea that less shrinkage contributes to lower polymerization stress, no advantages of silorane-based composite over methacrylate-based composite have been observed in clinical studies.[14,17,18] Shrinkage values of 1% and 1.7% have been reported for Filtek Silorane[4] and X-tra Fil, respectively (http://www.voco.com/us/product/x_tra_fil/index.html). Although this difference is distinct in the laboratory, it was difficult to show the effect in the clinic, where so many factors, such as chemical and physical properties, influence the final restoration. Thus, it might be concluded that the low shrinkage of materials may not be a determinant factor for clinical success.

In the current study, none of the restorations had Charlie scores in terms of color match, which was similar to the results of other studies.[16,17]

Secondary caries have been attributed to poor oral hygiene and plaque accumulation.[29] No secondary caries were detected over the 24-month period of this study. This finding may be a result of our selection of patients with good oral hygiene. On the other hand, this short period of time may not be sufficient for observing the formation of secondary caries. The smooth surface texture of the restorations may be another reason. Only one restoration from each group was scored as Bravo during the clinical trial. Charlie scores were not recorded, denoting that all the restorations were acceptable in terms of surface texture. Comparable results were reported in other clinical studies with clinically acceptable surface textures of silorane restorations.[16,19]

This study has several limitations. First, it was impossible to blind the operating dentist (EK) because she had to follow the different treatment protocols for the two materials during placement. Second, the 24-month recall rate of 81% might be modest. The reason was that the patients had moved and did not want to spend their time and money just for re-examination. However, in future studies, patients might be instructed to return for a refund. Third, long-term clinical evaluations are required to fully assess the performance of this material and warranted to confirm our results, as this was a short-term follow-up of a 24-month study with a small number of evaluable restorations.

CONCLUSIONS

Within the limitations of this clinical study, it can be concluded that the clinical performance of a silorane-based composite was acceptable at the end of the 24-month evaluation period, with no obvious advantage compared to methacrylate-based packable composite. Both silorane- and methacrylate-based resin composite restorations showed no significant clinical difference in class II slot preparations after 24 months of evaluation.

Regulatory Statement

This study was conducted in accordance with all the provisions of the local human subjects oversight committee guidelines and policies of Hacettepe University. The approval code for this study is HEK 10/35.

Conflict of Interest

The authors of this article certify that they have no proprietary, financial, or other personal interest of any nature or kind in any product, service, and/or company that is presented in this article.

(Accepted 7 January 2017)

REFERENCES

1. Calheiros FC, Sadek FT, Braga RR, & Cardoso PE (2004) Polymerization contraction stress of low-shrinkage composites and its correlation with microleakage in class V restorations. *Journal of Dentistry* **32(5)** 407-412.
2. Gonzalez-Lopez S, Vilchez Diaz MA, de Haro-Gasquet F, Ceballos L, & de Haro-Munoz C (2007) Cuspal flexure of teeth with composite restorations subjected to occlusal loading. *Journal of Adhesive Dentistry* **9(1)** 11-15.
3. Leevailoj C, Cochran MA, Matis BA, Moore BK, & Platt JA (2001) Microleakage of posterior packable resin composites with and without flowable liners. *Operative Dentistry* **26(3)** 302-307.
4. Weinmann W, Thalacker C, & Guggenberger R (2005) Siloranes in dental composites. *Dental Materials* **21(1)** 68-74.
5. Karaman E, & Ozgunaltay G (2014) Polymerization shrinkage of different types of composite resins and microleakage with and without liner in class II cavities. *Operative Dentistry* **39(3)** 325-331.
6. Boaro LC, Goncalves F, Guimaraes TC (2010) Polymerization stress, shrinkage and elastic modulus of current low-shrinkage restorative composites. *Dental Materials* **26(12)** 1144-1150.
7. Karaman E, & Ozgunaltay G (2013) Cuspal deflection in premolar teeth restored using current composite resins with and without resin-modified glass ionomer liner. *Operative Dentistry* **38(3)** 282-289.
8. Santos PJ, Silva MS, Alonso RC, & D'Alpino PH (2013) Hydrolytic degradation of silorane- and methacrylate-based composite restorations: Evaluation of push-out strength and marginal adaptation. *Acta Odontologica Scandinavica* **71(5)** 1273-1279.
9. Gregor L, Bortolotto T, Feilzer AJ, & Krejci I (2013) Shrinkage kinetics of a methacrylate- and a silorane-based resin composite: Effect on marginal integrity. *Journal of Adhesive Dentistry* **15(3)** 245-250.
10. Parolia A, Adhauliya N, de Moraes Porto IC, & Mala K (2014) A comparative evaluation of microleakage around class V cavities restored with different tooth colored restorative materials. *Oral Health and Dental Management* **13(1)** 120-126.
11. Santos MJ, Podorieszach A, Rizkalla AS, & Santos GC Jr (2013) Microleakage and microtensile bond strength of silorane-based and dimethacrylate-based restorative systems. *Compendium of Continuing Education in Dentistry* **34(Special Issue 8)** 19-24.
12. Joseph A, Santhosh L, Hegde J, Panchajanya S, & George R (2013) Microleakage evaluation of silorane-based composite and methacrylate-based composite in class II box preparations using two different layering techniques: an in vitro study. *Indian Journal of Dental Research* **24(1)** 148.
13. Bogra P, Gupta S, & Kumar S (2012) Comparative evaluation of microleakage in class II cavities restored with Ceram X and Filtek P-90: An in vitro study. *Contemporary Clinical Dentistry* **3(1)** 9-14.
14. Schmidt M, Dige I, Kirkevang LL, Vaeth M, & Horsted-Bindslev P (2015) Five-year evaluation of a low-shrinkage silorane resin composite material: A randomized clinical trial. *Clinical Oral Investigations* **19(2)** 245-251.
15. Baracco B, Perdigao J, Cabrera E, & Ceballos L (2013) Two-year clinical performance of a low-shrinkage composite in posterior restorations. *Operative Dentistry* **38(6)** 591-600.
16. Mahmoud SH, Ali AK, & Hegazi HA (2014) A three-year prospective randomized study of silorane- and methacrylate-based composite restorative systems in class II restorations. *Journal of Adhesive Dentistry* **16(3)** 285-292.
17. Yazici AR, Ustunkol I, Ozgunaltay G, & Dayangac B (2014) Three-year clinical evaluation of different restorative resins in class I restorations. *Operative Dentistry* **39(3)** 248-255.
18. Walter R, Boushell LW, Heymann HO (2014) Three-year clinical evaluation of a silorane composite resin. *Journal of Esthetic and Restorative Dentistry* **26(3)** 179-190.
19. Yaman BC, Dogruer I, Gumustas B, & Efes BG (2014) Three-year randomized clinical evaluation of a low-shrinkage silorane-based resin composite in non-carious cervical lesions. *Clinical Oral Investigations* **18(4)** 1071-1079.
20. Schmidt M, Kirkevang LL, Horsted-Bindslev P, & Poulsen S (2011) Marginal adaptation of a low-shrinkage silorane-based composite: 1-year randomized clinical trial. *Clinical Oral Investigations* **15(2)** 291-295.
21. Cvar JF, & Ryge G (1971) Criteria for the clinical evaluation of dental restorative materials US Public Health Service Publication No 790-244 *San Francisco: Government Printing Office*.
22. Papadogiannis D, Kakaboura A, Palaghias G, & Eliades G (2009) Setting characteristics and cavity adaptation of low-shrinking resin composites. *Dental Materials* **25(12)** 1509-1516.
23. Sampaio RK, Wang L, Carvalho RV (2013) Six-month evaluation of a resin/dentin interface created by methacrylate and silorane-based materials. *Journal of Applied Oral Science* **21(1**) 80-84.
24. Van Meerbeek B, Braem M, Lambrechts P, & Vanherle G (1993) Evaluation of two dentin adhesives in cervical lesions. *Journal of Prosthetic Dentistry* **70(4)** 308-314.
25. Versluis A, Tantbirojn D, Pintado MR, DeLong R, & Douglas WH (2004) Residual shrinkage stress distribu-

tions in molars after composite restoration. *Dental Materials* **20(6)** 554-564.

26. Bicalho AA, Valdivia AD, Barreto BC (2014) Incremental filling technique and composite material—Part II: Shrinkage and shrinkage stresses. *Operative Dentistry* **39(2)** E83-E92.
27. Kenshima S, Francci C, Reis A, Loguercio AD, & Filho LE (2006) Conditioning effect on dentin, resin tags and hybrid layer of different acidity self-etch adhesives applied to thick and thin smear layer. *Journal of Dentistry* **34(10)** 775-783.
28. Feilzer AJ, De Gee AJ, & Davidson CL (1987) Setting stress in composite resin in relation to configuration of the restoration. *Journal of Dental Research* **66(11)** 1636-1639.
29. Kohler B, Rasmusson CG, & Odman P (2000) A five-year clinical evaluation of class II composite resin restorations. *Journal of Dentistry* **28(2)** 111-116.

©Operative Dentistry, 2017, **42-4,** E111-E120

Clinical Performance of Different Solvent-based Dentin Adhesives With Nanofill or Nanohybrid Composites in Class III Restorations: Five Year Results

M Demirci • S Tuncer • HS Sancaklı • N Tekçe • C Baydemir

Clinical Relevance

The clinical performance of different solvent-based dentin adhesives with nanofill or nanohybrid composites in Class III restorations was satisfactory. Marginal discoloration and marginal integrity deterioration were reasons for the failure of the self-etch adhesive systems in Class III cavities.

SUMMARY

Purpose: To evaluate the clinical performance of water, acetone, ethanol, and ethanol-water solvent-based dentin adhesives with nanofill or nanohybrid composites in Class III restorations.

Methods and Materials: A total of 22 patients aged between 14 and 48 years (mean age: 25.2 years) participated in the study. Each patient received four Class III restorations, which were performed using water (Scotchbond Multipurpose), acetone (Prime&Bond NT), ethanol (XP Bond) and ethanol-water (Xeno V) solvent-based dentin adhesive systems with a nanofill (Filtek Supreme XT) or nanohybrid composite (CeramX Duo). Two experienced examiners evaluated the restorations with regard to retention, color match, marginal discoloration, wear/loss of anatomic form, caries formation, marginal adaptation, and surface texture at baseline and at one-, two-, three-, four-, and five-year recalls.

Results: The five-year survival rates were 100% for Scotchbond Multipurpose, Prime&Bond

Mustafa Demirci, DDS, PhD, professor, Faculty of Dentistry, Department of Restorative Dentistry, Istanbul University, Istanbul, Turkey

*Safa Tuncer, DDS, PhD, associate professor, Faculty of Dentistry, Department of Restorative Dentistry, Istanbul University, Istanbul, Turkey

Hande Şar Sancaklı, DDS, PhD, associate professor, Faculty of Dentistry, Department of Restorative Dentistry, Istanbul University, Istanbul, Turkey

Neslihan Tekçe, DDS, PhD, assistant professor, Kocaeli University, Faculty of Dentistry, Department of Restorative Dentistry, Kocaeli, Turkey

Canan Baydemir, PhD, associate professor, Kocaeli University Faculty of Medicine, Department of Biostatistics and Medical Informatics, Kocaeli, Turkey

*Corresponding author: Çapa, 34390 Istanbul, Turkey; e-mail: tuncers@istanbul.edu.tr

DOI: 10.2341/16-326-C

NT, and XP Bond and 81.2% for Xeno V–bonded restorations. Only three Xeno V–bonded restorations failed. With the exception of marginal discoloration, there were no statistically significant differences among the four adhesive-bonded restorations in any of the evaluation periods in terms of the evaluation criteria.

Conclusions: With the exception of marginal discoloration and marginal integrity deterioration of Xeno V–bonded restorations, all four adhesive-bonded restorations exhibited good long-term results. However, adhesion strategy (such as self-etch or etch-and-rinse) is more important than the solvent content of dentin adhesive systems in the success of Class III restorations.

INTRODUCTION

Bonding to enamel and dentin occurs through the replacement of minerals removed from the hard dental tissue by resin monomers, which become micromechanically interlocked in the newly created porosites.[1] Adhesives are classified according to their underlying adhesion mechanism into "etch & rinse," "self-etch," and "resin-modified glass ionomer adhesives, in addition to the number of application steps."[2]

Solvents are key elements of adhesive systems. The low viscosity of primers and primer-adhesive resins is in part caused by the dissolution of monomers in a solvent, which improves the diffusion ability in the porous substrate. Therefore, solvents are important to ensure the diffusion of monomers into demineralized dentin.[3] However, polymerization may be jeopardized, voids created, and the permeability of the adhesive may be increased as a result of the dilution of monomers; therefore, any remaining solvent must be removed from the adhesive after diffusion.[4,5] Water, ethanol, and acetone are the most frequently used solvents in adhesives.[6] Water is an indispensable compound of self-etch adhesives for ionizing acidic monomers.[6] In etch-and-rinse adhesives, water has the ability to re-expand the collapsed and shrunken collagen network.[7,8] Water is not an ideal solvent for organic compounds because they are typically quite hydrophobic; however, the addition of secondary solvents such as ethanol or acetone helps to negate this problem. Water's higher boiling point and low vapor pressure make its removal from adhesive solutions difficult after use,[6] and ethanol's higher vapor pressure enables superior evaporation in air-drying. Ethanol is usually used alongside water as a co-solvent. Thus, the occurrence of hydrogen bonds between water and ethanol molecules provides greater evaporation of water-ethanol aggregates than is obtained with pure water alone.[6] Acetone also combines hydrophobic and hydrophilic components. Its main advantage is its high vapor pressure; however, acetone-containing adhesives may have shorter shelf lives because the high volatility of acetone may cause rapid evaporation.[6] Acetone is often used alone as a solvent, but it is used as a co-solvent with water in self-etch adhesives.[6]

A new category of composites resins, known as nanocomposites, has been developed.[9] There are several nanocomposite products on the market, including Filtek Supreme (3M ESPE, St Paul, MN, USA), which contains nanometric particles (nanomers) and nanoclusters, and CeramX (Dentsply-DeTrey, Konstanz, Germany), which contains glass fillers.[10] Nanocomposites enable increased filler loading and reduce the resin requirement, thereby reducing shrinkage during polymerization while simultaneously maintaining esthetics and strength.[10] Knowledge of the composition, characteristics, and mechanisms of each adhesive system used in etch-and-rinse or self-etch systems is crucially important in the creation of ideal bonding strategies in the clinical setting.[3] Nanocomposites with solvent-containing adhesive systems have been extensively used in Class III cavities. However, few clinical studies have been conducted to investigate their clinical performance in such cavities.[9] The aim of this study was to evaluate the clinical performance of water, acetone, ethanol, and ethanol-water solvent-based dentin adhesives with nanofill or nanohybrid composites in Class III restorations.

METHODS AND MATERIALS

Study Design

Approval for the study was granted by the local ethics committee of Istanbul University Medical Faculty (#32859). The brands, chemical compositions, and manufacturers of the materials used are shown in Table 1. The restorations were performed between July 2008 and January 2010 in the Department of Restorative Dentistry, Faculty of Dentistry, Istanbul University. A total of 22 patients (nine males, 13 females) aged between 14 and 48 years (mean age: 25.2 years) participated in the study. The inclusion criteria included the following: patients with four primary caries in the approximal area on the maxillary anterior teeth; patients who displayed good oral hygiene and had no active periodontal or pulpal diseases and were willing to

Table 1: *Materials, Compositions, and Application Steps*

Adhesive	Compositions	Application Steps	Manufacturer
Scotchbond Multipurpose	Etchant: 35% H_3PO_4, water, and silica Primer: 2-hydroxyethylmethacrylate, polyalkenoic acid, copolymer, water Adhesive: 2-hydroxyethylmethacrylate, Bis-GMA, photoinitiator	Apply the conditioner for 15 s. Rinse the surface for 15 s and dry the surface slightly, leaving a visible moist surface. Apply the primer and dry gently for 5 s. Apply the bond and light-cure for 20 s.	3M/ESPE, St Paul, MN, USA
Prime&Bond NT	Etchant: 36% phosphoric acid (DeTrey conditioner 36 gel) PENTA, UDMA resin, resin R5-62-1, T-resin, D-resin, nanofiller, initiators, stabilizer, cetylamine hydrofluoride, acetone	Gently extrude conditioner to cavity surface, at least 15 s for enamel, 15 s or less for dentin. Rinse the surface for at least 15 s. Remove water from cavity with a soft air blow. Avoid desiccating the dentin; leave a moist surface. Apply the adhesive and leave undisturbed for 20 s. Air blow gently for at least 5 s. Light cure for at least 10 s.	Dentsply DeTrey, Konstanz, Germany
XP Bond	Etchant: 36% phosphoric acid PENTA, TCB, UDMA, TEGDMA, HEMA, camphorquinone, DMABE, butylated benzenediol, tert-butanol	Apply conditioner to the dentin surface for 15 s. Rinse thoroughly for 15 s and air-dry. Apply the adhesive and leave undisturbed for 20 s. Air blow for a minimum of 5 s. Light-cure for 20 s.	Dentsply DeTrey, Konstanz, Germany
Xeno V	Bifunctional acryl resin with amide function, acryloylamino alkylsulfonic acid, "inverse" functionalized phosphoric acid ester, acrylic acid, camphorquinone, coinitiator, butylated benzenediol, water, tertiary butanol	Apply Xeno V sufficiently, wetting all cavity surfaces uniformly. Then gently agitate the adhesive for 20 s. Air blow with air until there is no more movement of the adhesive, but for at least 5 s. Light-cure for a minimum of 20 s.	Dentsply DeTrey, Konstanz, Germany
Filtek Supreme XT	Bis-GMA, UDMA, TEGDMA, Bis-EMA, silica, filler, zirconia, filler, aggregated zirconia/silica, cluster, filler	Tooth color to be restored selected from a Vitapan classical shade guide before isolating the tooth. The corresponding body shade was selected. In 2-mm layers or less increments of body shade applied. Each increment light-cured 20 s.	3M/ESPE, St Paul, MN, USA
CeramX Duo	Methacrylate modified polysiloxane, dimethacrylate resin, fluorescence pigment UV stabilizer, camphorquinone, ethyl-4(dimethylamino)benzoate, barium-aluminum-borosilicate glass, methacrylate functionalized silicon dioxide nanofiller, iron oxide pigments and titanium oxide pigments and aluminum sulfo silicate pigments	Tooth color to be restored selected from a Vitapan classical shade guide before isolating the tooth. The corresponding combination of CeramX Duo enamel and dentin shade was selected. In 2-mm layers or less dentin shade applied and light-cured for 40 s. Then enamel layer in 2-mm layers or less applied and light-cured 10 s.	Dentsply DeTrey, Konstanz, Germany

Abbreviations: BIS-EMA, ethoxylated bisphenol A glycol dimethacrylate; Bis-GMA, bisphenol A diglycidyl methacrylate; DMABE, ethyl-4-(dimethylamino)benzoate; H_3PO_4, phosphoric acid; HEMA, 2-hydroxyethyl methacrylate; PENTA, dipentaerythritol pentaacrylate monophophate; UDMA, urethane dimethacrylate; TCB, butan-1,2,3,4-tetracarboyxlic di-2-hydroxyethylmethacrylate ester; TEGDMA, triethylene glycol dimethacrylate.

Table 2: *Distribution of Class III Composite Restorations According to Adhesives/Composite Combination and Tooth Number*

Dentin Adhesive/Composite	n	Tooth No.					
		11	12	13	21	22	23
Scotchbond Multipurpose/Filtek Supreme XT	22	8	4	1	6	2	1
XP Bond/CeramX Duo	22	9	1	0	8	4	0
Prime&Bond NT/CeramX Duo	22	8	4	0	6	4	0
Xeno V/CeramX Duo	22	2	7	1	5	6	1
Sum of restorations	88	27	16	2	25	16	2

return for follow-up examinations as outlined by the investigators. Exclusion criteria included the following: patients with uncontrolled parafunction; those presenting with insufficient oral hygiene; those presenting with spontaneous pain or pain to percussion; patients who were pregnant or nursing; and patients who had periodontal or gingival disease.[11-13] Each patient received four restorations for primary caries of the anterior teeth prior to evaluation; there were 88 restorations in total. The distribution of Class III restorations according to adhesives/composite combination and tooth number is presented in Table 2. All teeth had contact from opposing and adjacent teeth.

Treatment Protocol

Each patient received four Class III restorations: a water (Scotchbond Multipurpose), acetone (Prime& Bond NT), ethanol (XP Bond), and ethanol-water (Xeno V) solvent-based dentin adhesive system with nanofill composite (Filtek Supreme XT) or nanohybrid composite (CeramX Duo). Randomization was performed by first selecting the water solvent–based dentin adhesive and tooth number by flipping a coin, followed by the selection of acetone, ethanol, ethanol-water, and tooth number, also accomplished by the flip of a coin.

Restoration Procedure

All teeth were cleaned using pumice-water slurry and a rubber cup to remove the pellicle and residual dental plaque. Cavity preparation was limited to the removal of caries. The incisal margins of the cavities were cervical to the incisal edge of the teeth, and the cervical margins were at/or incisal to the cementoenamel junction and extended.[14] In addition, the cavity margins could extend onto the facial or/and lingual surface depending on the amount of tooth structure missing. If possible, the outline form did not include the entire proximal contact area, extend onto the facial surface, or become extended subgingivally.[15] For etch-and-rinse adhesive systems (Scotchbond Multipurpose, Prime&Bond NT, and XP Bond), all enamel margins were beveled 0.5-1.0 mm at approximately 45° to the external cavosurface using a high-speed, water-cooled, rotary hand-piece, with a medium-grit diamond bur. For the self-etch adhesive system (Xeno V), enamel margins were not beveled and the acid-etching procedure was not performed. After the cavities were prepared, the manufacturer's instructions were closely adhered to regarding cavity treatment and placement of the restorative materials (Table 1). Isolation was achieved with cotton rolls and saliva ejectors.[14] Cavity treatment and application and polymerization of dentin adhesives were performed by the same practitioner (HS), who was experienced with the materials in the present study. Polymerization was performed using a halogen curing unit (VIP; Bisco Inc, Schaumburg, IL, USA). The composite shade was chosen using the relative composite guide or composite samples. All cavities were restored using a Mylar strip and wooden wedge to rebuild the anatomic form and proximal contacts of the teeth. With restorations having depths of more than 2 mm, composite was applied incrementally. The first composite layer was light-cured after being applied to the pulpal walls; this was followed by a second layer, which was cured in the same manner as the first. The composite was placed in a single increment in shallow cavities.[14] Light curing, contouring, and finishing were performed as described in our previous publication.[13]

Evaluation

Two experienced examiners evaluated the restorations using a dental explorer and mirror, in accordance with the modified Ryge criteria (Table 3).[16,17] Examiners were not involved with the operation and insertion of restorations and were fully blinded to the experimental protocol. For consistency, both examiners were provided photographs as reference instruments to illustrate scoring for each criterion. The examiners then clinically evaluated 20 Class III restorations with two days' separation between the

Table 3: *Direct Clinical Evaluation Criteria (Modified Ryge Criteria)*

Rating	Aspect	Method
Color match		
Alpha (A)	There is no a mismatch in color, shade, and/or translucency between the restoration and the adjacent tooth structure.	Visual inspection
Bravo (B)	There is a mismatch in color, shade, and/or translucency between the restoration and the adjacent tooth structure, but the mismatch is within the normal range of tooth color, shade, and/or translucency.	Visual inspection
Charlie (C)	The mismatch is between restoration and adjacent tooth structure outside the normal range of tooth color, shade, and/or translucency.	Visual inspection
Cavosurface marginal discoloration		
Alpha (A)	There is no discoloration anywhere on the margin between the restoration and the tooth structure.	Visual inspection
Bravo (B)	There is discoloration anywhere on the margin between the restoration and the tooth structure, but the discoloration has not penetrated along the margin of the restorative material in an enamel direction and can be polished away.	Visual inspection
Charlie (C)	The discoloration has penetrated along the margin of the restorative material in an enamel direction.	Visual inspection
Wear/anatomic form		
Alpha (A)	The restoration is not undercontoured: that is, the restorative material is not discontinuous with existing anatomic form.	Visual inspection and explorer
Bravo (B)	The restoration is undercontoured: that is, the restorative material is discontinuous with existing anatomic form, but sufficient restorative material is not missing so as to expose the enamel or base.	Visual inspection and explorer
Charlie (C)	Sufficient restorative material is missing so as to expose the enamel or base.	Visual inspection
Caries		
Alpha (A)	There is no evidence of caries contiguous with the margin of the restoration.	Visual inspection
Bravo (B)	There is evidence of caries contiguous with the margin of the restoration.	Visual inspection
Marginal adaptation		
Alpha (A)	There is no visible evidence of a crevice along the margin into which the explorer will penetrate.	Visual inspection and explorer
Bravo (B)	There is visible evidence of a crevice along the margin into which the explorer will penetrate. The enamel or base is not exposed.	Visual inspection and explorer
Charlie (C)	There is visible evidence of a crevice along the margin into which the explorer will penetrate. The enamel or base is exposed.	Visual inspection and explorer
Delta (D)	The restoration is fractured or missing in part or *in toto*.	Visual inspection and explorer
Surface texture		
Alpha (A)	Surface of restoration is smooth.	Explorer
Bravo (B)	Surface of restoration is slightly rough or pitted, can be refinished.	Explorer
Charlie (C)	Surface deeply pitted, irregular grooves (not related to anatomy), cannot be refinished.	Explorer
Delta (D)	Surface is fractured or flaking.	Explorer

examinations. These restorations were not included in the present study. The evaluation phase of study was initiated when at least 85% intra- and interexaminer agreement was achieved in the calibration phase.[18] Color match, wear or loss of anatomic form, marginal discoloration, caries, marginal adaptation, and surface texture were evaluated at baseline and at one-, two-, three-, four-, and five-year recalls. Restorations were scored as Alpha (A) = ideal clinical condition; Bravo (B) = acceptable; Charlie (C) = unacceptable, replacement required; and Delta (D) = fractured, mobile, or missing restoration, immediate replacement required. Scoring conflicts were resolved by consensus.[16,18]

Statistical Analysis

All analyses were performed using SPSS for Windows version 20.0 (SPSS, Chicago, IL, USA). Data obtained were statistically analyzed using the Friedman test to evaluate changes over the five-year study period. Comparisons of data among the four

dentin adhesives were performed using the Mann-Whitney *U*-test and Kruskal-Wallis one-way analysis of variance and the Dunn post hoc test. When a statistically significant difference was identified for any criterion, the Dunn post hoc test was used for multiple comparisons between each recall time interval for each composite. Kaplan-Meier survival analysis was used to determine the probability of clinical survival of the composites. Statistical significance was considered at $p < 0.05$. Cohen kappa was used to examine inter- and intraexaminer agreement.

RESULTS

During the five-year evaluation, six patients with 24 restorations (six Scotchbond Multipurpose–bonded restorations, six Prime&Bond NT–bonded restorations, six XP Bond–bonded restorations, and six Xeno V–bonded restorations) left the study (Figure 1). The cumulative recall rate was 72.7% at the end of five years.

Cohen kappa (0.89) exhibited strong agreement between the examiners ($p>0.05$). The results of the Kaplan-Meier survival analysis displayed as follows: At one-year recall, one Xeno V–bonded restoration was lost (95.5% success rate). A 100% success rate was observed at the two- and three-year recalls for Scotchbond Multipurpose, XP Bond, and Prime&Bond NT, and a 95.2% success rate was observed for Xeno V–bonded restorations. At the end of four years, two Xeno V–bonded restorations failed as a result of marginal discoloration with Charlie rating (82.4% success rate). There were no restoration failures at the end of the fifth year with Scotchbond Multipurpose, Prime&Bond NT, or XP Bond (100% success rate), and Xeno V–bonded restorations were 81.2% successful.

With the exception of three failed Xeno V–bonded restorations, no restorations were clinically unacceptable with regard to retention, color, wear or loss of form, caries formation, marginal adaptation, or surface texture after the fifth-year evaluation. Other than marginal discoloration, there were no statistically significant differences among the four restorations in any of the evaluation periods with regard to the evaluation criteria. There was, however, a statistically significant difference between four years or five years and baseline marginal discoloration rates for Xeno V.

After the fifth year, 93.8% of Scotchbond Multipurpose–bonded restorations, 87.5% of the Prime&Bond NT– and XP Bond–bonded restorations, and 84.6% of Xeno V–bonded restorations showed clinically ideal (Alpha) color-match rates. At the end of five years, 6.3% of XP Bond–bonded restorations and 30.8% of Xeno V–bonded restorations exhibited marginal discoloration (Bravo). However, this discoloration was superficial, anywhere along the margin, did not penetrate toward the pulp along the margin of the restorative material, and could be polished away. On the other hand, 12.5% of the Xeno V–bonded restorations showed marginal discoloration at Charlie rating and had to be replaced after four years. With regard to wear and anatomic form, 100% of Scotchbond Multipurpose–, XP Bond–, Prime&Bond NT–bonded restorations and 92.3% of Xeno V–bonded restorations achieved an Alpha rating after five years. With respect to marginal adaptation rates, 100% of XP Bond– and Prime&Bond NT–bonded restorations and 93.8% of Scotchbond Multipurpose–bonded restorations were clinically ideal at the end of five years. One Xeno V–bonded restoration (4.5%) was lost after one year; this restoration therefore received a Delta score for marginal adaptation. After five years, 100% of Scotchbond Multipurpose–, XP Bond–, Prime&Bond NT–, and Xeno V–bonded restorations were rated an Alpha with regard to caries and surface texture.

DISCUSSION

The prevalence rate of Class III restorations has fallen along with the reduction of proximal caries.[19] However, a large demand for Class III restorations has been observed, and resin composites accompanied by different dentin adhesive system types have been extensively used in Class III cavities. There are limited data regarding the effect of adhesive systems on long-term clinical performance of Class III restorations.[20] Therefore, we evaluated the five-year clinical performance of water (Scotchbond Multipurpose), ethanol (XP Bond), acetone (Prime&Bond NT), and ethanol-water solvent-based (Xeno V) dentin adhesives with nanofill (Filtek Supreme XT) or nanohybrid composites (CeramX Duo) in Class III restorations.

According to our findings, the five-year survival rates were 100% for Scotchbond Multipurpose–, XP Bond–, and Prime&Bond NT–bonded restorations and 81.2% for Xeno V–bonded restorations. Scotchbond Multipurpose, XP Bond, and Prime&Bond NT showed the same excellent success rates. In agreement with our findings, identical (100%)[21] or slightly lower (96%)[22] success rates have been reported in Class III/IV or Class III restorations, respectively, after five years. Also, in a 20-year clinical study,[23]

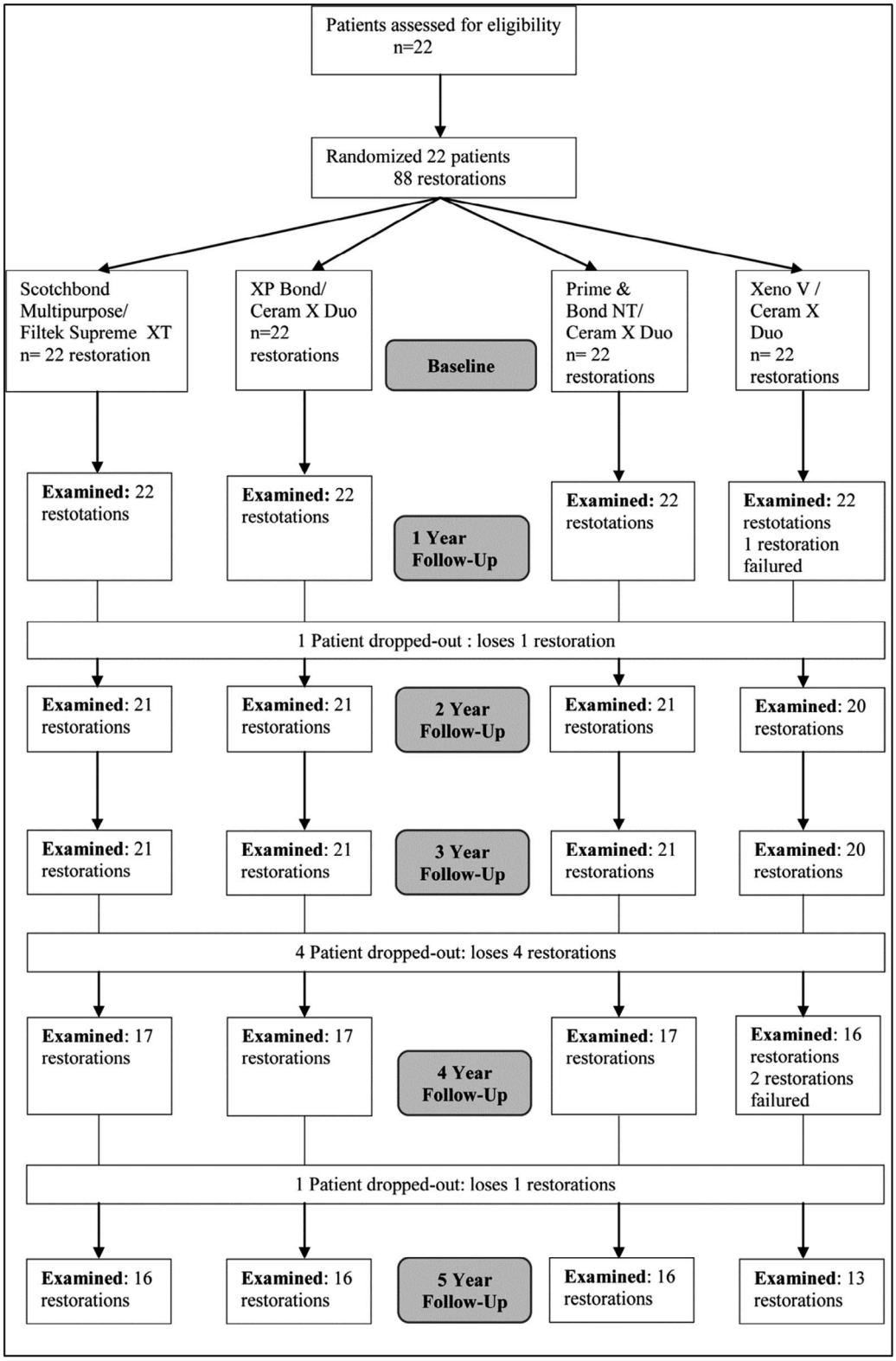

Figure 1. *Flow diagram history of restorations.*

survival rate was 100% for five-year periods in anterior restorations, which included Class III and IV restorations. In a meta-analysis,[19] 10-year survival rates for Class III and Class IV restorations were 95% and 90%, respectively, which corresponded with the annual failure rates of around 0.5% and 1%. A systematic review[24] involving long-term survival of anterior restorations, including Class III and Class IV restorations, showed annual failure rates varying between 0% and 4.1%. In another study,[25] in accordance with the findings of the present study, the success rate after three years was found to be 100% in Class III cavities with additional acid-etching. In contrast, Moura and others[26] reported a lower survival rate (91.8%) after three years for Class III restorations than was obtained in the present study. However, in their study restorations were placed by undergraduate dental students; the main cause of failure was the loss of restoration due to limited adhesiveness. The authors[26] stated that the debonding of the restorations may have been due to operator inexperience with the adhesive technique. In our study, there were no significant differences between the four dentin adhesives with regard to survival rates. On the other hand, Xeno V exhibited lower survival rates than did Scotchbond Multipurpose, XP Bond, and Prime&Bond NT, which are etch-and-rinse adhesive systems; Xeno V is a self-etch adhesive system. Self-etch systems are more user friendly. These adhesives eliminate the etch-and-rinse step, which not only reduces the clinical application time but also significantly minimizes the technique sensitivity or the risk of making errors during application.[2] In addition, it was revealed[14,19] that beveling of enamel did not significantly affect the clinical outcome variables in direct anterior restorations. Therefore, enamel margins were not beveled and etched with phosphoric acid. For etch-and-rinse adhesive systems, enamel margins were beveled and etched with phosphoric acid. Beveling enamel provides more exposed enamel rod ends and makes the enamel prisms more reactive to acid conditioning and produces an additional area for bonding.[27,28] Therefore, with any preparation that utilizes the acid-etch technique, such as etch-and-rinse systems, it is important to expose as many enamel rod ends as possible to increase resin retention.[28] Contradictory to this finding, although different dentin adhesives were used in the present study, Van Dijken and others[22] found no difference in the survival rates of three adhesives that were investigated after five years. The authors[22] did not confirm their hypothesis that use of bonding systems improved the durability of Class III restorations. Also, it was shown[25] that there was no difference in the retention rates of these two applications in Class III cavities when a self-etch adhesive was applied with and without acid-etching after three years. In agreement with the findings of the present study, although a one-step self-etch adhesive was shown[29] to have a higher cumulative failure rate than a two-step etch-and-rinse adhesive after 48 months, there was no significant difference between these two adhesives in Class III cavities. On the other hand, in Class III cavities, the two-step self-etch adhesive with etch group showed a significantly lower survival compared with the non-etch group and two-step etch-and-rinse adhesive groups.[20]

In the present study, self-etch (Xeno V) –bonded restorations exhibited significantly higher marginal discoloration than did three etch-and-rinse adhesive-bonded restorations. The reason for the failure of two of the three Xeno V failed restorations was marginal discoloration at the Charlie level. However, with respect to marginal adaptation, there were no significant differences between the four adhesive-bonded restorations. Only one Xeno V restoration was lost as a result of marginal adaptation at the Delta level. In agreement with these findings, it was reported[29] that a one-step self-etch adhesive showed higher marginal discoloration and lower marginal integrity than a two-step etch-and rinse adhesive in Class III/IV cavities after four years. On the other hand, marginal discoloration was not found as a reason for failure associated with three dentin adhesives in Class III cavities pretreated with oxalic or phosphoric acid.[22] Moreover, additional etching of the enamel margins was reported[25] to improve the marginal quality of mild two-step self-etch adhesives by protecting against small marginal defects and superficial marginal discolorations in Class III cavities after three years. A clear tendency for marginal staining has been reported with self-etching primers compared with enamel etching. The marginal seal of direct restorations can only be measured clinically through the evaluation of marginal discoloration and detectable margins.[19] The bond with enamel is vital to protect against marginal discoloration and for a good seal because almost all of the visible margin of Class III/IV restorations is in the enamel.[19] The best current method for establishing a microretentive pattern that permits good bonding to ground enamel is achieved through etching with 37% phosphoric acid.[19,30] Less discoloration was observed when enamel was etched with phosphoric acid compared with restorations performed with alternative conditioning systems.[19] In

addition, in support of our findings related to marginal adaptation and marginal discolorations, it was reported[19] that the marginal integrity did not depend on the system or method of tooth conditioning because no differences were found between acid-etching and no etching in Class III restorations; detectable margins do not always result in stained margins.

After five years, there was no statistically significant difference among the four adhesive bonded restorations with respect to color match. However, nanofill composite restorations (Filtek Supreme XT) with Scotchbond Multipurpose exhibited more ideal restorations than did nanohybrid composite restorations (CeramX) with XP Bond, Prime&Bond NT, and Xeno V. It was stated that the initial gloss of many restoratives was quite good, but in hybrid composite (microhybrids, nanohybrids) plucking of the larger fillers caused loss of gloss. In contrast, nanoclusters shear at a rate similar to that of the surrounding matrix during abrasion in nanofilled composites, which allows restorations to retain a smoother surface for long-term polish retention.[31] This was likely the reason why we obtained more ideal nanofill composite restorations (Filtek Supreme XT) with respect to color match after five years.

In the current study, no caries were observed adjacent to the restoration margins in any of the four products tested, and all showed ideal (Alpha rate) surface texture. During the five-year observation period, 92.3% of the CeramX restorations and Xeno V (7.7%) restorations were ideal (Alpha) for wear and anatomic form, and only 1.2% of the restorations were at clinically acceptable (Bravo) levels for wear and anatomic form. On the other hand, the other three adhesive bonded restorations were ideal for wear and anatomic form. This finding was similar to the findings of our previous study,[13] in which the same composites were used to restore space closure by build-up restorations on anterior teeth. The use of nanotechnology-based composites may account for the greater number of ideal restorations.

CONCLUSIONS

Adhesion strategy, such as self-etch or etch-and-rinse, is a more important factor than solvent content of dentin adhesive systems in the success of Class III restorations. With the exception of marginal discoloration and marginal integrity deterioration of Xeno V–bonded restorations, modern composites such as nano-composites and nanohybrids could provide high-quality restorations and good long-term results.

Regulatory Statement

This study was conducted in accordance with all the provisions of the local human subjects oversight committee guidelines and policies of the University Ethical Committee of Istanbul University. The approval code for this study is 32859.

Conflict of Interest

The authors of this manuscript certify that they have no proprietary, financial, or other personal interest of any nature or kind in any product, service, and/or company that is presented in this article.

(Accepted 7 January 2017)

REFERENCES

1. Van Meerbeek B, Vargas M, Inoue S, Yoshida Y, Peumans M, Lambrechts P, & Vanherle G (2001) Adhesives and cements to promote preservation dentistry *Operative Dentistry* **26(Supplement 6)** 119-144.
2. Van Meerbeek B, De Munck J, Yoshida Y, Inoue S, Vargas M, Vijay P, Van Landuyt K, Lambrechts P, & Vanherle G (2003) Buonocore memorial lecture. Adhesion to enamel and dentin: Current status and future challenges *Operative Dentistry* **28(3)** 215-235.
3. Silva e Souza MH Jr, Carneiro KG, Lobato MF, Silva e Souza Pde A, & de Góes MF (2010) Adhesive systems: Important aspects related to their composition and clinical use *Journal of Applied Oral Science* **18(3)** 207-214.
4. Ikeda T, De Munck J, Shirai K, Hikita K, Inoue S, Sano H, Lambrechts P, & Van Meerbeek B (2005) Effect of evaporation of primer components on ultimate tensile strengths of primer-adhesive mixture *Dental Materials* **21(11)** 1051-1058.
5. Jacobsen T, & Söderholm KJ (1995) Some effects of water on dentin bonding *Dental Materials* **11(2)** 132-136.
6. Van Landuyt KL, Snauwaert J, De Munck J, Peumans M, Yoshida Y, Poitevin A, Coutinho E, Suzuki K, Lambrechts P, & Van Meerbeek B (2007) Systematic review of the chemical composition of contemporary dental adhesives *Biomaterials* **28(26)** 3757-3785.
7. Carvalho RM, Yoshiyama M, Brewer PD, & Pashley DH (1996) Dimensional changes of demineralized human dentine during preparation for scanning electron microscopy *Archives of Oral Biology* **41(4)** 379-386.
8. Carvalho RM, Mendonça JS, Santiago SL, Silveira RR, Garcia FC, Tay FR, & Pashley DH (2003) Effects of HEMA/solvent combinations on bond strength to dentin *Journal of Dental Research* **82(8)** 597-601.
9. Loguercio AD, Lorini E, Weiss RV, Tori AP, Picinatto CC, Ribeiro NR, & Reis A (2007) A 12-month clinical evaluation of composite resins in Class III restorations *Journal of Adhesive Dentistry* **9(1)** 57-64.
10. Chen MH (2010) Update on dental nanocomposites *Journal of Dental Research* **89(6)** 549-560.
11. Wolff D, Kraus T, Schach C, Pritsch M, Mente J, Staehle HJ, & Ding P (2010) Recontouring teeth and closing diastemas with direct composite buildups: A clinical

evaluation of survival and quality parameters *Journal of Dentistry* **38(12)** 1001-1009.

12. Gresnigt MM, Kalk W, & Ozcan M (2012) Randomized controlled split-mouth clinical trial of direct laminate veneers with two micro-hybrid resin composites *Journal of Dentistry* **40(9)** 766-775.
13. Demirci M, Tuncer S, Öztaş E, Tekçe N, & Uysal Ö (2015) A 4-year clinical evaluation of direct composite build-ups for space closure after orthodontic treatment *Clinical Oral Investigations* **19(9)** 2187-2199.
14. Demirci M, Yildiz E, & Uysal O (2008) Comparative clinical evaluation of different treatment approaches using a microfilled resin composite and a compomer in Class III cavities: Two-year results *Operative Dentistry* **33(1)** 7-14.
15. Roberson TM, Heymann HO, Ritter AV, & Pereira PNR (2002) Classes III, IV, and V direct composite and other tooth-colored restorations In: Sturdevant CM (ed) *The Art and Science of Operative Dentistry* **4th edition** C.V. Mosby Co, St Louis, MO 501-536.
16. Ryge G (1980) Clinical criteria *International Dental Journal* **30(4)** 347-358.
17. Barnes DM, Blank LW, Gingell JC, & Gilner PP (1995) A clinical evaluation of a resin-modified glass ionomer restorative material *Journal of the American Dental Association* **126(9)** 1245-1253.
18. Cvar JF, & Ryge G (2005) Reprint of criteria for the clinical evaluation of dental restorative materials *Clinical Oral Investigations* **9(4)** 215-232.
19. Heintze SD, Rousson V, & Hickel R (2015) Clinical effectiveness of direct anterior restorations—A meta-analysis *Dental Materials* **31(5)** 481-495.
20. Kubo S, Kawasaki A, & Hayashi Y (2011) Factors associated with the longevity of resin composite restorations *Dental Materials Journal* **30(3)** 374-383.
21. Deliperi S (2008) Clinical evaluation of nonvital tooth whitening and composite resin restorations: Five-year results *European Journal of Esthetic Dentistry* **3(2)** 148-159.
22. van Dijken JW, Olofsson AL, & Holm C (1999) Five year evaluation of Class III composite resin restorations in cavities pre-treated with an oxalic- or a phosphoric acid conditioner *Journal of Oral Rehabilitation* **26(5)** 364-371.
23. Baldissera RA, Corrêa MB, Schuch HS, Collares K, Nascimento GG, Jardim PS, Moraes RR, Opdam NJ, & Demarco FF (2013) Are there universal restorative composites for anterior and posterior teeth? *Journal of Dentistry* **41(11)** 1027-1035.
24. Demarco FF, Collares K, Coelho-de-Souza FH, Correa MB, Cenci MS, Moraes RR, & Opdam NJ (2015) Anterior composite restorations: A systematic review on long-term survival and reasons for failure *Dental Materials* **31(10)** 1214-1224.
25. Ermis RB, Temel UB, Celik EU, & Kam O (2010) Clinical performance of a two-step self-etch adhesive with additional enamel etching in Class III cavities *Operative Dentistry* **35(2)** 147-155.
26. Moura FR, Romano AR, Lund RG, Piva E, Rodrigues Júnior SA, & Demarco FF (2011) Three-year clinical performance of composite restorations placed by undergraduate dental students *Brazilian Dental Journal* **22(2)** 111-116.
27. Schroeder M, Reis A, Luque-Martinez I, Loguercio AD, Masterson D, & Maia LC (2015) Effect of enamel bevel on retention of cervical composite resin restorations: A systematic review and meta-analysis *Journal of Dentistry* **43(7)** 777-788.
28. Moore DH, & Vann WF Jr (1988) The effect of a cavosurface bevel on microleakage in posterior composite restorations *Journal of Prosthetic Dentistry* **59(1)** 21-24.
29. Häfer M, Schneider H, Rupf S, Busch I, Fuchß A, Merte I, Jentsch H, Haak R, & Merte K (2013) Experimental and clinical evaluation of a self-etching and an etch-and-rinse adhesive system *Journal of Adhesive Dentistry* **15(3)** 275-286.
30. De Munck J, Van Meerbeek B, Satoshi I, Vargas M, Yoshida Y, Armstrong S, Lambrechts P, & Vanherle G (2003) Microtensile bond strengths of one- and two-step self-etch adhesives to bur-cut enamel and dentin *American Journal of Dentistry* **16(6)** 414-420.
31. Sakaguchi RL, & Powers JM (2012) *Craig's Restorative Dental Material*s Elsevier Mosby, Philadelphia, PA.